EFFICIENT AND RESPONSIBLE USE OF PRIOR INFORMATION AND JOINT PARAMETER ESTIMATION FOR ESTIMATING PARAMETERS OF GROUNDWATER FLOW MODELS

by

RICHARD A. WEISS

B.Sc., The Colorado School of Mines, 1986
M.Sc., The Pennsylvania State University, 1989

A THESIS SUBMITTED IN PARTIAL FULFILLMENT OF

THE REQUIREMENTS FOR THE DEGREE OF

DOCTOR OF PHILOSOPHY

in

THE FACULTY OF GRADUATE STUDIES

Department of Geological Sciences

We accept this thesis as conforming

to the required standard

THE UNIVERSITY OF BRITISH COLUMBIA

April 1994

In presenting this thesis in partial fulfilment of the requirements for an advanced degree at the University of British Columbia, I agree that the Library shall make it freely available for reference and study. I further agree that permission for extensive copying of this thesis for scholarly purposes may be granted by the head of my department or by his or her representatives. It is understood that copying or publication of this thesis for financial gain shall not be allowed without my written permission.

(Signature)

Department of Geological Sciences

The University of British Columbia
Vancouver, Canada

Date 5-26-94

DE-6 (2/88)

Abstract

Parameter estimation problems for groundwater flow systems are often non-identifiable or unstable using only hydraulic head data. Prior information on parameters or joint parameter estimation including tracer concentrations may be used to stabilize the parameter set. Response surfaces and multiparameter confidence regions are used to identify the most efficient and responsible use of prior information and joint data sets for the purpose of parameter estimation.

Prior information on some of the parameters are used to stabilize the parameter set for parameter estimation. Efficient use of prior information involves identifying those parameters for which prior information will stabilize the model parameter set the most. Responsible use of prior information involves identifying how errors in the prior information will influence the parameter estimates. The most responsible parameters for prior information are those parameters for which errors in the prior information have the least influence on the final parameter estimates. Guidelines are developed for efficient and responsible use of prior information in parameter estimation based on an analysis of the parameter space using response surfaces and eigenspace decomposition.

Joint parameter estimation is used when more than one data set is available to estimate the model parameters. Response surfaces and confidence regions are used to show how multiple data sets reduce parameter uncertainty. The value of

future data in reducing the uncertainty of parameter estimates is explored. For weighting data sets in joint parameter estimation, three criteria based on parameter space analysis are proposed. These three criteria are evaluated and compared to the more traditional weighting method based on an analysis of data residuals.

A groundwater model for the San Juan Basin, New Mexico, is constructed and calibrated using the methods developed in this thesis. Hydraulic head data, ^{14}C concentration data, and prior information on the model parameters is used to calibrate the model in an efficient and responsible manner. The model is calibrated in two stages. In the first stage, prior information on the hydraulic conductivity parameters for the lower model layers was found to be both efficient and responsible in stabilizing the parameter set. In the second stage, the parameter estimates and uncertainties based on the four weighting criteria were compared.

Table of Contents

List of Tables

List of Figures

Acknowledgements

From the moment I arrived at the University of British Columbia, Dr. Leslie Smith guided the way toward the completion of this thesis. He has been an outstanding research supervisor, devoting an extraordinary amount of attention toward my work. I would like to thank him for his time, energy, and most of all his understanding. This research has been supported by University Graduate Fellowships from the University of British Columbia, as well as grants from the Natural Sciences and Engineering Research Council of Canada (NSERC). I would like to thank Martin Shute for the use of his unpublished ^{14}C data for the San Juan Basin. I would also like to thank Tom Clemo for his willingness to solve any computer problems that arose. Finally, I would like to thank my wife, Rosanna Weiss, who supported, encouraged and helped me continuously throughout this project.

CHAPTER 1. INTRODUCTION

Mathematical models are commonly used to simulate fluid flow and solute transport in subsurface environments. Site specific models are constructed in order to better understand the subsurface environment or to predict future values of hydraulic head and mass concentration. The simulated model results will be accurate only if the model is a reasonable representation of the true flow and transport system. While the mathematical and computational aspects of groundwater models are well developed, the question of how to choose appropriate parameter values for a specific flow and transport system is problematic. The process of choosing appropriate parameter values for a model is termed parameter estimation.

Groundwater flow can be described mathematically by a partial differential equation and associated boundary conditions. Models for groundwater flow require parameter values at every point in the model domain to solve for the dependent variable, the hydraulic head distribution in space and time. These parameters include hydraulic conductivity, storage coefficient, boundary conditions and initial conditions. It is impossible to directly identify a parameter such as hydraulic conductivity at every point in the domain being modelled, so some method of indirectly identifying the parameters must be found. The inverse method of parameter estimation uses observations of the dependent variable (hydraulic head) to estimate the parameters of the model.

Hydraulic head data have traditionally been used to estimate model parameters. However, the inverse problem using only head data is often ill-posed [*Emsellen and de Marsily,* 1971]. The ill-posed nature of the inverse problem leads to unstable and uncertain parameter estimates. Independent information (prior information) on parameter values, such as hydraulic conductivity estimates from pump tests, have been used to reduce the problems associated with the ill-posed nature of the inverse problem [*Cooley,* 1982]. Another way of reducing the problems due to the ill-posed nature of the inverse problem is to use an additional data set through joint parameter estimation. Environmental tracers (isotopes) are present throughout many groundwater systems, and the tracer data may be used in conjunction with hydraulic head data to provide improved parameter estimates. For large scale flow systems, environmental tracer data is a practical type of mass concentration data for use in estimating flow system parameters.

The work in this thesis was motivated by an attempt to understand how prior information and joint parameter estimation stabilize parameter estimates and reduce parameter uncertainty. In numerical experiments using a variety of models, it was noted that in some cases prior information significantly stabilized the parameter estimates, while in other cases prior information did not stabilize the parameter estimates at all. Similarly, for some models joint estimation stabilized parameter estimates significantly over single state parameter estimation, while for other models joint estimation did not stabilize parameter estimates at all. The work in this thesis has

focused on understanding why the above effects occur, and developing methods to determine how prior information and joint parameter estimation can be used in an efficient and responsible manner.

The most efficient parameters for prior information are those parameters for which prior information will stabilize the parameter estimates the most. Responsible use of prior information involves identifying how errors in the prior information will influence the parameter estimates. The most responsible parameters for prior information are those parameters for which errors in the prior information have the least influence on the final parameter estimates. For joint parameter estimation, parameter space analysis is used to determine the information available about the model parameters from each of the data sets. Several criteria are developed in this thesis to determine how to combine the information from each data set to produce the best parameter estimates.

1.1 Need for parameter estimation

Steady state groundwater flow is governed by the equation:

$$\nabla \cdot (\boldsymbol{K} \cdot \nabla h) + q = 0 \quad on\ R \tag{1.1}$$

subject to the boundary condition:

$$-\boldsymbol{K} \cdot \nabla h \cdot \boldsymbol{n} = Q \quad on\ \Gamma_1 \tag{1.2a}$$

$$h = H \quad on\ \Gamma_2 \tag{1.2b}$$

where R is the spatial domain of the flow system, Γ is the boundary of the flow system, ∇ is the gradient operator, $\boldsymbol{K}$ is the hydraulic conductivity tensor, h is the hydraulic head, q represents internal sources, $\boldsymbol{n}$ is the unit vector normal to the boundary, Q is the prescribed boundary flux on Γ_1, and H is the prescribed boundary head on Γ_2.

The solution of the flow equation requires the knowledge of the parameters $\boldsymbol{K}$, q, H, and Q over the entire flow domain and on its boundary. The output from the model are the simulated values of h throughout the domain of the model. In practice, the flow equation is often solved by numerical methods, and the parameters take on discrete values. These discrete parameter values will be referred to as the model parameter values.

The most straightforward way of constructing a model of a flow system is to obtain measurements of all the system parameters, use the measured parameter values as the model parameter values, and directly calculate the output head values. There are several problems with this approach. First, due to the heterogeneity of the media, measurements of the parameters would be required at every point in the flow domain. It is prohibitively difficult and expensive to measure all parameters at every

point in the flow domain. Parameters such as hydraulic conductivity are expensive to measure in the field, and in practice measurements are relatively scarce. Second, the scale of the measured parameters is often quite different from the scale of the model. A pump test measures hydraulic conductivity at a scale that is often much smaller than the scale of the model. These problems necessitate an alternate method of constructing a flow and transport model for a specific field site.

A more practical approach to constructing a model is the process of model calibration. One way of determining if a model is a good representation of the flow system is to compare the output head values from the numerical model to a set of field data. If the simulated head values match the field data closely, then the model is deemed to be a good representation of the system (at least for the purposes of simulating the model output). If the simulated head values are a poor match to the field data, then the model may be a poor representation of the system. Model calibration is the process of constructing a model so that the simulated data closely match the field data.

The traditional method of model calibration is manual trial and error. The values of the model parameters are adjusted manually until the simulated data match the observed data. When an adequate fit between the simulated and observed data is obtained, the model is deemed calibrated. The parameter values of the calibrated model are the model parameter estimates. The trial and error approach is often very

helpful in understanding how a flow system behaves. However, the trial and error process is often time consuming, frustrating, and subjective. It is difficult to determine whether the parameter estimates are the best estimates, or whether other, equally good or better sets of parameter estimates exist. The quality of the model and the model parameter estimates are difficult to evaluate using the trial and error approach.

Formalized parameter estimation methods offer a way to automate the trial and error model calibration process. The formalized parameter estimation schemes present a framework in which the most likely parameter estimates can be determined, and the reliability of these parameter estimates can be quantified. The calibration process is automated, yet the modeller still retains control over the calibration process.The parameter estimation methods are based on the solution of the inverse problem, which is the solution of equations (1.1) and (1.2) for the parameters (independent variables), given the values of the output variable h (the dependent variable). Chapter 2 provides an overview of many of the parameter estimation methods.

1.2 Ill-posedness of the inverse problem.

The inverse problem is the basis for formalized parameter estimation, but it is often ill-posed. Due to this ill-posed nature, strict conditions must be met in order to obtain a meaningful solution. For a groundwater flow problem, these conditions are that error free values of the hydraulic head must be known everywhere in the flow

domain, and either the hydraulic conductivity or the flux must be prescribed at one point along each streamline *[Emsellen and de Marsily,* 1971]. In addition, the model must be a true representation of the real system.

In practice, the data are generally sparse, available only at various point locations throughout the model domain. For a variety of reasons, the data are also in error with respect to the model [*Cooley,* 1979]. Examples of data errors are: (1) measurement errors due to instrument error; (2) errors in head data due to errors in surveyed elevation; (3) areal models assume that the data is averaged over the vertical, but the measurements may not be taken over the entire vertical interval; (4) in cross section models, there is some uncertainty in the depth of measurement when the screened interval of the well is long; (5) parameter variations smaller than the modeled scale may cause fluctuations in data values that are not accounted for in the model; (6) data may be influenced by a transient flow system, yet the model may be at steady state. All of these factors contribute to errors in the data with respect to the model, and the magnitude of these errors is often unknown.

In the field, parameters such as hydraulic conductivity vary continuously in space throughout the flow system. Numerical models of the flow system, either finite difference or finite element models, divide the flow system into elements. The continuous variation of the field parameter is replaced by a set of discrete model parameters. The model cannot represent the true variation in the field parameter, and

is therefore an approximation to the true flow system. For groundwater problems, the above factors lead to an ill-posed inverse problem. The ill-posed nature of the inverse problem often makes the inverse problem difficult to solve.

1.3 Uniqueness, identifiability, and stability issues

Three major issues result from the ill-posed nature of the inverse problem: uniqueness, identifiability, and stability. A detailed mathematical analysis of these issues is contained in *Carrera and Neuman* [1986b]. We present these issues in a conceptual context.

A solution to the inverse problem is said to be unique if the set of estimated parameters is the only set which satisfies the conditions to be a solution [*Carrera,* 1988]. Two types of non-uniqueness have been recognized [*Tarantola and Valette,* 1982]. One type is due simply to the paucity of data, that is, more parameters are to be identified than data available. The second type of non-uniqueness is due to the structure of the physical model. Multiple minima in the objective function surface are a symptom of non-uniqueness due to model structure. Non-uniqueness due to model structure may be relatively rare [*Carrera,* 1988].

A model parameter is non-identifiable if the model output is not sensitive to the parameter [*Chavent,* 1979]. For instance, in a one-dimension flow system with

prescribed head boundaries and a uniform hydraulic conductivity, the hydraulic conductivity is non-identifiable using head data. The value of hydraulic conductivity has no influence on the head distribution. If a parameter is non-identifiable, then the solution to the inverse problem is non-unique. However, a non-unique solution may occur even if all parameters are identifiable.

A group of parameters may also be non-identifiable. For example, when all model parameters are estimated using only head data, the set of model parameters are non-identifiable [*Cooley and Naff,* 1990]. The model output is not sensitive to the entire set of model parameters, considered jointly. A suite of different combinations of parameter values result in identical model outputs. Because of the non-identifiability of the entire set of model parameters, all model parameters are very seldom estimated. It is common practice to estimate only a subset of the model parameters, usually the internal model parameters. The model boundary conditions are commonly specified.

The major difficulty associated with parameter estimation arises from the instability of the parameter set being estimated. When a parameter set is unstable, small errors in the data can lead to large errors in the estimated parameters. Since errors in the data are unavoidable, large errors in estimated parameters are common in unstable problems. Unstable parameter sets also lead to large uncertainties in the estimated parameters. Unstable parameter sets are characterized by a large, nearly

flat region in the response surface (see Chapter 4). A side effect of parameter instability is that it slows the convergence rate of the iterative algorithms used for parameter estimation. Instability often leads to iterative algorithms that stop at points that are not the true minimum, leading to the (false) assumption that multiple local minima exist. Thus, instability is often confused with non-uniqueness. Some researchers have concluded that instability in the inverse problem is such a major problem that sensible parameter estimates are unattainable in many instances [*Yakowitz and Duckstein,* 1980].

1.4 Methods for controlling instability

Since parameter instability is a major issue in parameter estimation for groundwater flow problems, many researchers have focused on methods of controlling the parameter instability. Three approaches are possible: (1) reduction in parameter dimension; (2) incorporation of prior information on parameter values; and (3) collection of additional data.

1.4.1 Parameter dimension

The parameter dimension is the number of parameters to be estimated. In a numerical model, an independent model parameter may be assigned to each element for each type of parameter [eg. *Shah et al.,* 1978]. In this case, there will generally be

more parameters than data, and the resulting parameter estimates will be non-unique. To reduce the parameter dimension, elements may be grouped in zones, and a model parameter assigned to each zone [eg. *Cooley,* 1977]. Zones for one type of parameter, such as hydraulic conductivity, may not correspond to zones for another type, such as recharge.

As the number of zones increases, the fit of the simulated data to the observed data becomes better, while the uncertainty of the parameter estimates increases. As the number of zones decreases, the fit of the simulated data to the observed data becomes worse, but the parameter estimates have lower uncertainties. Several methods have been developed to determine the optimum number and arrangement of the zones (*Shah et al.,* 1978; *Yeh and Yoon,* 1981; *Sun and Yeh,* 1985; *Carrera and Neuman,* 1986a; *Cooley et al.,* 1986). All methods attempt to minimize the uncertainty of the parameter estimates while maximizing the fit of the data to the model. The methods select the simplest model compatible with the available data.

Reducing the number of zones (parameter dimension) may not always help to reduce the problems associated with the inverse problem. For the case of estimating all model parameters, the inverse problem is non-identifiable regardless of the number of parameter zones. In other cases, the geology of the site may impose a given number and arrangement of zones. It may not be possible to reduce the number of zones and still retain a credible model of the site.

1.4.2 Prior information

Independent information on the estimated parameters (called prior information) has been recognized as valuable in stabilizing the inverse problem. The prior information can either have a specified reliability [*Neuman and Yakowitz,* 1979] or an unknown reliability [*Cooley,* 1982]. For the case of estimating all the parameters for a groundwater flow model, the inverse problem becomes identifiable in the presence of prior information [*Carrera and Neuman,* 1986b]. Although identifiable, the inverse problem may still be very unstable.

Though prior information may be valuable in stabilizing the inverse problem, a cautious use of prior information may be advisable. Prior information may not significantly stabilize an inverse problem. There is little advantage to be gained by obtaining prior information about a parameter which will not be effective in stabilizing the model parameter set. In this thesis, guidelines are developed to identify those parameters for which prior information will most efficiently stabilize the parameter set.

Another concern when using prior information is that it may not be representative of the model parameter values. The prior information may be in error or biased with respect to the model for a number of reasons. First, prior information may be obtained at a scale which is different from the scale of the model. As an example, suppose the prior information about hydraulic conductivity for a model zone

is obtained using a slug test. The slug test samples smaller volume of the subsurface than the model zone, and the slug test may miss some large scale features that the model zone includes. The hydraulic conductivity obtained from the slug test would most likely be different than the hydraulic conductivity at the scale of the model. If prior information about all hydraulic conductivity zones were obtained from slug tests, the prior information would most likely be consistently biased with respect to the model hydraulic conductivity values. Second, prior information on parameters such as hydraulic conductivity is often extrapolated from measurements taken outside of the modelled region. This extrapolation introduces the possibility of errors in the prior information. Third, prior information may be obtained in parts of hydrogeological units that are not representative of the entire unit. As an example, in low permeability units, hydraulic conductivity measurements are often obtained in the higher permeability lenses within the units. Also, if the prior information is obtained from tests near the outcrop of a hydrogeological unit, it may not represent the parameter values for the same unit at depth. All of these factors contribute to the fact that the prior information may be unrepresentative of the model parameter values.

The influence of unrepresentative or biased prior information on the final model parameter estimates is explored in this thesis. The biased prior information influences not only those parameters with prior information, but the other model parameter estimates as well. In fact, small errors in prior estimates may lead to greatly magnified errors in the final estimates for other parameters. In this thesis, guidelines are

developed to identify those parameters for which errors in the prior information lead to the smallest possible errors in the final parameter estimates.

1.4.3 Additional data

Additional data on the dependent variable may be used to stabilize the inverse problem. This additional data may take the form of additional hydraulic head data, or it may be a new data type, such as mass concentration data. If the additional data are more hydraulic head data, they may or may not assist in stabilizing the inverse problem. When estimating a subset of the model parameters, the additional head data may help stabilize the parameter estimates. However, when estimating all model parameters, the additional head data will not stabilize the inverse problem. In this case, the inverse problem is non-identifiable regardless of the number of head data used.

Additional data may take the form of mass concentration data. The mass concentration data will yield information on the flow parameters, since the concentration is dependent on the fluid velocities, which are a function of the flow parameters. For this reason, the mass concentration data should assist in stabilizing the parameter estimates for the flow parameters, even when estimating all model flow parameters. The use of head and concentration data together falls under the concept of joint parameter estimation.

Solute transport of a single decaying nonreactive species is governed by the advection-dispersion equation:

$$\nabla \cdot \theta \, (\boldsymbol{D} \cdot \nabla c - Vc) - \lambda \theta c = \theta \frac{\partial c}{\partial t} \quad on \; R \tag{1.3}$$

subject to the initial conditions:

$$c = c_o \quad on \; R \quad at \; t = t_o \tag{1.4a}$$

and the boundary conditions:

$$(\theta \, \boldsymbol{D} \cdot \nabla c - \theta V c) \cdot \boldsymbol{n} = g_1 \quad on \; \Gamma_3 \tag{1.4b}$$

$$c = g_2 \quad on \; \Gamma_4 \tag{1.4c}$$

where $\boldsymbol{D}$ is the dispersion tensor, c is the mass concentration of the solute, V is the fluid velocity, λ is the decay coefficient, θ is the porosity, c_o is the initial concentration, g_1 is the specified mass flux along Γ_3, and g_2 is the specified concentration along Γ_4. The components of the fluid velocity are calculated from the solution to the flow equation by

$$V_i = \sum_{j=1,3} \left[-\frac{K_{ij}}{\theta} \frac{\partial h}{\partial x_j} \right] \tag{1.5}$$

The components of the dispersion coefficient are given by

$$D_{ij} = \alpha_T V \delta_{ij} + (\alpha_L - \alpha_T) \frac{V_i V_j}{V} + D_d \delta_{ij} \tag{1.6}$$

where α_L is the longitudinal dispersivity, α_T is the transverse dispersivity, V is the magnitude of the fluid velocity, D_d is the molecular diffusion coefficient, and δ_{ij} is the

Kronecker delta.

The solution to the solute transport equations requires the knowledge of additional parameters, such as α_L, α_T, θ, and the initial and boundary conditions on mass concentration. These additional parameters may either be estimated during the solution of the inverse problem, or independent information on these additional parameters could be obtained.

The concentration data may eliminate the non-identifiability of the parameter set and stabilize the parameter estimates. In some instances, concentration data will stabilize the parameter estimates and reduce parameter uncertainty significantly, while in other cases the concentration data may not stabilize the parameter estimates [*Weiss and Smith,* 1993]. Methods of determining whether the additional data will significantly stabilize the parameter estimates are developed in this thesis.

For joint parameter estimation, relative weights for each data set are required. Three methods of weighting are developed in this thesis, based on obtaining the best possible estimates given the data available. Another issue involved in incorporating concentration data is the question of the additional transport parameters needed to simulate the mass concentrations. If these additional parameters are specified using prior information, the parameter values may be in error. Methods are developed in this thesis to evaluate the influence of errors in the transport parameters on the estimates

of the flow parameters.

1.5 Outline of thesis

The objective of the thesis research is to develop methods for stabilizing parameter estimates for groundwater flow models in an efficient and responsible manner. For determining the usefulness of prior information, guidelines are developed to identify those parameters for which prior information will most efficiently stabilize the parameter set. Since the prior information may be in error with respect to the model, guidelines are also developed to identify those parameters for which errors in the prior information leads to the smallest possible errors in the final parameter estimates. Using prior information on the basis of these guidelines will result in an efficient and responsible method of stabilizing the inverse problem using prior information.

For joint parameter estimation, methods are developed to determine the usefulness of mass concentration data for the purposes of stabilizing the estimated parameter set. Several different weighting methods for the data sets in joint estimation are developed and evaluated. Methods of determining the influence of errors in the transport parameters on the estimates of the flow parameters are also developed. All of the above issues are explored through an examination of the model parameter space.

The thesis is organized as follows. Chapter 2 contains an overview of previous work in single state and joint parameter estimation, as well as parameter space analysis. Chapter 3 details the methods and philosophy of parameter estimation used in this work. An introduction to the concepts needed for parameter space analysis is provided in Chapter 4. In Chapter 5, the parameter space analysis is used to evaluate the use of prior information in parameter estimation. Guidelines are developed for efficient and responsible use of prior information. In Chapter 6, joint parameter estimation is analyzed in the context of parameter space analysis. A groundwater flow model for the San Juan basin, New Mexico, is constructed and calibrated to illustrate the methods developed in this work, and the results are presented in Chapter 7.

CHAPTER 2. REVIEW OF PARAMETER ESTIMATION

Parameter estimation for groundwater flow systems has been investigated for over three decades. The majority of the research has focused on single state parameter estimation, generally estimating flow parameters using a set of hydraulic head measurements. Less work has been done on coupled inverse problems, such as joint flow-mass transport or joint flow-thermal transport problems. This chapter describes past research on the major issues involved in single state and joint parameter estimation for groundwater models, as well as past work on analysis of models using parameter space methods.

2.1 Single state parameter estimation

A great deal of research has been done on parameter estimation for a single state variable in groundwater flow systems. Complete reviews may be found in *Yeh* [1986] and *Carrera* [1988]. The following is a short overview of the major issues involved in parameter estimation for a single state variable. The first issue, parameterization, concerns how the true parameter structure is represented by the discrete model parameters. The second issue, model construction, includes determining the correct model structure. The other issues concern estimating model parameters, assuming a given parameterization and model structure.

2.1.1 Parameterization

The field parameters, such as hydraulic conductivity, vary continuously in space. The boundary parameters, such as specified head, also vary continuously along the boundary. This continuous variation in the field parameter is replaced by a set of discrete model parameters. Parameterization refers to the method by which the true parameter variation is represented by a set of discrete model parameters. There are several popular parameterization methods:

1. Zonation: The flow region is divided into a number of subregions, or zones, and a constant parameter value is assigned to each region [eg. *Cooley*, 1979]. The zonation approach is conceptually simple, and the zonation may be based on geological or hydrogeological information. Since the number of parameters is less than the number of data, the reliabilities of the parameter estimates may be quantified. The major criticism of the zonation approach is that the zonation may be incorrect or unrepresentative of the true system. If the zonation is incorrect, then the parameter estimates for the zones may be incorrect or meaningless. The issue of determining the correct zonation is discussed under model construction below.

2. Interpolation: This approach is generally used with finite element methods. A value of the parameter is assigned to each node of the element, and interpolated within the element by a local basis function [eg. *Yeh and Yoon*, 1981]. The elements used for

parameter interpolation need not be the same as the elements used for the head interpolation.

3. Discretization: The discrete values of the parameters at every model node or within each element are taken as the model parameters. This approach can be used with either zonation or interpolation, and results in a large number of model parameters [eg. *Shah et al.,* 1978]. The advantages of this method are that the model structure does not need to be determined a priori. The disadvantages are that a large number of model parameters need to be estimated, often greater than the number of data. The inverse problem is underdetermined, and estimates of the parameter reliability are difficult to obtain.

4. Stochastic: The model parameters are viewed as random functions, characterized by a mean and covariance. The estimated parameters are the mean, trend and the covariance of the field parameters [eg. *Kitanidis and Vomvoris*, 1983].

All of the above parameterization methods are valid, and each has advantages and disadvantages. The method chosen is often determined by the type of information required about the system being modelled and the purpose for which the model is being developed.

2.1.2 Model construction

In order to adequately calibrate a numerical model for a flow and transport system, three major model construction steps need to be followed. First, the model should include all physical processes relevant to the flow and transport system. Second, the structure of the model should resemble that of the real system. Third, the values assigned to the model parameters need to be similar to the true system parameter values. Most of the work in parameter estimation for groundwater flow models has concentrated on the third step.

The physical processes of the system are represented in the model by the equations used for the numerical model. For steady state groundwater flow, equations (1.1) and (1.2) adequately represent the physics of the flow process. For solute transport, the advection-dispersion equation (1.3) has traditionally been used to represent the physics of the mass transport process. However, it is recognized that this representation using a constant dispersivity is not generally valid in a heterogeneous porous medium [eg. *Gelhar and Axness*, 1983].

The model structure needs to be defined correctly. The type of boundary conditions and the location of the model boundaries need to be determined. Within the model domain, the structure of the hydraulic conductivity, recharge, porosity, and dispersivity distributions need to be defined. When discrete values of the parameters

within each element of the model grid are sought, it is not necessary to determine the model structure before estimating the parameters. Since each element is a separate model parameter, the results of the parameter estimation will determine the model structure. More commonly, a zonation or interpolation scheme is used to parameterize the model. The shape of the parameter zones and the location of the boundaries of the zones need to be determined before the parameters are estimated. In some cases, the geology of the site will greatly assist in determining the shape and location of the internal zones. The model structure is defined by the shape and location of all model parameter zones.

One approach for determining the correct model structure consists of selecting the model structure which leads to the best model fit while maintaining parameter stability [*Shah et al.*, 1978; *Yeh and Yoon*, 1981]. Alternative models with different parameter structures are compared. *Sun and Yeh* [1985] have proposed a method for automatically determining the model structure without having to construct alternative models. However, their approach does not include prior information on the model parameters.

Linear hypothesis testing can be used to compare alternative models. *Cooley et al.* [1986] sequentially compared pairs of models for a large scale flow system using hypothesis testing. A simple model for the flow system was initially proposed, and more complex models were compared to this simple model. Models that significantly

improved the fit of the data were accepted. More complex models were often rejected, based on the fact that the fit to the data was not improved significantly.

Criteria-based approaches have been used to compare model structures. *Carrera and Neuman* [1986a] present four criteria, and use these criteria to discriminate between competing models. The criteria tend to select the simplest models that are compatible with the data. Additional complexity can be built into the models as the quantity and quality of the data increase.

Once the model structure has been determined, the parameters of the model need to be estimated. The remainder of this chapter concerns estimating the parameters of the model.

2.1.3 Direct and indirect techniques

The techniques used to solve the inverse problem can be classified as either direct or indirect. The direct technique treats the model parameters as unknowns, and uses the hydraulic head distribution and the spatial derivatives of this distribution to solve for the unknown parameters directly. The solution of the direct technique requires that an estimate of the hydraulic head be known everywhere in the system, and that a value of the transmissivity is known on every streamline in the system. There are methods of relaxing these requirements; for instance, using a flatness

criterion [*Emsellem and de Marsily,* 1971]. Most of the early work with parameter estimation used the direct formulation of the inverse problem [*Stallman,* 1956]. Many mathematical techniques can be applied to the direct method of parameter estimation, among them are linear programming [*Kleinecke,* 1971]; quadratic programming [*Hefez et al.,* 1975]; and kriging with matrix inversion [*Yeh et al.,* 1983].

The indirect technique uses an output error criterion, usually the difference between the measured head values and the model generated head values. The model parameters are iteratively updated until the output error is minimized. The indirect technique has been more popular because of its flexibility and stability. Prior information on parameters can be incorporated into the parameter estimation scheme, and several data types can be used. The indirect technique is implemented in the form of minimizing an objective function, resulting in a type of least squares minimization problem. Mathematical programming techniques for minimizing the objective function are often used, such as gradient search procedures [*Jacquard and Jain,* 1965]; quadratic programming [*Yeh,* 1975]; Gauss-Newton method [*Cooley,* 1977]; conjugate gradient method [*Neuman,* 1980]; maximum likelihood method [*Carrera and Neuman,* 1986a]; and the direct search method [*Woodbury et al.*, 1987].

2.1.4 Formulation of inverse problem

The specific aim of indirect parameter estimation techniques is to minimize the

difference between the measured and model generated hydraulic heads. However, the real objective of parameter estimation techniques should to be to estimate meaningful parameters. It is necessary to recognize that the hydraulic head data generally contains errors, and the parameter estimation needs to be performed in a statistical framework. Three primary statistical approaches have been introduced: non-linear regression, Bayesian, and maximum likelihood methods. Each of these approaches starts from a different philosophical background, however, they each result in a similar set of equations for parameter estimation. A fourth approach, based on the stochastic formulation, has also been proposed.

2.1.4.1 Non-linear regression

Non-linear regression generally results in a weighted least squares criterion for parameter estimation. The weighted least squares criterion attempts to match the model calculated hydraulic heads to the observed hydraulic heads in a least squares sense. For hydraulic head data and prior information on parameters, the objective function to be minimized is:

$$S = [(\boldsymbol{h}-\boldsymbol{h}^*)^T \boldsymbol{W}_h (\boldsymbol{h}-\boldsymbol{h}^*) + \lambda(\boldsymbol{p}-\boldsymbol{p}^*)^T \boldsymbol{W}_p (\boldsymbol{p}-\boldsymbol{p}^*)] \qquad (2.1)$$

where $\mathbf{h}^*$ is the vector of observed heads, $\mathbf{h}$ is the vector of model calculated heads at the observation points, $\mathbf{W}_h$ is a weighting matrix, T is the transpose operator, $\mathbf{p}^*$ is the vector of observed prior information on parameters, $\mathbf{p}$ is the model calculated prior

information, $\mathbf{W_p}$ is a weighting matrix, and λ is the trade-off between head and prior data. When S is minimized, the differences between the observed and calculated heads and the prior and calculated parameter values are minimized.

The main advantage of this approach is that it allows the use of a large body of literature [eg. *Graybill,* 1976] on hypothesis testing, definition of confidence regions, and model selection. The reliability of the estimated parameters can be determined from the linearized covariance matrix [*Yeh and Yoon,* 1981]. Non-linear confidence intervals for the estimated parameters can also be determined [*Vecchia and Cooley,* 1987; *Cooley,* 1993].

2.1.4.2 Bayesian estimation

The Bayesian approach assumes that the data on hydraulic heads and prior information on parameters can be represented as joint probability density functions, and the resulting parameter estimates have a probability density function. The most general approach is presented by *Tarantola and Valette* [1982], and the approach of *Gavalas et al.* [1976] is nearly equivalent. The observed hydraulic heads can be described by a probability density function *r(h)*. The prior information on parameters is described by the a priori probability density function *r(p)*. The calculated data obtained from the model is described by a conditional probability density function, *Q(h|p)*, that is, the probability that the head values are *h*, given that the model and its

parameter values are described by p. The posterior conditional probability density function of the parameter values, $s(p|h)$, is the solution to the parameter estimation problem. Bayes theorem states that $s(p|h) = Q(h|p)r(p)/r(h)$, thus the probability density function of the parameter estimates can be constructed by knowing the statistics of the prior information and the model.

If the parameters and measurement errors are normally distributed and the model is linear in its parameters, it can be shown that the posterior conditional probability density function $s(p|h)$ is normally distributed as:

$$s(p|h) \propto \exp\{-\frac{1}{2}[(\boldsymbol{h}-\boldsymbol{h}^*)^T\boldsymbol{C}_h^{-1}(\boldsymbol{h}-\boldsymbol{h}^*) + (\boldsymbol{p}-\boldsymbol{p}^*)^T\boldsymbol{C}_p^{-1}(\boldsymbol{p}-\boldsymbol{p}^*)]\} \qquad (2.2)$$

where $\mathbf{C}_h^{-1}$ is the hydraulic head covariance matrix, and $\mathbf{C}_p^{-1}$ is the parameter covariance matrix. The entire probability density function can be obtained. The estimated parameters can be described by a probability density function, but it is difficult and expensive to determine the entire distribution. The practical approach is to determine the maximum a posteriori point of the distribution. Maximum aposteriori estimation of a normal distribution is equivalent to minimizing the quadratic objective function:

$$S = (\boldsymbol{h}-\boldsymbol{h}^*)^T\boldsymbol{C}_h^{-1}(\boldsymbol{h}-\boldsymbol{h}^*) + (\boldsymbol{p}-\boldsymbol{p}^*)^T\boldsymbol{C}_p^{-1}(\boldsymbol{p}-\boldsymbol{p}^*) \qquad (2.3)$$

This objective function is identical to the objective function found using a least squares criterion, when the inverse covariance matrices equal the weight matrices. The least

squares criterion and the Bayesian estimation criterion with normally distributed data errors and parameters lead to minimizing the same objective function.

2.1.4.3 Maximum likelihood estimation

Maximum likelihood estimation calls for choosing parameters that maximize the likelihood function. If the data errors are normally distributed, the likelihood function is similar to equation (2.2) above. The chief differences between maximum likelihood estimation and Bayesian estimation are philosophical. Bayesian formulations consider the model parameters to be random variables, while maximum likelihood formulations consider the model parameters to be fixed but unknown. The lack of information causes the parameters to be uncertain, but the model itself is deterministic. Maximum likelihood estimation does not require that the model be capable of reproducing the true system exactly, because the parameters are chosen as most likely within the framework of a specific model structure. This recognition that the model is not exact leads to criteria for comparing competing models [*Carrera and Neuman,* 1986a].

2.1.4.4 Stochastic formulation

Stochastic formulations of the inverse problem emphasize capturing the spatial variability of the parameters. The parameters are considered random functions, and are estimated at every point in the aquifer. A statistical model is proposed to represent

the spatial variability of the parameter within the flow system. This statistical model can generally be characterized by its mean, covariance, and trend. The spatial variability of the heads are derived from the spatial variability of the parameters through a linearized flow equation. The parameters describing the mean, covariance and trend of the model parameters are estimated using a maximum likelihood approach, conditioned on the head and prior parameter data. Kriging is applied to provide minimum variance, unbiased, point estimates of the parameters using all available information. This approach has been described by *Kitanidis and Vomvoris* [1983] for a one dimensional flow system and *Hoeksema and Kitanidis* [1985] for two dimensional flow systems, while *Dagan* [1985] used analytical techniques for parameter estimation in an infinite medium and with statistically uniform parameters. *Dagan and Rubin* [1988] extend this approach to identifying different parameter types in an unsteady flow regime.

2.2 Joint parameter estimation

Joint parameter estimation methods for groundwater flow systems have mainly been studied in the context of joint flow-mass transport systems and joint flow-thermal transport systems. The joint parameter estimation methods were used because multiple data sets were available, and the joint estimates often resulted in lower parameter uncertainties than single state parameter estimates. Joint parameter estimation methods often allowed more parameters to be estimated than equivalent

single state parameter estimation methods.

In many parameter estimation studies using concentration data, the flow field and associated flow parameters are considered known, and only the transport parameters are estimated using the concentration data. *Umari et al.* [1979] used concentration data with a linearized version of the transport equation to estimate dispersivities. No estimates of the reliabilities of these estimates were possible in their formulation. *Wagner and Gorelick* [1986] estimated all transport parameters for a one dimensional system using concentration data, and included estimates of the reliability of the parameter estimates. *Carrera and Walters* [1985] estimated the transport parameters and boundary conditions for a one dimensional tracer test.

True joint parameter estimation studies estimate both the flow and transport parameters simultaneously. *Strecker and Chu* [1986] combine a method of characteristics solute transport simulation with quadratic programming to estimate transmissivities and dispersivities for a hypothetical aquifer. Because the observations of head and concentrations had no error, they were able to accurately estimate the unknown parameters. *Wagner and Gorelick* [1987] considered optimal groundwater quality management under parameter uncertainty in which a coupled flow-mass transport model was identified. *Mishra and Parker* [1989] considered parameter estimation for coupled unsaturated flow and transport. Coupled inverse problems in general were discussed by *Sun and Yeh* [1990a], and equations and synthetic

examples for adjoint state parameter estimation were derived for both joint flow-mass transport and flow-thermal transport. *Sun and Yeh* [1990b] discussed identifiability issues for joint flow-mass transport systems. *Gailey et al.* [1992] used an analysis of data residuals to determine the relative weights for the two data sets in applying parameter estimation for joint flow-mass transport to a field problem. *Xiang et al.* [1993] developed a composite L_1 estimator to identify parameters in a joint flow-mass transport model, and showed the L_1 estimator to be more robust in handling observation data containing outliers than the more traditional L_2 estimators.

Temperature data has been used in a joint inversion scheme to improve the parameter estimates [*Woodbury and Smith*, 1988; *Wang et al.*, 1989]. Using only hydraulic head data, *Woodbury and Smith* [1988] could estimate only the ratio between recharge and hydraulic conductivity. The introduction of temperature data allowed independent estimates for recharge and hydraulic conductivity. The solution to the joint inverse problem did result in an improvement in the parameter estimates [*Wang et al.*, 1989], but temperature data is not readily available at many field sites. Use of temperature data for parameter estimation in groundwater flow systems is restricted to more permeable systems with a significant component of vertical groundwater flow. Joint geophysical-hydrological parameter estimation has also been proposed by *Copty et al.* [1993]. They first estimated the flow parameters using only head and permeability data, then included seismic velocity data through Bayesian updating. Semiempirical relationships were used to correlate the seismic velocity and

and hydraulic properties.

Less formal methods of parameter estimation using environmental tracer data have been employed. *Campana and Simpson* [1983] used ^{14}C data to determine residence times, vertical flow velocities, and average recharge rates for an aquifer using discrete state compartmental models. *Phillips et al.* [1989] used hydraulic head and ^{14}C to determine the hydraulic conductivity distribution in two confined aquifers in the San Juan Basin, New Mexico. Dispersion was not considered when determining the ^{14}C travel times. They used the estimates of hydraulic conductivity determined from isotope travel times and the hydraulic head distribution to construct a numerical model of flow in the aquifers. *Krabbenhoft et al.* [1990a,1990b] used stable isotopes to estimate the discharge rates of a kettle lake to the surrounding aquifer. They used two methods to determine the recharge rates, an isotope mass balance method and a calibrated quasi three dimensional flow and transport model. The recharge rate to a shallow unconfined aquifer system has been investigated using hydraulic head data and tritium data [*Robertson and Cherry*, 1989]. A groundwater flow model was constructed using permeameter estimates of hydraulic conductivity, and recharge rates determined from the tritium distribution. The simulated hydraulic heads using this model compared well with the field measured hydraulic heads. The dispersivity of the medium was then calculated by comparing field measured tritium distributions to a one dimensional solution to the advection-dispersion equation. These less formal methods use the idea that environmental tracers provide additional information about the flow

system, but they lack a framework in which to quantify both parameter uncertainty and the role of the environmental tracer data in reducing parameter uncertainty.

2.3 Parameter space analysis

The results of most parameter estimation methods are typically a set of parameter estimates and associated uncertainties. Analysis of the parameter space allows the modeller to visualize the results of parameter estimation, and develop a clearer understanding of the results. Parameter identifiability and uniqueness issues can be clearly visualized using parameter spaces. Most parameter space analysis consists of visualizing response surfaces (objective function surfaces) in two dimensional parameter space.

Sorooshian and Arfi [1982] used two dimensional response surfaces to study the sensitivity of model parameter estimates in rainfall-runoff models. They believed that individual parameter sensitivity, measuring the sensitivity of one parameter while holding the other parameters constant, was a poor method of determining parameter sensitivity. They introduced two indices to measure two parameter concurrent sensitivities, based on the shape and orientation of the response surface in parameter space.

The relationship between model structure and parameter observability and

uniqueness in rainfall-runoff models was investigated by *Sorooshian and Gupta* [1983]. Response surface studies were used to investigate the effects of different model structures and different objective functions. *Sorooshian and Gupta* [1985] focused on evaluating a model based on whether the parameters could be identified. They introduced some multiparameter methods for evaluating the identifiability of model parameters. Reparameterization of rainfall-runoff models was suggested in order to improve parameter identifiability.

Two dimensional parameter uncertainty regions in rainfall-runoff models were investigated by *Kuczera* [1983a]. *Kuczera* [1983b] evaluated the effects of including independent information on the parameters. This study also showed the effects of different kinds of data on parameter uncertainty, as well as the compatibility of different kinds of data.

In groundwater modeling studies, parameter space or response surface analysis is rare. *Carrera and Neuman* [1986b] showed, using response surfaces, that log-transformation of the hydraulic conductivities generally resulted in better conditioned parameter estimates. They also used two dimensional response surfaces to demonstrate an example of parameter non-uniqueness. *Toorman et al.* [1992] used parameter response surfaces to evaluate the influence of two data types on parameter estimates in unsaturated one-step outflow experiments. They evaluated the influence of outflow and matric potential data on three model parameters, and concluded that

using both data types together generally resulted in more unique solutions. Parameter uncertainty was not evaluated.

This thesis extends the use of response surfaces and parameter space analysis in several ways. First, most of the work using response surfaces described above was restricted to two dimensional parameter space, since it is easy to visualize in two dimensions. Eigenspace decomposition is used in this thesis to visualize multi-dimensional response surfaces. Second, response surfaces and parameter space analysis are used to identify those parameters which most efficiently stabilize the parameter estimates. Third, parameter space analysis is used to determine the effects of errors in prior information, and to identify those parameters which lead to the smallest errors in the parameter estimates. Finally, response surfaces are used to show how joint data sets reduce parameter uncertainty, and parameter space analysis is used to develop several different weighting criteria in joint parameter estimation.

CHAPTER 3. PHILOSOPHICAL AND NUMERICAL ISSUES IN THE INVERSE PROBLEM

This chapter covers the philosophical and computational aspects of parameter estimation used in this work. The choice of philosophy is often controlled by the objectives of the study. Once a philosophy has been chosen, it controls the methods and results of parameter estimation, as well as the interpretation of the results. The type of parameterization and type of estimation are the philosophical issues considered. Computational aspects include the numerical scheme used for the forward simulations of flow and transport and the modifications to the basic parameter estimation method.

3.1 Philosophical issues

This work is geared toward the application of parameter estimation to joint groundwater flow and mass transport models for large scale flow systems. The underlying philosophy throughout the work is to develop responsible parameter estimates with minimum uncertainty. To accomplish these goals, a parameter estimation method that allows the calculation of estimated parameter reliabilities is required. The number of parameters needs to be smaller than the number of data in order to calculate the estimated parameter reliabilities. A zonation approach to parameterization will be used, with the zonation controlled by the geology of the site.

3.1.1 Parameterization

In numerical models, the continuous spatial variation in the field parameters must be replaced by a discrete set of model parameters. Methods of accomplishing this parameterization were discussed in Chapter 2. In this thesis, zonation is used to parameterize the internal model parameters and a combination of zonation and interpolation is used to parameterize the boundary conditions. This type of parameterization is chosen because zonation allows the number of parameters to be less than the number of data, which in turn allows the reliabilities of the parameter estimates to be calculated. If the number of parameters were greater than the number of data, parameter reliabilities could not be calculated.

The major criticism of the zonation approach is that the zonation may be incorrect or unrepresentative of the true system. If the zonation does not reflect the true structure of the system, the parameter estimates for the zones may be incorrect or meaningless. The philosophy of zonation taken in this work is that the geological data can be used to define the large scale zones. Geological or hydrostratigraphic units are mapped and used as the basis for zonation. There is often a sharp contrast in parameter values between geological units. Within each of these units, the parameter values vary continuously in space. If a trend in the parameter values within each unit is hypothesized, then the geological unit is subdivided into zones to reflect the trend in the parameter value. If no trend in the parameter value is hypothesized,

then the geological unit is not subdivided. Alternative models using different parameter structures may be compared to decide if a geological unit should be subdivided into multiple zones. Hypothesis testing [*Cooley et al.,* 1986] or criteria based methods [*Carrera and Neuman*, 1986c] can be used to select the proper zonation within each unit.

3.1.2 Method of parameter estimation

Any of the three statistical philosophies for parameter estimation introduced in Chapter 2 can be used, since they all lead to similar objective functions. In this thesis, a non-linear regression approach is adopted, with a linearized approximation for the parameter reliabilities. This approach allows the calculation of parameter uncertainties and parameter confidence regions, which are used extensively in this work.

3.2 Computational aspects of non-linear regression

In order to estimate parameters, two problems must be solved; the forward problem and the inverse problem. The forward problem consists of solving equations (1.1) and (1.3) for the dependent variables, hydraulic head and tracer concentration. The inverse problem estimates the independent variables in equations (1.1) and (1.3) using measurements of head and concentration. The forward problem is solved using finite element methods. The inverse problem is solved using a modified Gauss-Newton

scheme.

Three unique aspects are introduced in this thesis for the parameter estimation process. First, the forward transport problem is solved using the Arnoldi algorithm [*Woodbury et al.,* 1990], which allows rapid calculation of tracer concentrations in simulations with many time steps. The Arnoldi algorithm is extended to permit the calculation of sensitivity coefficients through the sensitivity equation method. Second, the matrices in the Gauss-Newton method are scaled using the parameter values. This scaling is performed so that the matrices are independent of the differences in parameter values, which is helpful when evaluating parameter uncertainties. Third, the Gauss-Newton equations are solved using singular value decomposition [*Press et al.,* 1986]. The singular values and vectors are used to allow a visual interpretation of parameter uncertainty through parameter space analysis.

3.2.1 Solution to the forward problem

The finite element method was used to solve both the flow and transport models. For steady state flow, the finite element method is straightforward to implement and can be solved rapidly. For transport using the standard Crank-Nicolson time stepping scheme, numerical dispersion and stability issues constrain the size of the elements and the time step length required for accurate solutions. For large scale flow systems, a large number of time steps are required for accurate solutions.

Consequently, a large amount of computer time is required in order to accurately simulate tracer concentrations, especially in large-scale settings. The forward problem must be solved many times during the parameter estimation process. If the computer time required to simulate tracer concentrations could be reduced, it would result in a large overall saving in computer time required to obtain parameter estimates. In order to be able to use parameter estimation methods in large scale flow and transport systems, an alternate time stepping method is desirable.

One alternative method for time stepping in finite element methods is the Arnoldi algorithm [*Woodbury et al.*, 1990]. The Arnoldi algorithm replaces the global stiffness and storage matrices with much smaller matrices, and steps through time in the reduced system. The finite element solution is a linear combination of Arnoldi vectors, and a small number of Arnoldi vectors can capture the essential characteristics of the solution. The Arnoldi vectors are calculated from the finite element matrices, and combined to create the reduced system of equations. The reduced system of equations is marched through time, and a reduced solution is determined at each time step. At times of interest, the reduced solution is expanded into the full solution. The numerical formulation of the Arnoldi algorithm is outlined in section 3.2.1, and the details of the Arnoldi algorithm for the transport equation are described in *Woodbury et al.,* [1990] and *Nour-Omid et al.* [1991].

For most problems, less than 15 Arnoldi vectors are needed to capture the

essential characteristics of the solution. Once all Arnoldi vectors are calculated, the small (less than 15 x 15) system is marched through time using a Crank-Nicolson scheme. The computer time required to march this small system through time is negligible. For a small number of time steps (less than 15) the Arnoldi method is slower than the Crank-Nicolson method. However, for many time steps, the Arnoldi method can be much faster than the Crank-Nicolson method.

In theory, the computer time required for the calculation of a single Arnoldi vector should be equivalent to a single Crank-Nicolson time step. However, this equivalence is not true when iterative methods are used to solve the system of equations. For the Crank-Nicolson method, after the initial time step, the starting point for the iterative solution at each time step is close to the true solution. The iterative methods converge rapidly, generally in less than 5 iterations for reasonable time steps. When calculating the Arnoldi vectors, the starting guess for the iterative methods is far from the solution, and an average of 25-50 iterations is required for convergence, more if the system of equations is poorly-conditioned. The algorithms in this work use the ORTHOMIN conjugate gradient method (*Mendoza et al.,* 1992) to solve the systems of equations. Using ORTHOMIN, the Arnoldi method really only starts to outperform the Crank-Nicolson method when more than 50 to 100 time steps are required.

3.2.2 Solution to the inverse problem

Non-linear regression is a common method for parameter estimation. The regression technique and solution methods used in this thesis follow *Cooley and Naff* [1985] and *Hill* [1992]. A set of observations Y_i, $i = 1,n$ of the physical system are fit to a model which has the parameters B_j, $j = 1,p$. The parameters B_j are the true unknown values of the parameters. The functional relationship between the observations and the model parameters is

$$\mathbf{Y} = f(\mathbf{B}) + \varepsilon \tag{3.1}$$

where ε is a vector of random variables assumed to have a distribution of

$$\varepsilon \sim N(0, \sigma^2 \mathbf{V}) \tag{3.2}$$

where **V** is a known (n x n) positive definite variance-covariance matrix. The matrix **V** defines the relative covariances between the data, and σ^2 is a scaling term with an unknown magnitude.

The parameter estimation problem for joint data sets actually uses three types of data; hydraulic head data, mass concentration data, and prior estimates of the parameters. Equations (3.1) and (3.2) can be applied to both the both the head and concentration data, though each data set will have different functional relationships and error terms. The functional relationship f(**B**) for the head data is the steady state groundwater flow equation (1.1), while the functional relationship f(**B**) for the concentration data is the mass transport equation (1.3). For the prior information on

model parameters, the functional relationship between the observations and model parameters is

$$\mathbf{Y} = \mathbf{B} + \varepsilon \tag{3.3}$$

and ε has a distribution defined by equation (3.2). In real world problems, the use of (3,2) for the errors in the prior information is not always valid. Chapter 5 examines the consequences of biased prior information.

The non-linear regression approach minimizes an objective function S(**b**) to estimate the parameters **b**, with the resulting parameter estimates defined as $\hat{\mathbf{b}}$. For the joint parameter estimation problem using head, concentration, and prior information on parameters, the objective function is:

$$S(\boldsymbol{b}) = w_h(\boldsymbol{Y}_h - f(\boldsymbol{b}))^T \boldsymbol{V}_h^{-1} (\boldsymbol{Y}_h - f(\boldsymbol{b})) + w_c(\boldsymbol{Y}_c - f(\boldsymbol{b}))^T \boldsymbol{V}_c^{-1} (\boldsymbol{Y}_c - f(\boldsymbol{b})) + (\boldsymbol{b}_p - \boldsymbol{b})^T \boldsymbol{V}_p^{-1} (\boldsymbol{b}_p - \boldsymbol{b}) \tag{3.4}$$

where the *h* subscript denotes those terms relating to head data, the *c* subscript denotes those terms relating to concentration data, and the *p* subscript denotes those terms relating to prior information on parameters. The w_h and w_c terms are weights designed to yield a trade-off between the parts of the objective function. The design and magnitude of these weighting terms are discussed in chapter 6.

A modified Gauss-Newton method will be used to determine the parameter estimates for the objective function given in (3.4). The basic Gauss-Newton method

and various modifications are given in *Cooley and Naff* [1985]. For this work, the Gauss-Newton method is modified by scaling the approximate Hessian matrix, augmenting the Hessian matrix using Marquardt's modification [*Marquardt*, 1964], and singular value decomposition (SVD) [*Press et al.,* 1986]. This combination of modifications is used not only to reduce problems associated with ill-conditioned parameter sets, but also to allow easy analysis of the uncertainties associated with the parameter estimates.

The basic Gauss-Newton method is based on computing, at each iteration, the minimum of the second order Taylor expansion of the objective function (3.4). The resulting set of equations are:

$$\mathbf{H}\,\mathbf{d}^k = \mathbf{g} \tag{3.5}$$

where

$$\mathbf{H} = \text{approximate Hessian Matrix} = \mathbf{X}^T\,\mathbf{V}^{-1}\,\mathbf{X} \tag{3.6}$$

$$\mathbf{g} = \text{Gradient Vector} = \mathbf{X}^T\,\mathbf{V}^{-1}\,(\mathbf{Y} - \mathrm{f}(\mathbf{b})) \tag{3.7}$$

The approximate Hessian matrix (also called the least squares coefficient matrix) is a first order approximate to the true Hessian matrix. The vector $\mathbf{d}^k$ is the correction to the parameter vector at the kth iteration. The matrix $\mathbf{V}^{-1}$ is the inverse of the combined data reliability matrix. The matrix $\mathbf{X}$ is the sensitivity matrix, whose elements are $\frac{\partial\{f(b)\}_i}{\partial b_j}$, where $\{\mathrm{f(b)}\}_i$ is the ith data point and b_j is the jth parameter. Because the objective function (3.4) is non-linear with respect to the parameters, more than one iteration is required to obtain the parameter estimates. A starting guess for the

parameters is used to initiate the procedure. The approximate Hessian matrix and the gradient vector are calculated using the initial estimates of the parameter values. Equation (3.5) is solved for the parameter corrections, and an updated set of parameter estimates is calculated. These updated parameter values are then used to recalculate the approximate Hessian matrix and gradient vector, and new parameter corrections are calculated. This process is continued until the parameter values converge within a given tolerance. The final parameter values are the parameter estimates. The calculation of the uncertainties in the parameter estimates, and their relationship to the response surfaces, are discussed in Chapter 4.

3.2.2.1 Calculation of the sensitivity matrix

For the Gauss-Newton method, calculating the sensitivity matrix of partial derivatives is the most time consuming portion of the parameter estimation process. Three methods are in use [*Yeh,* 1986].

1. Influence coefficient method. Each parameter is perturbed from its original estimate by a small amount, and a complete simulation is performed with the perturbed parameter. Since the method requires perturbing the parameters one at a time, the method requires $p+1$ forward simulations to determine the sensitivity matrix.
2. Sensitivity equation method. The governing equation is differentiated and rearranged so that the partial derivatives with respect to each parameter are used as

the dependent variable. The numerical solution to the set of equations yields one column of the sensitivity matrix. Again, *p+1* simulations are needed to determine the sensitivity matrix.

3. Adjoint state method. The adjoint state equations for the original partial differential equations must be derived. The number of adjoint equations to be solved to determine the sensitivity matrix is equal to the number of observations *n*.

The influence coefficient method is the least accurate method [*Sun and Yeh*, 1990a]. The sensitivity equation method is efficient if there are more observations than parameters to be identified. The adjoint state method is more efficient if there are more parameters to be identified than observations. For this work, there are always more data than parameters, so the influence coefficient and sensitivity equation methods are the best options. Both methods are used in this work, but in general the sensitivity equation method is superior, for reasons given below.

Sensitivity equation method applied to steady state flow equation

The discretized form of the flow equation is:

$$\mathbf{A}\,\mathbf{h} = \mathbf{f} \tag{3.8}$$

A is the (*l x l*) global stiffness matrix, where *l* is the number of nodes in the finite element mesh, **h** is the (*l x 1*) vector of hydraulic head values at each node of the finite element mesh, and **f** is the (*l x 1*) forcing vector, which includes boundary

conditions and flux terms. The sensitivity formulation of the flow equation is:

$$\boldsymbol{A}\frac{\partial \boldsymbol{h}}{\partial b_j} = \frac{\partial \boldsymbol{f}}{\partial b_j} - \frac{\partial \boldsymbol{A}}{\partial b_j}\boldsymbol{h} \qquad (3.9)$$

where b_j is the *j*th parameter. The variable to be solved for is $\frac{\partial \boldsymbol{h}}{\partial b_j}$, the sensitivity vector of the head to the jth parameter. The form of the equation is identical to the original discretized flow equation, and only the right-hand side changes for each parameter. The matrix consisting of the derivative of the stiffness matrix with respect to each parameter (second term on the RHS) is very sparse. Because only a sparse matrix needs to be formed for each parameter, and only the RHS of the system of equations is altered, the sensitivity equation method is very efficient. It is much faster than the influence coefficient method for calculating the sensitivity coefficients in the steady state flow equation.

Sensitivity equation method applied to the transient transport equation

The discretized form of the transport equation is:

$$[\mathbf{A} + (1/\Delta t)\,\mathbf{M}]\,\mathbf{c}_{t+\Delta t} = [(1/\Delta t)\,\mathbf{M}]\,\mathbf{c}_t + \mathbf{f} \qquad (3.10)$$

A is the global stiffness matrix for the transport equation (different from the flow equation), **M** is the global storage matrix, Δt is the time step length, $\mathbf{c}_{t+\Delta t}$ is the vector of concentrations at the new time step, $\mathbf{c}_t$ is the vector of concentrations at the previous time step, and **f** is the forcing vector. The sensitivity formulation of the transport equation is:

$$[\boldsymbol{A}+\tfrac{1}{\Delta t}\boldsymbol{M}]\ \{\frac{\partial \boldsymbol{c}}{\partial b_j}\}_{t+\Delta t} = \frac{\boldsymbol{M}}{\Delta \boldsymbol{t}}\ \{\frac{\partial \boldsymbol{c}}{\partial b_j}\}_{t} + \frac{\partial \boldsymbol{f}}{\partial b_j} - \frac{\partial \boldsymbol{A}}{\partial b_j}\ \{\boldsymbol{c}\}_{t+\Delta t} \qquad (3.11)$$

The variable to be solved for at each time step is $\{\frac{\partial \boldsymbol{c}}{\partial b_j}\}_{t+\Delta t}$, the partial derivative of concentration with respect to the jth parameter at the current time step. From the solution to equation (3.10), the concentrations at each time step are known. The derivative of the concentration with respect to the parameter is known at the previous time step. The form of the sensitivity equation is identical to the discretized form of the transport equation, only the right hand side is different. However, unlike the flow equation, the matrix of the derivatives of the stiffness matrix with respect to the parameters (third term on RHS) is a full matrix. Any change in the flow parameters alters the entire velocity field, on which the global stiffness matrix is based. For the transport equation, the sensitivity equation approach and the influence coefficient approach are approximately equal in terms of computer time required.

Sensitivity equation method applied to the Arnoldi transport equation

Since the Arnoldi algorithm is used for time stepping in the transport equation, the sensitivity matrix equations need to be derived with respect to the Arnoldi equations. The Arnoldi algorithm reduces the discretized transient transport equation (3.10) to a reduced set of equations:

$$[\mathbf{I} + (1/\Delta t)\ \mathbf{P}]\ \mathbf{w}_{t+\Delta t} = [(1/\Delta t)\ \mathbf{P}]\ \mathbf{w}_t + \mathbf{g} \qquad (3.12)$$

where:

I = Identity matrix

$\mathbf{P} = [\mathbf{Q}^T \mathbf{M} \mathbf{A}^{-1} \mathbf{M} \mathbf{Q}]$; (*mxm*)

$\mathbf{g} = \mathbf{Q}^T \mathbf{M} \mathbf{A}^{-1} \mathbf{f}$; (*mx1*)

$\mathbf{w} = \mathbf{Q}^T \mathbf{c}$; (*mx1*)

Q = matrix of Arnoldi vectors; (*lxm*)

m = number of Arnoldi vectors

Since the sensitivity equation is of the same form as the transport equation, the sensitivity equation (3.11) can also be reduced to the Arnoldi form. For each parameter b_j, the vector $\frac{\partial \boldsymbol{f}}{\partial b_j}$ and the matrix $\frac{\partial \boldsymbol{A}}{\partial b_j}$ must be formed. The vector $\frac{\partial \boldsymbol{f}}{\partial b_j}$ can immediately be reduced into Arnoldi dimensions by pre-multiplying by ($\mathbf{Q}^T \mathbf{M} \mathbf{A}^{-1}$). However, the matrix $\frac{\partial \boldsymbol{A}}{\partial b_j}$ must be multiplied by the concentrations at each time step, and the resultant vector then reduced to Arnoldi dimensions and added to the RHS vector. This operation, performed at each time step, is inefficient. The advantage of the Arnoldi reduction is wasted.

An approximate method for calculating the sensitivity coefficients using the Arnoldi algorithm was developed. Instead of multiplying the matrix $\frac{\partial \boldsymbol{A}}{\partial b_j}$ by the concentrations and then reducing the resultant vector at every time step, the multiplication and reduction is only done a few times during the entire time stepping scheme. The resulting sensitivity coefficients are not exact. The accuracy of the sensitivity coefficients depends on the number of times the multiplication and reduction is performed. One multiplication and reduction, using only the concentrations at the

end of the simulations, was generally not adequate. The convergence rate using these sensitivity coefficients was relatively slow. Using two multiplications and reductions, the sensitivity coefficients were generally adequate. More than five multiplications and reductions resulted in good approximations to the true sensitivity coefficients for most problems in this thesis.

Near the minimum of the objective function, especially in poorly conditioned problems, the sensitivity coefficients need to be quite accurate. Though increasing the number of time steps in which the true RHS vector is calculated does increase the accuracy of the sensitivity coefficients, it is at the expense of computer time. The algorithm used in this work switches from the sensitivity coefficient formulation for the transport problem to the influence coefficient method once the convergence rate slows significantly. It was found that the influence coefficient method, combined with the Arnoldi algorithm for transport, performs well near the minimum. For groundwater flow, the sensitivity coefficient formulation is used at all iterations, since it is much more efficient than the influence coefficient method.

3.2.2.2 Modifications to the basic Gauss-Newton method

To speed convergence for unstable problems and to allow consistent analysis of parameter uncertainties, three modifications to the basic Gauss-Newton method were made. The first is the Marquardt modification, which moves the descent direction

from a Newton direction toward a steepest descent direction if a reduction in the objective function does not occur at any iteration [*Marquardt,* 1964]. The implementation of this modification is described in *Cooley and Naff* [1985]. The second modification is scaling the approximate Hessian matrix and gradient vector by the parameter values. The third modification is to use singular value decomposition (SVD) to solve the Gauss-Newton system of equations while discarding small singular values.

The approximate Hessian matrix and the gradient vector are defined in equations (3.6) and (3.7). The elements of the approximate Hessian matrix and the gradient vector are scaled by the current parameter values.

$$H_{j,k} = H_{j,k} * b_j * b_k \tag{3.13}$$

$$g_j = g_j * b_j \tag{3.14}$$

This scaling is not the usual scaling performed in modified Gauss-Newton methods. Scaling the approximate Hessian matrix by the parameter values produces a matrix that is independent of the differences in parameter values. Later in this work, the scaled Hessian matrix is used to characterize the relative uncertainties of the parameters as they relate to the parameter space. If the approximate Hessian matrix were left unscaled, the parameter space would reflect not only the relative parameter uncertainties, but the differences in parameter values as well.

The third modification is to use singular value decomposition (SVD) to solve for

the parameter corrections at each iteration. The scaled approximate Hessian matrix is decomposed by SVD into eigenvectors and eigenvalues (for a square matrix, eigenvalues are identical to singular values).

$$\mathbf{H} = \mathbf{U}^*\Lambda^*\mathbf{U}^T \tag{3.15}$$

where **U** is the matrix of eigenvectors and Λ is the diagonal matrix containing the singular values. The parameter corrections at each iteration are calculated by:

$$\Delta\mathbf{b} = \mathbf{U}\Lambda^{-1}\,\mathbf{U}^T * \mathbf{g} \tag{3.16}$$

However, before the parameter corrections are calculated, the singular values of the scaled Hessian matrix are examined. If there are one or more singular values that are much smaller than the other singular values, these small singular values are set to zero. This procedure prevents the estimation routine from searching along very flat directions of the parameter space for a minimum, and allows the routine to concentrate on the steepest directions in parameter space. For poorly conditioned problems, this procedure speeds convergence and allows a set of parameters to be estimated where ordinary methods would fail to converge. The singular values are also used to characterize the shape and orientation of the parameter confidence regions, as described in Chapter 4.

CHAPTER 4. CONCEPTS OF PARAMETER SPACE ANALYSIS

Parameter space analysis can be a valuable tool for understanding and calibrating groundwater flow and mass transport models. The parameter space contains information about the parameter estimates and their associated uncertainties, and also the shape and orientation of the confidence region. The shape and orientation of the confidence region can provide information about the interaction of the model parameters and the data. This chapter introduces the concepts needed for parameter space analysis. Parameter spaces and response surfaces are defined, and the relationship between the response surface and the parameter confidence region is formalized. The linear approximation to the parameter confidence region is examined along with its representation by eigenvectors and eigenvalues. Examples of response surfaces and confidence regions for well- and poorly-conditioned parameter sets are shown.

4.1 Parameter space

The parameter space for a model is the p-dimensional space that contains all possible combinations of parameter values, where p is the number of model parameters. Each model parameter is represented by an axis in parameter space. If no information is available about the model parameters, any point in the parameter space is equally likely as the set of parameter estimates. The process of parameter

estimation identifies the most likely region of parameter space for the estimated parameters.

In this work, the parameter spaces are scaled. Each axis in parameter space is scaled by a value representing that parameter, usually the parameter estimate. The scaling is performed so that the parameter space represents the relative uncertainties in the parameter estimates, and not just differences in parameter values. For instance, if parameter b_1 has a value of 2000, and parameter b_2 has a value of 0.001, a 10% uncertainty in b_1 will be much larger than a 10% uncertainty in b_2. The unscaled parameter space creates the impression that b_1 is much more uncertain than b_2, while the scaled parameter space shows that b_1 and b_2 have similar relative uncertainties. Scaling parameter space is equivalent to comparing parameter coefficients of variation rather than comparing parameter variances.

4.2 Response surfaces

Using non-linear regression, an objective function is minimized to obtain parameter estimates and their associated uncertainties. For a joint parameter estimation problem using both hydraulic head and mass concentration data, and including prior information on the parameters, the objective function is given by equation (3.4). Values of the objective function can be mapped into the parameter space, and these values define a *p*-dimensional surface called the response surface

(also known as the objective function surface). The global minimum in this response surface defines the set of the parameter estimates.

A response surface can be constructed for a model when the following conditions have been met. First, a groundwater model needs to be defined and constructed. The location and type of boundary conditions, initial conditions, and distributed parameters need to be defined and a numerical model constructed. Second, calibration data and/or hydrogeological data need to be collected and available for parameter estimation. The process of parameter estimation simply searches the response surface for a minimum.

A unique response surface exists for each data value used to calibrate the model. The shape and orientation of the response surface can indicate what information the data has about the model parameters. The surfaces for each data value are superimposed to obtain the total response surface. The response surface for each data value, or each group of data values, can be analyzed. It is easy to discover whether data values contain similar or different information about the model parameters.

When only two model parameters are estimated, maps of the response surfaces can be constructed as follows. A two dimensional grid is defined, with one parameter represented by each axis. A lower and upper bound for each parameter

value and a step size for each parameter is selected. At each point on the grid (each combination of parameter values b_1 and b_2), a forward simulation is run, and the simulated values for the hydraulic heads and tracer concentrations are calculated. These simulated data values and the parameter values are substituted into equation (3.4), and a value for the objective function is calculated. The response surface can be visualized by contouring the values of the objective function throughout the grid area.

When more than two model parameters are estimated, it is more difficult to construct response surfaces. The process of constructing response surfaces with more than two parameters makes heavy demand on computer time, since the number of forward simulations needed increases as x^p, where p is the number of parameters. It is also very difficult to visualize the response surfaces in parameter spaces greater than two dimensions. We will present response surfaces for two parameter dimensions only, and use other techniques to visualize response surfaces for more than two parameter dimensions.

Using response surfaces, the estimated parameter values and associated uncertainties are easy to visualize. The Gauss-Newton method described in Chapter 3 allows both the minimum in the response surface and the shape of the response surface to be approximated without calculating the entire response surface. The matrices involved in the Gauss-Newton method can also be used to visualize

response surfaces for multi-parameter estimation problems.

4.3 Relationship between response surfaces and confidence regions

Contours of the response surface represent boundaries of the confidence region for the parameter estimates [*Ratowsky,* 1984]. Under the likelihood ratio method, and the assumptions that the uncertainties in the data are normally distributed, known and included in $\mathbf{V}_h$, $\mathbf{V}_c$, and $\mathbf{V}_p$, and that model error is negligible, an approximate (1-α)100% confidence region for the parameter set $\hat{\mathbf{b}}$ is given by:

$$\frac{S(\boldsymbol{b})-S(\hat{\boldsymbol{b}})}{\sigma^2} \leq \chi^2_{\alpha}(p) \tag{4.1}$$

where S(**b**) is the value of the objective function using the parameter set **b**, defined by equation (3.4), S($\hat{\mathbf{b}}$) is the value of the objective function at the estimated parameter set $\hat{\mathbf{b}}$, and $\chi^2(p)$ is a chi-square distribution with p degrees of freedom. The σ^2 term is often unknown, and can be estimated from the model. The estimate of σ^2 is s^2, defined as:

$$s^2 = \frac{S(\hat{\boldsymbol{b}})}{(n-p)} \tag{4.2}$$

where *n* is the number of data and *p* is the number of parameters. An approximate (1-α)100% confidence region for the parameter set $\hat{\mathbf{b}}$ is given by:

$$\frac{S(\boldsymbol{b})-S(\hat{\boldsymbol{b}})}{s^2} \leq pF_{\alpha}(p,n-p) \qquad (4.3)$$

where $F(p,n-p)$ is an F distribution with p and $(n-p)$ degrees of freedom. For large n, s^2 approaches σ^2 and $pF_{\alpha}(p,n-p)$ approaches $\chi^2(p)$, so the two confidence regions are equivalent.

Figure 4.1 illustrates a response surface and confidence regions for a two parameter system. The response surfaces are presented as $(S(\mathbf{b})-S(\hat{\mathbf{b}}))/s^2$ so that the confidence regions can be visualized. The parameter axes b_1 and b_2 are scaled by their estimated values, so the point in parameter space at $b_1=1.0$, $b_2=1.0$ represents the parameter estimates. Both univariate and joint confidence regions can be calculated from this response surface. A univariate confidence interval is the confidence interval for one parameter at a time, assuming the values of the other parameters remain fixed. For large n, the univariate confidence interval can be obtained from the $\chi^2(1)$ distribution. At a 68.6% confidence level (one standard deviation), $\alpha=.314$, and $\chi^2_{.314}(1)=1.0$, so the univariate confidence intervals are calculated from the 1.0 contour. The joint confidence region is the confidence region for both parameters, where both can vary simultaneously. For a two parameter system, the joint confidence region is obtained from the $\chi^2(2)$ distribution. At a 68.6% confidence level, $\chi^2_{.314}(2)=2.3$, so the joint confidence region is based on the 2.3 contour. Both the univariate and joint confidence regions are shown in Figure 4.1.

4.4 Linearized confidence regions

The confidence region defined by the response surface reflects the true non-linearity of model parameters. It is often convenient to work with a linearized approximation to this non-linear confidence region. The linearized confidence region can be calculated from the matrices involved in the Gauss-Newton parameter estimation scheme. The linearized confidence region is defined as

$$(\boldsymbol{b}-\hat{\boldsymbol{b}})^T\, \hat{\boldsymbol{X}}^T \boldsymbol{V}^{-1}\, \hat{\boldsymbol{X}}\, (\boldsymbol{b}-\hat{\boldsymbol{b}}) \leq ps^2 F_\alpha(p,n-p) \qquad (4.4)$$

where $\hat{\mathbf{X}}$ is the sensitivity matrix evaluated at the parameter estimates [*Ratowsky,* 1984]. The boundary of (4.4) forms an ellipsoid in parameter space centered on $\hat{\mathbf{b}}$.

This ellipsoid in *p*-dimensional space is often hard to visualize. It is more convenient to calculate the major axes of this ellipsoid. The length and orientation of these axes can be calculated from either the sensitivity matrix, the approximate Hessian matrix, or the variance-covariance matrix evaluated at the final parameter estimates. For this work, these axes are calculated from the approximate Hessian matrix because it is readily available in scaled form, and can be manipulated by adding and subtracting data without changing dimension. The scaled Hessian matrix is decomposed by SVD into singular values and associated vectors (equivalent to eigenvalues and eigenvectors for a square matrix). The square root of the inverse of the eigenvalues are the lengths (L) of the axes of the ellipsoid. The associated eigenvectors are unit vectors (**U**) defining the orientation of the axes of the ellipsoid

with respect to the parameter axes.

The boundary of the ellipsoid is calculated to coincide with the 1.0 contour of the response surface. The projection of the ellipsoid onto each parameter axis defines the univariate confidence intervals for the estimated parameters at one standard deviation. Since the parameter space is scaled by the estimated parameter values, the univariate confidence intervals are for the coefficient of variation of the estimated parameters.

For the response surface shown in Figure 4.1, a linearized confidence region can be calculated from the scaled approximate Hessian matrix. The SVD decomposition of the scaled approximate Hessian matrix yields eigenvectors and eigenvalues, which can be converted into lengths and orientation of the axes associated with the linearized confidence ellipse. Table 4.1 summarizes the lengths and orientation of the axes of the confidence ellipse.

Table 4.1 Axes of confidence ellipsoid

Lengths of Axes	L_1 = .008	L_2 = .024
Unit Vectors	$\mathbf{U_1}$	$\mathbf{U_2}$
b_1 axis	.98	.16
b_2 axis	.16	-.98

Constructing the ellipse from the information contained in Table 4.1 is straightforward. The ellipse has two axes, a short axis with a length L_1 = .008, and a long axis with a length L_2 = .024. The unit vector $\mathbf{U}_1$ defines the orientation of the short axis with respect to the parameter axes b_1 and b_2. The unit vector $\mathbf{U}_1$ has a projection of 0.98 in the direction of parameter axis b_1, and a projection of 0.16 in the direction of parameter axis b_2. To plot the short axis, the total projection in each parameter axis direction is required. The total projection is the product of the axis length and the unit vector in the direction of each parameter axis. The total projection of the short axis in the b_1 axis direction is (0.008) * (0.98) = 0.0078. The total projection of the short axis in the b_2 axis direction is (0.008) * (0.16) = 0.0013. The construction of the short axis using these total projections is shown in Figure 4.2. For the long axis, the construction is similar. The total projection of the long axis in the b_1 axis direction is (0.024) * (0.16) = 0.0034. The projection of the long axis in the b_2 axis direction is (0.024) * (0.98) = 0.023. These total projections are used to construct the long axis of the confidence ellipse, as shown in Figure 4.2. This confidence ellipse coincides with the 1.0 contour of the confidence region.

The ratio of the lengths of the longest axis of the confidence region to the shortest axis of the confidence region is termed the condition number (CN) for the parameter estimates [*Sorooshian and Gupta,* 1985]. The CN is a measure of the stability of the parameter estimates, with smaller CNs indicating more stable parameter estimates. For this parameter set, the CN = 3.0.

4.5 Examples of response surfaces

Response surfaces are very useful in understanding and diagnosing problems associated with ill-conditioned parameters. The axes of the confidence regions can yield similar information. Figure 4.1 and 4.3 are examples of two parameter response surfaces. Figure 4.1 is a response surface for a well-conditioned parameter set, while Figure 4.3 shows a more poorly-conditioned parameter set.

For the well-conditioned set of parameters (Figure 4.1), the response surface has a well-defined minimum. The joint parameter confidence region enclosed by the 2.3 contour is relatively small. The condition number, CN = 3.0, is relatively small. The response surface for the poorly-conditioned parameter set (Figure 4.3) contains a valley with a very flat bottom. The minimum of the response surface lies somewhere along this valley. For poorly-conditioned problems, this flat-bottomed valley is the cause of small errors in data values leading to large errors in estimated parameter values. Small errors in the data values can move the minimum in the response surface to anywhere along the bottom of the valley, covering a wide range of parameter estimates. The joint confidence region for the parameter estimates enclosed by the 2.3 contour is relatively large. The condition number for this parameter set is large (CN = 17), showing that one axis of the confidence region is much longer than the other.

When more than two parameters are estimated, it is difficult to visualize response surfaces. The axes of the confidence ellipsoid are used to understand the shape and orientation of the response surface. The CN can give an indication of the conditioning of the parameter set. As the parameter dimension increases, the CN will increase, so no absolute scale can be assigned to the magnitude of the CN. A closer inspection of the parameter axes will give more detailed information. For instance, if all the axes of the confidence region are of similar length, then the parameter set is generally well-conditioned, and the CN will be small. If one axis of the confidence region is much longer than the other axes, a flat-bottomed valley exists in the p-dimensional response surface. If two axes of the confidence region are much longer than the other axes, a plane in p-dimensional space has values of the response surface near the minimum. The last two examples both represent poorly conditioned parameter sets.

The orientation of the confidence ellipsoid relative to the parameter axes is also important. The orientation of the confidence region will determine how an error in the estimate of one of the parameters translates into errors in the other parameters. This concept is discussed in Chapter 5. The orientation of the confidence ellipsoid is also important when using joint data sets, as the difference in orientations of the confidence regions for the two data sets will determine the reduction in parameter uncertainty for the joint estimates. These concepts are discussed in Chapter 6.

4.6 Relative contribution to the coefficient of variation

To better understand the confidence region, it is helpful to know the contribution from each axis of the confidence ellipsoid to the coefficient of variation of the parameter estimates. The total coefficient of variation for each parameter, CV_i, is the square root of the element (i,i) of the inverse scaled approximate Hessian matrix. CV_i can also be calculated from the axes of the confidence ellipsoid as

$$CV_i = \sqrt{\sum_{j=1,p} (U_{i,j}L_j)^2} \tag{4.5}$$

Conceptually, the squared projection of all axes of the confidence region *j* in the direction of the parameter *i* are summed. The total coefficient of variation is the square root of this sum. Figure 4.4 is the confidence ellipse for the response surface of Figure 4.1. The axes of the confidence region and the contribution of each axis to the total coefficient of variation of parameter b_1 are labeled. The relative contribution to the total coefficient of variation of each parameter *i* from each parameter axis *j* is

$$RC_{i,j} = \frac{(U_{i,j}L_i)^2}{CV_i^2} \tag{4.6}$$

The relative contribution ($RC_{i,j}$) has values ranging from zero to one. If a relative contribution $RC_{i,j}$ is near zero, then ellipsoid axis *j* has a very small contribution to the total coefficient of variation of parameter *i*. If a relative contribution $RC_{i,j}$ is near one, then ellipsoid axis *j* has a very large contribution to the total coefficient of variation of parameter *i*. The relative contributions for the axes of the confidence ellipse in Table

4.1 are shown in Table 4.2.

Table 4.2 Relative contribution to total CV from each axis of the confidence region

	Axis 1	Axis 2
Parameter b_1	.81	.19
Parameter b_2	.01	.99

4.7 Summary

This chapter introduced the concepts needed for parameter space analysis. Response surfaces are a picture of the objective function in parameter space. Both univariate and joint confidence region for the parameter estimates can be determined from the response surface. A linearized approximation to the confidence region may be calculated from the approximate Hessian matrix, and SVD used to calculate the axes of the confidence ellipsoid. The total coefficient of variation and the relative contribution to the coefficient of variation from each axis of the joint confidence ellipsoid can be determined. Examples have been presented for well- and poorly-conditioned parameter sets.

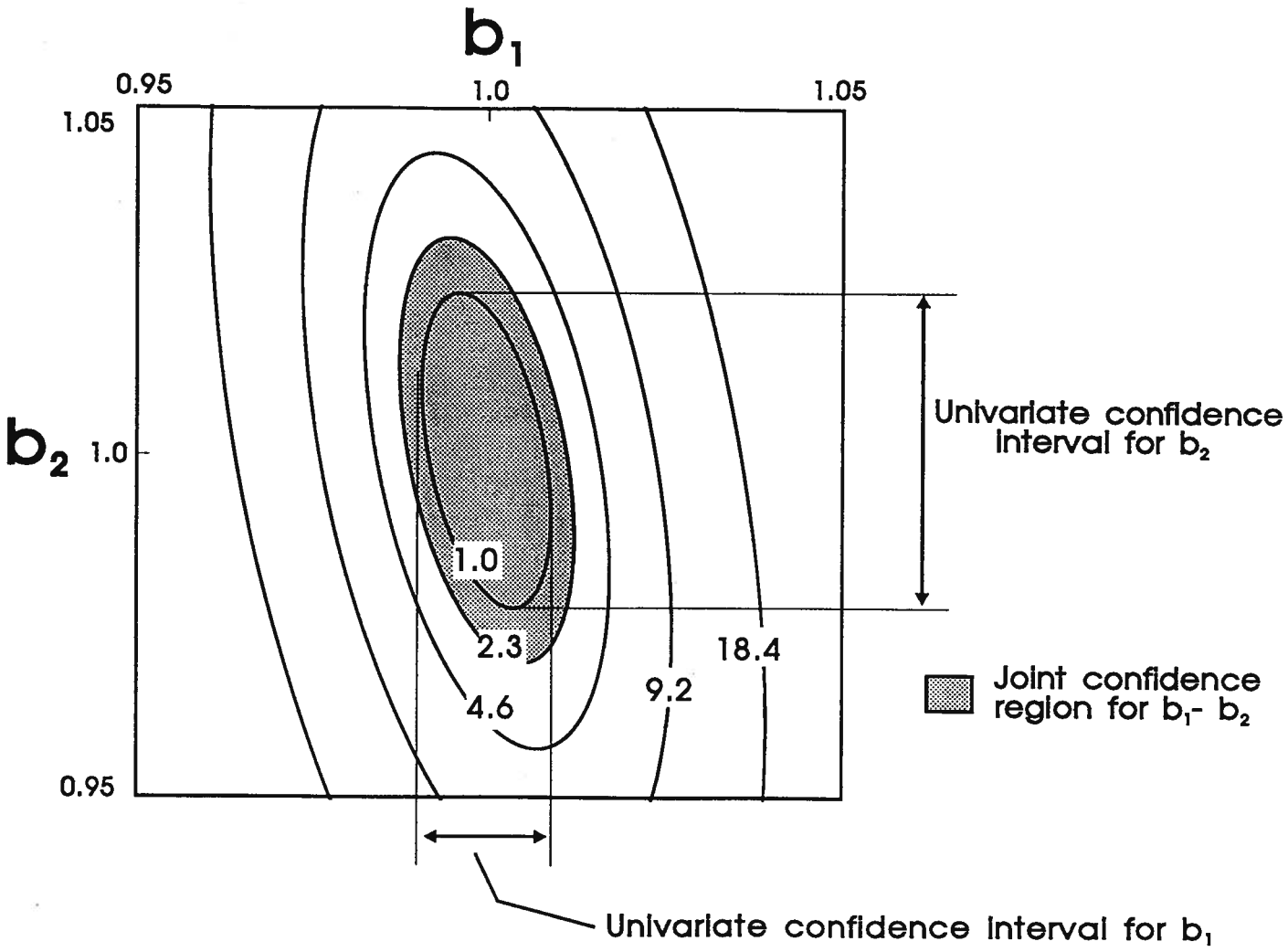

Figure 4.1 Response surface, univariate confidence intervals and joint confidence region for parameters b_1 and b_2

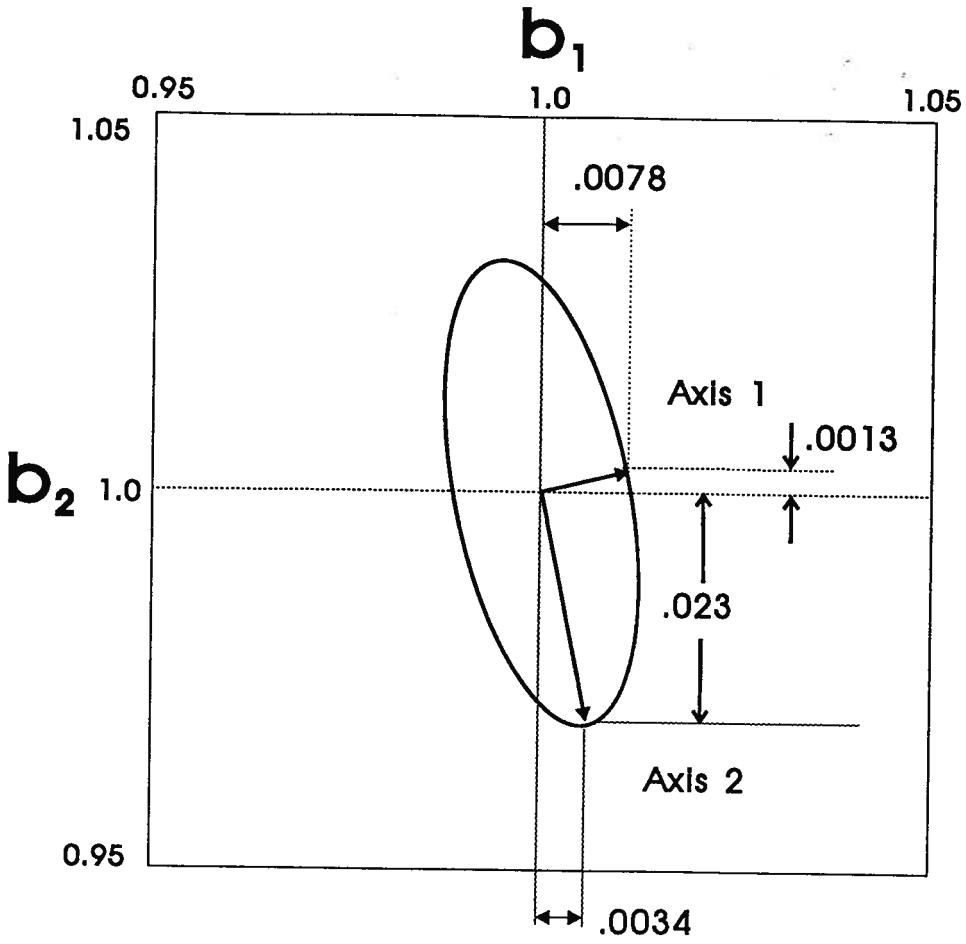

Figure 4.2 Construction of the axes of the confidence ellipse from the axis lengths and unit vectors

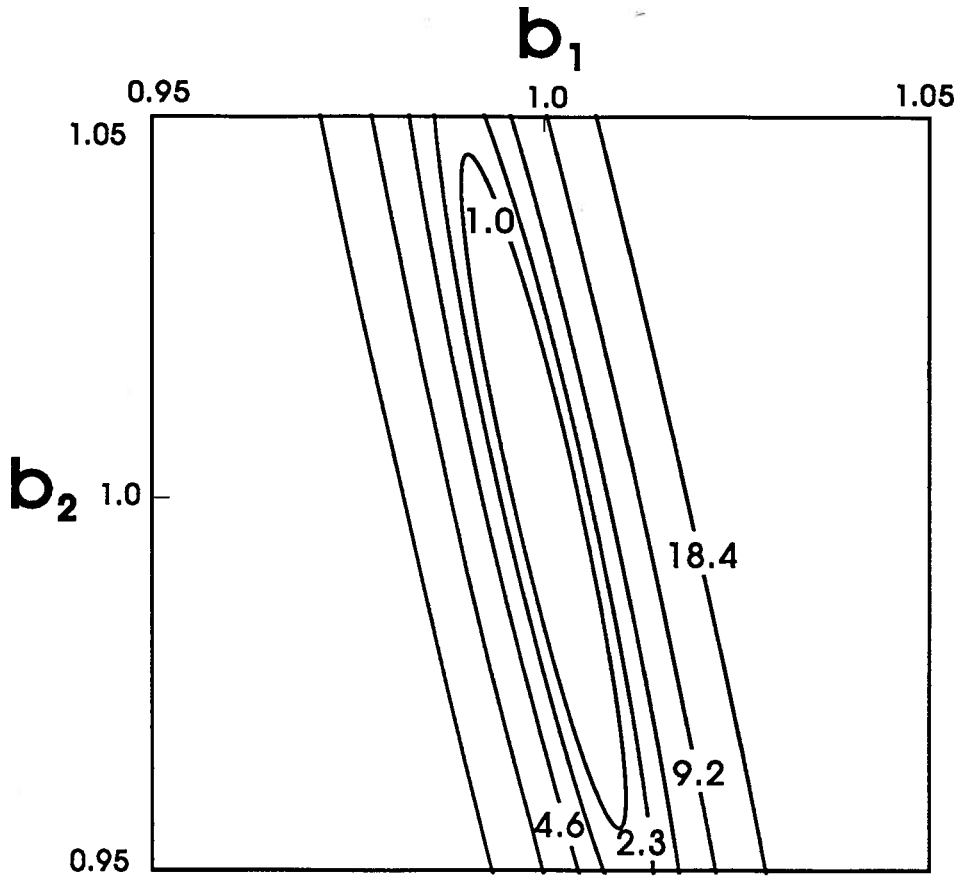

Figure 4.3 Example of a response surface for a poorly-conditioned parameter set.

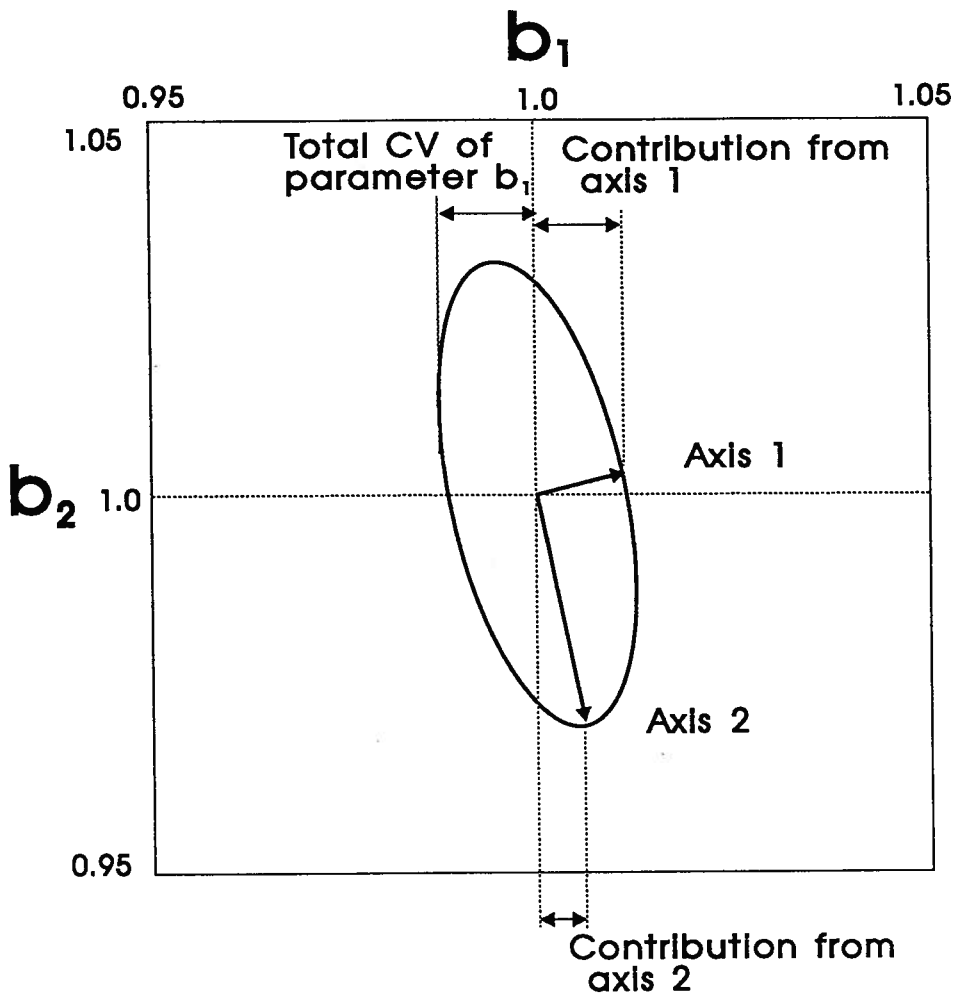

Figure 4.4 Axes of confidence region showing partial coefficient of variation from each axis of the confidence region.

CHAPTER 5. PARAMETER SPACE ANALYSIS FOR EFFICIENT AND RESPONSIBLE USE OF PRIOR INFORMATION

Parameter space analysis can be used to develop guidelines for efficiently and responsibly stabilizing the inverse problem using prior information. When a flow model is constructed, all parameters associated with the model need to be defined, both the internal model parameters such as hydraulic conductivity and recharge, and the boundary values such as specified head and specified flux. If all model parameters are estimated using only hydraulic head data, the inverse problem will be non-identifiable. This non-identifiability can be observed in the response surface for the parameter set. The response surface will contain a perfectly flat-bottomed valley cutting across the entire parameter space.

To change this non-identifiable inverse problem into an identifiable problem, prior information is needed. This prior information can take one of two forms: (1) a specified value for a given parameter, assuming no uncertainty in the specified value, or (2) a prior value with some uncertainty. Specifying a parameter value with no uncertainty is equivalent to eliminating a dimension in parameter space. Prior information with uncertainty alters the topology of the response surface in the full parameter space. These two uses of prior information are treated separately in this chapter because they act differently in parameter estimation problems and produce different results in parameter space. In this work, prior information without uncertainty

is referred to as specifying a parameter value. Prior information with uncertainty is termed prior information.

In many cases, when either of the above approaches is used to eliminate the non-identifiability of the parameter set, the parameter set remains unstable. This instability can be observed in the response surface for the parameter set. The response surface will contain a valley with a nearly flat bottom. The unstable parameter set is identifiable, since a unique minimum does exist, but it is very difficult to find this minimum. The response surfaces for non-identifiable and unstable parameter sets are very similar. The same remedies used to correct problems with non-identifiable parameter sets can be used to correct problems with unstable parameter sets.

When prior information is used to stabilize a set of parameter estimates, it must be recognized that the prior information may be in error with respect to the model. As discussed in Chapter 2, the prior information may be biased. If errors in the prior estimates are present, the final parameter estimates for all parameters may be influenced by the erroneous prior information. The influence of errors in the prior information on the parameter estimates can be determined using response surfaces and parameter space analysis.

In this chapter, guidelines will be developed to ensure the most efficient and

responsible use of prior information. Those parameters for which prior information will reduce the overall uncertainty in the parameter estimates the most and produce the most stable parameter set will be the most efficient parameters. Responsible use of prior information involves identifying how errors in the prior information will influence the final parameter estimates. Those parameters for which errors in the prior information will have the least influence on the final parameter estimates will be the most responsible parameters. Both the most efficient and most responsible parameters can be identified through an examination of the model parameter space and response surfaces.

This chapter is organized as follows. First, a synthetic flow model is introduced. The parameter space of this synthetic model is used to illustrate the concepts developed in this chapter. The effect of specifying parameter values is explored using a two parameter subset of the synthetic model. The effect of prior information is explored using the same two parameter subset. Guidelines for identifying those parameters for which prior information is most efficient are developed. Next, the consequences of error in the prior parameter values is explored using a three parameter subset of the synthetic model. Guidelines for identifying those parameters which result in the most responsible parameter estimates are developed. Finally, the concepts and methods developed using the simple two and three parameter systems are demonstrated on a more complicated multi-parameter system.

5.1 Synthetic model

A simple synthetic flow model is used to illustrate the concepts developed in this chapter. A two-dimensional flow system is constructed. The flow system is 6 km by 6 km, and contains two transmissivity zones, one zone of enhanced areal recharge, and two constant head boundary zones (Figure 5.1). The remaining model boundaries are no-flow boundaries. The flow system is at steady state. Fifteen observation points are used. Observed values of the hydraulic head are simulated by running a forward simulation using the true parameter values, and calculating the data values at the sampling locations. Random Gaussian errors with an uncertainty of 1 meter are added to these data values to generate the observed data values. These observed data values are used to estimate the parameters.

There are five parameters in the flow system: the two transmissivity zones (T_1 and T_2); one recharge zone (R); and two specified head zones (H_1 and H_2). During parameter estimation, the transmissivity parameters are log-transformed, and the other parameters are untransformed. For ease of presenting response surfaces, generally only two parameters will be estimated at one time. The other three parameters are fixed at their true values. In the following sections, the effects of including prior information are examined using the parameter space for parameters T_1 and R. This parameter space is examined using both the response surface and the axes of the confidence region.

5.1.1 Parameter space T_1-R

Figure 5.2 illustrates the response surface for the parameters T_1 and R. The response surface is plotted as $[S(\mathbf{b})-S(\hat{\mathbf{b}})]/s^2$, so the contours represent the height of the response surface above the minimum. Since the parameter space is scaled by the parameter estimates, the parameter estimates are at the point $T_1 = 1.0$, $R = 1.0$ in parameter space. The response surface contains a long, narrow valley. The axis of this valley is oriented such that is makes a much smaller angle with respect to the R parameter axis than the T_1 parameter axis.

The confidence ellipse is a linearized picture of the response surface, with the boundary of the ellipse corresponding to the 1.0 contour of the response surface. This ellipse can be characterized by its major axes, calculated from SVD decomposition of the scaled Hessian matrix at the parameter estimates. Table 5.1 gives the axes of the confidence ellipse for this parameter set. L_1 and L_2 are the lengths of the two axes, and $\mathbf{U}_1$ and $\mathbf{U}_2$ are the unit vectors showing the orientation of the axes. The condition number for this parameter set is 16.8, indicating that axis 2 is approximately 17 times longer than axis 1.

Both the response surface and the axes of the confidence ellipse indicate that along the direction of axis 2 the response surface is relatively flat. The parameter set T_1-R is relatively unstable. Using equations (4.5) and (4.6), the relative contributions

Table 5.1 Axes of confidence ellipse for T_1-R parameter set

Lengths of Axes	L_1 = .0077	L_2 = .129
Orientation of Axes	U_1	U_2
T_1 axis	-.94	-.32
R axis	.32	.94

to the parameter coefficient of variation from each axis of the confidence region can be calculated (Table 5.2). Axis 2 is the major contributor to the uncertainty to both parameters. If the length of axis 2 could be reduced, then the uncertainty in both parameter estimates would be decreased.

Table 5.2 Relative contributions to the parameter CV from each axis of the confidence region for parameter set T_1-R

	Axis 1	Axis 2
Parameter T_1	.029	.971
Parameter R	.001	.999

5.2 Efficient use of prior information

In order to stabilize this parameter set, prior information can be used. The prior information may either be prior information without uncertainty (equivalent to specifying a parameter value), or prior information with uncertainty. First, consider specifying a parameter value, which results in removing a parameter dimension from parameter

space. The response surface for this reduced parameter set can be visualized by taking a cross section through the two-dimensional response surface (Figure 5.2) perpendicular to the specified parameter axis, intersecting that axis at a point corresponding to the specified value. The intersection of this cross section with the 1.0 contour is the univariate confidence interval at one standard deviation. If parameter R is specified at a scaled value of 1.0 and parameter T_1 estimated, the 68% confidence interval for T_1 is approximately $0.99<T_1<1.01$. If parameter T_1 is specified at a scaled value of 1.0 and parameter R is estimated, then the confidence interval for R is approximately $0.97<R<1.03$. Specifying R results in a smaller confidence interval than specifying T_1. For the purpose of reducing parameter uncertainty, it is more efficient to specify R than to specify T_1. This simple example demonstrates that is it most efficient to specify the parameter whose axis is most closely aligned with the valley in the response surface.

When one parameter is specified, and thereby removed from the inverse problem, that parameter is assigned a single value with no uncertainty. However, the parameter whose axis is most closely aligned with the valley in the response surface is often the one with the most uncertainty associated with it. The above analysis suggests that using prior information on this parameter will most efficiently stabilize the remaining parameter estimates. This can be puzzling; the parameter with the most uncertainty is replaced with a parameter with no uncertainty. It is the structure of the response surface which makes this demand - based on the data available, the

response surface contains the least information about this parameter. If this parameter, about which the response surface space contains very little information, does not need to be estimated, the other parameters can be estimated more precisely. However, there is an obvious danger in specifying a value of a parameter. If the value of the specified parameter is in error, the estimate of the remaining parameter will also be in error, and this error will not be accounted for in the calculation of the confidence region. This issue is discussed in section 5.4.

Prior information with uncertainty can also be used to stabilize the parameter set. Figure 5.3 illustrates the response surface for prior information on parameter R only, where the scaled prior value equals 1.0 with an uncertainty of 2%. The total response surface for head and prior information is shown in Figure 5.4. The size of the confidence region is reduced, and the parameter set is more stable than using head data only. To demonstrate the efficiency of prior information on different parameters, the lengths of the longest axis of the confidence region after including prior information can be compared. The length of the longest axis of the confidence region using only head data was 0.129 (from Table 5.1). For head and prior information on T_1, the length of the longest axis is 0.068. For head and prior information on R, the length of the longest axis is 0.031. Prior information on R is most efficient, since it reduces the length of the longest axis of the confidence region the most with a given quality of prior information.

These graphical approaches using response surfaces can be formalized using the axes of the confidence region. Prior information on the parameter with the largest element of the longest axis of the confidence region will reduce the uncertainty of the remaining parameter estimates most efficiently. The parameter with the largest element of the longest axis of the confidence region is the parameter whose axis is most closely aligned with the longest axis of the confidence region. From Table 5.1, axis 2 is the longest axis, and parameter R has the largest element of that axis (0.94). Prior information is most efficient for those parameters with the largest elements of the longest axis of the confidence region.

5.3 Effect of errors in prior information

Using prior information is an effective way to stabilize an unstable or non-identifiabe inverse problem. However, if errors exist in the prior information, these errors will influence the estimates of the remaining parameters. Prior information without uncertainty is used to illustrate the consequences of errors in prior information and develop the methods of minimizing the consequences of these errors. These methods are then extended to using prior information with uncertainty.

Based on examining a number of cases, it is apparent that in some cases an error in the specified value of a model parameter leads to very large errors in the estimated parameter values of the other model parameters. In other cases, an error

in the specified value of a model parameter value leads to relatively small errors in the estimated parameter values of the other model parameters. The ratio of a scaled error in an estimated parameter value to a scaled error in a specified parameter value is termed the error ratio. This section examines the causes of the error ratio, and the reason for different error ratios for different model parameters. The underlying factor that determines the magnitude of the error ratio is shown to be the orientation of the confidence region in parameter space, which leads to a method of approximating the error ratios.

5.3.1 Consequences of errors in prior estimates

To illustrate the consequences of error in prior estimates, the flow system introduced above is used, and parameters T_1 and T_2 are estimated using hydraulic head data. The data has an uncertainty with a standard deviation of 1 meter. In this system, there are three other parameters that have been assigned specified values. These are the inflow head boundary, the outflow head boundary, and the recharge zone. When the parameters T_1 and T_2 are estimated using only the head data, and the true values of the other parameters are used, the true values of parameters T_1 and T_2 are estimated. Figure 5.5 is the response surface for the parameter set T_1-T_2 using only head data, with the confidence region due to uncertainty in the head data.

If an error exists in the specified value of one of the other parameters, the

estimates of parameters T_1 and T_2 will not be equal to their true values. Table 5.3 illustrates the consequences of an error in the inflow head boundary (H) and Table 5.4 illustrates the consequences of an error in the recharge (R) parameter. For the parameter H, relatively small errors in the specified value lead to large errors in the estimate of parameter T_2. The error ratio is calculated as a ratio of the percentage error in the estimated parameter to a percentage error in the specified value.The error ratios for parameter T_2 are much larger than one. The errors in the estimate of T_1 are approximately of the same magnitude as the errors in the specified head value, with the error ratios of approximately one. When specifying R, errors in the specified value lead to much smaller errors in the estimate of both T_1 and T_2. The error ratios for specifying R are much smaller than one.

Table 5.3 Consequences of error in specified head boundary value

Value of H	% Error in H	Estimate of T_1	% Error in T_1	Error Ratio	Estimate of T_2	% Error in T_2	Error Ratio
200.00	0.00	1.290	0.00	0.00	2.231	0.00	0.00
201.00	0.50	1.294	0.31	0.62	2.308	3.45	6.90
205.00	2.50	1.314	1.86	0.74	2.884	29.27	11.71
210.00	5.00	1.360	5.43	1.09	6.701	200.36	40.07
199.00	-0.50	1.282	-0.62	1.24	2.163	-3.05	6.10
195.00	-2.50	1.262	-2.17	0.87	1.958	-12.24	4.89
190.00	-5.00	1.241	-3.80	0.76	1.779	-20.26	4.05
180.00	-10.00	1.212	-6.34	0.63	1.531	-33.67	3.37
150.00	-25.00	1.124	-12.87	0.51	1.100	-50.69	2.03

Table 5.4 Consequences of error in specified value of recharge

Value of R	%Error in R	Estimate of T_1	% Error in T_1	Error Ratio	Estimate of T_2	% Error in T_2	Error Ratio
0.00040	0.00	1.290	0.00	0.00	2.231	0.00	0.00
0.00041	2.50	1.299	0.70	0.28	2.242	0.49	0.20
0.00042	5.00	1.310	1.55	0.31	2.250	0.85	0.17
0.00044	10.00	1.330	3.10	0.31	2.273	1.88	0.19
0.00045	12.50	1.340	3.88	0.31	2.283	2.33	0.19
0.00050	25.00	1.386	7.44	0.30	2.329	4.39	0.18
0.00060	50.00	1.465	13.57	0.27	2.408	7.93	0.16
0.00080	100.00	1.590	23.26	0.23	2.534	13.58	0.14
0.00039	-2.50	1.279	-0.85	0.34	2.220	-0.49	0.20
0.00038	-5.00	1.270	-1.55	0.31	2.211	-0.90	0.18
0.00036	-10.00	1.245	-3.49	0.35	2.188	-1.93	0.19
0.00035	-12.50	1.230	-4.65	0.37	2.173	-2.60	0.21
0.00030	-25.00	1.173	-9.07	0.36	2.104	-5.70	0.23
0.00020	-50.00	0.989	-23.33	0.47	1.930	-13.49	0.27
0.00010	-75.00	0.688	-46.67	0.62	1.628	-27.03	0.36

The effect of errors in the specified parameter values is summarized graphically in Figure 5.6. The parameter estimates produced when errors are present in the specified parameter values are plotted in the scaled parameter space T_1-T_2. For errors in H, the parameter estimates plot along a slightly curved line in parameter space. The errors are much larger if H is overestimated than if H is underestimated, and even a 5% overestimate in H produced parameter estimates which plotted outside of the

diagram. For errors in R, the parameter estimates plot along a relatively straight line in parameter space, and the error ratios are nearly constant. The orientation of the line in parameter space reflecting errors in R is different from the orientation of the line reflecting errors in H.

For this synthetic example, several observations can be made about the consequences of errors in specified parameter values on parameter estimates.

1. Errors in the values of specified parameters lead to errors in estimated parameter values.
2. The estimated parameter values produced when errors are present in the specified parameter values plot in relatively straight or slightly curved lines in parameter space.
3. The orientation of the line in parameter space connecting the estimated parameter values produced when errors are present in specified parameter values bears no relation to the orientation of the parameter confidence region.
4. Errors in the specified value of recharge lead to much smaller error ratios for the parameters T_1 and T_2 than errors in the specified value along the inflow head boundary.
5. The orientation of the line in parameter space based on errors in R is different from the orientation of the line based on errors in H.

5.3.2 Conceptual relationship between confidence region and error ratio

In order to predict the consequences of errors in prior information, the confidence region for both the estimated parameters and the parameters with prior information must be examined. For example, the confidence region for T_1, T_2, and H must be examined to determine the consequences of errors in H on the estimates of T_1 and T_2. A three dimensional parameter space is required. It is possible to use the axes of the linearized confidence ellipsoid to represent the three dimensional confidence region.

The confidence region for the parameters T_1, T_2, and H is examined first. SVD decomposition of the scaled Hessian matrix using the true parameter values is used to calculate the principal axes of the confidence region (Table 5.5). Axis 3 is the longest axis, about five times as long as axis 2 and 50 times as long as axis 1, and $\mathbf{U}_3$ gives the orientation of the unit vector associated with the longest axis. Figure 5.7 shows the orientation of the longest axis of the ellipsoid in the three dimensional parameter space, with the shaded box included to show the orientation of the axis.

The longest axis of the parameter confidence ellipsoid represents the trace of the smallest value of the response surface in three dimensional space. If all three parameters are considered, then the overall minimum of the response surface is at the center of the ellipsoid. To determine the parameter estimates and confidence

Table 5.5 Axes of confidence region for T_1-T_2-H parameter set

Axis Lengths	0.005	0.020	0.100
Unit Vectors	U_1	U_2	U_3
T_1	-0.17	0.98	-0.06
T_2	-0.10	-0.07	-0.99
H	0.98	0.17	-0.11

region for T_1 and T_2 at any value of H, a slice parallel to the T_1-T_2 plane is taken, intersecting the H axis at the specified value of H. The point where the minimum in the response surface intersects this slice is approximately the parameter estimates for T_1 and T_2. This minimum in the response surface is closely related to the point where the longest axis of the confidence ellipsoid intersects the slice.

In this example, the confidence ellipsoid is oriented in such a way that the angle between its longest axis and the parameter axis T_2 is relatively small (see Figure 5.7). The angles between the longest axis of the parameter confidence ellipsoid and the other two parameter axes are relatively large. If the value of H is equal to the true value, then the estimates for T_1 and T_2 will be the equal to their true values as well. If the specified value of H is larger than the true value, the parameter estimate for T_2 changes significantly. Since the longest axis is aligned closely with the orientation of the T_2 axis, small errors in the specified value of H result in large errors in the value of T_2. However, errors in the specified value of H are approximately equal to the errors in the estimated values of T_1. Comparing Figure 5.7 to Figure 5.6, the

line of parameter estimates at different errors in H is approximately the trace of the longest axis of the parameter confidence region in three dimensional space projected onto the T_1-T_2 plane. The orientation of this axis explains the fact that small errors in H resulted in large errors in the estimate of T_2.

The same analysis can be carried out for errors in the recharge parameter. The longest axis of the parameter confidence ellipsoid in the parameter space T_1-T_2-R is shown in Figure 5.8, and all axes are listed in Table 5.6. In this case, the longest axis of the confidence ellipsoid is 375 times as long as the next longest axis. The three parameters are very unstable when considered together, and the system is ill-conditioned. The longest axis of the confidence region is oriented at a small angle to the parameter axis R, and at large angles to the parameter axes T_1 and T_2. The parameter estimates of T_1 and T_2 at any value of recharge can be determined by the point of intersection of the long axis with a slice taken parallel to the T_1-T_2 plane at that value of R. The longest axis is oriented at a small angle to the axis of parameter R, so large errors in recharge result in relatively smaller errors in T_1 and T_2. The line of parameter estimates in Figure 5.6 is the projection of the long axis in three dimensional space on the T_1-T_2 plane.

The error in the estimated parameters as a result of an error in the specified value of a parameter depends on the orientation of the joint confidence region. If the longest axis of the confidence region is nearly parallel to the specified parameter axis,

Table 5.6 Axes of confidence region for T_1-T_2-R parameter set

Axis Lengths	0.016	18.100	0.048
Unit Vectors	U_1	U_2	U_3
T_1	-0.93	0.30	0.21
T_2	-0.16	0.17	-0.97
R	0.33	0.94	0.11

then the error ratio is small. If the longest axis is oriented nearly perpendicular to the specified parameter axis, then the error ratio for at least one of the estimated parameters is large.

5.3.3 Calculation of error ratios from confidence region

It is possible to calculate the error ratio from the parameter confidence region. Figure 5.9 is a generic confidence ellipse in two parameter dimensions with the parameter axes scaled by the parameter estimates. Using linearized error analysis, the shape and orientation of the confidence ellipse is constant for any contour of the response surface, so the confidence ellipse in Figure 5.9 can represent any contour of the response surface. The error ratio is defined as the ratio of an error in the estimated parameter value to an error in the specified parameter value. If b_1 is the specified parameter, the error ratio can be graphically constructed by using a line perpendicular to the b_1 axis tangent to the confidence ellipse. This line is represented by A - A'. The parameter estimates, given an error in b_1, are at the point where the

line A - A' intersects the confidence ellipse, labelled as point (X,Y). The objective function has a minimum along the line A - A' at that point. The error in the specified parameter b_1 is given by $(X - X_0)$. The error in the estimated parameter is given by $(Y - Y_0)$. The error ratio is therefore $(Y-Y_0)/(X-X_0)$. Because the shape and orientation of the confidence ellipse is constant for any contour of the response surface, the distance $(X-X_0)$ can be scaled to any error in the specified parameter. The error ratio remains constant for any error in the specified parameter.

The conceptual method presented above can be used in simple two and three dimensional parameter spaces, but not for multi-parameter problems. The error ratio can be calculated from the axes of the parameter confidence ellipse. The error ratio is

$$ER_{i,j} = \frac{\sum_{k=1,p} [U_{i,k} U_{j,k} L_k^2]}{CV_j^2} \qquad (5.1)$$

where $ER_{i,j}$ is the error ratio for an error in the ith estimated parameter, given an error in the jth specified parameter. CV_j is the total coefficient of variation for the specified parameter, defined in equation (4.5). This error ratio is termed the linearized error ratio because it is calculated from the linearized confidence ellipsoid.

The error ratio depends on two factors; the orientation of the confidence region and the shape of the confidence region. If the confidence region has a large condition number (long and narrow), the error ratio will depend mainly on the orientation of the longest axis of the confidence region. Figure 5.10a shows an example of a confidence

region with a large condition number, along with the longest axis of the confidence region. The line perpendicular to b_1 axis, tangent to the confidence region, intersects the confidence region near the longest axis of the confidence ellipsoid. The ratio of the elements of the eigenvector of the longest axis of the confidence region approximates the linearized error ratio. If the confidence region is well-conditioned, the contribution to the coefficient of variation from the longest axis for the fixed parameter will be less than one, and the error ratio will be reduced from that calculated using only the elements of the eigenvector. Figure 5.10b shows an example of a well conditioned confidence region, and the longest axis of the confidence region. The line perpendicular to the P_1 axis, tangent to the confidence region, intersects the confidence region at a point somewhat below the longest axis of the confidence region. Thus the linearized error ratio is less than that calculated only using the longest axis of the confidence region.

5.3.4 Using error ratios to identify responsible parameters for prior information

When prior information is used to reduce the uncertainty in parameter estimates and stabilize parameter sets, it should be recognized that errors in the prior information may lead to errors in the estimated parameters. It is necessary to know the influence of errors in the prior information on the parameter estimates in order to use the prior information in a responsible manner. If errors exist in the prior information, it would be responsible use prior information which minimizes the effects

of these errors. The parameters that lead to the smallest error ratios are the most responsible parameters for prior information.

Tables 5.7 and 5.8 show the linearized error ratios calculated from equation (5.1) for the two parameter sets described above. These tables can be used to choose the responsible parameters for prior information. For the parameter set T_1-T_2-H, the largest linearized error ratio results from estimating T_2 while parameter H is specified. Errors in specified values of H will be magnified over 7 times when T_2 is estimated. At the same time, errors in the estimate of T_1 will be smaller than the error in the specified value of H. From examining Table 5.7, it is apparent that specifying the value of T_2 leads to the smallest error ratios for the estimates of the remaining parameters. The errors in estimates of both T_1 and H will much smaller than errors in the specified value of T_2. The choice of T_2 as the most responsible parameter to specify is consistent with the examination of the parameter confidence region. The longest axis of the confidence region is sub-parallel to the T_2 parameter axis, so errors in T_2 will not result in large error ratios.

Table 5.7 Error ratios for the T_1-T_2-H parameter set

	Fixed T_1	Fixed T_2	Fixed H
Estimated T_1	1.0	.057	.86
Estimated T_2	1.35	1.0	7.11
Estimated H	.30	.111	1.0

For the parameter set T_1-T_2-R, the error ratios are shown in Table 5.8. The smallest error ratios result from specifying parameter R. This result is consistent with the fact that the confidence region for this parameter set is sub-parallel to the parameter axis R.

Table 5.8 Error ratios for the T_1-T_2-R parameter set

	Fixed T_1	Fixed T_2	Fixed R
Estimated T_1	1.0	1.7	.32
Estimated T_2	.57	1.0	.19
Estimated R	3.1	5.4	1.0

It is important to note that the error ratios for the parameter subset T_1-T_2 are not always the same. From Table 5.7, an error in the specified value of T_1 leads to a 1.2 error ratio for parameter T_2. However, from Table 5.8, an error in the specified value of T_1 lead to a .57 error ratio for parameter T_2. The full confidence region for the parameter set determines the error ratio. The confidence regions for these two parameter sets are different, so error ratios for the same parameters are different.

5.3.5 Influence of non-linear confidence regions

Throughout the above analysis, linear approximations to the confidence regions have been used to calculate the axes of the confidence ellipsoids and the linearized error ratios. These linear approximations do not account for the non-linearity of the true confidence regions. Three indications of non-linearity are apparent in the examples presented, especially in the T_1-T_2-H system.

1. The lines in parameter space reflecting the trace of the axis of the confidence region are slightly curved for the confidence region including parameter H. This curvature implies that the axis of the confidence region is curved in parameter space. For a linear model, the axis of the confidence region would be straight.
2. Errors in specified parameters that overestimate the true parameter values result in different errors in the estimated parameters than errors in specified parameters that underestimate the true parameter values. The confidence region is not symmetrical about the true parameter value. In a linear system, the confidence region would be symmetrical.
3. The true error ratios are not constant as the error in specified parameter values increases. A combination of curved and non-symmetrical confidence regions are the cause of the non-constant error ratios. For a linear system, the error ratio would be constant for any error in the specified parameter value. The linearized error ratios are considered constant.

Even though there are indications of model non-linearity, the non-linearity is generally not severe. The curvature of the confidence region is slight, while the non-symmetry is somewhat greater. However, since the linearized error ratio analysis depends mainly on the orientation of the parameter confidence region, and not on the symmetry of this region, the linear approximation is generally robust. The true error ratios may differ from the linearized error ratios, but the conclusions based on the linearized error ratios are valid. The parameters that result in the smallest error ratios will most likely be the same even if the true non-linearity were taken into account.

5.4 Error ratios for prior information with uncertainty

Using prior information with uncertainty is generally an improvement over simply specifying a single value for a parameter. In parameter space, specifying a single value is equivalent to taking a slice in parameter space perpendicular to that parameter axis at the specified value. The ill-conditioning is reduced by reducing the parameter dimension. Prior information retains all the parameters in the inverse problem, but adds a penalty term to the response surface for deviations from the prior estimate. A better conditioned, more stable response surface is the result.

The error ratio method developed above can be extended to using prior information with uncertainty. In terms of error ratio, the major difference between using prior information with uncertainty and specifying a parameter value without uncertainty

lies in how close the final estimate is to the prior estimate. When a parameter value is specified, it cannot change during parameter estimation, and the final estimate is equal to the prior information. When using prior information with uncertainty, the prior estimate and the final estimate are different.

Two factors determine how close the final estimate are to the prior estimate; the assigned uncertainty in the prior information and the shape of the response surface before prior information is included. If the uncertainty assigned to the prior estimate is small, there is a large penalty in moving away from this prior estimate, and the final estimate will be close to the prior estimate. Conversely, if the uncertainty in the prior estimate is large, the penalty for moving away from the prior estimate is small.

If the response surface using only head data reflects a poorly-conditioned problem, the final estimate will be close to the prior estimate. A poorly conditioned parameter set is characterized by a valley with a flat bottom. The prior information, even if it has a large uncertainty, will produce a definite minimum in the valley at the value of prior estimate. The final estimate will be very close to the prior estimate. If the response surface using only head data is well conditioned, the minimum defined by the head data will have a large influence on the final parameter estimates. Even if the prior information has large errors, the final estimates will be controlled by the response surface for the head data.

When prior information is assigned for more than one parameter, the relationships between the prior and final estimate are more complicated. In addition to the factors described above, the final estimates also depend on the relationship between the orientation of the data response surface and the location of the minimum and shape of the response surface using prior information. These relationships are too complicated to form any specific conclusions. In general, we find that for an inverse problem that is ill-conditioned before adding prior information, one or more of the final estimates will be very constrained by the prior estimate. If the final estimate is in error, it will introduce errors in the final parameter estimates of the other parameters.

Thus, for an ill-conditioned or non-identifiable inverse problem, the final parameter estimates will be close to the prior estimates, regardless of the assigned uncertainty in the prior estimates. The error ratio method will be valid for determining the effects of errors in the prior information. For a well-conditioned problem, the final estimates may not be close to the prior estimates, and the error ratios may be less than those calculated by the linearized error ratios.

5.4.1 Example of the influence of the topology of the data response surface

Response surfaces T_1-T_2 and T_1-R are used to illustrate the influence of the topology of the response surface on the difference between the prior and the final estimate. The response surface for T_1-T_2 (Figure 5.5) reflects a well-conditioned

parameter set, and the response surface for T_1-R (Figure 5.2) is poorly-conditioned. Assume that the prior estimate has a value of T_1 (prior) = 1.02 in scaled space, and thus is in error. Figure 5.11 shows the response surface for the prior information on T_1, with an uncertainty in the prior information equal to one percent of the prior parameter estimate. The final parameter estimates for the two parameter sets are quite different. The total response surfaces are shown in Figure 5.12 and 5.13. Note that the two response surfaces are not shown at the same scale. For the parameter set T_1-R (Figure 5.12), the final parameter estimate for T_1 is the same as the prior parameter estimate. The response surface using head data alone does not have a unique minimum, but instead contains a nearly flat bottomed valley. All along this valley, the values of the response surface are very close to the minimum. The prior value of the parameter T_1 defines where the minimum will lie along this valley. Since the prior estimate for T_1 was in error, the final estimates for both T_1 and R are in error. For the parameter set T_1-T_2 (Figure 5.13), the parameter estimate for T_1 moves away from the prior estimate toward the parameter estimate based on the head data only. The head data alone produce a response surface with a definite minimum. This minimum has a large influence on the total response surface, and pulls the final estimates toward this minimum.

In parameter set T_1-T_2, the parameter space is well conditioned, and the minimum is well defined using only head data without prior information. When prior information is included, the parameter estimates are pulled toward the minimum using

head data only. Even when the prior information has large errors, the final estimates are controlled by the information contained in the head data. In parameter set T_1-R, the parameter space is poorly conditioned using only head data, as shown by a long, flat bottomed valley in the response surface. The prior information does help transform this problem into a well-conditioned inverse problem, with a well-defined minimum. However, the location of the minimum (and therefore the parameter estimates) is completely dependent on the specified value of the prior information. If the prior information is accurate, there is no problem. However, if the prior information is in error, even if a large uncertainty is assigned to the prior information, the value of the parameter estimates depends on the incorrect value of the prior information.

5.5 Summary of guidelines for use of prior information

Parameter space analysis has been used to develop guidelines for the efficient and responsible use of prior information in groundwater flow models. The axes of the confidence region can be used to identify the most efficient parameters for prior information. Those parameters with the largest elements of the longest axis of the confidence region will be the most efficient parameters for reducing parameter uncertainty and increasing parameter stability.

A linearized error ratio matrix can be calculated from the axes of the confidence region, and used to identify the most responsible prior information. The linearized error

ratio matrix is calculated based on prior information without uncertainty, but is also valid for prior information with uncertainty. For ill-conditioned or non-identifiable inverse problems, the error ratio method will be valid for determining the effects of errors in prior information with uncertainty. For a well-conditioned problem, the error ratios may be less than those calculated by the linearized error ratios.

To minimize the effects of possible errors in the prior estimates, those parameters with the smallest error ratios are the most responsible parameters for prior information. Errors in these parameters will have the least influence on the parameter estimates for the remaining parameters. Those parameters that are the most efficient are often the same ones as those that are the most responsible. Both guidelines lead to selecting parameters whose axes are closely aligned with the longest axis of the parameter confidence region.

5.6 Application to a multi-parameter system

The guidelines developed above for the efficient and responsible use of prior information to stabilize an inverse problem were applied to a synthetic multiparameter system. The flow system is taken from Carrera and Neuman (1986c) and shown in Figure 5.14. The data consist of 18 head measurements with uncertainties of 1 meter. The parameters to be estimated include 9 transmissivity zones, 2 recharge zones, one specified flux boundary and one specified head boundary. All model parameters,

including those describing the domain boundaries, were estimated, which resulted in a non-identifiable parameter estimation problem. When estimating parameters, the final estimates were found to depend on the initial values of the parameters.

Table 5.9 gives the parameter estimates and uncertainties for two sets of initial parameter values. The transmissivity parameters are log transformed, all other parameters are untransformed. One set of initial estimates is close to the true values of the parameters, the other set of initial estimates is far from the true values of the parameters. The two final sets of parameter estimates are very different. The standard errors of the estimates from the two sets of initial estimates are very similar, so only one set is given. The standard errors of the estimates are very large compared to the values of the estimates, leading to very large coefficients of variation for nearly all parameters. The correlation matrix, which is not presented here, shows correlations of greater than .99 between all parameters except H_1, which showed very little correlation with the other parameters. The resulting parameter estimates are very poor, due to the ill-conditioning of the problem.

5.6.1 Parameter space of multi-parameter problem

Before using prior information to stabilize this problem, the shape and orientation of the parameter confidence region must be understood. The axes of the parameter confidence region are calculated using SVD decomposition of the scaled

Table 5.9 Parameter estimates and uncertainties for multiparameter problem

		Parameter Estimates			
Parameters	True Value	Run #1	Run #2	Standard Error	CV
T_1	2.17	2.22	1.81	5.76	3.16
T_2	2.17	2.09	1.68	5.66	3.36
T_3	2.17	2.00	1.60	5.31	3.32
T_4	2.17	2.28	1.88	5.53	2.94
T_5	1.69	1.68	1.27	5.46	4.26
T_6	1.17	1.20	0.79	5.28	6.61
T_7	1.69	1.79	1.39	5.52	3.96
T_8	1.17	1.21	0.81	5.33	6.62
T_9	0.70	0.73	0.32	5.25	15.92
R_1	2.74e-04	2.98e-04	1.17e-04	1.49e-03	12.70
R_2	1.37e-04	1.42e-04	5.60e-05	7.00e-04	12.63
H	100.0	98.3	98.3	1.75	0.02
F	50.0	70.8	27.9	386.24	13.73

Hessian matrix calculated using the estimated parameter values. Either of the two sets of parameter estimates listed in Table 5.9 leads to confidence regions of similar shape and size, though centered on different points in parameter space. Table 5.10 gives the axes of the confidence region. Table 5.11 shows the relative contribution to the total coefficient of variation from each axis of the confidence region. Table 5.12 is the error ratio matrix for this problem.

The longest axis of the confidence region is axis 13, which is 75 times longer than any other axis. The valley in the multidimensional response surface is oriented

Table 5.10 Axes of parameter confidence region for multiparameter problem

Axis Lengths	2.1e-03	8.2e-03	1.0e-02	2.2e-02	2.5e-02	2.7e-02	3.8e-02	5.6e-02	8.3e-02	2.0e-01	2.2e-01	3.0e-01	22.30
Unit Vectors	U_1	U_2	U_3	U_4	U_5	U_6	U_7	U_8	U_9	U_{10}	U_{11}	U_{12}	U_{13}
T_1	-0.30	0.08	-0.24	0.18	-0.08	0.68	-0.44	0.22	-0.06	0.28	0.09	-0.01	0.10
T_2	-0.12	0.03	0.00	0.01	-0.02	0.15	-0.02	0.15	0.83	-0.49	-0.05	0.02	0.11
T_3	-0.06	-0.01	0.08	-0.10	0.06	-0.13	0.09	-0.18	0.50	0.79	-0.04	0.19	0.10
T_4	-0.20	-0.07	-0.54	-0.02	0.10	0.10	0.10	-0.77	0.00	-0.15	0.03	-0.04	0.10
T_5	-0.13	-0.14	-0.09	-0.32	-0.07	0.39	0.77	0.26	-0.12	0.03	-0.06	0.10	0.14
T_6	-0.11	-0.24	0.17	-0.70	0.45	0.05	-0.37	0.00	-0.09	-0.09	-0.08	0.06	0.22
T_7	-0.15	-0.06	-0.66	0.04	0.25	-0.48	-0.02	0.48	0.00	0.05	0.05	0.05	0.13
T_8	-0.11	-0.35	-0.08	-0.24	-0.81	-0.21	-0.21	-0.02	-0.04	-0.03	-0.02	0.19	0.22
T_9	-0.10	-0.66	0.24	0.54	0.23	0.02	0.04	-0.03	-0.06	-0.05	0.00	0.28	0.30
R_1	0.20	0.50	0.02	0.02	0.02	0.00	-0.02	-0.05	-0.13	-0.13	0.11	0.64	0.50
R_2	0.07	0.12	0.00	0.11	-0.04	-0.04	-0.02	0.00	-0.06	0.05	-0.76	-0.38	0.49
H	0.86	-0.29	-0.31	-0.06	0.01	0.24	-0.09	0.03	0.12	0.06	0.00	0.01	0.00
F	0.07	-0.01	0.13	-0.04	-0.04	-0.06	0.07	0.00	0.03	0.04	0.63	-0.53	0.53

Table 5.11 Relative contribution to the CV from each axis of the confidence ellipsoid

Parameters	U_1	U_2	U_3	U_4	U_5	U_6	U_7	U_8	U_9	U_{10}	U_{11}	U_{12}	U_{13}
T_1	0.00	0.00	0.00	0.00	0.00	0.00	0.00	0.00	0.00	0.00	0.00	0.00	1.00
T_2	0.00	0.00	0.00	0.00	0.00	0.00	0.00	0.00	0.00	0.00	0.00	0.00	1.00
T_3	0.00	0.00	0.00	0.00	0.00	0.00	0.00	0.00	0.00	0.00	0.00	0.00	1.00
T_4	0.00	0.00	0.00	0.00	0.00	0.00	0.00	0.00	0.00	0.00	0.00	0.00	1.00
T_5	0.00	0.00	0.00	0.00	0.00	0.00	0.00	0.00	0.00	0.00	0.00	0.00	1.00
T_6	0.00	0.00	0.00	0.00	0.00	0.00	0.00	0.00	0.00	0.00	0.00	0.00	1.00
T_7	0.00	0.00	0.00	0.00	0.00	0.00	0.00	0.00	0.00	0.00	0.00	0.00	1.00
T_8	0.00	0.00	0.00	0.00	0.00	0.00	0.00	0.00	0.00	0.00	0.00	0.00	1.00
T_9	0.00	0.00	0.00	0.00	0.00	0.00	0.00	0.00	0.00	0.00	0.00	0.00	1.00
R_1	0.00	0.00	0.00	0.00	0.00	0.00	0.00	0.00	0.00	0.00	0.00	0.00	1.00
R_2	0.00	0.00	0.00	0.00	0.00	0.00	0.00	0.00	0.00	0.00	0.00	0.00	1.00
H	0.01	0.02	0.03	0.00	0.00	0.11	0.03	0.01	0.37	0.38	0.00	0.02	0.01
F	0.00	0.00	0.00	0.00	0.00	0.00	0.00	0.00	0.00	0.00	0.00	0.00	1.00

Table 5.12 Error ratio matrix for multiparameter system

	Specified Parameters												
Estimated Parameters	T_1	T_2	T_3	T_4	T_5	T_6	T_7	T_8	T_9	R_1	R_2	H	F
T_1	1.00	0.95	0.88	1.04	0.72	0.47	0.78	0.47	0.33	0.21	0.22	40.2	0.22
T_2	1.05	1.00	0.92	1.09	0.76	0.49	0.82	0.50	0.33	0.22	0.23	39.8	0.23
T_3	1.14	1.08	1.00	1.18	0.82	0.53	0.89	0.54	0.32	0.24	0.25	39.8	0.25
T_4	0.96	0.92	0.85	1.00	0.70	0.45	0.75	0.46	0.32	0.20	0.21	40.0	0.21
T_5	1.39	1.32	1.22	1.44	1.00	0.65	1.08	0.66	0.41	0.30	0.30	49.2	0.30
T_6	2.13	2.03	1.87	2.21	1.54	1.00	1.66	1.01	0.59	0.46	0.46	70.1	0.46
T_7	1.28	1.22	1.13	1.33	0.93	0.60	1.00	0.61	0.41	0.27	0.28	49.2	0.28
T_8	2.11	2.01	1.86	2.19	1.52	0.99	1.65	1.00	0.59	0.45	0.46	70.2	0.46
T_9	3.03	3.04	3.11	3.12	2.43	1.69	2.44	1.68	1.00	0.62	0.64	101.	0.57
R_1	4.61	4.39	4.06	4.79	3.33	2.16	3.60	2.19	1.63	1.00	1.00	124.	1.00
R_2	4.61	4.39	4.06	4.79	3.33	2.16	3.60	2.19	1.62	1.00	1.00	124.	1.00
H	0.00	0.00	0.00	0.00	0.00	0.00	0.00	0.00	0.00	0.00	0.00	1.0	0.00
F	4.61	4.39	4.06	4.79	3.33	2.16	3.60	2.19	1.74	1.00	1.00	125.	1.00

in the direction of this axis, and is very long and flat, leading to high correlations between any parameters that contribute to this axis. Examining the unit vector that corresponds to axis 13, all parameters except H have a component in the direction of axis 13. The axes of parameters F, R_1 and R_2 are most closely aligned with the axis 13. Based on the contribution to the parameter CV matrix (Table 5.11), axis 13 contributes nearly all the uncertainty to every parameter except H. If axis 13 could be shortened, the uncertainty in all parameters except H would be reduced.

The linearized error ratio matrix (Table 5.12) shows that errors in parameters R_1, R_2, and F lead to small error ratios for the other parameters. Errors in the transmissivity zones lead to larger error ratios for the other parameters. Errors in the head boundary value lead to the largest error ratios.

The confidence region for the parameter estimates can be interpreted as follows. There is one axis that is much longer than the others, and this axis contributes nearly all the uncertainty to all parameters except H. This axis is oriented most closely with parameter axes F_1, R_1 and R_2, and is perpendicular to parameter axis H. This implies that parameter H is virtually independent of the other parameters, and can be estimated from the data even in this ill-conditioned problem.

The unit vector associated with the longest parameter axis has some interesting properties. The magnitudes of the components of the unit vector seem to fall into

three distinct groups. The first group contains the transmissivity parameters. The components of the unit vector range from 0.10 to 0.30, and seem to be inversely correlated with the magnitude of the estimated parameter. Since the confidence region reflects the coefficient of variation, the smaller the value of the estimated parameter, the larger the coefficient of variation. The parameter estimates for T_1 through T_9 have approximately equal variances, so their coefficients of variation are inversely proportional to their estimated values. In this confidence region, the longest axis contributes nearly all the uncertainty to all parameters, so the components of the unit vector are closely correlated to the coefficients of variation. The second group of components contain the recharge and flux parameters. All three parameters have components of the longest vector of similar magnitude, and thus similar coefficients of variation. The variances of these parameters are quite different, but their coefficients of variation are similar. This is the opposite of what was observed in the first set. The third group consists of the specified head parameter, which has no contribution to the longest axis of the confidence region.

5.6.2 Anticipated influence of prior information based on parameter space

From the parameter space, three groups of parameters emerge. The head boundary value can be identified quite well using head data only. Prior information on parameter H will not reduce the ill-conditioning of the parameter set significantly. However, errors in the prior information for H would cause very large errors in the

other parameter estimates. Prior information for parameter H would be a poor choice, since it is not necessary, provides no advantage in identifying the other parameter estimates, and leads to large error ratios.

The flux boundary value and the recharge parameters all have large components of the unit vector associated with the long axis of the confidence region. These three parameters also have the smallest error ratios. Any of these three parameters are good choices for prior information because they efficiently reduce the ill-conditioning of the parameter set while reducing the influence of any errors in the prior information.

The transmissivity parameters have smaller but still significant components of the unit vector associated with the longest axis of the confidence region. Prior information for any of these parameters will reduce the ill-conditioning of the parameter set significantly, but at the expense of potentially magnifying any errors in the specified values of the parameters.

5.6.3 Comparison of parameter space and modelled results

Based on the analysis of the parameter space, the flux boundary and the recharge parameters should be the most efficient and responsible parameters for prior information. The transmissivity parameters are less efficient and responsible, while

prior information on the head boundary would be both inefficient and irresponsible. These results need to be checked against the actual modelled results.

First, the issue of which parameters most efficiently stabilize the inverse problem is examined. Two types of prior information are considered: prior information without uncertainty and prior information with uncertainty. Table 5.13 shows the effect of specifying various parameters at their true values, with no uncertainty in the prior information. The component of the longest axis for each parameter is listed, along with the average CV and the CN for the parameter set after specifying each parameter. Specifying those parameters with large components of the longest axis should result in the most stable parameter sets with the smallest average coefficient of variation.

Table 5.13 Calculated results from specifying some representative parameters at their true values

	Full Parameter Set	Specify T_1	Specify T_5	Specify T_9	Specify R_1	Specify F	Specify H
Comp. of L_{max}	N/A	0.10	0.14	0.30	0.50	0.53	0.00
CN	9900.0	289.8	180.6	168.4	164.3	165.1	8944.0
Average CV	5.510	0.181	0.113	0.102	0.097	0.099	5.490

The full parameter set (all 13 parameters) results in a very large CN and a large average CV. Specifying parameter H does not significantly reduce either the CN

or average CV. Specifying any of the other parameters does significantly stabilize the problem, because the dimension in parameter space in which all the parameters were correlated is removed. Table 5.13 shows that specifying parameter T_9 reduces parameter uncertainty more than specifying parameters T_1 or T_5. Parameter T_9 has a larger component of the longest axis than the other transmissivity parameters, so specifying T_9 should reduce parameter uncertainties more than any other transmissivity parameters. The parameters with the largest components of the longest axis are R_1, R_2, and F. Table 5.13 shows that specifying parameters R_1 and F result in the most stable parameter estimates with the lowest uncertainties. The behavior of parameter R_2 is similar to parameter R_1. Specifying those parameters with large components of the longest axis are generally the most efficient in stabilizing the parameter set.

Table 5.14 illustrates the effect of prior information with uncertainty. Prior information is added to one parameter at a time, where the uncertainty in the prior information is ±25% of the prior value. The CN and average parameter CV are presented for prior information on representative parameters. Prior information on R_1 and F resulted in the most stable parameter estimates with the lowest uncertainties of any parameters. If only transmissivity parameters are considered, prior information on T_9 resulted in the best parameter estimates. Prior information on parameters with the largest elements of the unit vector associated with the longest axis of the confidence region are most effective in reducing the average CV.

Table 5.14 Calculated results from prior information on various parameters

	All Parameters	Prior T_1	Prior T_5	Prior T_9	Prior R_1	Prior F	Prior H
Comp. of L_{max}	N/A	0.10	0.14	0.30	0.50	0.53	0.00
Condition Number	9900.0	1181.9	973.6	413.2	274.0	295.0	8944.0
Average CV	5.510	0.628	0.512	0.242	0.174	0.187	5.490

To determine for which parameters prior information will most responsibly stabilize the inverse problem, error ratios can be calculated. Prior information was included one parameter at a time, where the prior value was 25% greater than the true value. Table 5.15 gives the calculated error ratios, calculated as the ratio of the percentage error in the estimated parameter to the percentage error in the prior value. The first column of Table 5.15 are the calculated error ratios for the full set of estimated parameters, where the starting estimate is equal to the true value of the parameter. The other columns are the calculated error ratios when one parameter at a time is specified at a value 25% higher than its true value. Because the data have errors, the calculated error ratios do not equal the linearized error ratios from Table 5.12. However, the calculated error ratios do follow the trend of the linearized error ratios estimated from the parameter space. For instance, when T_1 is specified, the error ratios for T_1 through T_5 are near one, T_6 through T_8 are between one and two, T_9 is above two, and the recharge and flux parameters are much higher. The

calculated error ratios for specified recharge and flux parameters are much lower than the error ratios for specified transmissivities. There is one pattern that the linearized error ratios did not predict, that is the fact that the errors in the flux boundary value as a consequence of errors in specified values for other parameters are consistenty larger than errors in recharge. The linearized error ratios predict that these errors will be similar in magnitude. The cause of this discrepance may be the difference between the true and estimated parameter values. The estimate of the value of the flux parameter is much farther from its true value than the estimates of the recharge parameters from their true values, even though the coefficient of variation for all these parameters is similar in magnitude. This error due to data uncertainty may carry the whole way through the error ratio analysis. No error ratios for H were calculated, because the parameters set was so ill-conditioned when using only prior information on H that parameter estimates could not be reliably estimated.

Because the parameter set is ill-conditioned without prior information, the final estimates do not depend on the uncertainty assigned to the prior information. Even if the prior information is assigned an uncertainty of 100%, the final estimates are identical to those using prior information without uncertainty. Table 5.15 is unchanged for any reasonable uncertainty in the prior information.

If prior information is provided for more than one parameter, the situation becomes more complicated. The relationship between the location of the prior

Table 5.15 Calculated error ratios due to 25% error in the specified parameter

Parameters	True Values	Estimate	Error Ratio	Error ratio due to error in specified parameters					
				Specify T_1	Specify T_5	Specify T_8	Specify T_9	Specify R_1	Specify F
T_1	150.00	144.00	-0.03	1.00	0.89	0.56	0.34	0.19	-0.02
T_2	150.00	109.00	-0.25	0.37	0.66	0.33	0.11	-0.04	-0.24
T_3	150.00	86.90	-0.44	0.63	0.49	0.16	-0.07	-0.21	-0.42
T_4	150.00	168.00	0.09	0.92	-0.10	0.68	0.46	0.31	0.10
T_5	50.00	41.80	-0.18	0.93	2.42	0.57	0.28	0.10	-0.17
T_6	15.00	13.80	-0.12	1.46	1.59	0.97	0.57	0.27	-0.10
T_7	50.00	54.40	0.09	1.23	1.26	0.84	0.55	0.37	0.10
T_8	15.00	14.07	-0.09	1.49	1.61	1.00	0.57	0.27	-0.07
T_9	5.00	4.70	-0.15	2.52	2.71	1.67	0.97	0.53	-0.11
R_1	2.74e-04	2.58e-04	-0.23	7.11	8.00	3.93	2.01	1.00	-0.16
R_2	1.37e-04	1.24e-04	-0.39	6.54	7.50	3.56	1.72	0.76	-0.35
H	100.00	98.30	-0.07	-0.05	-0.07	-0.07	-0.07	-0.07	-0.07
F	50.00	61.40	0.91	11.70	11.61	6.30	3.81	2.50	1.00

estimates in parameter space, the relative uncertainties of the prior estimates, and the location of the valley in parameter space determine the final parameter estimates. For instance, when prior information on F, R_1 and R_2 is provided, and all three prior estimates are 25% greater than their true value, the final parameter estimate for R_1 and R_2 are approximately 15% greater than their true values, and the final estimate for F is approximately 35% greater than its true value. In another example, when the prior estimate of F is 25% less than its true value, and the prior estimates of R_1 and R_2 are 25% greater than their true values, then all three final estimates are within 5% of the true parameter values. The errors in the prior estimates are averaged, and the final estimates do not reflect the errors in the prior estimates.

5.6.4 Discussion of results for multi-parameter system

In order to responsibly stabilize this problem, the parameters F, R_1 and R_2 were found to be the most efficient and responsible parameters to select for prior information. Practically, these three parameters may be the most difficult to measure in order to obtain the prior information. It is difficult to estimate the value of a flux boundary independent of the model. Recharge is also a difficult parameter to estimate without the use of the model unless a detailed field measurement program is implemented. However, errors in the prior estimates of these parameters translate into relatively small errors in the estimates of transmissivity parameters. Prior estimates on these three parameters, even if they are in error or have large uncertainties, may

be better for parameter estimation than prior information in the transmissivity parameters. A systematic underestimation of prior estimates on transmissivity parameters may lead to large errors in the estimation of the recharge and flux parameters.

Should prior information on parameters be used if it is highly uncertain or has the potential for significant errors? Three factors need to be considered: the conditioning of the parameter set without prior information, the error ratio of the parameters with prior information, and the distribution of the prior information. If the parameter set is ill-conditioned without the prior information, then the prior information will constrain the model parameter estimates. If the error ratio is large for the parameters with prior information, then errors in the prior values may lead to large errors in the estimated values of the other parameters. If the prior information has the potential to systematically over or underestimate the true parameter values, then the prior information may lead to errors in parameter estimates. If the prior information is randomly distributed about the true value of the parameter estimate, then the prior information might not lead to significant errors in the final parameter estimates. However, the assumption that prior information is randomly distributed about the true parameter value is rarely fulfilled in practice.

In this synthetic system, the full parameter set is ill-conditioned without prior information. Parameters R_1, R_2 and F lead to small error ratios, but these are difficult

parameters to measure independent of the model. The transmissivity parameters lead to larger error ratios, but are easier to measure in the field. However, it is common for prior information on transmissivity to be significantly biased, because of scaling differences between the measurement of transmissivity in the field and the model transmissivity. One solution to this dilemma is to provide prior information on parameter T_9. This parameter leads to the smallest error ratios of any of the transmissivity parameters. Errors in this parameter value will not be magnified as much as errors in any of the other transmissivity parameters.

If at this point the parameter set was still unstable, or a further reduction in parameter uncertainty was required, the same analysis could be carried out to select a second parameter for prior information. The reduced parameter space (12 parameters now) would be analyzed, and a parameter selected. This process is easy to accomplish, since the parameter estimation in the 12 parameter system has already been done. The scaled Hessian matrix at the parameter estimates would be used to construct the three tables given above for the 12 parameter system. This parameter space would be analyzed, and a second parameter selected.

5.7 Summary and conclusions

Parameter estimation problems are often non-identifiable or unstable using only head data. Prior information on some of the parameters may be used to stabilize the

parameter set for the purpose of parameter estimation. Guidelines have been developed for efficient and responsible use of prior information in parameter estimation.

An analysis of the parameter space is used to select parameters for prior information. The most efficient parameters for prior information are those with the largest element of the unit vector (eigenvector) associated with the longest axis of the parameter confidence region. The axes of these parameters in parameter space are most closely aligned with the longest axis of the confidence region. To minimize the effects of error in prior estimates, the most responsible parameters for prior information are those which lead to the smallest error ratios. The linearized error ratios can be calculated from the axes of the parameter confidence region. The parameters that lead to the smallest error ratios are often the same parameters that have the largest element of the unit vector associated with the longest axis of the parameter confidence region.

The parameter space analysis was applied to a multi-parameter system with good results. The parameter space was used to gain an understanding of the interaction of the model parameters and the data set. The parameters for which prior information most efficiently and responsibly stabilized the parameter set were correctly identified using the parameter space. The linearized error ratios followed the pattern observed in the true error ratios. The parameter space analysis may lead to selecting

parameters about which reliable prior information is difficult to obtain. The modeller must make a judgement regarding the reliability of the prior information against the potential effects of errors in the prior estimate. The parameter space analysis gives the modeller a tool to judge the potential effects of errors in the prior estimates.

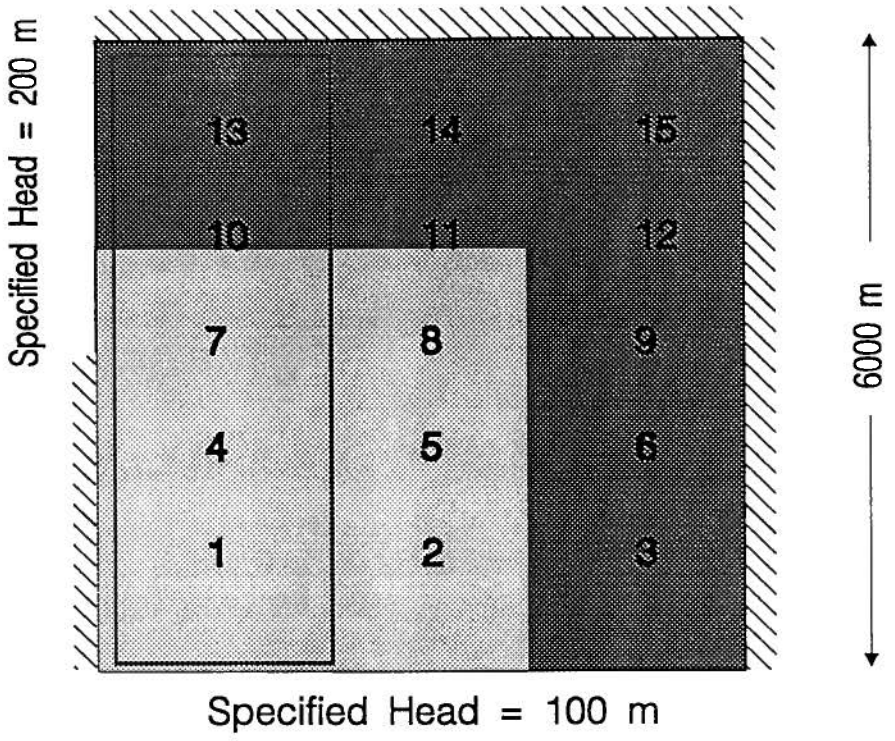

Transmissivity Zone 1
T_1 = 20 m^2/day

Transmissivity Zone 2
T_2 = 200 m^2/d

Boundary of Recharge Zone
R = 0.0004 m/d

13 Sample Location

Figure 5.1 Five parameter synthetic flow system.

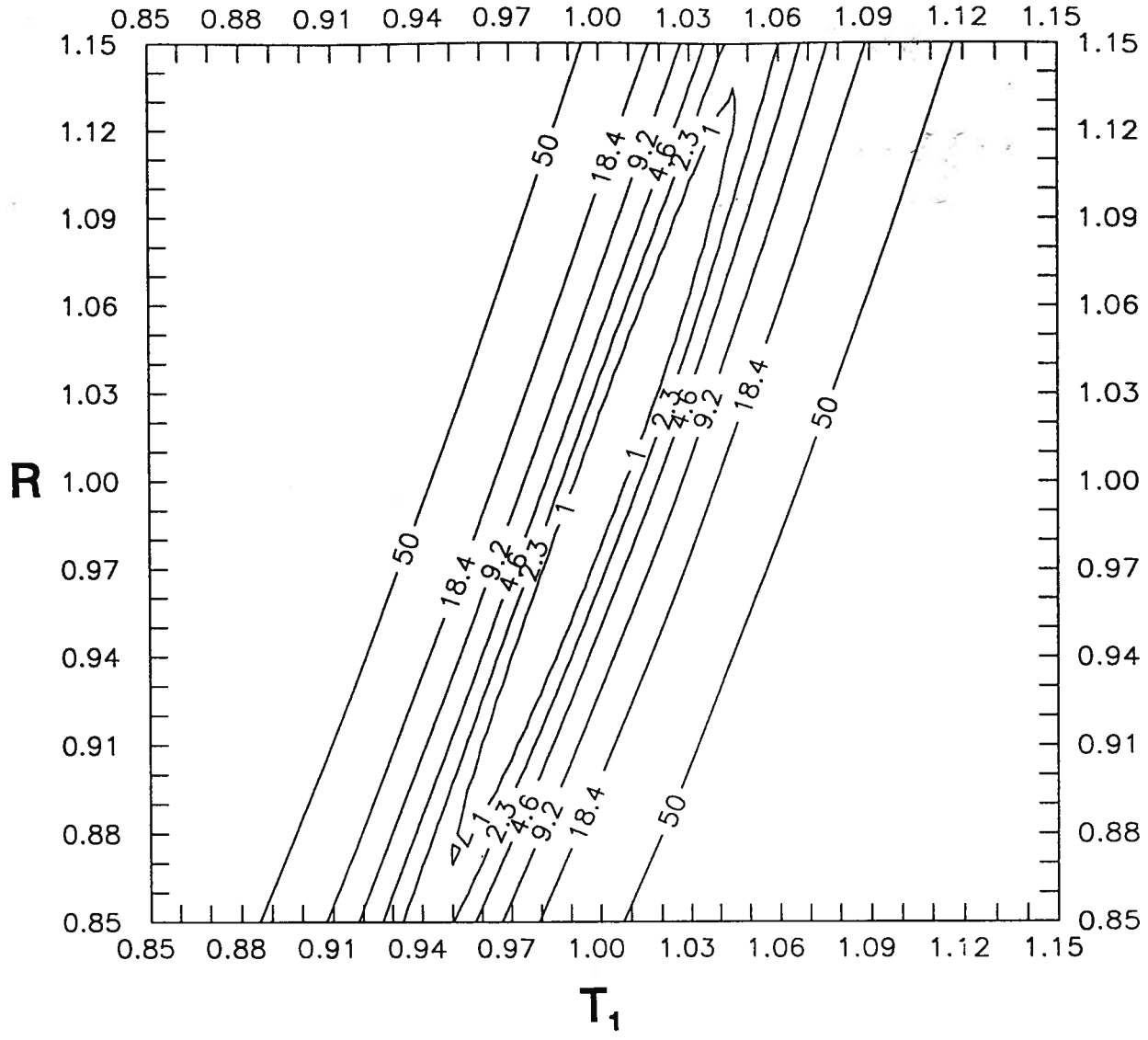

Figure 5.2 Response surface for T_1-R parameter set using hydraulic head data

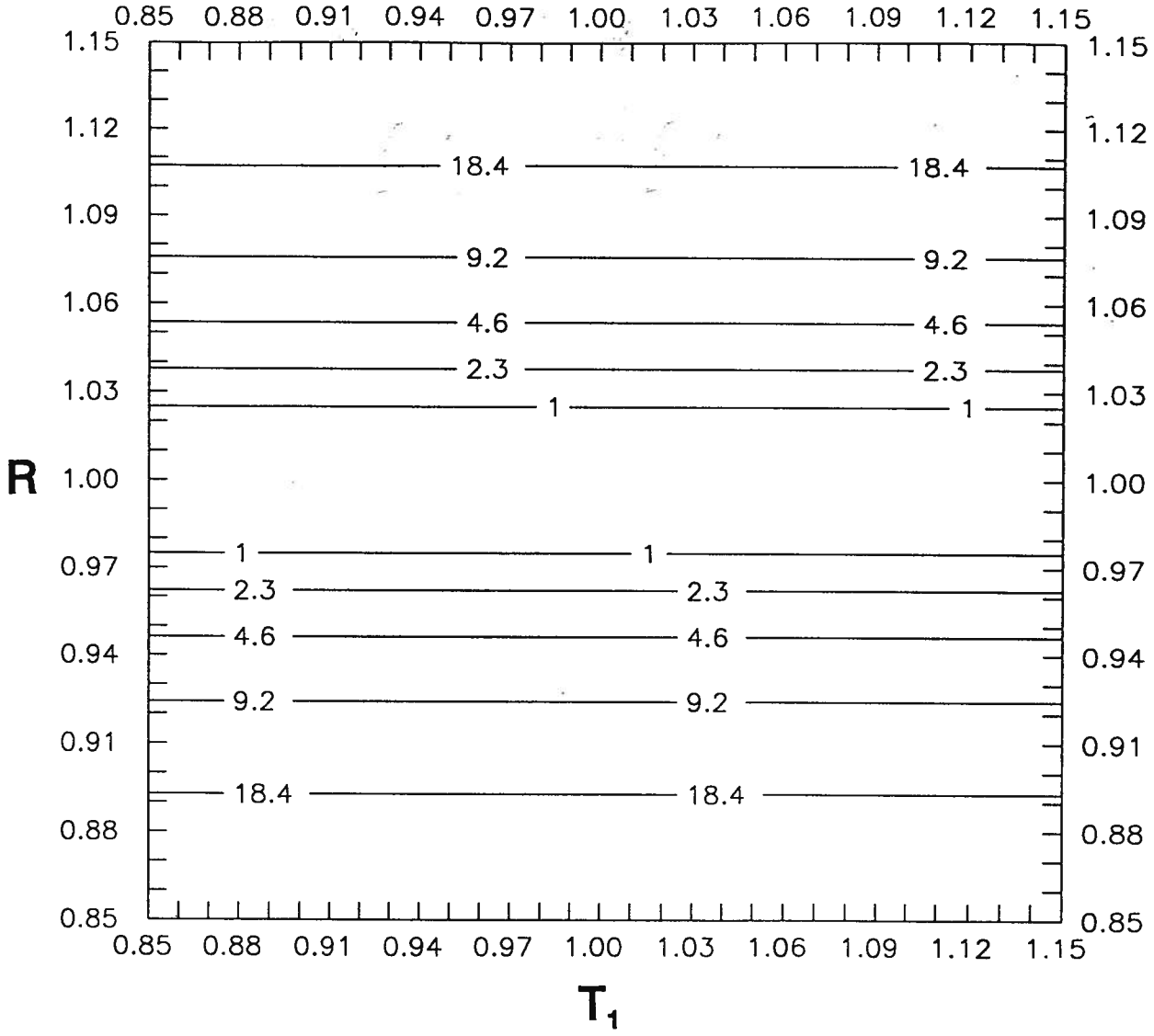

Figure 5.3 Response surface for T1-R parameter set using prior information on R.

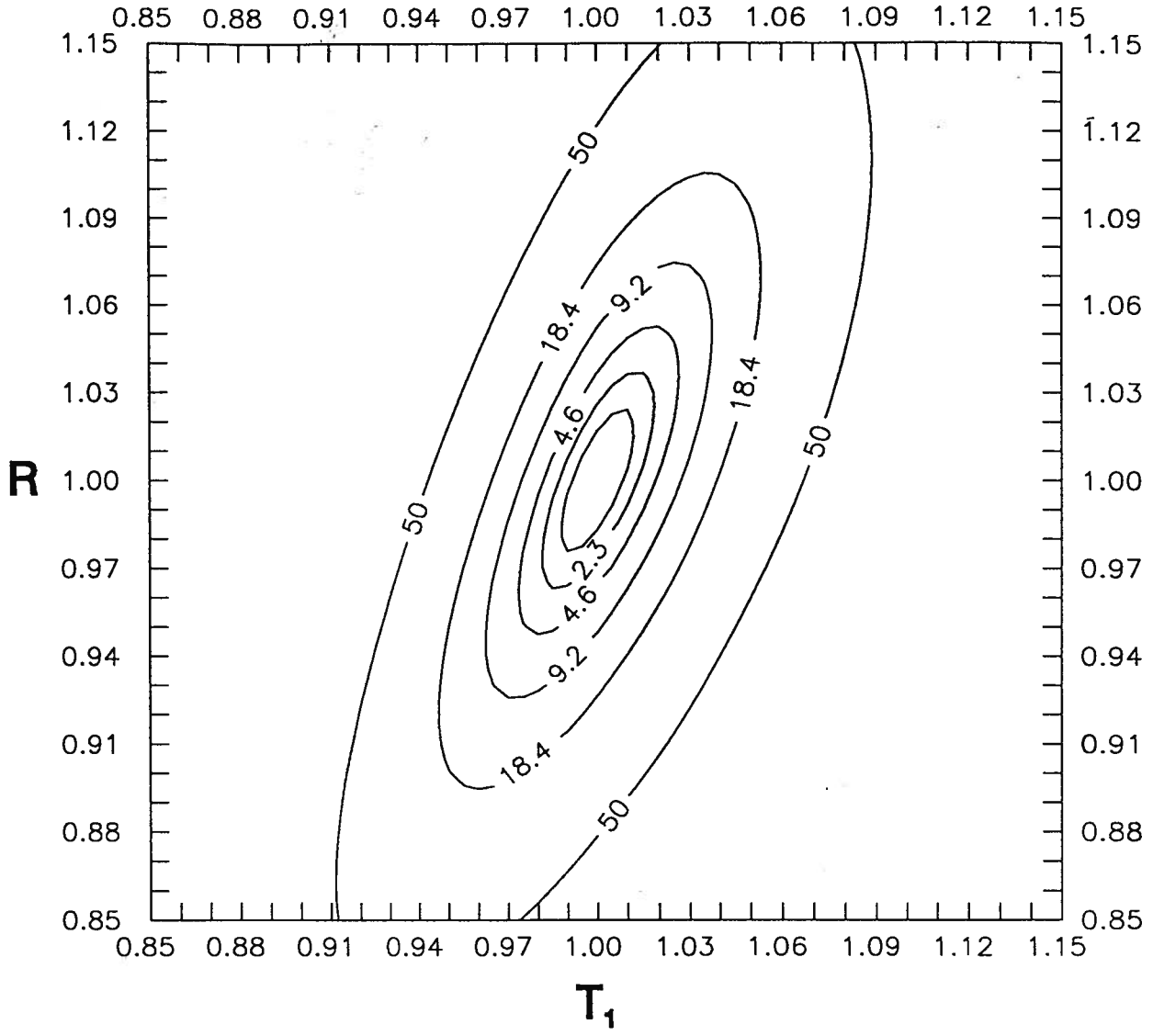

Figure 5.4 Response surface for T_1-R parameter set using head and prior information on R

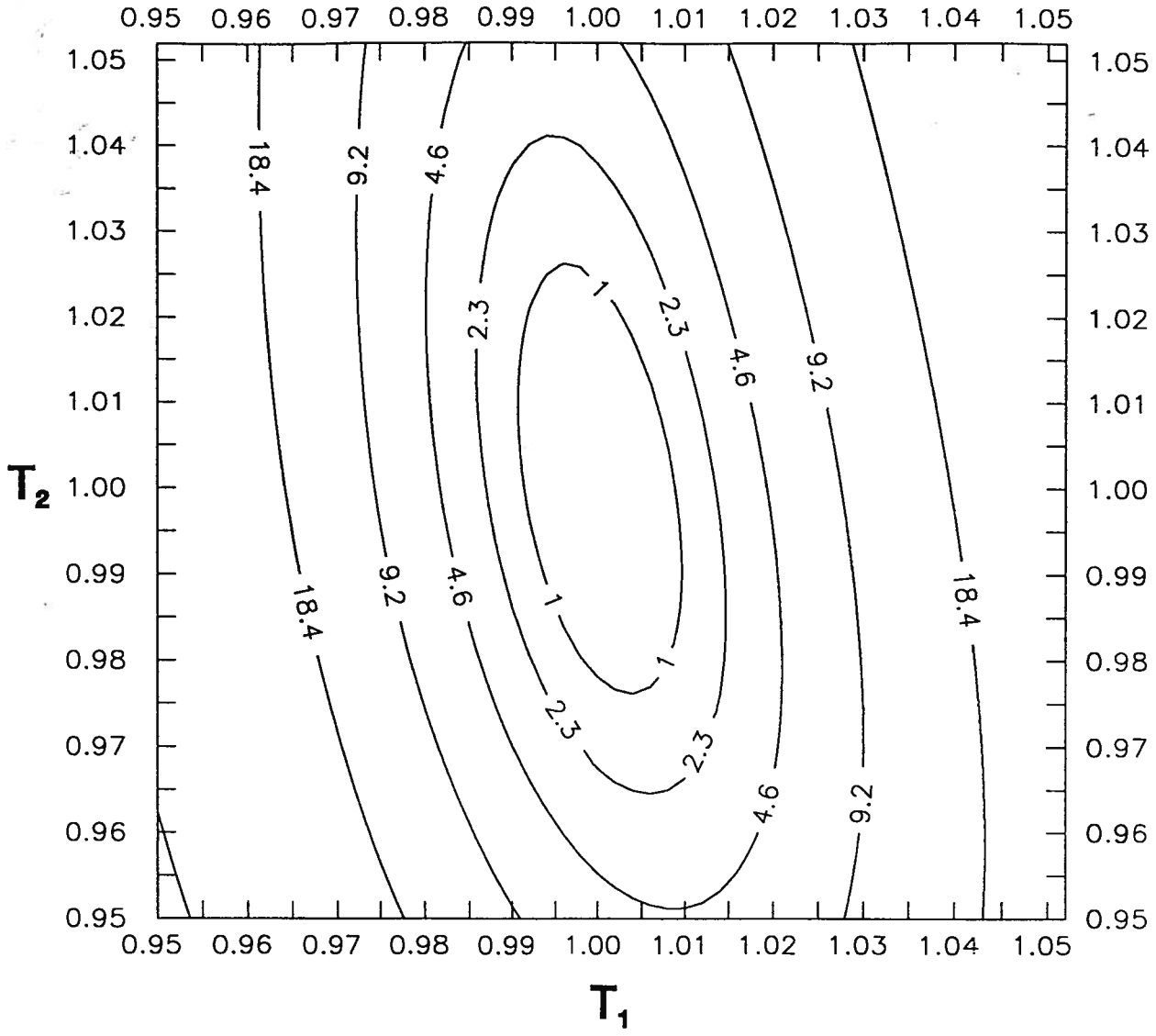

Figure 5.5 Response surface for T_1-T_2 parameter set using hydraulic head data

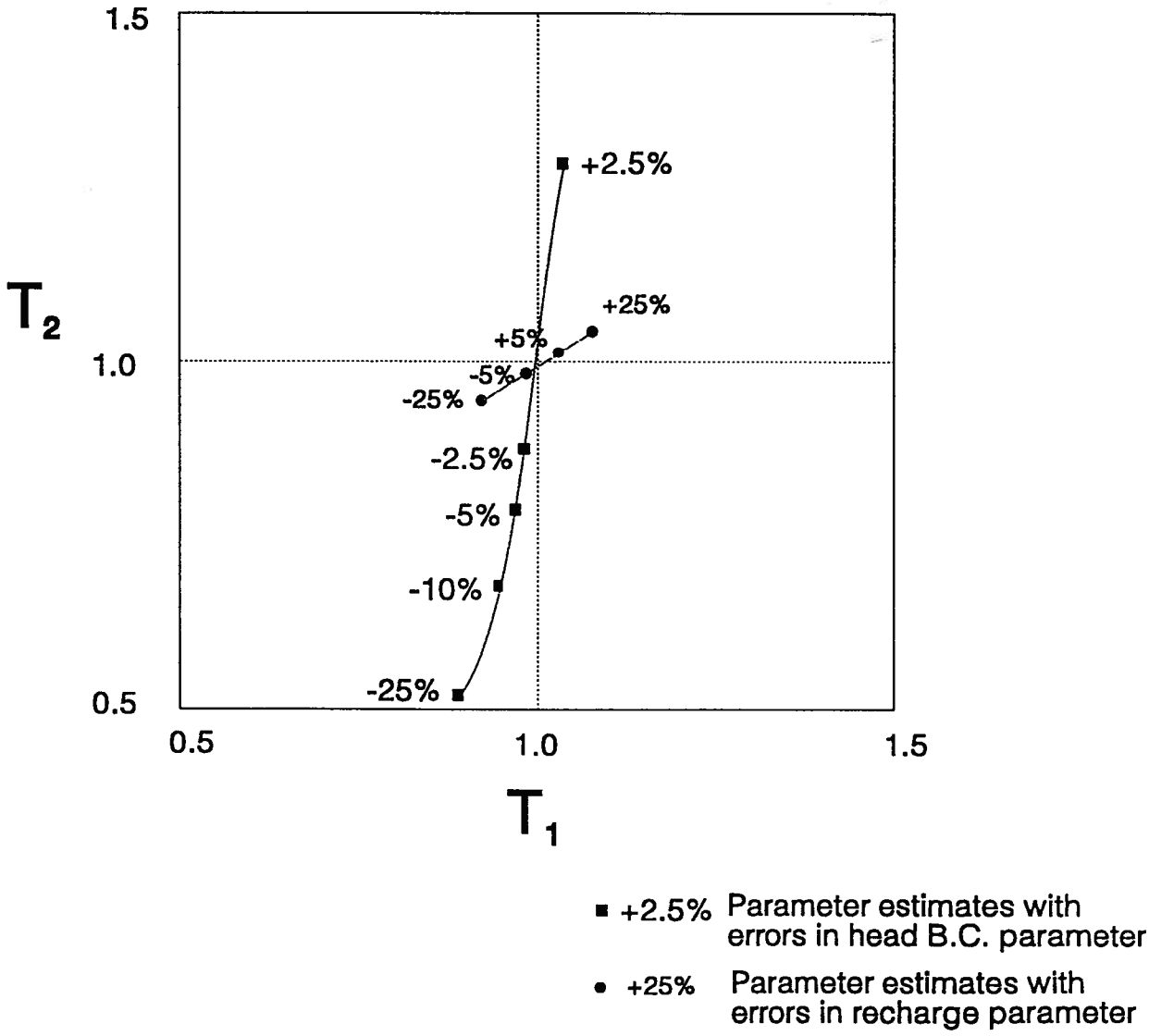

Figure 5.6 Effect of errors in head and recharge parameter values on estimates of T_1 and T_2

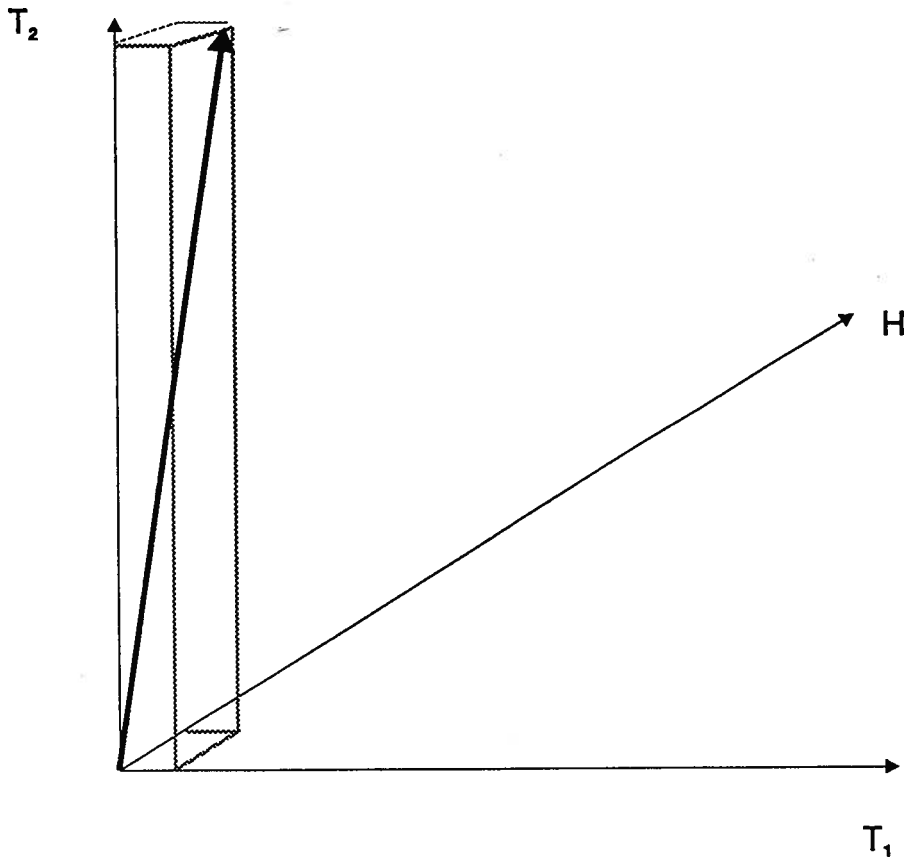

Figure 5.7 Orientation of longest axis of T_1-T_2-H confidence ellipsoid

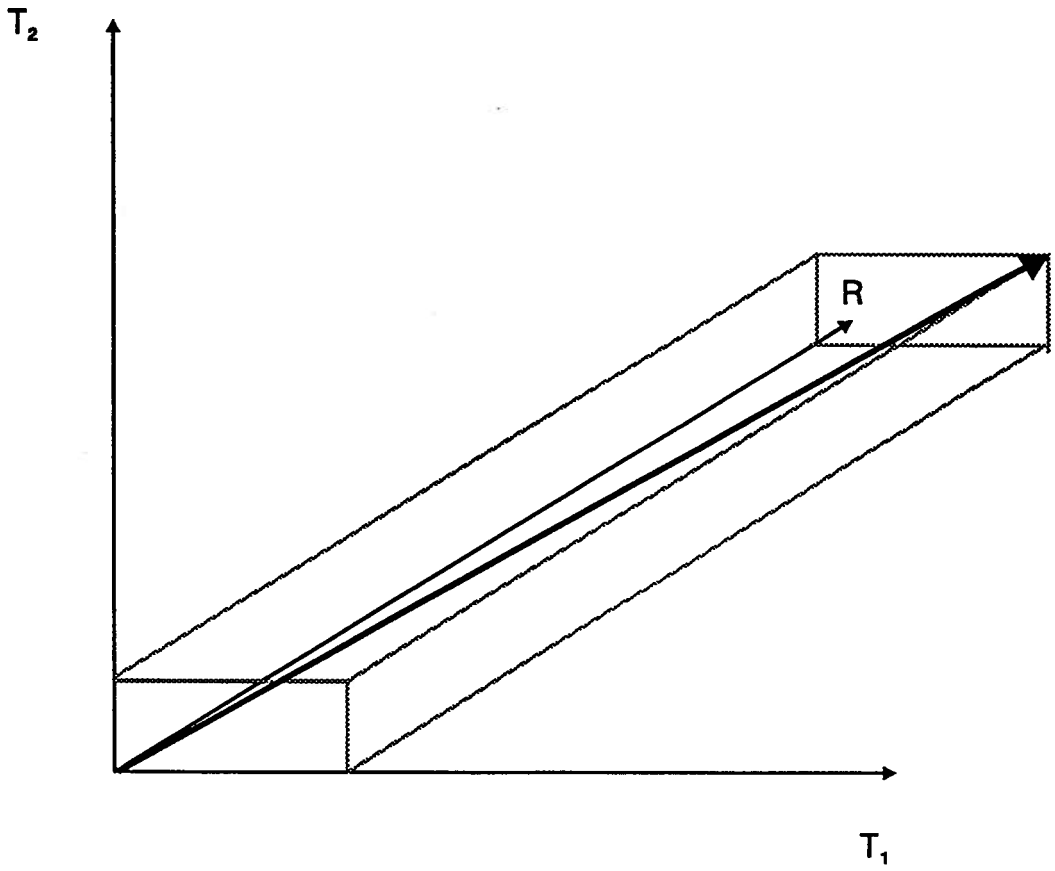

Figure 5.8 Orientation of longest axis of T_1-T_2-R confidence ellispoid

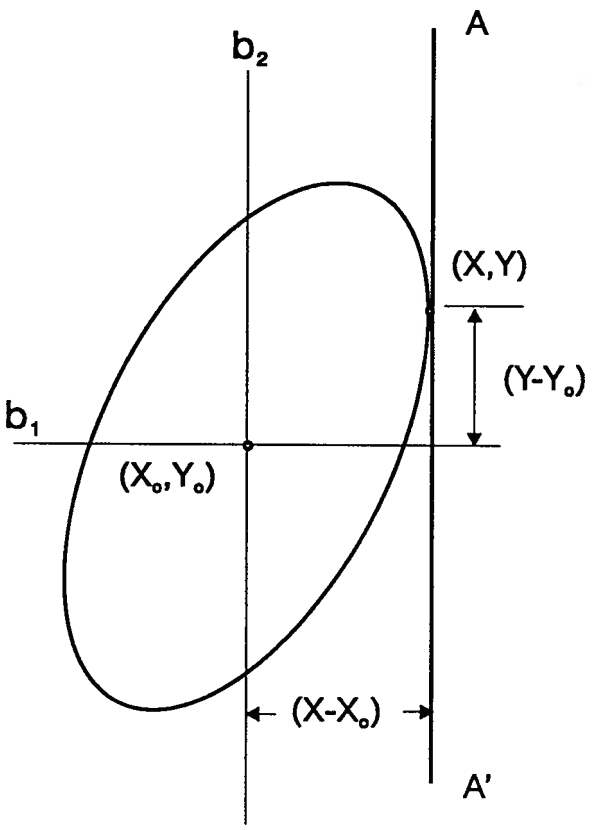

Figure 5.9 Generic confidence ellipse to show calculation of error ratio for parameter b_2 due to an error in parameter b_1

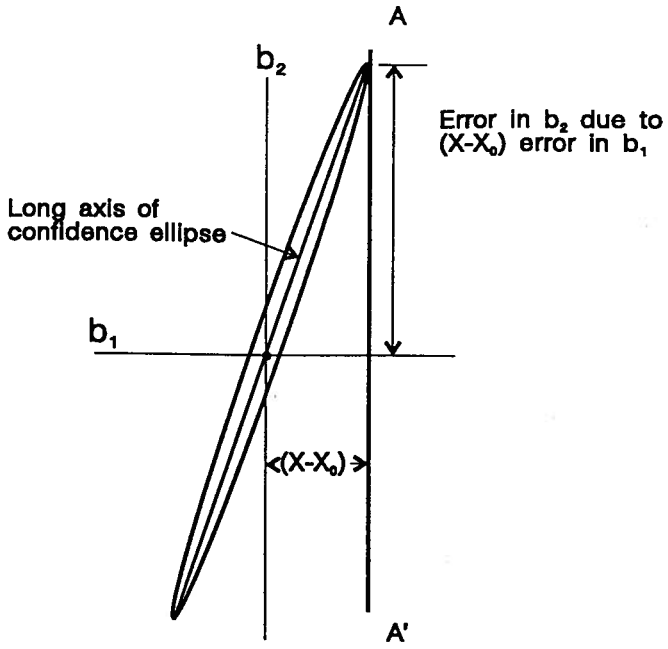

(a) Poorly-conditioned confidence ellipse.

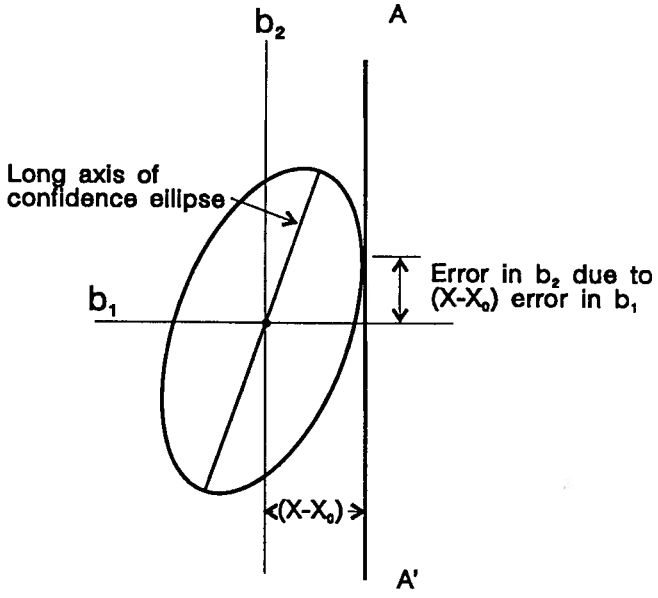

(b) Well-conditioned confidence ellipse.

Figure 5.10 Influence of shape of confidence ellipse on error ratio for (a) well-conditioned and (b) poorly-conditioned confidence regions

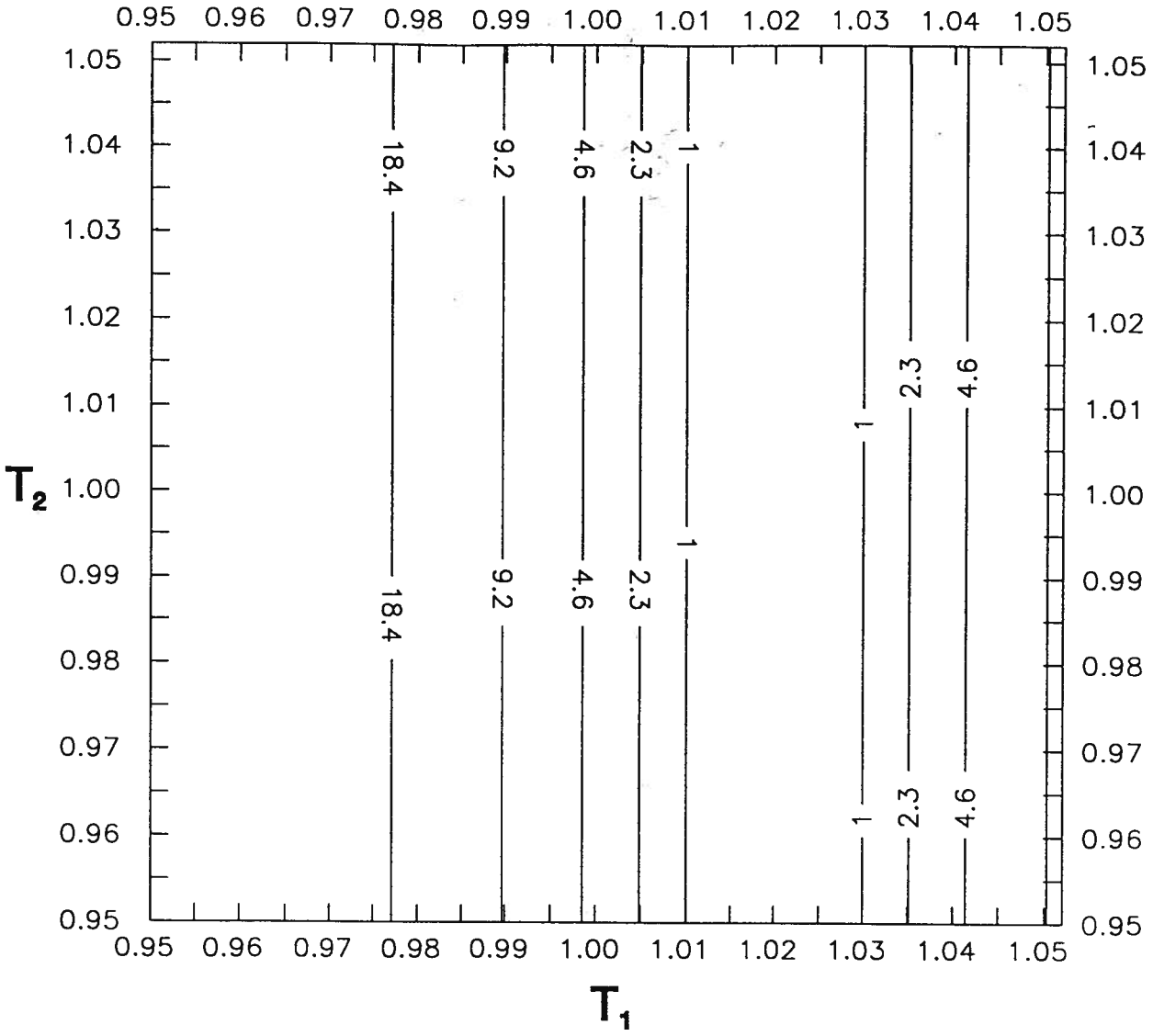

Figure 5.11 Response surface for T_1-T_2 parameter set using incorrect prior information on T_2

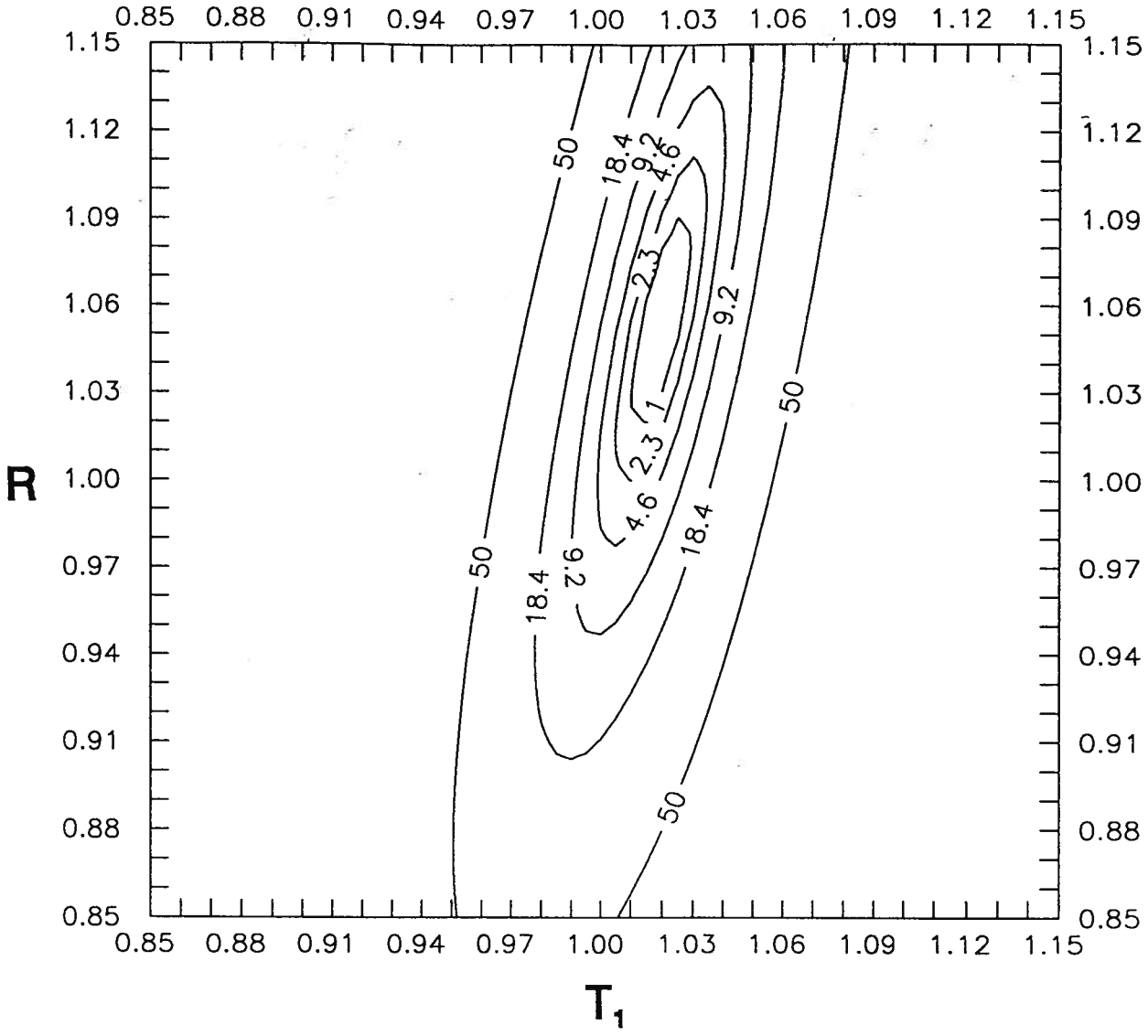

Figure 5.12 Response surface for T_1-R parameter set using head and incorrect prior information on T_1

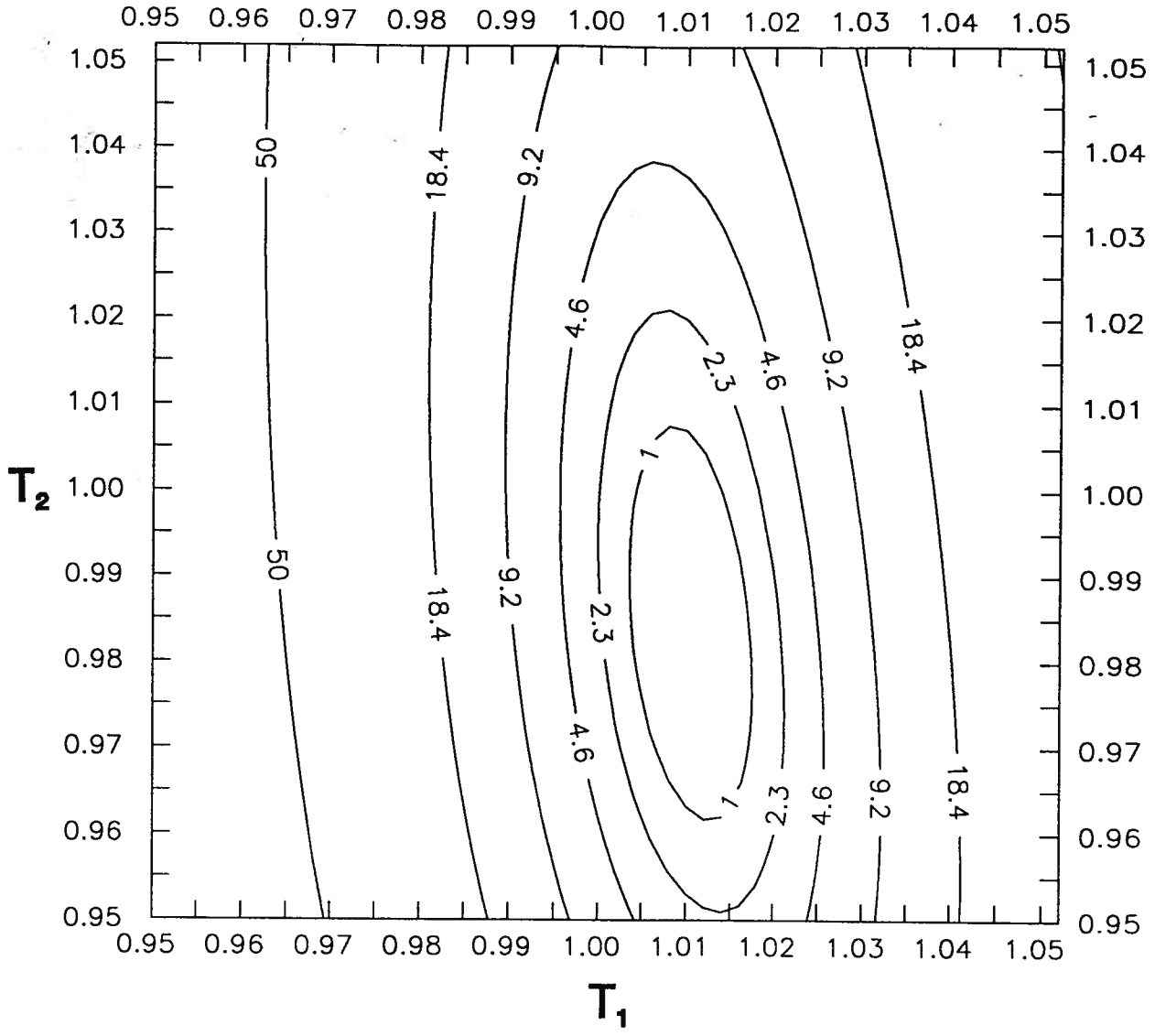

Figure 5.13 Response surface for T_1-T_2 parameter set using head and incorrect prior information on parameter T_2

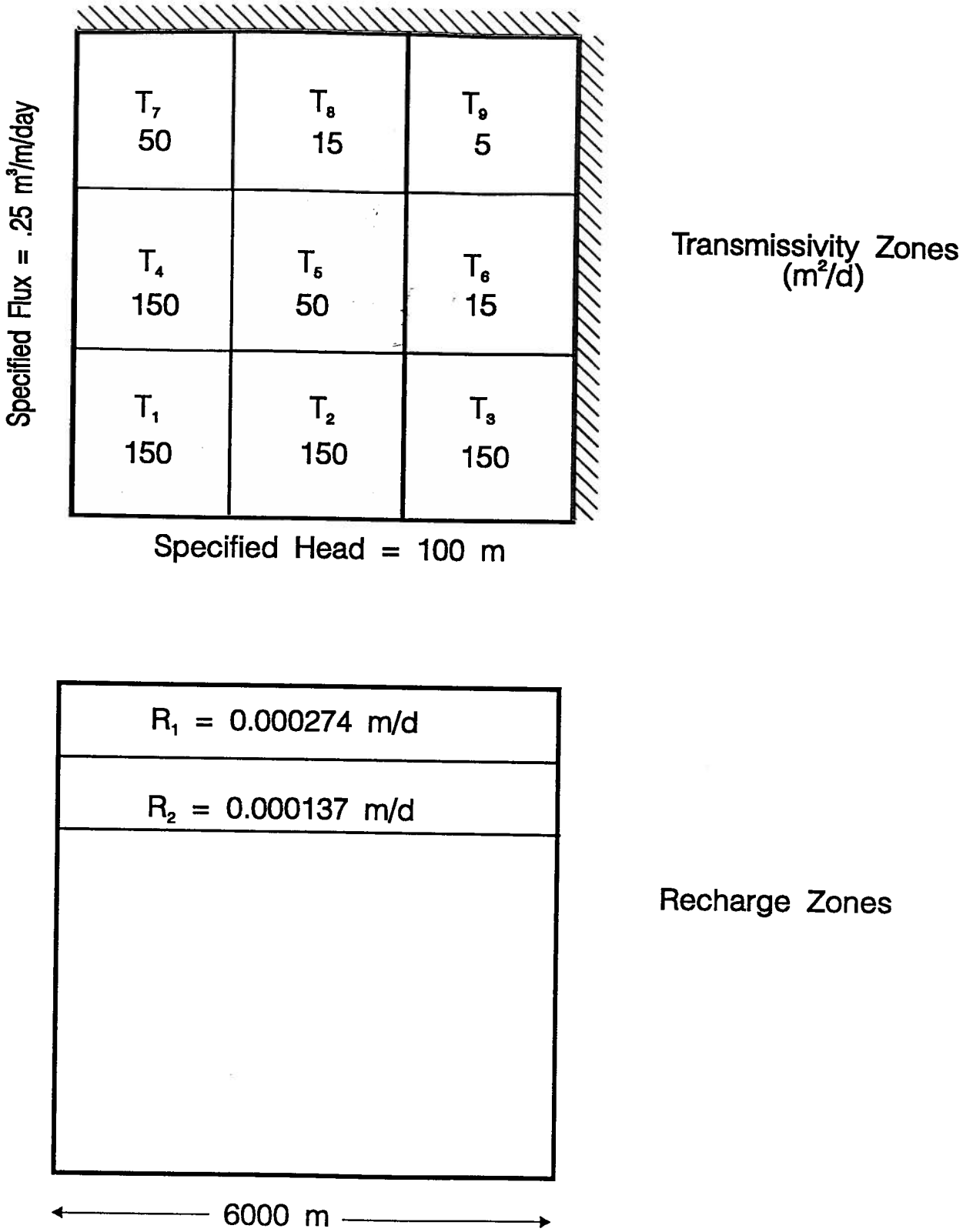

Figure 5.14 Multi-parameter synthetic flow system showing arrangement of transmissivity and recharge zones

CHAPTER 6. PARAMETER SPACE METHODS IN JOINT PARAMETER ESTIMATION

Parameter estimation for hydrogeological models using hydraulic head data is frequently plagued by difficulties due to the ill-posed nature of the inverse problem. In Chapter 5, guidelines were developed for using prior information to overcome these difficulties in an efficient and responsible manner. Joint parameter estimation provides another method for overcoming these difficulties. Incorporating a second set of observation data of a different data type through joint parameter estimation may assist in stabilizing the inverse problem.

Joint parameter estimation extends the concept of single state parameter estimation by incorporating more than one set of observation data in the parameter estimation process. In this thesis, the two data sets are hydraulic head data and tracer concentration data. The tracer concentration data is used to help estimate the flow parameters. Transport parameters are not estimated, and need to be specified. However, effects of errors in the specified transport parameters can be evaluated. The governing equations and boundary conditions for the simulation of flow and mass transport have been introduced in Chapter 1. This chapter examines joint parameter estimation in the context of parameter space analysis.

Three issues in joint parameter estimation are examined in this chapter. First,

parameter space analysis is used to show how the two data sets interact to yield improved parameter estimates. Second, parameter space information can be exploited to determine a priori if a future data set will improve parameter estimates significantly, before the second data set is collected. The third issue explored is the weighting of the different data sets in joint estimation. Four methods of weighting data sets for the purposes of minimizing parameter uncertainty with the available data are presented and evaluated.

6.1 Parameter space analysis of multiple data sets

Parameter space analysis is useful for understanding how two data sets interact to produce an improved set of parameter estimates. This improvement is manifested in a better conditioned, more stable set of parameter estimates with a smaller parameter confidence region. The hydraulic head data set defines a response surface. If the model parameters are poorly conditioned, the response surface will contain a valley with a flat bottom. The response surface defines the parameter confidence region for the head data. A second data set, the tracer concentration data, defines a new response surface. The total response surface used in joint estimation is the sum of the individual response surfaces. If the tracer concentration response surface has a shape and orientation that is significantly different from the head response surface, then the total response surface will be better conditioned than the initial head response surface. If the tracer concentration response surface has a shape and

orientation that is similar to the head response surface, then the parameter confidence region will not be reduced significantly.

The confidence regions defined by the response surfaces can be approximated by the linearized confidence ellipsoids (Equation 4.4). The difference in orientation of the confidence regions for the two data sets can be expressed in terms of their confidence ellipsoids. The angle between the longest axes of the two confidence ellipsoids can be used to approximate the difference between the two confidence regions. This angle, called the angle of interaction (β), can be calculated using:

$$\cos(\beta) = U_{h,l} \cdot U_{c,l}$$

where $U_{h,l}$ is the unit vector corresponding to the longest axis of the confidence ellipsoid using the head data set, and $U_{c,l}$ is the unit vector corresponding to the longest axis of the confidence ellipsoid using concentration data set. A small angle of interaction represents confidence regions with similar orientations, while a large angle of interaction represents confidence regions with very different orientations. The larger the angle of interaction, the greater the potential increase in stability and decrease in the uncertainty of the parameter estimates using the joint data set over the initial data set.

6.1.1 Demonstration using a two parameter set

The five parameter synthetic flow system introduced in Chapter 5 is used to

demonstrate response surface analysis for multiple data sets. Tracer transport is simulated within this flow system. A specified concentration is introduced along the inflow head boundary, and the tracer concentrations are measured at the same locations as the head data after 500 days. For this simulation, all units are assigned an effective porosity of 0.2, and the specified concentration parameter values are α_L=100 m, α_T = 10 m, and c_{init} = 1.0. Figure 6.1 shows the concentration distribution throughout the flow system at 500 days. The leading edge of the plume has moved most of the way through the flow system. Some of the concentration samples, in the center of the lower permeability zone, are not sensitive to changes in the parameter values. The simulated measurements of tracer concentration are corrupted with Gaussian distributed errors with an uncertainty of 5.0%.

Response surfaces are used to show how information from the two data sets interact to produce smaller confidence regions in joint parameter estimation. Only two parameters are estimated in order to visualize the response surfaces. Response surfaces and confidence regions are discussed for two sets of parameters: (1) Set A: transmissivity zone 1 (T_1) and recharge zone (R); and (2) Set B: transmissivity zone 1 (T_1) and transmissivity zone 2 (T_2). These two parameter sets provide good examples of the influence of a second data set on the uncertainty and stability of the parameter estimates.

Table 6.1 lists the parameter estimates and uncertainties, along with the

Table 6.1 Parameter estimates and uncertainties for parameter sets A and B

	Head Data	Concentration Data	Combined Data
T_1 Estimate	1.320	1.326	1.320
R Estimate	0.00042	0.00042	0.00042
Std (T_1)	0.0498	0.0956	0.0430
Std (R)	4.4e-05	9.4e-05	3.9e-05
CV (T_1)	0.0377	0.0619	0.0345
CV (R)	0.1064	0.2120	0.0988
Average CV	0.0721	0.1370	0.0667
T_1 Estimate	1.303	1.303	1.303
T_2 Estimate	2.284	2.297	2.297
Std (T_1)	0.0102	0.0143	0.0079
Std (T_2)	0.0468	0.0089	0.0078
CV (T_1)	0.0079	0.0110	0.0061
CV (T_2)	0.0204	0.0043	0.0034
Average CV	0.0141	0.0076	0.0047

coefficient of variation, for the two parameter sets. The parameter estimates for T are given in log-transformed values, and the parameter estimates for R in units of m/d. Equal weights are assigned to each data set for joint estimation. Table 6.1 contains the estimates for both the individual data sets and the joint data sets.An average coefficient of variation is included to allow easy comparison between the data sets. This table shows that for parameter set A, the additional concentration data does not reduce the parameter uncertainties significantly, as measured by the coefficient of variation. The average CV for the combined data set is only slightly better than for the

head data set. For parameter set B, the additional concentration data does reduce the parameter uncertainties significantly. The average CV for the combined data set is much smaller than for either the head or concentration data sets. An analysis of the response surfaces shows why the two parameter sets behave differently under joint parameter estimation.

The response surfaces for parameter sets A and B are shown in Figure 6.2 and 6.3. Each figure has three parts: (a) is the response surface using only head data, (b) is the response surface using only concentration data, and (c) is the total response surface. The 68% joint confidence region is defined by the area inside the 2.3 contour of the response surface.

The response surface for parameter set A (Figure 6.2a) using only head data contains a long, narrow valley with a nearly flat bottom. The estimates of T_1 and R are highly correlated, and the parameter set is ill-conditioned. The confidence region using concentration data only (Figure 6.2b) is similar in shape and orientation to that using head data, but is larger in size. The confidence region for the combined data sets (Figure 6.2c) is slightly smaller than that for head or concentration data alone, and is very similar in shape and orientation. The angle of interaction calculated from the linearized confidence ellipsoids is 3 degrees, so the orientation of the confidence ellipsoids are very similar. Since the two confidence regions are very similar, addition of the second data set does not significantly increase the stability nor reduce the

uncertainty of the parameter estimates.

The response surface using head data only for parameter set B (Figure 6.3a) is better conditioned than that for parameter set A. A definite minimum is observed, but it still contains a valley oriented almost parallel to the T_2 axis. The confidence region using concentration data (Figure 6.3b) is oriented nearly parallel to the T_1 axis, and is smaller than the confidence region using head data. The angle of interaction for this parameter set is 77 degrees, confirming that the orientations of the two confidence regions are significantly different. The confidence region for the combined data set (Figure 6.3c) is much smaller than the confidence regions for the individual data sets. The parameter estimates are stable, and the uncertainty in the parameter estimates has decreased substantially. The data sets can be combined to yield stable, well-defined parameter estimates.

For parameter sets A and B, the addition of concentration data led to very different behaviors. With parameter set A, the concentration data did not reduce the uncertainty of the parameter estimates significantly. With parameter set B, the combined data sets resulted in stable parameter estimates with low uncertainties. The angle of interaction reflects the difference in orientation of the confidence regions.

It is often difficult to estimate both transmissivity and recharge together [eg. *Woodbury et al.,* 1987]. This analysis shows that when estimating T_1 and R

simultaneously, the head data and the concentration data contain similar information about the model parameters. Both data sets are very sensitive to the value of parameter T_1, and not very sensitive to the value of parameter R. The joint data set does a poor job in estimating the two parameters. Another example, estimating T_2 and R simultaneously, is not presented here in detail but shows a different result. For the parameter set T_2 and R, the head data and concentration data contain different information about the parameter values. The response surfaces are different in shape and orientation, with an angle of interaction of 39°, and the joint parameter estimates are more stable than either of the single state estimates. There seems to be no clear physical explanation as to why, in one case, the head and concentration data contain similar information about the parameters, and in the second case the head and concentration data contain different information about the parameters.

6.1.2 Multiple parameter dimensions

In most parameter estimation problems, more than two parameters are estimated. In these cases, the response surfaces cannot be visualized. The response surface in the form of the parameter confidence ellipsoid can be approximated. The longest axes of the parameter confidence ellipsoid correspond to the directions of maximum uncertainty in parameter space.

As with the two parameter problem, the confidence ellipsoids can be calculated

for both data sets. The topologies of the ellipsoids for the two data sets can be compared by comparing the lengths and directions of the longest axes. If the longest axis of the confidence regions for the two data sets are similarly oriented and similar in size, the second data set will not reduce the parameter uncertainties or instabilities significantly. If the longest axes are similarly oriented but of different sizes, the joint parameter estimates will be similar to those of the data set with the smaller confidence ellipsoid. If the longest axes are oriented in significantly different directions, the second data set has the potential to significantly reduce the parameter uncertainties. However, simply using the orientation as measured by the angle of interaction between the longest axes can be misleading in multiparameter estimation problems. Several axes of the confidence ellipsoid may contribute to the ill-conditioning or large uncertainties in the parameter estimates, and these other axes are not taken into account using the angle of interaction.

It may be helpful to identify the largest axes for each data set by examining the eigenspace, and then calculate the angle of interaction between each of these axes. For instance, if each confidence ellipsoid had two axes that were much longer than the others, a total of four angles of interaction would be calculated. If all angles of interaction were large, then the ellipsoids would be significantly different. If one or two of the angles were small, then the combined ellipsoid would still contain a direction where the parameter confidence had not been reduced very much. The parameter estimates may not improve significantly.

A second method of comparing the confidence ellipsoids is to compare the eigenspaces for the two data sets. The magnitude of all axes of the confidence ellipsoid for the head data set should be examined to see how many contribute significantly to the uncertainty of the parameter estimates. The relative contribution to the uncertainty of each parameter from each of these long axes can be calculated. The directions of the largest axes for the head data set are then compared to the long axes for the concentration data set. This method has the advantage of a more thorough analysis of the parameter space, leading to a better understanding of the model. However, it has the disadvantage of not producing a single number that allows the comparison between the two confidence regions. These methods are used in section 6.4, when a multi-parameter example is examined.

6.1.3 Multiple sampling periods

The above examples used tracer concentration data sampled at a single point in time for parameter estimation. These samples provide a single snapshot in time of the concentration distribution. Numerical experiments were also conducted for the tracer concentration data sampled at multiple time intervals, at 100, 500, 1000 and 1500 days, as the tracer moved through the system.

The response surfaces with the concentration data sampled at multiple time intervals are similar in shape and orientation to the response surfaces sampled at a

single snapshot in time. There are two differences between the response surfaces presented for a single sampling period and the response surfaces for multiple sampling periods. First, the response surfaces for multiple sampling periods result in smaller confidence regions, because more data exists. Second, the confidence regions for the data from the multiple sampling intervals are generally better conditioned than the confidence region for the single sampling period. For the trial with a single snapshot in time, some of the sampling locations are insensitive to changes in the parameter values. For the trial with multiple sampling periods, all of the sampling locations are sensitive to changes in parameter values for at least one sampling period. Since the response surface for each sample location is slightly different, the total response surfaces for the concentration data are somewhat better conditioned when multiple sampling periods are used. Numerical experiments were also conducted for a decaying environmental tracer, sampled at its steady state concentration distribution. The response surfaces for the environmental tracer are very similar to the response surfaces for a single snapshot in time.

6.2 Predicting the usefulness of a second data set

The use of response surfaces described above can be extended to predict how additional data will influence the uncertainty of the parameter estimates before the data is collected. The basis for this prediction is an analysis of the parameter space for both the actual data set and a proposed future data set. The initial data set will

produce a set of parameter estimates along with the parameter confidence region in the form of a response surface. The general shape of the response surface for the future data can be calculated even without knowing the actual values of the future data, although the position of the confidence region in parameter space cannot be determined until the data is collected. The superposition of the two response surfaces will produce the total response surface for both the initial data and the proposed future data, from which the size and shape of the confidence region can be calculated. If the response surfaces for the initial and future data sets are similar, the future data set will not significantly reduce the uncertainty in the parameter estimates. If the response surfaces are quite different, the addition of the future data set will improve the parameter estimates significantly.

Even though the actual values of the future data are unknown, and the value of the resulting parameter estimates are unknown, the general shape and size of the parameter confidence region can be calculated. The topology of the response surfaces (and thus the confidence regions) depend on how the data interact with the model parameters. The location of the minimum in the response surface depends on the actual data values, but the overall shape of the response surface depends on the interaction of the data with the model parameters. If the true data values are unknown, then the location of the minimum in the response surface is unknown. However, as long as the physical location of the data samples are known, the general topology of the response surface can be calculated. The size and shape of the confidence region

for the parameter estimates can then be calculated.

The general procedure is:

1. Design a model and estimate parameters based on the initial data set.
2. Use the model and parameter estimates to simulate a proposed future data set.
3. Calculate the confidence region for the future data set.
4. Compare the confidence region for the initial data set to the confidence region for the future data set, using either the angle of interaction or analysis of confidence ellipsoids.
5. Evaluate the potential reduction in parameter uncertainty based on the difference between confidence regions for the two data sets.

6.2.1 Demonstration using the T_1-T_2 parameter set

To illustrate the above method, the parameter set T_1-T_2 can be used. The initial data set consists of hydraulic head data at the 15 observation locations, with a 1 meter standard error. The proposed future data set includes 15 concentration data taken at 500 days after the source is introduced. It is assumed that the future concentration data have a 5% standard error due to measurement uncertainty. This example is similar to the one presented above, except for the assumption that the concentration data has not been collected before the process of parameter estimation.

Estimates for T_1 and T_2 are obtained using the initial hydraulic head data set (from Table 6.1). The response surface for the hydraulic head data has been presented in Figure 6.3a. These estimates of T_1 and T_2 are used in a forward model to calculate the synthetic concentration distribution, and the concentrations are sampled at the observation locations. These synthetic concentration data, with no added error, are used to estimate the parameters again. This time, the parameter estimates are not the major focus, since the estimates are the same as the estimates using the initial head data set. The parameter values obtained from the head data set were used to simulate the future concentration data, so these parameter values are recovered when using the synthetic concentration data to estimate the parameters. Instead, the parameter confidence region is the main concern. The response surface is calculated for the synthetic concentration data (Figure 6.4a). Comparison of the response surface for the synthetic concentration data to the response surface using head data (Figure 6.3a) shows that the orientation of the valley in the response surfaces are quite different. The joint confidence region (Figure 6.4b) is much smaller than either region considered separately. The point estimates are the same as for the head data alone.

The synthetic future data set will not have the same values as the actual future data set. Therefore, the parameter estimates based on the synthetic data set will not be the same as for the actual future data set. The general shape of the response surface for the actual future data set and the synthetic future data set will be similar,

although the location of the minimum are different. For example, the actual future data set may have a response surface shown in Figure 6.4c. (This response surface was generated by adding Gaussian noise to the synthetic concentration data, and thus represents a possible concentration data set.) Note that the shape of the response surface is similar to the synthetic future data set (Figure 6.4a), but the location of the minimum is different. The combined response surface for the head data set and the actual future data set is shown in Figure 6.4d. It is similar in shape to the combined response surface for the initial data set and the synthetic future data set (Figure 6.4b), but the location of the minimum is different.

In the above example, the future data set would significantly improve the parameter estimates. However, for an example using the T_1-R parameter set, the future data would not improve the parameter estimates significantly. The response surfaces for the initial and future data sets are quite similar, so the future data will not significantly reduce the parameter ill-conditioning or uncertainty. It may not be worth the expense of collecting additional data in this case.

6.2.2 Discussion of worth of future data

This section has presented a method for evaluating the worth of future data for the purpose of reducing parameter uncertainty. The size of the confidence region for the combined present data set and the proposed future data set can be evaluated.

These confidence regions are compared to determine if the future data will significantly impact the parameter uncertainties. The actual parameter estimates cannot be calculated, since the true values of the future data are unknown. Different sets of future data can be evaluated with respect to reducing parameter uncertainty.

There are two major assumptions implicit in this method. First, the model for the initial data set and the model for the future data set are the same. The model parameters and their uncertainties are being compared, so the model, including the zonation and boundary conditions must remain unchanged. The initial data set should allow the construction of a model and estimation of reasonable parameter estimates. The future data are being evaluated on their ability to improve the parameter estimates.

The second assumption is that the method is based on a linear analysis of parameter uncertainty. If the model is highly non-linear with respect to the parameters, then the confidence regions become curved and non-symmetric. In these cases, the shape of the region depends on the value of the parameter estimates. If the model is linear with respect to the parameters, then the shape of the ellipsoid is independent of the value of the parameter estimates. Evaluating the worth of future data using parameter space analysis relies on the fact that the response surface does not change significantly when the parameter values change. Even in the case where the model is highly-nonlinear in its parameters, this method may provide a first

approximation to the worth of the future data in reducing parameter uncertainty.

The above analysis allows the worth of the future data to be quantified based on its ability to reduce parameter uncertainties. The reduced parameter uncertainties will result in a model that has more accurate predictive capabilities. The benefits of the data must be weighed against the cost of collecting the data. A decision analysis framework may be used to determine the worth of the data based on the ultimate purpose of the model [*Freeze et al.,* 1990]. The future data is only worthwhile if the benefits produced by the future data exceeds the cost of the data collection.

6.3 Weighting data sets in joint parameter estimation

The key difference between joint parameter estimation and single state parameter estimation is the presence of multiple data sets. With multiple data sets, a decision must be made regarding the importance of each of the individual data sets. Each data set contains different, possibly unique, information on model parameter values and uncertainties, yet some data sets contain more information than others. The importance of each data set is manifested as a set of weights in the parameter estimation process, as in equation (3.4). The data set containing more, or better, information should be weighted more heavily than data set containing less information. However, even data sets with poor quality information may be important since they may contain unique information not found in the other data sets. It is important to

assign an appropriate set of weights to each data set in order to obtain the best set of parameter estimates possible. A well designed set of weights will extract the maximum information from each data set. A poorly designed set of weights might ignore essential information contained in some of the data sets. The use of parameter space information allows the modeller to design a set of weights during the parameter estimation process.

In this section, several methods designed to select an appropriate set of weights in a joint parameter estimation problem are investigated. An analysis of data residuals is the traditional method for weighting of the data sets in joint parameter estimation [*Gailey et al.,* 1992]. Using this method, a set of weights is selected so that the residuals for each data set have approximately equal variance. In addition, three parameter space methods are proposed to select a set of weights. These parameter space methods select a set of weights based on an analysis of the parameter space of the individual data sets. Weights can be selected to satisfy any of the following goals:

1. Maximize parameter stability for the final parameter estimates.
2. Minimize the total uncertainty of the final parameter estimates.
3. Minimize the longest axes of the parameter confidence region.

Each of the parameter space approaches are designed to accomplish different goals, and may lead to different sets of weights. All of the approaches are based on an analysis of the parameter space. The final set of weights is selected to extract the

most information from each data set with respect to the goal that is required.

6.3.1 Analysis of data residuals

The analysis of data residuals method uses the data residuals to determine the relative weights of the data sets. This method was first proposed for using both hydraulic head and prior information on parameters [*Neuman and Yakowitz*, 1979]. It has also been used with joint head-thermal data [*Woodbury and Smith*, 1988], and joint head-concentration observations [*Sun and Yeh*, 1990; *Gailey et al.*, 1992]. The weights are assigned so that the variance of the weighted data residuals for each data type are approximately equal.

The following is an outline of the above approach for two data sets. For the joint parameter estimation problem using head and concentration data the objective function is:

$$S(\boldsymbol{b}) = w_h(\boldsymbol{Y}_h - f(\boldsymbol{b}))^T \boldsymbol{V}_h^{-1} (\boldsymbol{Y}_h - f(\boldsymbol{b})) + w_c(\boldsymbol{Y}_c - f(\boldsymbol{b}))^T \boldsymbol{V}_c^{-1} (\boldsymbol{Y}_c - f(\boldsymbol{b})) \qquad (6.1)$$

where the h subscript denotes those terms relating to head data and the c subscript denotes those terms relating to concentration data. The $\mathbf{V}_h$ and $\mathbf{V}_c$ matrices contain the relative reliabilities of the data within each data set. The w_h and w_c terms are weights for each portion of the objective function, or each data set. The weights w_h and w_c are to be determined. The general procedure for determining the weights is as follows (although it varies slightly from author to author):

1. Minimize the objective function S(**b**) with $w_h = w_c = 1.0$
2. At minimum S(**b**), calculate variance of weighted data residuals for each data set separately.

$$s_h^2 = \frac{w_h S_h}{n_h} \qquad s_c^2 = \frac{w_c S_c}{n_c}$$

where S_h and S_c are the minimum of the objective function using each data set individually, and n_h and n_c are the number of data in each data set.

3. Compute the ratio of the variances.

$$Ratio = \frac{s^2_h}{s^2_c}$$

4. Adjust the weights so that the ratio of the variances is equal to one, and estimate the parameters with the new set of weights.
5. Repeat steps 2,3,and 4 until the ratio of the variances stabilizes [*Neuman and Yakowitz*, 1979] or is approximately equal to one [*Gailey et al.,* 1992]. The iterative steps are necessary because the data residuals may change with different sets of weights.
6. Calculate the final parameter estimates and uncertainties.

The key point for the analysis of data residuals method is that the weights are chosen so that the variances of the weighted residuals for each data set are approximately equal. In the examples which follow, the criterion which chooses weights based on the analysis of data residuals will be termed the RESID criterion.

6.3.2 Methods based on analysis of parameter space.

The parameter space contains information about the parameters being estimated. This information can be used to select the weights in joint parameter estimation problems. Three methods have been developed to choose the weights for each data set. Each method emphasizes a different aspect for the final parameter estimates. The three goals for the final parameter estimates are:

1. Parameter estimates with maximum parameter stability.
2. Parameter estimates with minimum total uncertainty.
3. Parameter estimates with the largest uncertainties minimized.

The sections 6.3.2.1 through 6.3.2.3 outline the concepts for each of the weighting methods, and section 6.3.2.4 outlines the procedural details for calculating the weights for all parameter space methods.

6.3.2.1 Maximum parameter stability

Stable parameter estimates have the characteristic that uncertainties in the data values do not influence the value of the parameter estimates greatly. When parameter estimates are unstable, small errors in the data values can cause large errors in the values of the parameter estimates.

Each data set has a unique response surface. Often these response surfaces

for individual data sets are somewhat unstable, containing a narrow valley. When the orientation of the valleys are different for each data set (measured using angle of interaction), the data sets can be combined to yield more stable parameter estimates. A specific combination of the data sets will produce parameter estimates with the maximum parameter stability.

In order to choose weights to obtain parameter estimates with maximum stability, the condition number (CN) of the scaled Hessian matrix is minimized. The CN for each data set is the ratio of the longest to the shortest axis of the parameter confidence ellipsoid. Using joint parameter estimation, the shape of the confidence ellipsoid will change based on the weighting of each data set in the joint problem. The weights that minimize the CN of the joint problem are to be selected.

The advantage of this weighting scheme is that the parameter estimates are as stable as possible, given the model being calibrated and the data available. Its major disadvantage is that the method may assign greater weights to the data set with a larger confidence region just to produce circular confidence regions. The method may produce stable parameter estimates with larger uncertainties than other weighting schemes.

6.3.2.2. Minimum total parameter uncertainty

The overall parameter uncertainty can be measured by calculating the volume of the parameter confidence region. To minimize the overall parameter uncertainty, the volume of this region is minimized [*Sun and Yeh,* 1985]. The volume of the region is calculated using the axes of the parameter confidence ellipsoid, with the volume proportional to the product of the lengths of the axes. During joint parameter estimation, the shape and size of the confidence ellipsoid will change based on the weighting of each data set in the joint problem. The weights that minimize the volume of the confidence region for the joint problem are identified.

The advantage of this method is that the final set of parameter estimates have a confidence region with the smallest possible volume. Having confidence region with a small volume is good, and this type of criterion is often used in experimental design for the purpose of discriminating among competing models [*Hill,* 1978]. However, the smallest volume confidence region does not necessarily lead to individual parameter estimates with minimum uncertainty. As an example, consider two confidence regions with the same volume, Figure 6.5a and 6.5b. It is apparent that the confidence region in Figure 6.5a leads to individual parameter estimates with much larger uncertainties than those in Figure 6.5b. The parameter estimates represented by Figure 6.5a are more unstable than those represented by Figure 6.5b.

Selecting weights which minimize the volume of the parameter confidence region often tends to reduce the smallest axes of the parameter confidence ellipsoid before reducing the largest axes. Reducing the smallest axes of the confidence ellipsoid reduces the volume much faster than reducing the largest axes. The result of minimizing the volume of the parameter confidence ellipsoid is that the stability of the estimated parameters is often decreased.

6.3.2.3 Minimizing longest axes of parameter confidence region.

The above weighting methods minimize either the volume of the confidence region or maximize the parameter stability, often at the expense of the other criterion. A third weighting method, selecting weights that minimize the length of the longest axes of the parameter confidence ellipsoid, strikes a compromise. When the longest axes of the parameter confidence region are minimized, the parameter estimates tend to become more stable. The individual parameter uncertainties also tend to be reduced. The requirements of maximum parameter stability and minimum parameter uncertainty are balanced. The parameter estimates based on the set of weights satisfying this criterion should be relatively stable, and have relatively small individual parameter uncertainties.

6.3.2.4 Procedure for weighting by the parameter space methods.

The procedures for all three proposed parameter space methods are similar. The differences lie in what criterion is minimized during the selection of weights. For maximum parameter stability, the CN is minimized. For minimum overall variance, the volume of the parameter confidence region is minimized. The length of the longest axis of the parameter confidence region is minimized as the third criterion.

The basis for all of the parameter space methods is that each data set produces an individual parameter confidence region. As the data sets are combined using different weights, the shape and orientation of the joint parameter confidence ellipsoid changes. For a particular set of weights, a confidence ellipsoid is obtained that minimizes the required criterion. The general procedure is:

1. Minimize the objective function S(**b**) with $w_h = w_c = 1.0$
2. At minimum S(**b**), separate the approximate Hessian matrix into two parts, each part containing only head or only concentration information.

$$\mathbf{H}_t = w_h \mathbf{H}_h + w_c \mathbf{H}_c \tag{6.2}$$

3. Scale the approximate Hessian matrices by the current parameter values.
4. Scale the approximate Hessian matrices by $\frac{1}{s_t^2}$, where s_t^2 is:

$$s_t^2 = \frac{S(\min)}{n-p} \tag{6.3}$$

where S(min) is the minimum value of the combined objective function, n is the

total number of data, and p is the number of parameters being estimated. This scaling is done so that the inverse approximate Hessian matrix reflects the linearized parameter confidence region. The s_t^2 term also represents the overall variance of the data.

5. Varying the weights between 0 and 1, search for a set of weights that minimizes the appropriate criterion. At each set of weights, decompose the total Hessian matrix into eigenvalues and eigenvectors that describe the parameter confidence ellipsoid. The square roots of the inverses of the eigenvalues are the lengths of the axes of the confidence region. These lengths are used to calculate the criteria. The three criteria are:

   (1) MINCN: minimize the CN of confidence region

$$CN = \frac{L(\max)}{L(\min)} \tag{6.4}$$

   (2) MINVOL: minimize the volume of confidence region

$$VOL = \prod_{i=1,p} L_i \tag{6.5}$$

   (3) MINLEN: minimize the length of longest axis

$$LEN = L(\max) \tag{6.5}$$

6. Using the set of weights that minimized the appropriate criteria, estimate the parameters again. Repeat steps 2 through 6 until the set of weights stabilize. Less than three iterations are generally required for the weights to stabilize.

The proposed weighting methods produce unequal weighted residuals for each data set. This is not in accordance with standard regression techniques, which demand that the weighted residuals have equal variance. However, for joint data sets, the unequal variances of the weighted residuals may be necessary. Just as the data and the model interact to define the parameter confidence region, the interaction of the data and model combine to determine the calculated variance of the data residuals. The variance of the data residuals for each data set are unique to that data set, and this variance is somewhat model dependent. Due to this model dependence, unequal variances of the weighted residuals for each data type may produce the best parameter estimates for a given model.

Because the variances of the individual data sets are unequal, the assumptions for classical weighted regression are violated. The calculated parameter variances may not be equal to, and may underestimate, the true parameter variances. In the following analysis, the parameter CV's and uncertainties are calculated based on standard weighted regression. The calculated CV's are used to compare the different weighting criteria. These calculated CV's may not be equal to the true CV's, and are used for comparison purposes only.

6.3.3 Discussion of residual vs parameter space weighting criteria

What are the advantages of using the parameter space methods rather than

the analysis of data residuals method of selecting weights? The parameter space methods are designed to use more of the information available about the model being calibrated. The set of weights is designed based on the relative information each data set carries about the model parameters. The set of weights reflects the information each data set has about all the parameters of the model.

The parameter space methods incorporate information about the shape and orientation of the individual confidence regions in weighting the data sets. The data residuals approach determines the value of each data set (and therefore the weights) by the average residual variance for that data set. Two data sets may have similar residual variances, yet their confidence regions may be quite different. If the confidence region for head data is much larger than the confidence region for concentration data, then the estimates using head data are probably further from the true values than the estimates using concentration data. The concentration data lead to better estimates, and should probably be weighted more heavily. In many cases, one set of data may provide better information on one of the parameters, while the second set of data provides better information on other parameters. The parameter space methods allow the selection of weights based on the information each data set has about all the model parameters.

The parameter space methods can also adapt the weights to changes in the model or parameter set being calibrated. If the model being calibrated is altered, or

the number of parameters being estimated is changed, the response surface for the parameter estimates will change. These different response surfaces result in different confidence regions, and parameter space methods can adapt the weights to the information contained in these confidence regions. In section 6.3.4.1, an example is presented to show how the parameter space criteria adapt the weights to changes in the model. In Chapter 7, a flow model is calibrated for two different parameter sets, illustrating how the parameter space criteria adapt the weights to different numbers of parameters being estimated.

6.3.4 Comparison of weighting criteria

The four weighting criteria can be compared using the synthetic flow and transport system introduced earlier. Only two parameters are estimated; T_1 and T_2. The residual variances for each data set are approximately equal ($s_h^2 = 0.95$; $s_c^2 = 0.96$). Gaussian random noise at a specified level of uncertainty was used to produce the data set, and the data covariance matrix is chosen to reflect these known data uncertainties. This choice results in residual variances for each data set which are approximately equal to 1.0. Therefore, using the RESID criterion, the two data sets would be weighted equally. Figure 6.3a and 6.3b, introduced earlier, are the response surfaces for head and concentration data respectively.

When the parameters are estimated with the joint data set, any of the four

Table 6.2 Parameter estimates and uncertainties for joint parameter set using four different weighting criteria

	Weighting Criteria					
	Head Data	Tracer Data	RESID	MINCN	MINVOL	MINLEN
w_h	1.00	0.00	1.00	1.00	0.65	1.00
w_c	0.00	1.00	1.00	0.21	1.00	0.40
T_1 Estimate	1.303	1.303	1.303	1.302	1.303	1.302
T_2 Estimate	2.284	2.297	2.297	2.296	2.297	2.297
Std (T_1)	0.0102	0.0143	0.0079	0.0074	0.0082	0.0070
Std (T_2)	0.0468	0.0089	0.0078	0.0121	0.0076	0.0097
CV (T_1)	0.0079	0.0110	0.0063	0.0054	0.0063	0.0055
CV (T_2)	0.0204	0.0040	0.0034	0.0052	0.0032	0.0039
Average CV	0.0142	0.0075	0.0049	0.0053	0.0048	0.0047
CN	2.94	3.01	1.87	1.24	2.07	1.39
Volume of Region	2.00e-04	4.30e-05	2.60e-05	2.95e-05	1.99e-05	2.48e-05
L_{max}	2.40e-02	1.14e-02	6.90e-03	6.06e-03	6.44e-03	5.80e-03

criteria for choosing weights may be used. Table 6.2 shows the weights, the parameter estimates and uncertainties for the four sets of weights. Figure 6.6a.,b.,c. and d. show the total response surfaces for the parameter estimates using the RESID, MINCN, MINVOL, and MINLEN criterion respectively.

The MINCN criterion produces a parameter confidence region that is the most circular with the smallest CN, at the expense of larger parameter uncertainties (Figure 6.6b). The parameter estimates based on the MINCN criterion have the largest volume parameter confidence region, the longest length of the maximum axis, and the largest average CV of any of the weighting schemes. The MINCN criterion weights the head data set more heavily than the concentration data set in order to obtain the most rounded confidence region. Because the head data set has larger parameter uncertainties the confidence region for the joint parameter estimates using the MINCN criterion weights is large.

The MINVOL criterion weights the concentration data set more than the head data set (Figure 6.6c). This criterion results in a confidence region with the smallest volume, but the parameter set has a larger condition number than any other criterion. The MINLEN criterion weights the head data set more than the concentration data set (Figure 6.6d), but not as severely as the MINCN criterion. The resulting parameter estimates have a relatively small CN and volume of the confidence region. The average CV of the parameter estimates using the MINLEN criterion is the lowest. The

RESID criterion creates a parameter confidence region that is nearly as small as the MINVOL and MINLEN criterion. The parameter estimates for the MINLEN, MINVOL and RESID criterion are not significantly different.

6.3.4.1 Adaptability to changes in the model

One way to illustrate the adaptability of the parameter space methods is to change the model being calibrated. The same flow and transport system as above is used, and the same parameters (T_1 and T_2) are estimated. The model is changed so that the inflow boundary is a specified flux boundary rather than a constant head boundary. The specified flux is calculated to produce the same head distribution throughout the modelled area as the constant head boundary, and this flux value is specified with no uncertainty. The data set used for parameter estimation is the same as the original data set. This model is called the alternate model. The parameters T_1 and T_2 are estimated, first using the head and concentration data sets individually. The parameters are then estimated using the four weighting criteria to determine the weights for the joint data set.

Figures 6.7a and b show the response surfaces for the individual data sets for the parameter set T_1-T_2 using the alternate model. The parameter estimates and the confidence regions are very different from the original model, even though the same parameters are being estimated with the same data set. The data yield different

information about the model parameters because the model boundary conditions are different. The head data alone produce much better parameter estimates than the concentration data alone. In fact, the concentration data alone are virtually non-identifiable with respect to the two parameters being estimated. Because the confidence regions are different, the set of weights required to minimize the parameter space criteria are different.

Table 6.3 contains the parameter estimates, uncertainties, CV's for the individual data sets and the joint data sets using the four weighting criteria. The response surfaces for the RESID, MINCN and MINVOL criteria are shown in Figure 6.8a,b and c respectively. The RESID criterion yields the same set of weights (w_h = 1.0, w_c = 1.0) as the original model. However, the same set of weights does not produce the same parameter estimates or confidence region for the joint data set. The alternate model yields parameter estimates with smaller confidence regions for the joint data set than the original model when using RESID or MINLEN weighting criteria.

Using this alternate model, each of the parameter space criteria produce different sets of weights. The MINCN criterion (Figure 6.8b) weights the concentration data more than the head data, even though the concentration data alone yields a non-identifiable parameter set. The shapes and orientations of the confidence regions dictate that weighting the concentration data more than the head data results in a joint confidence region that is as round as possible. The MINVOL criterion (Figure 6.8c)

Table 6.3 Parameter estimates and uncertainties for joint data set using four weighting criteria for the alternate model

	Weighting Criteria					
	Head Data	Tracer Data	RESID	MINCN	MINVOL	MINLEN
w_h	1.00	0.00	1.00	0.05	1.00	0.98
w_c	0.00	1.00	1.00	1.00	0.10	1.00
T_1 Estimate	1.303	1.225	1.301	1.299	1.303	1.301
T_2 Estimate	2.299	2.225	2.300	2.301	2.299	2.300
Std (T_1)	0.0086	7.0700	0.0059	0.0076	0.0059	0.0059
Std (T_2)	0.0045	7.0700	0.0033	0.0065	0.0031	0.0033
CV (T_1)	0.0066	5.9000	0.0045	0.0058	0.0045	0.0045
CV (T_2)	0.0020	3.1600	0.0014	0.0028	0.0013	0.0014
Average CV	0.0043	4.5300	0.0030	0.0043	0.0029	0.0030
CN	6.92	588	4.58	2.21	6.32	4.58
Volume of Region	6.60e-06	6.50e-01	4.65e-06	1.67e-05	3.66e-06	4.65e-06
L_{max}	6.70e-03	7.11e+00	4.60e-03	6.08e-03	4.87e-03	4.60e-03

weights the head data more than the concentration data, resulting in a joint confidence region that has the minimum volume. However, the MINVOL criterion produces parameter estimates with the largest CN. For this alternate model, the MINLEN criterion results in the same set of weights as the RESID criterion. The MINLEN criterion and the RESID criterion result in parameter estimates that balance the need for parameter stability and minimum volume of the joint parameter confidence region.

This alternate model example simply demonstrates that even when estimating the same parameters with the same data set, the confidence regions can be very different. Under the RESID weighting criterion, the weights are unchanged, but the confidence regions are different. Under the parameter space criteria, the weights change in response to the change in confidence regions. The weights change because the parameter space methods recognize the change in information available from each data set.

6.3.5 Discussion of results from four weighting criteria

The parameter space methods presented above offer an alternative to the data residuals weighting method for joint parameter estimation. The parameter space methods have the apparent advantage of incorporating information about parameter confidence regions. From a conceptual standpoint, the MINLEN criterion would seem to result in the most sensible set of parameter estimates. It balances the need for

maximizing parameter stability and minimizing the total parameter uncertainty.

In examples presented, the MINCN criterion often resulted in parameter estimates with the largest uncertainties. This was a direct result of the MINCN criterion minimizing the condition number at all costs. The MINVOL criterion did result in minimizing the volume of the joint parameter confidence region, but the parameter estimates often had the largest condition numbers. The MINLEN criterion generally resulted in the parameter estimates with the lowest average coefficient of variation. The volume of the confidence region and the condition number of the parameter set were both usually small.

The RESID criterion also performed well, as measured by the average coefficient of variation, volume of joint confidence region, and condition number. The RESID criterion seemed to do a good job in balancing the different criteria used to assess the parameter estimates. Based on the examples presented, as well as other examples not presented, the MINLEN and the RESID criterion seem to be the most reasonable to use for weighting data sets in joint parameter estimation. Both criteria resulted in parameter estimates which balance the need for maximizing parameter stability and minimizing parameter uncertainty.

It may be appropriate to ask why the RESID criterion performs as well as the MINLEN criterion when it doesn't include information from the parameter space. The

explanation may be that, for these lower dimensional parameter spaces, a wide range of weights produce a joint confidence region that changes in shape, but doesn't change the length of the longest axis significantly. As the weights change, the shape of the joint confidence region does change, but this change is constrained by the shape and orientation of the individual confidence regions. Though the MINLEN criterion does minimize the length of the longest axis, this minimum length is not much different than the length for any reasonable set of weights. The RESID criterion results in a reasonable set of weights, and therefore does about as good a job as the MINLEN criterion. When more than two parameters are estimated, the differences between the parameter estimates using the parameter space criteria and the RESID criteria should be greater. Examples of multi-parameter estimation are shown in the following section and Chapter 7.

6.4 Analysis of multi-parameter system using joint data sets

A multi-parameter problem was examined using only hydraulic head data in Chapter 5. The axes of the confidence region were analyzed to determine the most efficient and responsible use of prior information to stabilize the parameter set. If concentration data can be collected for this system, the additional data set may be able to significantly stabilize this parameter set. The contribution of a concentration data set is evaluated in this section.

The flow model and boundary conditions have been introduced in Chapter 5 (Figure 5.14). To simulate a concentration data set, a constant concentration conservative tracer is introduced along the western 2000 meters of the northern boundary of the recharge zones. For this simulation, all units are assigned an effective porosity of 0.2, and the specified transport parameter values are α_L=100 m, α_T = 10 m, and c_{init} = 1.0. This tracer is sampled at the 18 sampling locations at 5000 days. The standard error in the tracer concentration data is 5.0% of the concentration value. The concentration distribution within the flow system at 5000 days is shown in Figure 6.9. The potential for this data set to reduce the non-identifiability of the 13 parameter set is to be evaluated.

6.4.1 Analysis of parameter space based on concentration data set

The confidence region for the concentration data set needs to be defined. The 13 flow parameters are estimated using only the concentration data. Using the scaled Hessian matrix evaluated at the parameter estimates, the axes of the parameter confidence region are given in Table 6.4. Table 6.4 shows that axis 13 of the confidence ellipsoid is very long and nearly parallel to axis H. The orientation of this longest axis of the confidence region indicates that H is an insensitive parameter. The model has no way of detecting the value or uncertainty of parameter H using the concentration data. Table 6.5 lists the relative contribution to the uncertainty in each parameter from each axis of the confidence region. Axis 13 contributes all the

uncertainty to parameter H, and contributes some of the uncertainty to the other parameters. However, axis 12 also contributes significantly to the uncertainty of all parameters except H and R_2.

Table 6.6 contains the error ratios for parameters using the concentration data set. The error ratios for the concentration data set are generally similar in magnitude to the error ratios for the head data set, with the exception of errors in the specified head boundary. Using concentration data only, errors in the specified head boundary have no influence on the estimates of the other parameters. However, errors in the other parameters may have a large influence on the estimate of the head boundary value. The error ratios for the transmissivity parameters show no distinct pattern, unlike the error ratios using the head data only. The error ratios for the recharge parameters, especially R_1, are the largest, indicating that the estimates of the other parameters are most sensitive to errors in recharge.

In a multiparameter inverse problem, determining the difference in shape and orientation of the parameter confidence regions is more complicated than in the two parameter problem. If only the longest axes were compared, axes 13 for both data sets would be used. However, for the concentration data, axis 13 contributes mainly to the uncertainty in parameter H and gives little information on the uncertainty of the other parameters. Using head data, axis 13 gives information on the uncertainty of all other parameters except H. In this example, parameter H is weakly correlated with all

Table 6.4 Axes of parameter confidence region for multiparameter problem based on concentration data

Axis Lengths	1.2e-02	1.7e-02	3.6e-02	4.7e-02	1.1e-01	1.3e-01	1.6e-01	2.7e-01	4.5e-01	9.2e-01	1.2e+00	1.1e+01	2.2e+05
Parameters	U_1	U_2	U_3	U_4	U_5	U_6	U_7	U_8	U_9	U_{10}	U_{11}	U_{12}	U_{13}
T_1	-0.30	0.21	-0.02	0.72	-0.08	0.49	-0.11	0.26	-0.05	0.10	-0.07	0.10	0.00
T_2	0.01	0.07	0.16	0.01	-0.68	-0.44	-0.14	0.26	-0.04	0.34	0.16	0.31	0.00
T_3	0.06	-0.07	-0.18	-0.17	0.54	0.07	-0.28	0.23	0.18	0.42	0.26	0.48	0.00
T_4	-0.40	0.26	-0.23	0.18	0.29	-0.60	-0.36	-0.08	-0.25	-0.06	0.00	-0.20	0.00
T_5	0.16	-0.04	0.43	-0.21	-0.01	0.28	-0.63	0.05	-0.48	-0.08	0.08	-0.16	0.00
T_6	0.18	-0.31	-0.26	0.04	0.09	-0.09	0.27	0.69	-0.41	-0.01	0.02	-0.26	0.00
T_7	-0.51	0.20	-0.39	-0.59	-0.26	0.32	-0.02	0.13	-0.04	0.07	-0.08	-0.09	0.00
T_8	-0.21	0.36	0.63	-0.15	0.27	-0.09	0.25	0.36	0.22	0.17	-0.09	-0.24	0.00
T_9	0.14	-0.21	-0.14	0.10	-0.09	0.02	-0.26	-0.09	0.33	0.57	-0.18	-0.60	0.00
R_1	-0.59	-0.75	0.26	0.02	0.01	-0.05	-0.02	-0.02	0.07	-0.05	0.01	0.06	0.00
R_2	-0.10	0.02	0.08	0.02	0.08	0.08	0.39	-0.41	-0.55	0.56	0.19	0.00	0.00
H	0.00	0.00	0.00	0.00	0.00	0.00	0.00	0.00	0.00	0.00	0.00	0.00	1.00
F	0.07	-0.05	0.03	-0.06	0.08	-0.08	-0.03	0.00	-0.20	0.15	-0.90	0.32	0.00

Table 6.5 Relative contribution to the CV from each axis of the confidence ellipsoid using the concentration data

Parameters	U_1	U_2	U_3	U_4	U_5	U_6	U_7	U_8	U_9	U_{10}	U_{11}	U_{12}	U_{13}
T_1	0.00	0.00	0.00	0.00	0.00	0.00	0.00	0.00	0.00	0.01	0.01	0.86	0.12
T_2	0.00	0.00	0.00	0.00	0.00	0.00	0.00	0.00	0.00	0.01	0.00	0.92	0.07
T_3	0.00	0.00	0.00	0.00	0.00	0.00	0.00	0.00	0.00	0.00	0.00	0.71	0.28
T_4	0.00	0.00	0.00	0.00	0.00	0.00	0.00	0.00	0.00	0.00	0.00	0.71	0.29
T_5	0.00	0.00	0.00	0.00	0.00	0.00	0.00	0.00	0.01	0.00	0.00	0.87	0.11
T_6	0.00	0.00	0.00	0.00	0.00	0.00	0.00	0.00	0.00	0.00	0.00	0.74	0.26
T_7	0.00	0.00	0.00	0.00	0.00	0.00	0.00	0.00	0.00	0.00	0.01	0.57	0.42
T_8	0.00	0.00	0.00	0.00	0.00	0.00	0.00	0.00	0.00	0.00	0.00	0.66	0.34
T_9	0.00	0.00	0.00	0.00	0.00	0.00	0.00	0.00	0.00	0.01	0.00	0.69	0.31
R_1	0.00	0.00	0.00	0.00	0.00	0.00	0.00	0.00	0.00	0.00	0.00	0.60	0.40
R_2	0.00	0.00	0.00	0.00	0.00	0.00	0.01	0.02	0.09	0.38	0.08	0.00	0.44
H	0.00	0.00	0.00	0.00	0.00	0.00	0.00	0.00	0.00	0.00	0.00	0.00	1.00
F	0.00	0.00	0.00	0.00	0.00	0.00	0.00	0.00	0.00	0.00	0.06	0.61	0.32

Table 6.6 Error ratio matrix for multiparameter problem based on concentration data

	Parameters with Prior Information												
Estimated Parameters	T_1	T_2	T_3	T_4	T_5	T_6	T_7	T_8	T_9	R_1	R_2	H	F
T_1	1.00	0.25	0.18	-0.54	-0.55	-0.37	-0.89	-0.40	-0.16	1.61	-0.42	0.00	0.04
T_2	2.62	1.00	0.67	-2.04	-2.08	-1.41	-3.34	-1.50	-0.62	6.07	-1.58	0.00	0.14
T_3	3.73	1.34	1.00	-2.89	-2.96	-2.00	-4.75	-2.14	-0.88	8.62	-2.25	0.00	0.19
T_4	-1.17	-0.42	-0.30	1.00	0.93	0.63	1.50	0.67	0.28	-2.72	0.71	0.00	-0.06
T_5	-0.92	-0.33	-0.24	0.72	1.00	0.50	1.17	0.53	0.22	-2.13	0.56	0.00	-0.05
T_6	-1.74	-0.62	-0.45	1.35	1.38	1.00	2.21	1.00	0.41	-4.01	1.05	0.00	-0.09
T_7	-0.57	-0.21	-0.15	0.44	0.45	0.31	1.00	0.33	0.13	-1.32	0.35	0.00	-0.03
T_8	-1.66	-0.60	-0.43	1.29	1.32	0.89	2.11	1.00	0.39	-3.83	1.00	0.00	-0.09
T_9	-4.05	-1.46	-1.04	3.14	3.21	2.18	5.16	2.32	1.00	-9.36	2.44	0.00	-0.21
R_1	0.41	0.15	0.11	-0.32	-0.33	-0.22	-0.52	-0.24	-0.10	1.00	-0.25	0.00	0.02
R_2	-0.69	-0.25	-0.18	0.53	0.55	0.37	0.88	0.39	0.16	-1.59	1.00	0.00	-0.04
H	789.	663.	853.	913.	1024.	592.	455.	828.	933.	1044.	1128.	1.00	1241.
F	0.68	0.25	0.17	-0.53	-0.54	-0.37	-0.87	-0.39	-0.16	1.58	-0.41	0.00	1.00

other parameters for both data sets, but is well defined using head data alone and insensitive using concentration data alone. The longest axes cannot be compared blindly; a comparison of only the orientations of axes 13 for both data sets for the purposes of determining if a reduction in parameter uncertainty will occur would be a mistake in this case.

Table 6.5 can be used to determine which axes of the confidence ellipsoid contribute most to the uncertainty of the parameters. Axis 12 contributes the majority of the uncertainty to all parameters except H and R_2. Axis 13 contributes the majority of the uncertainty to these two parameters. To determine if concentration data can increase the stability of the inverse problem for the majority of the parameters, the angle between axis 13 (head data) and axes 12 and 13 for the concentration data need to be determined. Comparing axis 13(head) to axis 13(conc), $\beta = 89.8°$, and comparing axis 13(head) to axis 12(conc), $\beta = 82.3$. The angle of interaction is quite large for both cases, indicating the concentration data may help stabilize and improve the parameter estimates significantly.

6.4.2 Joint parameter estimation using head and concentration data sets

For joint parameter estimation, weights must be selected for each data set. These weights can be selected on the basis of any of the four criteria given in section 6.3. The weights for all criteria, along with the parameter uncertainties, CV's, and CN's

of the parameter sets, are given in Table 6.7. This table also gives the parameter uncertainties and CV's for the head data set and the concentration data set alone. The average CV for all weighting criteria are given to allow easy comparison between criteria. The RESID criterion weights both data sets equally. The MINCN criterion weight the head data much less than the concentration data, while the MINLEN and MINVOL criteria weight the concentration data much less than the head data.

The concentration data alone yields parameter uncertainties similar to those using head data alone, except for parameter H, which has an extremely large uncertainty. The large uncertainty of parameter H occurs because it is insensitive. Any combination of data sets produce parameter estimates which are much better by any criterion than the parameter estimates using individual data sets. The MINCN criterion results in parameter estimates with a low condition number, but the CV of the parameter estimates is larger than any other criterion. This behavior is typical of the MINCN criterion, which maximizes parameter stability at the expense of increasing the uncertainty in the parameter estimates. The RESID criterion results in reasonably good parameter estimates. However, both the MINVOL and the MINLEN criteria produce somewhat better parameter estimates, as measured by the average coefficient of variation. The MINLEN criterion results in the smallest average CV, yet has the largest CN of any of the criteria. It is difficult to single out one criterion as the best, because the criterion which produce smaller average CV's also produce the larger CN's.

Table 6.7 Parameter uncertainties for joint data set using four weighting criteria for multiparameter problem

	Head Data Only		Concentration Data		RESID Criteria		MINCN Criteria		MINVOL Criteria		MINLEN Criteria	
w_h	1.0		0.0		1.0		0.02		1.0		1.0	
w_c	0.0		1.0		1.0		1.0		0.19		0.10	
Parameters	Std	CV	Std	CV	Std	CV	Std	CV	Std	CV	Std	CV
T_1	5.76	2.59	7.15	2.49	0.11	0.05	0.45	0.22	0.09	0.04	0.08	0.04
T_2	5.66	2.70	16.86	3.81	0.11	0.05	0.52	0.21	0.10	0.05	0.10	0.05
T_3	5.31	2.65	12.31	2.89	0.23	0.12	0.70	0.30	0.18	0.09	0.17	0.09
T_4	5.53	2.42	2.41	1.22	0.11	0.05	0.21	0.10	0.08	0.04	0.07	0.03
T_5	5.46	3.24	2.56	1.48	0.05	0.03	0.12	0.07	0.04	0.03	0.04	0.02
T_6	5.28	4.39	3.73	2.72	0.04	0.03	0.09	0.08	0.03	0.03	0.03	0.03
T_7	5.52	3.07	4.67	2.29	0.06	0.04	0.18	0.10	0.04	0.02	0.04	0.02
T_8	5.33	4.41	5.79	3.74	0.02	0.02	0.08	0.06	0.02	0.02	0.02	0.02
T_9	5.25	7.15	5.99	7.56	0.01	0.02	0.04	0.06	0.01	0.02	0.01	0.02
R_1	3.80e-03	12.70	7.0e-05	0.254	5.3e-06	0.0199	8.0e-06	0.025	1.00e-05	0.025	1.00e-05	0.025
R_2	1.80e-03	12.63	1.6e-04	1.3	2.3e-05	0.164	2.6e-05	0.295	2.00e-05	0.162	2.00e-05	0.165
H	1.75	0.02	1.8e+06	1.8e+05	1.38	0.01	4.05	0.04	0.98	0.01	0.91	0.01
F	971.77	13.73	298.20	6.62	16.40	0.28	39.54	1.00	11.54	0.19	10.79	0.17
Average CV		5.515		1.6e+05		0.069		0.195		0.056		0.053
Condition Number	1.1e+04		1.8e+07		134.		74.		144.		148.	
Volume of Region	1.32e-16		2.6e-04		2.17e-19		6.77e-15		5.43e-20		6.53e-20	
Length of Max Axis	22.55		2.2e+05		0.3695		1.002		0.3039		0.2992	

6.4.3 Analysis of joint confidence region

Using the scaled version of the approximate Hessian matrix containing both hydraulic head and mass concentration data, evaluated at the parameter estimates, the axes of the joint confidence region can be calculated. Two aspects of this joint confidence region relating to error ratios are evaluated; the influence of errors in the transport parameters, and a comparison of the error ratios for the head and joint data sets.

For this flow system, the concentration data reduce the uncertainty of the parameter estimates significantly. However, some assumptions were made when concentration data was simulated. Additional parameters were required to simulate the concentration distribution. These parameter are the porosity of the internal zones, the source strength, and the dispersivity of the medium. All of these parameters were assigned a specified value without uncertainty. The effect of possible errors in these parameter values on the parameter estimates needs to be determined. In particular, it would be nice to know if errors in these specified parameters will lead to large errors in the estimated parameters. The linearized error ratio matrix for all parameters, including the transport parameters, must be calculated from the confidence region using the joint data set, even though these transport parameters only enter into the tracer data. If the linearized error ratios for any of the transport parameters are large,

then it may be better to estimate those parameters with large error ratios rather than specify them.

The portion of the linearized error ratio matrix, calculated using equation (5.1), containing these transport parameters is included in Table 6.8. The porosity of each transmissivity zone is defined as a separate parameter, (given as P_1 through P_9 in Table 6.8), but the longitudinal and transverse dispersivities are considered a single parameter throughout the entire flow domain. It can be seen that errors in the concentration source value contribute the most to errors in the estimated parameters. For the porosity parameters, the error ratios are generally small. However, the error ratios for lower transmissivity zones are larger than the error ratios for the higher transmissivity zones. In granular porous media, porosity is relatively easy to estimate independently of the model, and large errors in estimates of porosity are uncommon. The dispersivity parameters have very small error ratios. Large errors in the specified value of dispersivity will only lead to small errors in the estimated values of the other parameters. Estimates of dispersivities are scale dependent and usually very difficult to obtain independent of the model. The small error ratios for the dispersivity parameters means that poor estimates of the dispersivities will not introduce large errors in the estimates of the flow parameters. From this examination of the error ratio matrix, the only transport parameter that may need to be estimated is the source strength. We can cautiously state that the concentration data added significantly to the parameter stability and reduced parameter uncertainty without requiring accurate

estimates of the additional transport parameters.

Table 6.8 Error ratio matrix for transport parameters using joint data set

Estimated Parameters	Transport Parameters											
	P_1	P_2	P_3	P_4	P_5	P_6	P_7	P_8	P_9	α_L	α_T	C_{init}
T_1	0.00	-0.02	-0.01	0.01	0.02	0.06	-0.01	0.06	0.09	0.00	0.00	-3.8
T_2	0.00	-0.01	-0.01	0.00	0.01	0.04	0.00	0.04	0.06	0.00	0.00	-4.0
T_3	0.00	-0.02	-0.02	0.01	0.02	0.07	-0.01	0.07	0.10	0.00	0.00	-3.5
T_4	0.00	-0.01	-0.01	0.00	0.01	0.04	0.00	0.04	0.06	0.00	0.00	-5.8
T_5	0.00	-0.02	-0.01	0.01	0.02	0.06	-0.01	0.06	0.09	0.00	0.00	-6.8
T_6	0.00	-0.02	-0.02	0.01	0.02	0.08	-0.01	0.08	0.12	0.00	0.00	-4.7
T_7	0.00	-0.02	-0.01	0.01	0.02	0.06	-0.01	0.06	0.09	0.00	0.00	-6.9
T_8	0.00	-0.02	-0.02	0.01	0.02	0.08	-0.01	0.08	0.12	0.00	0.00	-11.1
T_9	0.00	-0.04	-0.03	0.01	0.04	0.14	-0.02	0.13	0.21	0.00	0.00	-58.2
R_1	-0.01	-0.07	-0.05	0.02	0.07	0.23	-0.03	0.22	0.36	-0.01	-0.01	-18.0
R_2	-0.01	-0.07	-0.06	0.02	0.07	0.24	-0.03	0.23	0.37	-0.01	-0.01	-19.2
H	0.00	0.00	0.00	0.00	0.00	0.00	0.00	0.00	0.00	0.00	0.00	0.00
F	-0.01	-0.09	-0.07	0.03	0.09	0.30	-0.03	0.29	0.47	-0.01	-0.01	-18.9

It is informative to compare the error ratio matrix for the parameter estimates using the joint data set to the error ratio matrix for the parameter estimates from the head data set alone. The error ratio matrix for the joint data set is shown in Table 6.9. The error ratios are generally smaller for the joint data set than for the single data sets (Table 5.12 for head data; Table 6.6 for concentration data). The error ratios for the parameter F is the exception to this generalization. Parameter F has the most uncertainty associated with its estimate during joint parameter estimation. The longest axis of the joint parameter confidence region is nearly parallel to the axis of F in parameter space, resulting in large error ratios when estimating F. The parameter confidence region for the joint data set is much smaller than the confidence region for the single data set, and much better conditioned. These two factors allow the data set to compensate for errors in prior information. However, since this joint data set is well-conditioned for the 13 flow parameters, it is not imperative to use prior information to estimate the parameter. The two data sets together will do a good job in estimating all the parameters. Prior information with uncertainty may be used to decrease the size of the confidence region, if the uncertainty in the prior information is less than the uncertainty of the parameter from parameter estimation. Errors in prior information will not have a significant effect on the final estimates, as these estimates are defined by the well-conditioned response surface for the data.

Table 6.9 Error ratio matrix for the multiparameter problem using the joint data set

Estimated Parameters	Parameters with Prior Information											
	T_1	T_2	T_3	T_4	T_5	T_6	T_7	T_8	T_9	R_1	R_2	H	F
T_1	1.00	0.02	-0.07	0.28	-0.09	-0.12	0.56	-0.74	-0.34	-0.15	-0.04	-0.26	0.11
T_2	0.06	1.00	-0.01	0.04	-0.01	-0.02	0.08	-0.11	-0.05	-0.02	-0.01	-0.04	0.02
T_3	-0.33	-0.02	1.00	-0.22	0.07	0.10	-0.45	0.60	0.27	0.12	0.03	0.21	-0.09
T_4	0.24	0.01	-0.04	1.00	-0.05	-0.07	0.33	-0.44	-0.20	-0.09	-0.02	-0.15	0.06
T_5	-0.05	0.00	0.01	-0.03	1.00	0.01	-0.07	0.09	0.04	0.02	0.00	0.03	-0.01
T_6	-0.06	0.00	0.01	-0.04	0.01	1.00	-0.08	0.11	0.05	0.02	0.01	0.04	-0.02
T_7	0.29	0.01	-0.05	0.19	-0.06	-0.08	1.00	-0.52	-0.24	-0.10	-0.03	-0.18	0.07
T_8	-0.14	-0.01	0.02	-0.09	0.03	0.04	-0.18	1.00	0.11	0.05	0.01	0.09	-0.03
T_9	-0.05	0.00	0.01	-0.03	0.01	0.01	-0.07	0.09	1.00	0.02	0.00	0.03	-0.01
R_1	-0.04	0.00	0.01	-0.02	0.01	0.01	-0.05	0.06	0.03	1.00	0.00	0.02	-0.01
R_2	-0.63	-0.03	0.10	-0.42	0.14	0.18	-0.85	1.14	0.51	0.22	1.00	0.40	-0.16
H	-0.03	0.00	0.00	-0.02	0.01	0.01	-0.04	0.05	0.02	0.01	0.00	1.00	-0.01
F	3.86	0.19	-0.61	2.58	-0.83	-1.10	5.21	-6.97	-3.15	-1.36	-0.34	-2.45	1.00

6.5 Summary

Three aspects of joint parameter estimation have been discussed in this chapter. First, response surfaces and confidence regions were used to show how multiple data sets reduced parameter uncertainty. Second, the use of confidence regions was extended to predict the value of future data in reducing the uncertainty of parameter estimates, before the data are collected. Third, parameter space approaches were introduced for selecting the weights for the individual data sets in joint parameter estimation. Four weighting criteria were compared using both simple two parameter problems and a multi-parameter problem.

Each data set produces a unique response surface and confidence region. If these surfaces are oriented differently for the two data sets, the parameter uncertainty are significantly reduced when the second data set is included. If these surfaces are similar for two data sets, the second data set will not reduce the parameter uncertainty significantly. In simple two parameter examples, the response surfaces were visualized. For multiparameter examples, the axes of the confidence ellipsoid need to be analyzed to determine the difference in orientation of the confidence regions for the two data sets.

Future data can be simulated using the model and the parameter estimates from the original data set. The confidence region for the future data set can be

estimated using these simulated data values. The confidence regions for the initial and future data sets can be compared to determine the potential reduction in parameter uncertainty for the future data set. Though the actual future data will not produce the same parameter estimates as the simulated future data, the actual future data will produce similar values for parameter uncertainty.

For weighting data sets in joint parameter estimation, the analysis of data residuals method was compared to three methods based on parameter space analysis. The parameter space based methods have the advantage of incorporating information about parameter confidence regions. Three criteria based on parameter space analysis have been proposed (minimum condition number, minimum volume of confidence region, and minimum longest axis of confidence region). Each criterion results in the "best" parameter estimates in some sense. The parameter space criteria can adapt the weights to changes in the model. The MINCN criterion often resulted in parameter estimates with the largest uncertainties, but lowest condition number. The MINVOL criterion resulted in parameter estimates with the smallest sized joint confidence region, but the estimated parameter set often had larger condition numbers compared to other weighting criteria. In the examples presented, the MINLEN criterion and the RESID criterion seemed to be the most reasonable to use for weighting data sets in joint parameter estimation. They both balanced the need for maximizing parameter stability and minimizing the total parameter uncertainty.

A multi-parameter flow system was used to demonstrate the reduction in parameter uncertainty during joint parameter estimation. The parameter set was non-identifiable using only head data. Tracer concentration data significantly reduced parameter uncertainty and ill-conditioning. Additional transport parameters were needed to simulate the tracer concentrations, but errors in the specified values of these parameters were found to lead to very small errors in the estimates of the flow parameters, based on linearized error ratio analysis. The concentration data added significantly to the parameter stability and reduced parameter uncertainty without requiring accurate estimates of the transport parameters. With respect to weighting the data sets, it was difficult determine which criterion performed the best. The MINLEN criterion resulted in the smallest average coefficient of variation, but it also resulted in the largest condition number. The RESID criterion, MINVOL criterion and MINLEN criterion all resulted in reasonably good parameter estimates.

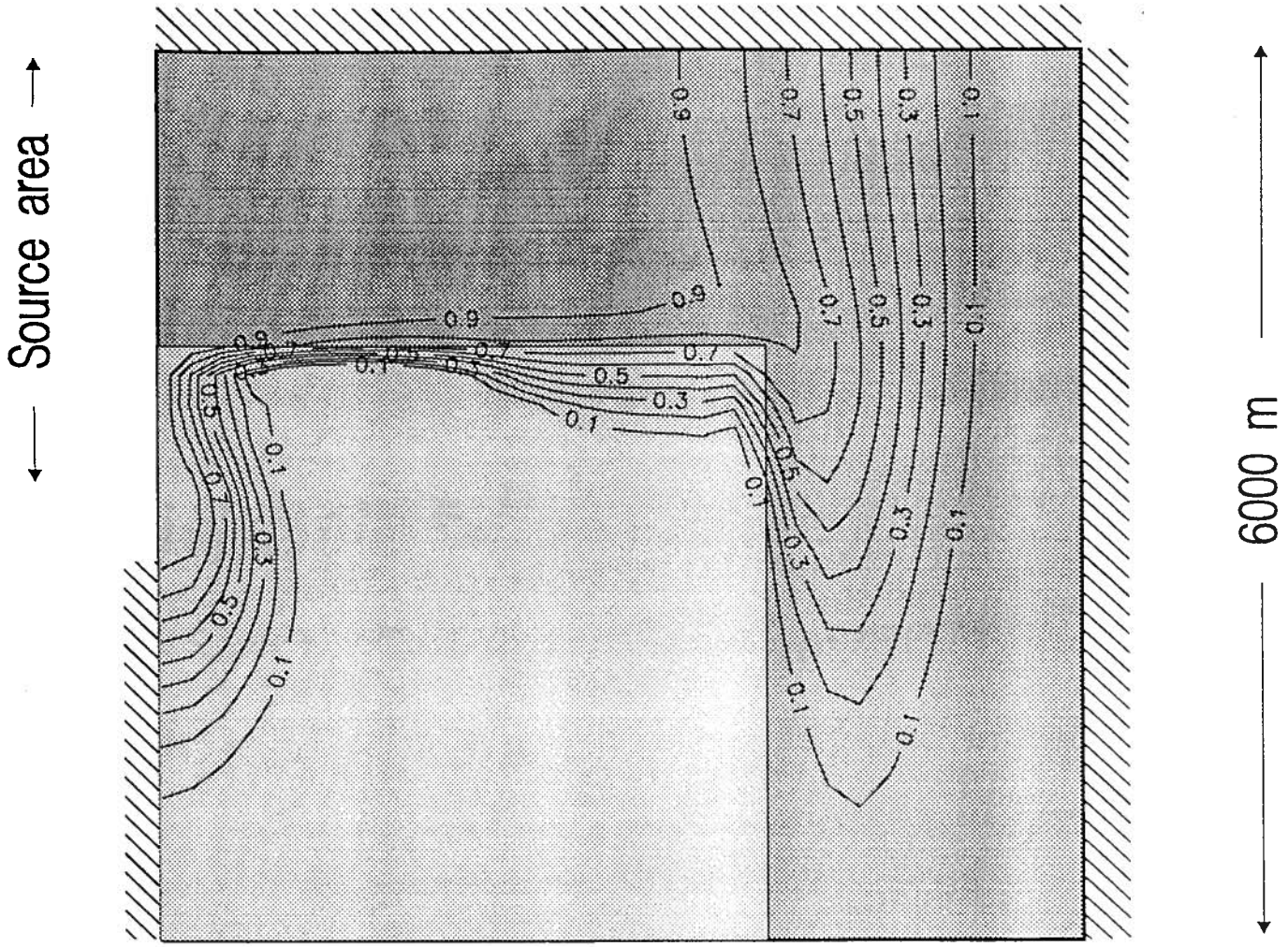

Figure 6.1 Tracer concentration distribution for 5 parameter flow system at 500 days

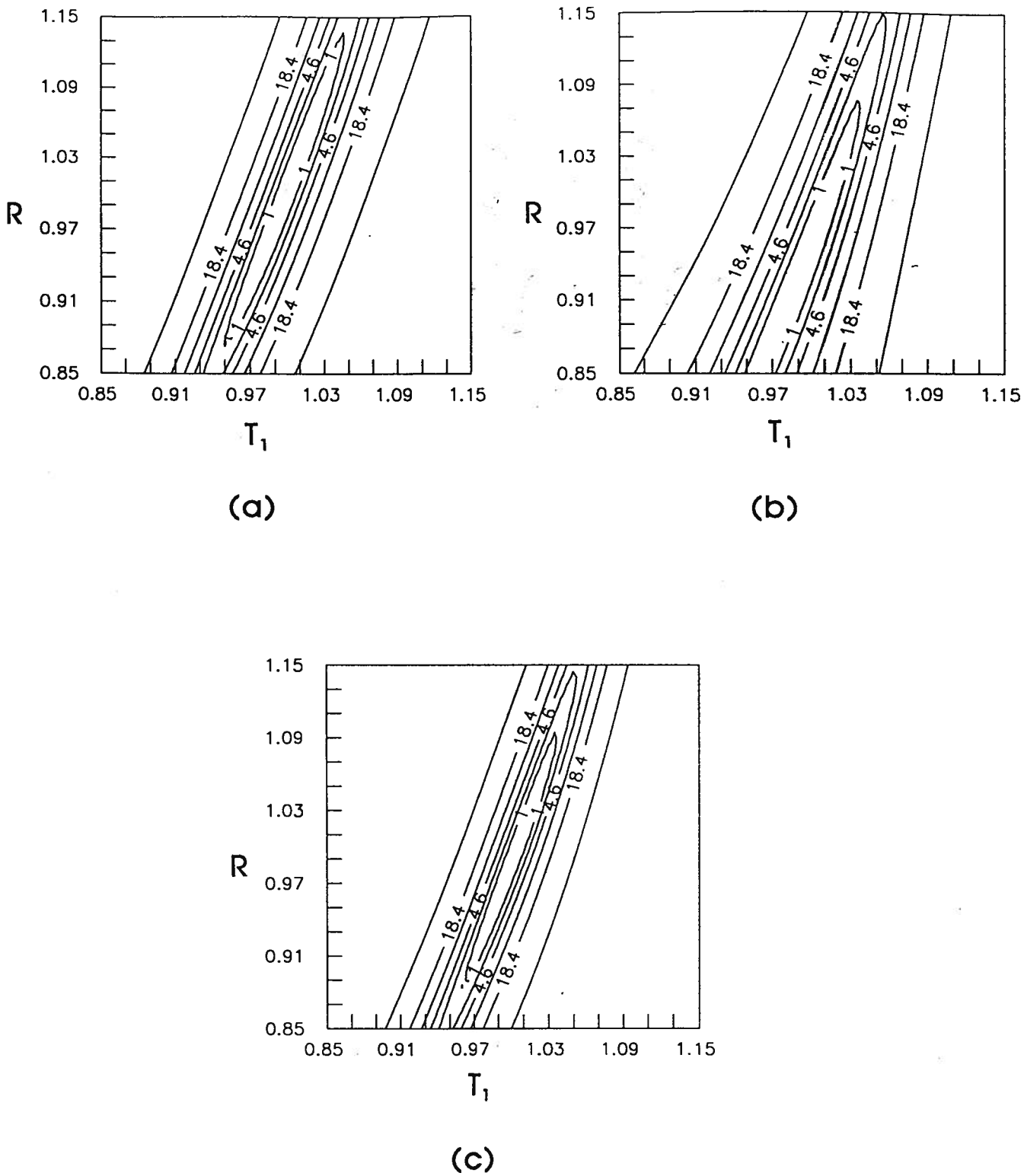

Figure 6.2 Response surfaces for parameter set A: (a) head data; (b) concentration data; (c) joint data set

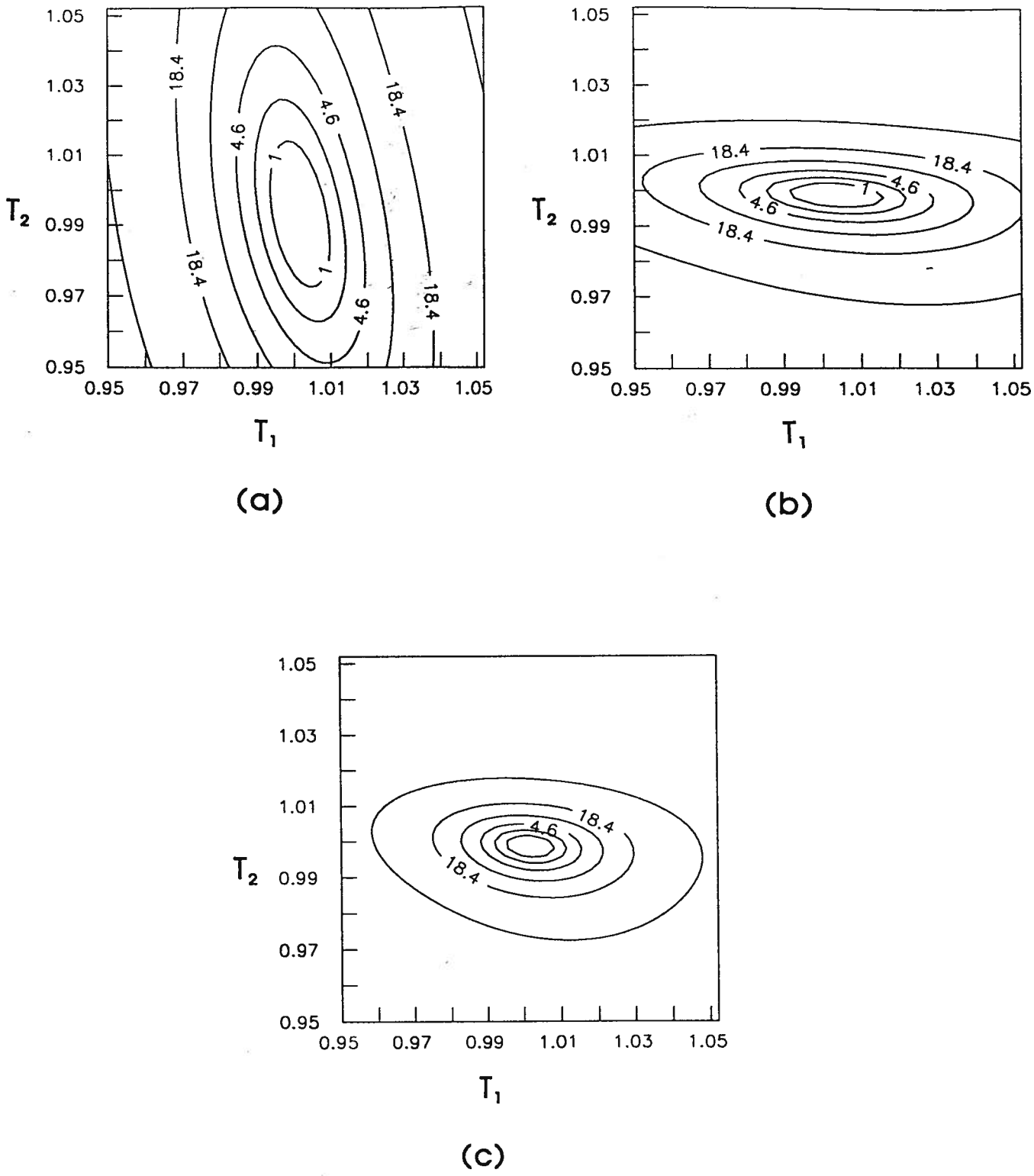

Figure 6.3 Response surfaces for parameter set B: (a) head data; (b) concentration data; (c) joint data set

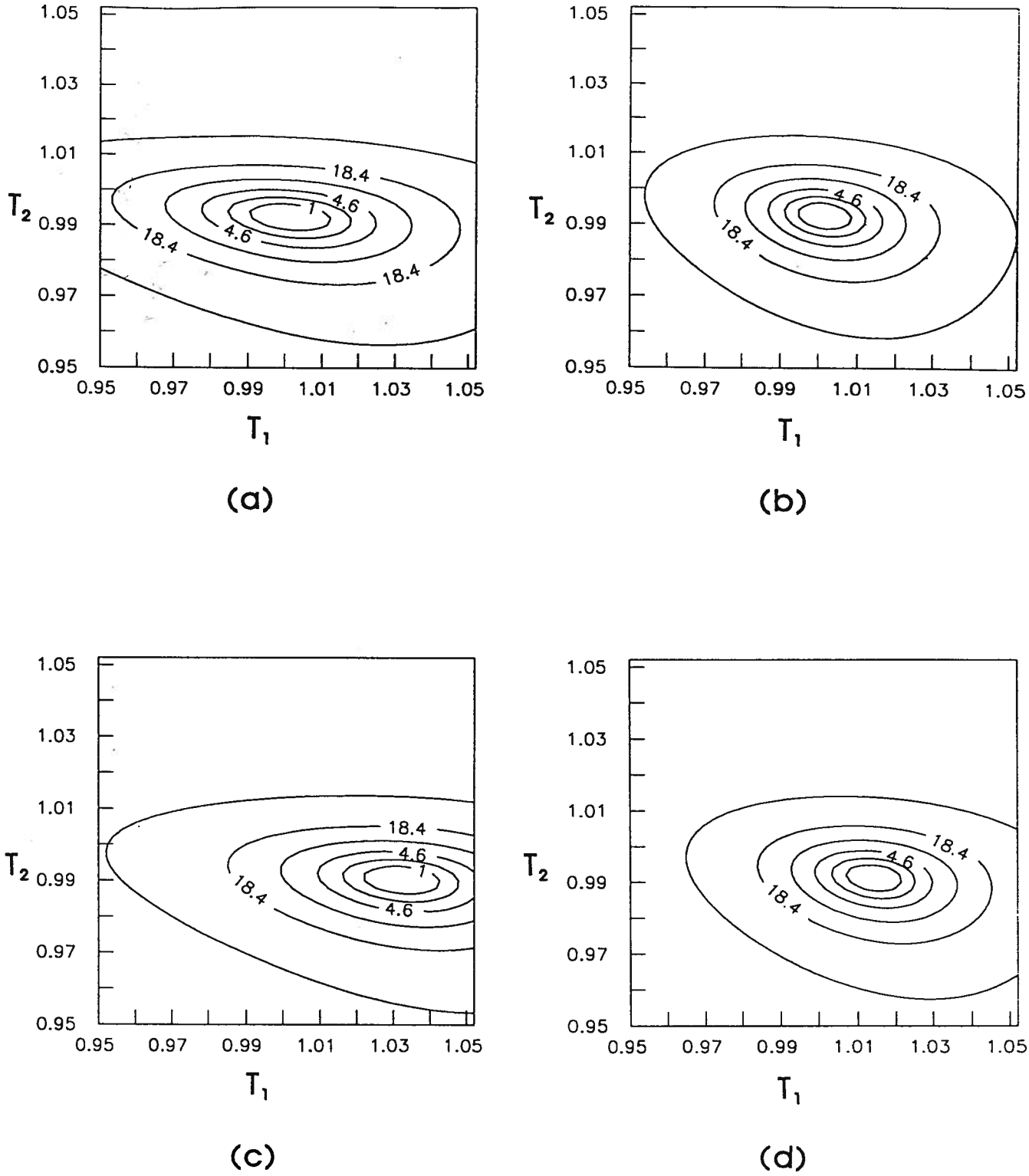

Figure 6.4 Response surfaces for T_1-T_2 parameter set: (a) synthetic future concentration data; (b) head and synthetic future concentration data; (c) actual concentration data; (d) head and actual concentration data

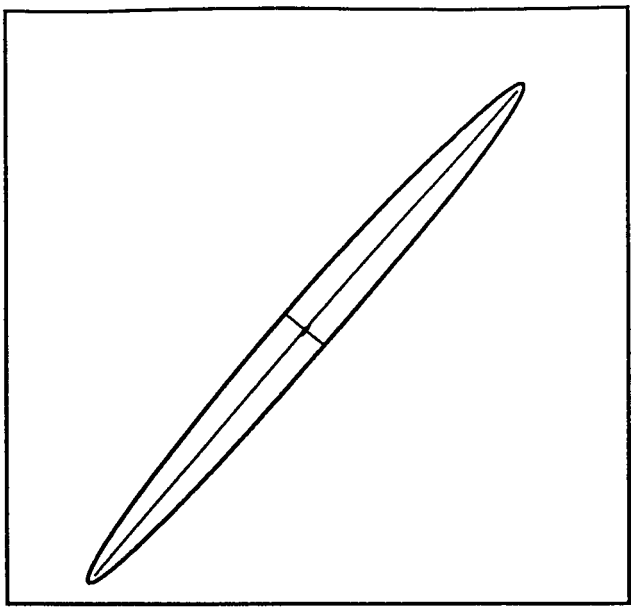

(a)

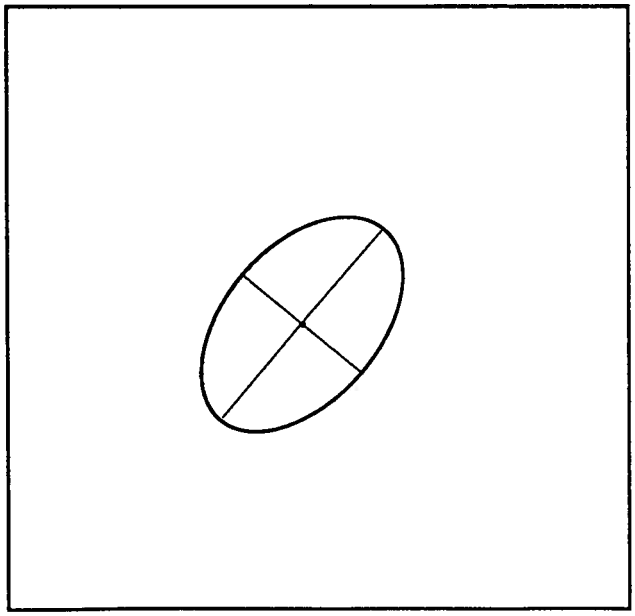

(b)

Figure 6.5 Two confidence ellipses with the same volume and orientation, but different stabilities and parameter uncertainties

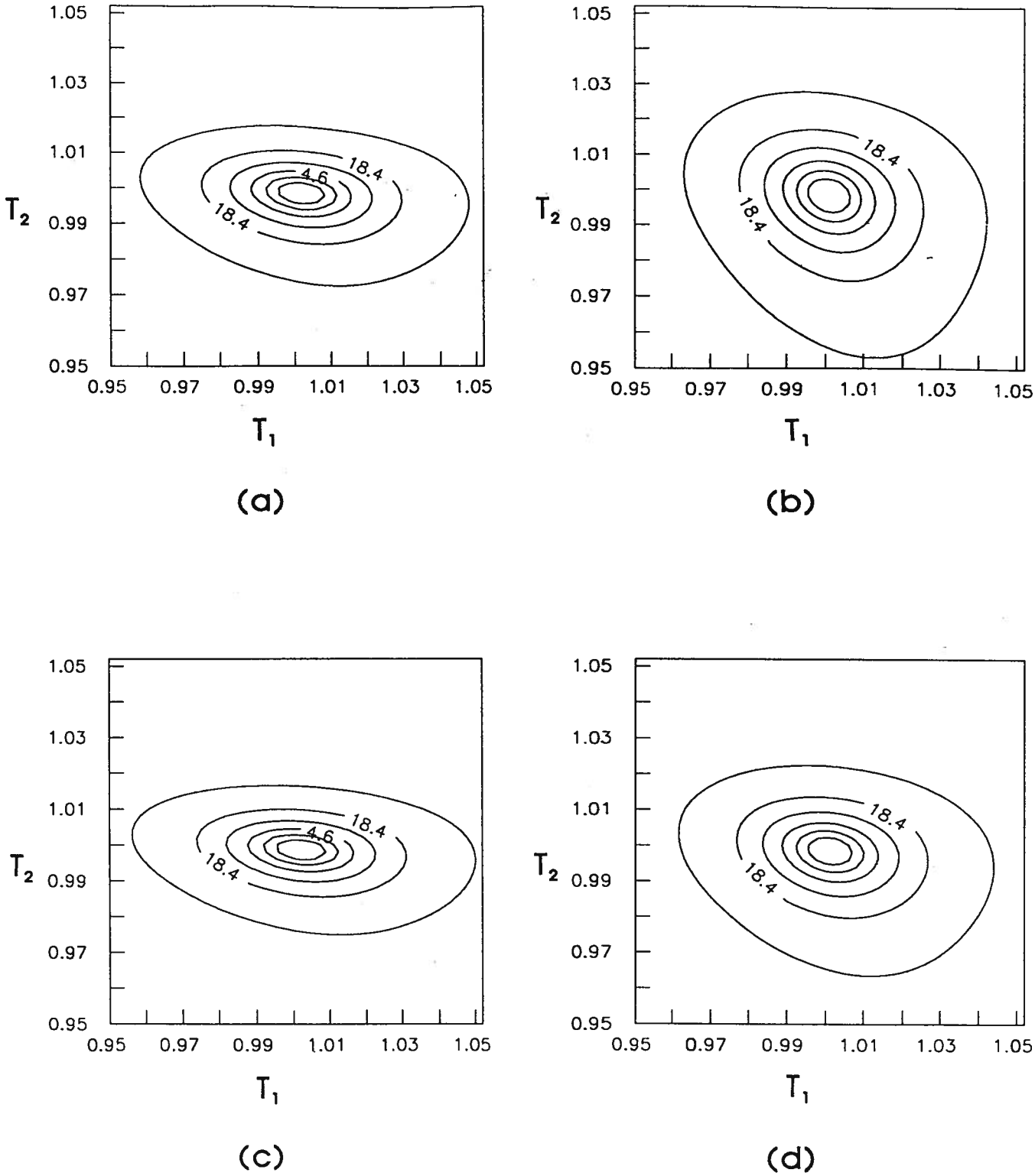

Figure 6.6 Response surfaces for T_1-T_2 parameter set using joint data sets: (a) RESID weights; (b) MINCN weights; (c) MINVOL weights; (d) MINLEN weights

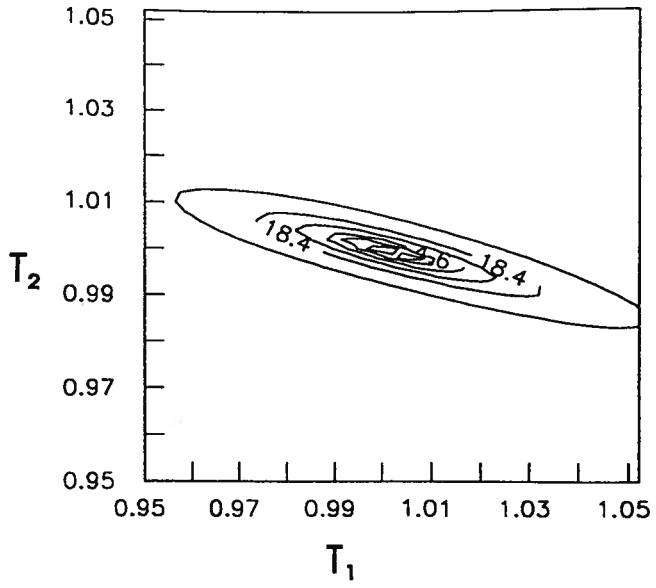

(a)

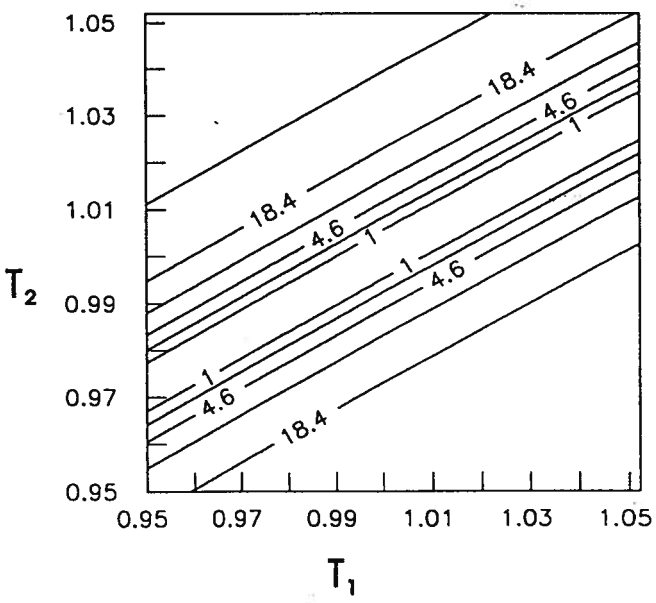

(b)

Figure 6.7 Response surfaces for alternate model: (a) head data; (b) concentration data

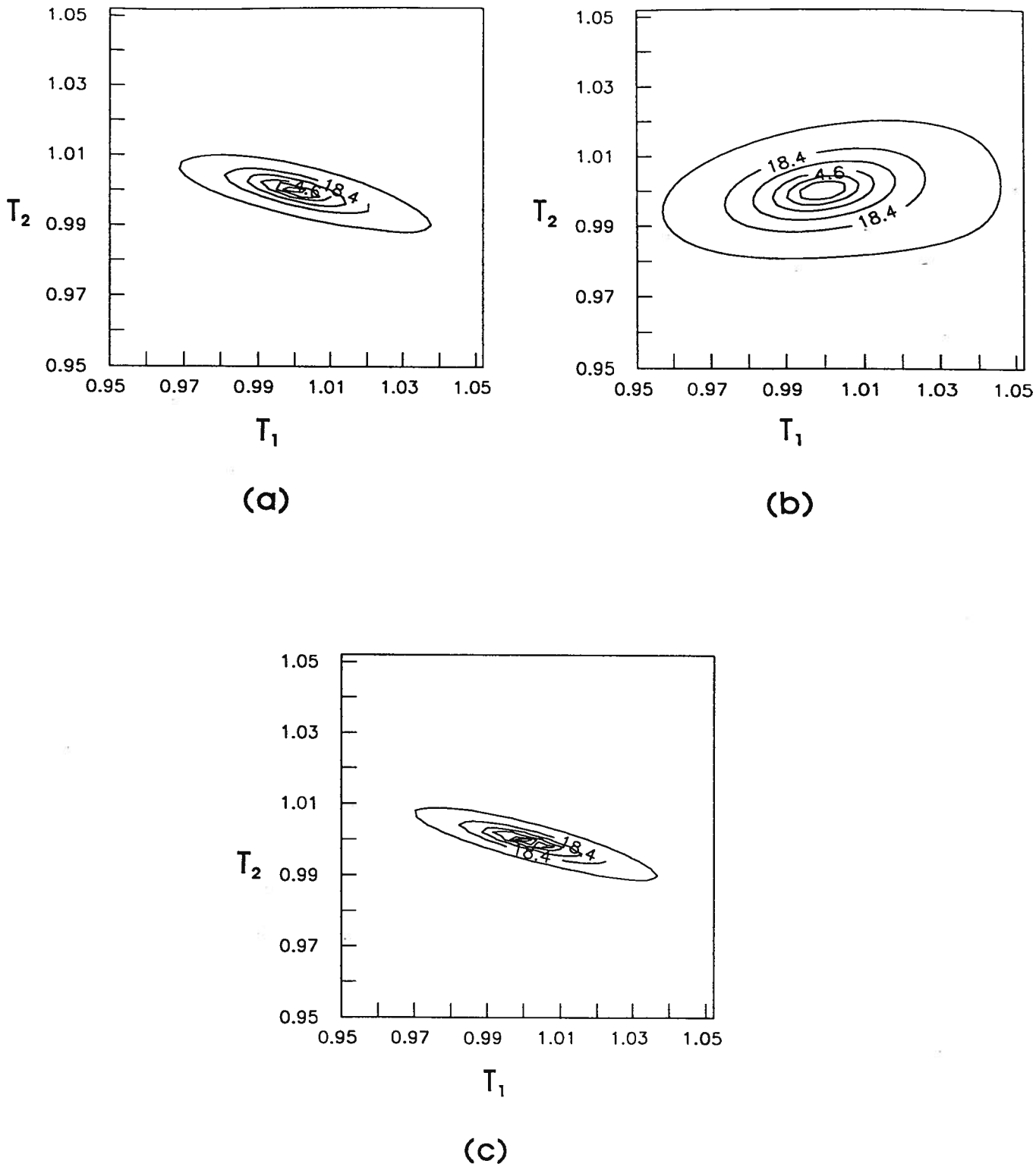

Figure 6.8 Response surfaces for alternate model using joint data sets: (a) RESID weights; (b) MINCN weights; (c) MINVOL weights

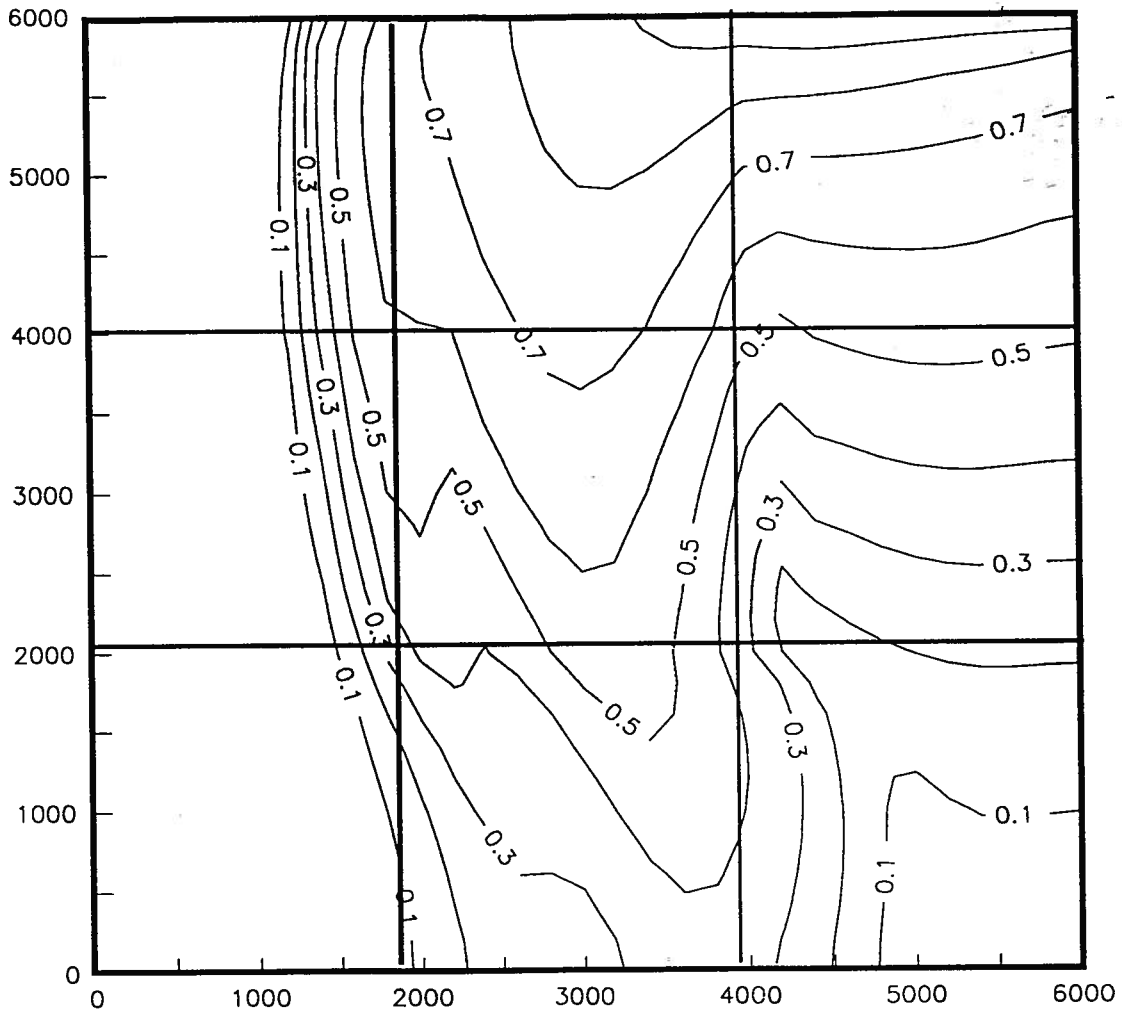

Figure 6.9 Concentration distribution for multi-parameter flow system at 5000 days

CHAPTER 7. JOINT PARAMETER ESTIMATION FOR THE SAN JUAN BASIN USING PARAMETER SPACE METHODS

In this chapter, the development and calibration of a groundwater flow model for the San Juan Basin, New Mexico, is discussed. Hydraulic head data, ^{14}C data, and prior information on parameter values are used for parameter estimation in the San Juan Basin. A cross-sectional model of the hydrogeological units in the west-central portion of the basin is constructed. The purpose of constructing the model is to demonstrate the utility of the methods developed in this thesis for calibrating a hydrogeological model in an efficient and responsible manner using joint data sets. The geology of the basin has been investigated by *Baltz* [1967] and *Fasset and Hinds* [1971]. The hydrogeology of the basin has been summarized by *Stone et al.* [1983].

7.1 Study area

The San Juan basin is a large structural basin (77000 km^2) in northwestern New Mexico and southwestern Colorado (Figure 7.1). The basin lies in a relatively flat upland region south and east of the Rocky Mountains. Altitudes range from 2400 m in the northern part of the basin to about 1550 m where the San Juan river exits the basin. The central part of the basin is a dissected plateau, the surface of which slopes gently to the west. Figure 7.1 is a plan view of the San Juan Basin, showing the surface outcrop of the major Cretaceous and Tertiary units. The line A-A' in the

southwestern portion of the basin is the line of section along which the model is constructed. The model extends from Chaco Canyon in the south to the San Juan river in the north, along the center of R10W.

The climate throughout the basin is arid to semi-arid. The rainfall in the basin is about 10 cm a year at the lower altitudes of the modelled cross section. The major stream in the basin is the San Juan River, which flows westward in the New Mexico portion of the basin. Many intermittent streams also drain the basin. The Chaco River is the largest intermittent stream, draining the southern and western parts of the basin and flowing into the San Juan on the western side of the basin.

7.2 Geology

The San Juan basin is nearly circular in plan view. It is an asymmetric structural depression which contains sedimentary rocks ranging in age from Cambrian to Quaternary. This study will concentrate on groundwater flow in the upper Cretaceous and Tertiary units of the basin. Figure 7.2 is a schematic cross section of the upper Cretaceous and Tertiary units along the modelled section.

The upper Cretaceous rocks of the basin are over 1830 m thick and consist of intertonguing marine and non-marine units that represent three basin-wide transgressive-regressive cycles of deposition. These cycles laid down the Menefee

Formation, the Cliff House Sandstone, the Lewis Shale, with the final regression of the sea resulting in the deposition of the Pictured Cliffs Sandstone. The Pictured Cliffs is overlain by two Cretaceous units of continental origin, the Fruitland Formation and the Kirtland Shale. The Tertiary rocks in the study area consist of the Ojo Alamo Sandstone and the Nacimiento Formation. The Nacimiento contains interbedded mudstone with sandstone lenses. Quaternary deposits consist of Pleistocene and Holocene terrace gravels and alluvium.

7.3 Hydrogeology

Three types of hydrogeological information are available to construct a hydrogeologic model of the basin; hydraulic head data, ^{14}C data, and direct information on parameter values.

The head data were obtained from *Stone et al.* [1983]. *Phillips et al.* [1989] kriged 24 head data in the Ojo Alamo and 26 head data in the Nacimiento to calculate the potentiometric surface for each aquifer. The head distribution indicates recharge along the outcrops and discharge to the San Juan River. The head distribution also shows that the hydraulic head contours are generally perpendicular to the modelled cross section.

For this study, all head data available in R9W, R10W and R11W from Chaco

Canyon in the south to the San Juan river in the north were analyzed for use in the cross section model. The sample locations are plotted on Figure 7.3, along with the information about which formation each well sampled. Most of the wells were completed in the Ojo Alamo and Nacimiento formations, but several were completed and sampled in lower formations. The screened intervals for the wells range from 5m to over 100m, with an average of approximately 20m. Table 7.1 contains the well data used in this study, listing a well identifier, well location, the elevation of the midpoint of the screened interval, and the hydraulic head. The well identifier consists of a number and letters. The letters indicate which formation the well was reported to have sampled. The letter identifiers are:

(q) Quaternary Alluvium

(n) Nacimiento

(o) Ojo Alamo

(k) Kirtland/Fruitland

(pc) Pictured Cliffs

(l) Lewis

(ch) Cliff House

The hydraulic head data set consists of all wells in R9W, R10W, and R11W, up to 15 km from the line of section. Figure 7.4 shows the modelled cross section, along with the midpoint of the screened interval for all wells in the head data set.

The assigned uncertainty in the head data is determined in part by the distance

Table 7.1 Hydraulic head data used for calibrating the San Juan Basin model

Well Identifier	Distance from Chaco Canyon (m)	Midpoint of Screened Interval (m)	Hydraulic Head (m)	Standard Error (m)
29n	30323.0	1993.0	2018.0	35.0
35n	27443.0	1976.0	1986.0	30.0
39n	42181.0	1833.0	1953.0	30.0
40n	42011.0	1860.0	1927.0	25.0
46n	54547.0	1857.0	1855.0	45.0
48n	47771.0	1833.0	1908.0	55.0
51n	52683.0	1822.0	1838.0	55.0
52n	47093.0	1775.0	1855.0	50.0
56n	62847.0	1840.0	1840.0	25.0
59n	67252.0	1738.0	1747.0	40.0
62n	69115.0	1654.0	1669.0	60.0
72n	75000.0	1658.0	1660.0	30.0
73n	74875.0	1652.0	1678.0	30.0
19o	25749.0	1906.0	2026.0	60.0
20o	25241.0	1915.0	2009.0	60.0
21o	25749.0	1909.0	1920.0	60.0
30o	28629.0	1928.0	1932.0	45.0
31o	33541.0	1960.0	1975.0	20.0
32o	33711.0	1857.0	1912.0	30.0
33o	32017.0	1856.0	1893.0	20.0
34o	27443.0	1924.0	1930.0	20.0
36o	33711.0	1920.0	1920.0	55.0
37o	40656.0	1845.0	1930.0	35.0
38o	40148.0	1810.0	1887.0	35.0
41o	40487.0	1870.0	1935.0	20.0
43o	37099.0	1816.0	1889.0	20.0

Table 7.1 (continued)

Well Identifier	Distance from Chaco Canyon (m)	Midpoint of Screened Interval (m)	Hydraulic Head (m)	Standard Error (m)
44o	39809.0	1846.0	1876.0	55.0
45o	45230.0	1812.0	1850.0	60.0
52o	47093.0	1773.0	1855.0	50.0
61o	69285.0	1625.0	1658.0	55.0
74o	74028.0	1526.0	1654.0	60.0
53q	46416.0	1880.0	1880.0	45.0
68q	74738.0	1663.0	1663.0	30.0
69q	74399.0	1679.0	1683.0	30.0
70q	74044.0	1710.0	1719.0	20.0
4q	4743.0	1949.0	1946.0	30.0
16q	8131.0	1874.0	1874.0	30.0
17q	7623.0	1871.0	1871.0	30.0
25q	17448.0	1957.0	1956.0	30.0
26q	17787.0	1957.0	1956.0	30.0
8k	11180.0	1862.0	1862.0	50.0
10k	15754.0	1839.0	1893.0	20.0
12k	14568.0	1902.0	1915.0	20.0
13k	12197.0	1876.0	1894.0	25.0
14k	12366.0	1872.0	1891.0	30.0
15k	11858.0	1833.0	1880.0	30.0
20k	25241.0	1825.0	1935.0	60.0
27k	25579.0	1320.0	1787.0	60.0
58k	57765.0	1576.0	1737.0	40.0
1ch	4913.0	1826.0	1898.0	35.0
2ch	4913.0	1664.0	1852.0	50.0
6pc	14399.0	1815.0	1938.0	60.0
9ch	11350.0	1619.0	1731.0	50.0
11pc	14399.0	1798.0	1882.0	25.0
18ch	11180.0	1821.0	1849.0	45.0

of the well from the line of cross-section. This uncertainty has several sources, all of which contribute to the modelled data not matching the measured data exactly. Some of these sources are: (1) an uncertainty about which vertical point in the aquifer is sampled due to the length of the screened interval of the well; (2) an uncertainty due to the fact that the wells do not lie on the line of section; and (3) the uncertainty due to the natural variation in hydraulic conductivity and other parameters within each unit, which is present in the field but not included in the model. For wells within 0.8 km (one section) of the line of the cross-section, the standard error of measurement is 20 meters. For wells further from the line of the cross-section, the standard error of measurement is 20 meters, plus 5 meters for each section (approximately 1.6 km) away from the cross section. This method of assigning uncertainty based on the distance from the modelled section is rather arbitrary, but qualitatively seems to be a reasonable method of assigning uncertainty in a cross sectional model. The baseline uncertainty of 20 m may seem to be large for measurements of hydraulic head, but it is consistent with the large scale of the model. Table 7.1 also contains the assigned standard error of measurement for each well.

The ^{14}C data were obtained from *Phillips et al.* [1989] and *Shute* [personal communication, 1994]. These data are available only in the Ojo Alamo and Nacimiento formations. The ^{14}C data available in R9W, R10W, and R11W were used for this study. Table 7.2 contains the ^{14}C data, reported in percent modern carbon, along with the well locations and midpoint of the sampling interval. Some of the wells sampled

Table 7.2 The ^{14}C data used to calibrate the San Juan Basin model

Well Identifier	Shute Well Number	Phillip Well number	Distance from Chaco Canyon (m)	Midpoint of Screened Interval (m)	C-14 [Shute] (pmc)	C-14 [Phillip] (pmc)	Standard Error
28n		SJB-24-O	35405	1934		51.2 ± 0.6	9.1
39n	NM05	SJB-22-N	42181	1833	12.6	12.3 ± 0.5	2.3
40n	NM22		42011	1860	19.9	-----	2.5
48n	NM07	SJB-35-N	47771	1833	8.39	9.2 ± 0.4	4.4
81n	NM01	SJB-21-N	67500	1553	1.4	<1.73	0.5
82n	NM08		57700	1681	4.49	-----	3.9
20o	NM10		25241	1915	37.9	-----	7.8
22o		SJB-13-O	25750	1909		10.16 ± .56	5.0
23o	NM17	SJB-04-O	17800	1934	50.5	51.22 ± 1.14	7.5
32o	NM09	SJB-02-O	33711	1857	27.2	28.66 ± .85	3.7
33o		SJB-17-O	32017	1856		40.3 ± 0.9	4.0
34o		SJB-05-O	27443	1924		5.52 ± .85	0.5
38o	NM11	SJB-08-O	40150	1810	8.33	8.99 ± .9	2.3
52o	NM13		47093	1773	8.14	-----	3.8
57o	NM03		62800	1626	2.79	-----	3.7
58o	NM02	SJB-15-O	57765	1624	3.96	10.25 ± .75	2.4
83o	NM23	SJB-12-O	51500	1700	8.85	4.40 ± 1.5	1.8
84o		SJB-11-O	47000	1756		4.70 ± 0.6	1.4

by *Phillips et al.* were re-sampled by *Shute*, and the ^{14}C concentrations are in agreement for most of the wells. Two wells sampled in both studies have different ^{14}C concentrations: wells 58o and 83o. In this study, the more recent sample concentrations are used for model calibration.

Figure 7.5 is a location map of the wells from which the ^{14}C data was collected. Eight wells lie within R10W, and the remaining 10 wells are further from the line of section. Figure 7.6 shows the modelled cross section, along with the locations of the midpoint of the sampling interval for the wells. Some of the same wells sampled for head data are also sampled for ^{14}C data. For most of the wells, the midpoint of the screened interval for hydraulic head data is identical to the midpoint of the sampling interval for the concentration data. Two wells are different. Well 34o (SJB-05-O) is reportedly screened in the Ojo Alamo, but *Phillips et al.* [1989] stated that the water chemistry indicated that it came from the Kirtland Shale. For the model calibration, the sampling interval is located in the Kirtland Shale. Well 58 (SJB-15-O) was screened as deep as the Pictured Cliffs, but was probably sampled in the Ojo Alamo, so the sampling interval is placed in the Ojo Alamo.

The assigned uncertainty in the ^{14}C data is determined using two factors: (1) the magnitude of the ^{14}C concentration and (2) the distance of the well from the line of cross-section. The sources of uncertainty in the ^{14}C data are the same as those for the hydraulic head data, as well as the measurement uncertainty reported by *Phillips et al.* [1989]. It is important to link the uncertainty in the ^{14}C concentrations to the magnitude of the concentrations in order to capture the pattern of concentration distribution. If the uncertainty were not linked to the magnitude of the concentrations, the match between the simulated concentrations and the observed concentrations would be dominated by the high concentration samples. The lower concentration

samples need to be matched more closely than the higher concentration samples in order to capture the overall pattern of the concentration distribution. The assigned uncertainty for each sample is calculated as 10% of the ^{14}C concentration, plus 0.5 pmc for each section (approximately 1.6 km) away from the cross section. Table 7.2 also contains the assigned standard error of measurement for each well.

The direct information on hydraulic conductivities is from *Stone et al.* [1983]. This direct information can be used as either prior information on parameter values or initial parameter estimates for model calibration purposes. However, the prior information may not be representative of the model parameter values for several reasons. First, the prior information is obtained from drill stem tests, slug tests, and pump tests, which sample the subsurface at a much smaller scale than the model parameter zones. The prior information may underestimate the model parameter values due to differences in scale. Second, the prior information in low permeability units is often obtained in the more permeable sandstone lenses within a lower permeability mudstone or shale unit. The sandstone lenses are often not interconnected, and the prior information obtained from the lenses may overestimate the overall permeability for the units. Third, the prior information is often from locations far from the modelled area. This prior information is often taken near the outcrop, and may not be representative of parameter values at depth. Table 7.3 contains the prior information available on the hydraulic conductivity values for the units in the model, along with the source of the prior information and the estimation method. Several prior

values are available for some of the units.

A second source of prior information is the model of *Phillips and Tansey* [1984]. They constructed a quasi three-dimensional groundwater flow model of the Ojo Alamo and Nacimiento formations, using ^{14}C ages to obtain the hydraulic conductivity distribution. They divided the Nacimiento into three units; an aquifer and two aquitards. The thickness of the aquifer was obtained by adding the thicknesses of the sandstone lenses throughout the Nacimiento together, and considering this total thickness an aquifer located in the center of the Nacimiento. An aquitard was located above and below this aquifer. The model was calibrated by adjusting the permeability of the aquitards. Table 7.3 also contains the prior information available from the *Phillips and Tansey* [1984].

7.4 Model construction

A cross-sectional model of the hydrogeological units in the west-central portion of the basin, representing the southern limb of the basin, is constructed. The purpose of constructing the model is to demonstrate the utility of the methods developed in this thesis for calibrating a hydrogeologic model in a responsible manner. Hydraulic head contours for the basin show that the flow direction is generally N-S, so the model is constructed along a north-south cross section through the middle of R10W. The southern boundary of the model coincides with the bottom of Chaco Canyon, and the

Table 7.3 Prior information on the parameters in the San Juan Basin model

Formation	Prior Hydraulic Conductivity	Source	Test Method
Nacimiento aquitard	0.63 m/yr	Phillips and Tansey [1984]	thermal gradients
Nacimiento aquitard	0.015 m/yr	Phillips and Tansey [1984]	model calibration
Nacimiento aquifer	6-15 m/yr	Phillips and Tansey [1984]	calculated from flow path and ^{14}C data
Nacimiento aquifer	11 m/yr	Stone et al., [1983]	estimated
Ojo Alamo	15-50 m/yr	Phillips and Tansey [1984]	calculated from flow path and ^{14}C data
Ojo Alamo	55-177 m/yr	Brimhall [1973]	aquifer pump tests
Fruitland/Kirtland	0.001-0.01 m/yr	Stone et al. [1983]	estimated based on variety of tests
Fruitland/Kirtland	0.015 m/yr	Phillips and Tansey [1984]	thermal gradients
Pictured Cliffs	.001-3.3 m/yr	Stone et al. [1983]	aquifer tests
Pictured Cliffs	0.7 m/yr	Stone et al. [1983]	permeability data from Reneau and Harris [1953]
Lewis Shale	-	-	no data
Cliff House	1.11 m/yr	Stone et al. [1983]	recovery test
Cliff House	0.11 m/yr	Stone et al. [1983]	permeability data from Reneau and Harris [1953]
Menefee	1.0e-6 to 1.1 m/y	Stone et al. [1983]	aquifer tests

northern boundary is located at the San Juan River. The distance from Chaco Canyon to the San Juan River is approximately 75 km along R10W.

7.4.1 Model boundary conditions

The locations of the model boundaries were chosen so that simple boundary conditions could be applied. Figure 7.7 is a conceptualized cross section showing the layering and boundary conditions. The flow system is assumed to be at steady state.

1. Upper Boundary

The upper boundary of the model is chosen to coincide with the elevation of the water table in the uppermost unit. From south to north along the cross section, the surface elevation starts at 1820 meters at the base of Chaco Canyon, and increases gradually to the outcrop of the Ojo Alamo, at approximately 2000 m. A plateau continues for about 15 km north of the outcrop of the Ojo Alamo, and then surface elevations decrease to the San Juan River, at approximately 1690 meters.

The upper boundary is represented as a specified head boundary. To impose this boundary, four nodes are located along the top of the flow system, one at Chaco Canyon, one at the outcrop of the Ojo Alamo (20 km), one at 35 km, and the fourth at the San Juan River (75 km). The value of the hydraulic head at each of these nodes is estimated, and the hydraulic head along the rest of the boundary is interpolated linearly between these nodes. During model calibration, the elevations of the top boundary change, and the FEM grid can adjust to reflect these changes. The initial estimate of the head along the top boundary is the surface elevation.

2. Lower Boundary

The lower boundary is represented by a no-flow boundary within the Menefee Formation. The Menefee Formation is the unit below the Cliff House, and is a relatively thick sequence of marine shales and siltstone lenses. Though more permeable formations do exist below the Menefee Formation, the flow across the Menefee represents a small percentage of the total flow through the system. The hydraulic conductivity of the Menefee is assigned a value of 1.0e-6 m/yr, and is not estimated. Several factors were taken into account in order to locate the domain boundary below the Cliff House. First, no hydraulic head or ^{14}C data was available in units below the Cliff House near the cross section, so the parameters for lower units would have been extremely difficult to estimate. Second, numerical experiments showed that including the units below the Cliff House in the model resulted in very little change in the hydraulic head or ^{14}C concentration distribution in the upper layers. Including the lower units was not necessary in order to simulate flow and transport in the units where data exists.

3. Southern Boundary.

The southern boundary of the model is chosen to coincide with the bottom of Chaco Canyon. This canyon is a surface water and shallow groundwater divide. It may not be a groundwater divide for the deeper regional groundwater system. However, the units intersecting this boundary are low permeability, so the no-flow boundary specification is probably reasonable.

4. Northern Boundary

The northern boundary is specified to be a no-flow boundary. The San Juan River marks the lowest elevation (in a N-S cross section) of the basin, and also marks the axis of the basin. The San Juan River should be both a shallow groundwater and a regional groundwater divide, so a no-flow boundary is appropriate.

7.4.2 Hydrogeological units in the model

Six major hydrogeological units are included in the model. The vertical location and dip of these units were obtained by plotting all data from the well logs, and fitting the units to the well log completion intervals. The distribution and thickness of the hydrogeological units in the model is shown in Figure 7.7. The Cliff House Sandstone, the lowest stratigraphic unit estimated using the model, crops out in Chaco Canyon at an elevation of approximately 1820 m. Based on well data, it dips to the north at an angle of about 1.5°. It is represented as a 50m thick unit. All other units dip to the north at an angle of about 1°. The Lewis Shale crops out just north of Chaco Canyon. It is relatively thin near the outcrop and increases in thickness northward up to 525m. The Pictured Cliffs Sandstone crops out about 8km north of Chaco Canyon, and maintains a constant thickness of 25m throughout the model domain. The Kirtland/Fruitland Shale is represented as a unit 200 meters thick. The Ojo Alamo Sandstone crops out about 15 km north of Chaco Canyon, and dips north at 1°. It is represented as a 50 m thick layer. The Nacimiento Formation is the highest

stratigraphic unit in the cross section. It is present only north of the outcrop of the Ojo Alamo, and ranges in thickness from 0 to 150 meters. For this model, the Nacimiento is considered a single hydrogeologic unit. Though the Nacimiento contains interbedded mudstone and sandstone lenses, it is not known whether the sandstone lenses are interconnected. Defining the Nacimiento as a single hydrogeologic unit is more reasonable than breaking it into several units, since the location and extent of multiple units would be difficult to determine.

7.4.3 Concentration boundary conditions and parameters

In order to simulate the ^{14}C data, the boundary conditions and parameters that are specific to the tracer concentration field are required. The ^{14}C is introduced along the top boundary of the model, where it enters the groundwater flow system at the water table. This boundary is a specified concentration boundary. The required parameters are the half life of the ^{14}C isotope, the initial concentration at the inflow boundary, the horizontal and transverse dispersivities, and the effective porosity for each unit.

The determination of the initial concentration of ^{14}C at the water table is not straightforward. *Phillips et al.* [1989] used six different correction models to estimate the initial concentration of ^{14}C samples in the San Juan basin, and obtained values ranging from 31 to 150 pmc. *Phillips et al.* [1989] determined that the correction model

of *Vogel* [1967] compared favorably with the other correction models they examined. The correction model of Vogel assigns an initial activity of 85 pmc to every sample. For the model in this thesis, an initial concentration of 85 pmc is used at the water table. This boundary condition was applied along the water table in the region where downward flow from the water table to the aquifer was present. In the discharge portion of the upper boundary, a third-type boundary was applied.

The horizontal and transverse dispersivities are not straightforward to determine. *Phillips et al.* [1989] used well logs and stochastic transport theory to estimate horizontal dispersivities of approximately 300 meters. However, using a one dimensional transport model, they showed that the concentration distribution was not very sensitive to the horizontal dispersivity for a decaying solute. Comparing horizontal dispersivities ranging from 0 to 1500 m, the maximum difference in ^{14}C ages was found to be 11%, within the measured uncertainty in the ^{14}C concentrations. For the model in this thesis, a horizontal dispersivity of 300 meters is used. The transverse dispersivity is estimated at 10 meters. The effective porosity is assigned a value of 0.2. After the parameters are estimated using the joint data set, the consequences of incorrectly specifying the parameters controlling the concentration distribution are examined.

The half life of ^{14}C is approximately 5740 years [*Fontes,* 1980]. Since the flow system is at steady state and is presumed to have been relatively unchanged for a

long period of time relative to the half life of ^{14}C, the ^{14}C concentrations are also at steady state. The time needed to reach a steady state distribution depends on the distance from the source. For a wide range of aquifer properties, it was determined that concentrations were relatively unchanged within the model domain after 50,000 years. The maximum simulation time is specified to be 50,000 years.

The ^{14}C distribution is calculated both using standard Crank-Nicolson time stepping and the Arnoldi algorithm. Using the Crank-Nicolson time stepping procedure, relatively accurate steady state distributions can be calculated using time steps of 500 years, so only 100 time steps are needed to calculate the ^{14}C distribution. Using the Arnoldi algorithm, the amount of computer time required to accurately calculate the steady state ^{14}C distributions is dependent on the contrast in hydraulic conductivity between the model layers. In general, at least 10 Arnoldi vectors are needed for moderate contrasts, and up to 15 Arnoldi vectors are needed when the contrast in hydraulic conductivity between layers is greater than 3 orders of magnitude. In addition, many more iterations are needed to solve for each Arnoldi vector when the contrast between the layers is large. Because the hydraulic conductivity of each layer is variable during the parameter estimation procedure, and contrasts of greater than six orders of magnitude are common, the Arnoldi algorithm performs poorly during parameter estimation for this model. The Crank-Nicolson procedure is more robust, and hence more reliable during parameter estimation. It is often faster as well.

7.4.4 Model grid

The model is based on a finite element technique using triangular elements. The mesh is aligned with the regional slope of the hydrogeological units. This alignment allows easy representation of the units, and allows the elements to be aligned with the streamlines in the more permeable units. The upper boundary of the mesh is adjustable so that it can coincide with the elevation of the water table in the upper units. For the flow model, the elements are 250 meters long and between 5 and 15 meters high.

7.5 Model calibration strategy

The flow model, as described above, contains 10 parameters that need to be estimated. There are 4 head boundary parameters; the value of hydraulic head at each of the 4 nodes that define the upper surface of the cross section. There are also 6 hydraulic conductivity parameters, one for each layer in the model. The anisotropy for each model hydraulic conductivity zone also needs to be defined, but this parameter is not estimated initially. The anisotropy is assigned a value of 100 for each model layer, and subsequently the effect of errors in the specified value of anisotropy on the parameter estimates are determined.

The model is calibrated in two stages. In the first stage, all 10 model

parameters are estimated. The hydraulic head and ^{14}C data are used both individually and jointly to estimate the model parameters. The parameter space for the joint data set is examined to determine how to use prior information to stabilize the parameter set most efficiently and responsibly. It is shown that the uncertainties in the estimates of hydraulic conductivity parameters in the lower layers of the model are many orders of magnitude larger than the uncertainties of the other parameters. The uncertainties in these parameters dominate the model parameter space, both in the single state and joint parameter estimates. It is also shown that prior information on these parameters stabilizes the parameter space, and leads to very small error ratios for the remaining parameters.

The second stage of model calibration builds on the first stage. The hydraulic conductivity parameters in the upper model layers are the most interesting, since most of the data is available in these layers. In the second stage, prior information is used to specify the parameter values for the lower model layers, and the remaining parameters are estimated. The relative weighting of the hydraulic head and the ^{14}C data for the joint data set is examined. The effects of possible errors in the anisotropy, ^{14}C source strength, and dispersivity is analyzed using the parameter space during the second stage of parameter estimation.

7.6 Model calibration for 10 flow parameters

In the first stage of model calibration, the model parameter space using hydraulic head and ^{14}C data is analyzed. Those parameters for which prior information will most efficiently and responsibly stabilize the model parameter set are identified.

7.6.1 Parameter estimates based on the hydraulic head data set

The hydraulic head data set contains 55 hydraulic head data, 14 in the Nacimiento, 18 in the Ojo Alamo, 8 in the Quaternary Alluvium, 8 in the Kirtland/Fruitland, 2 in the Pictured Cliffs, and 4 in the Cliff House. The distribution of these data is shown in Figure 7.4. No data are available in the Lewis shale. The initial parameter estimates are listed in Table 7.4. The hydraulic conductivity parameters are the horizontal hydraulic conductivities, in units of m/yr. For the hydraulic conductivity parameters, the initial estimates are based on the average values of the independent information for each of the hydrogeological units. For the head boundary parameters, the initial estimates are equal to the surface elevation at each node, in units of meters.

The final parameter estimates are listed in Table 7.4, along with the standard error of the parameter estimates and the coefficient of variation. When a different set of initial estimates were used, the final parameter estimates for the hydraulic conductivity parameters were found to be dependent on the initial estimates. The final

Table 7.4 Parameter estimates and uncertainties based on hydraulic head data

Parameters	Initial Estimate	Final Estimate	Std. Error	CV
K_{ch}	1.1	1.1	21.3	498.3
K_f	1.30e-02	1.4e-04	30.2	7.9
K_{pc}	7.00e-01	8.5e-01	49.3	706.4
K_k	1.40e-02	6.1e-04	44.5	13.8
K_o	100.0	209.6	55.7	24.0
K_n	10.0	149.2	52.1	23.9
H_1	1820.0	1805.0	43.7	0.024
H_2	2000.0	1975.0	23.2	0.012
H_3	1990.0	1940.0	13.3	0.007
H_4	1690.0	1686.0	13.3	0.008

parameter estimates for the head boundary parameters were independent of the initial estimates. Figure 7.8 shows the head distribution for the flow system using the final parameter estimates from the head data set.

For the hydraulic conductivity parameters, the standard error is given in log transformed units. A standard error of one implies an uncertainty in the parameter estimate of one order of magnitude. The standard errors range from 21 to 55, implying the hydraulic conductivities are virtually non-identifiable using this data set. These parameter uncertainties exceed the physical bounds on hydraulic conductivity, since the parameter values are not constrained in the estimation procedure. For this flow model and boundary conditions, it could be expected that the hydraulic conductivity parameters are non-identifiable using the hydraulic head data. The coefficients of

variation (CV) is the standard error divided by the log transformed parameter value. For hydraulic conductivity parameters with an estimate near one, the log transformed estimate is small, and the CV is large. For instance, K_{pc} and K_k have similar standard errors, but the log transformed estimate for K_{pc} is much smaller than K_k, and the CV of K_{pc} is much larger than the CV of K_k.

For the head boundary parameters, the standard errors are given in meters. The standard errors range from 13 to 43 meters, with the largest uncertainty in the estimate of the hydraulic head at the node located in the position of Chaco Canyon, node 1. From Figure 7.4, very little data exists in the vicinity of H_1, and the most data exists in the vicinity of H_4, so it is reasonable that H_1 has the most uncertainty and H_4 has the least uncertainty. The CV's for the head parameters are the standard error divided by the estimate, and the values of CV are relatively small. H_3 has the smallest coefficient of variation, since the standard error of H_4 and H_3 are nearly equal, while the estimate of H_3 is larger than the estimate of H_4. The head parameters are reasonably well defined by the data.

Table 7.5 presents the fit of the simulated and the observed data, along with some statistics describing the fit. The actual differences between the simulated and observed data range from 2.2 m to 104.2 m. The weighted difference is the actual difference divided by the assigned standard error for each data point. The weighted differences range from 0.07 to 2.69. The number of residuals greater than zero is

slightly more than the number of residuals less than zero, and the average weighted residual is near zero. The value of the objective function at the minimum is 58.69. The goodness of fit can be evaluated by the s^2 statistic, defined in Chapter 4 as the minimum of the objective function divided by the number of data minus the number of parameters. If the weighted errors in the data are normally distributed and have a unit variance, the goodness of fit should be about equal to one. The goodness of fit is equal to 1.3, implying the standard errors that were assigned to the data are slightly smaller than they should be, assuming the model is an accurate representation of the flow system.

7.6.2 Parameter space based on head data set

Table 7.6 lists the axes of the confidence region for the final parameter estimates using the head data set. Axis 10 is the longest axis of the confidence region, with a length of 690 units. The response surface is the flattest in the direction of axis 10. Axis 9 is about half as long as axis 10, and axis 8 is an order of magnitude shorter than axis 9. All four of the longest axes are greater than 5.1 units in length, which means that the parameters which have large components from these axes have coefficients of variation greater than 5. Examining the unit vectors, which define the orientations of the axes of the confidence region, the two longest axes only have components from the hydraulic conductivity parameters. The head parameters have no components of the unit vectors that define the orientations of the longest axes of

Table 7.5 Fit of observed and simulated head data at the parameter estimates based on the head data

Data Identifier	Observed Data	Simulated Data	Difference	Weighted Difference
28n	1969.0	1936.5	32.5	0.54
29n	2018.0	1952.1	65.9	1.88
35n	1986.0	1958.6	27.4	0.91
39n	1953.0	1898.4	54.6	1.82
40n	1927.0	1898.8	28.2	1.13
46n	1855.0	1824.6	30.4	0.67
48n	1908.0	1864.7	43.3	0.79
51n	1838.0	1835.1	2.9	0.05
52n	1855.0	1869.1	-14.1	-0.28
56n	1840.0	1772.6	67.4	2.69
59n	1747.0	1744.3	2.7	0.07
62n	1669.0	1730.7	-61.7	-1.03
72n	1660.0	1689.6	-29.6	-0.99
73n	1678.0	1691.8	-13.8	-0.46
19o	2026.0	1949.1	76.9	1.28
20o	2009.0	1949.2	59.8	1.00
21o	1920.0	1949.1	-29.1	-0.49
30o	1932.0	1955.6	-23.6	-0.52
31o	1975.0	1944.1	30.9	1.54
32o	1912.0	1941.9	-29.9	-1.00
33o	1893.0	1942.7	-49.7	-2.48
34o	1930.0	1955.5	-25.5	-1.27
36o	1920.0	1943.2	-23.2	-0.42
37o	1930.0	1907.9	22.1	0.63
38o	1887.0	1910.0	-23.0	-0.66
41o	1935.0	1907.0	28.0	1.40
43o	1889.0	1924.1	-35.1	-1.75
44o	1876.0	1911.3	-35.3	-0.64
45o	1850.0	1880.7	-30.7	-0.51
52o	1855.0	1869.1	-14.1	-0.28
61o	1658.0	1729.8	-71.8	-1.31
74o	1654.0	1700.7	-46.7	-0.78

Table 7.5 (continued)

53q	1880.0	1873.5	6.5	0.14
68q	1663.0	1690.1	-27.1	-0.90
69q	1683.0	1690.9	-7.9	-0.26
70q	1719.0	1694.4	24.6	1.23
16q	1874.0	1868.3	5.7	0.19
17q	1871.0	1864.2	6.8	0.23
25q	1956.0	1948.0	8.0	0.27
26q	1956.0	1951.2	4.8	0.16
8k	1862.0	1885.8	-23.8	-0.48
10k	1893.0	1891.9	1.1	0.06
12k	1915.0	1910.0	5.0	0.25
13k	1894.0	1889.9	4.1	0.16
14k	1891.0	1890.1	0.9	0.03
15k	1880.0	1886.0	-6.0	-0.20
20k	1935.0	1921.6	13.4	0.22
27k	1787.0	1836.6	-49.6	-0.83
58k	1737.0	1811.5	-74.5	-1.86
1ch	1898.0	1842.0	56.0	1.60
2ch	1852.0	1834.2	17.8	0.36
6pc	1938.0	1887.3	50.7	0.85
9ch	1731.0	1835.2	-104.2	-2.08
11pc	1882.0	1883.3	-1.3	-0.05
18ch	1849.0	1879.1	-30.1	-0.67
Average Weighted Residual:				0.0882
Number of Weighted Residuals greater than 0 : 29				
Number of Weighted Residuals less than 0.0 : 26				
Value at Objective Function Minimum = 58.69				
s^2 = 1.3				

the confidence region.

Table 7.6 Axes of confidence region for parameter estimates based on head data set

Axis Lengths	4.1e-03	5.9e-03	6.7e-03	1.3e-02	1.9e-01	4.0e-01	5.1e+00	2.8e+01	3.0e+02	6.9e+02
Parameters	U_1	U_2	U_3	U_4	U_5	U_6	U_7	U_8	U_9	U_{10}
K_{ch}	0.00	0.00	0.00	0.00	0.00	0.00	0.00	0.01	-0.87	0.50
K_l	0.00	0.00	0.00	0.00	0.11	0.00	0.98	-0.16	0.00	0.00
K_{pc}	0.00	0.00	0.00	0.00	0.02	0.00	0.00	-0.02	0.50	0.87
K_k	0.01	-0.01	0.02	0.00	-0.99	-0.03	0.11	-0.02	0.01	0.02
K_o	0.00	-0.01	-0.01	0.00	-0.02	0.71	-0.11	-0.70	-0.01	-0.01
K_n	0.00	0.01	0.01	0.00	0.02	-0.71	-0.11	-0.70	-0.01	-0.01
H_1	-0.09	0.16	-0.52	0.83	-0.02	0.00	0.00	0.00	0.00	0.00
H_2	-0.28	0.35	-0.71	-0.54	-0.02	0.00	0.00	0.00	0.00	0.00
H_3	-0.91	0.18	0.37	0.10	0.00	0.01	0.00	0.00	0.00	0.00
H_4	-0.30	-0.91	-0.29	-0.04	0.00	-0.01	0.00	0.00	0.00	0.00

The unit vector for axis 10, the longest axis of the confidence region, shows that the largest components come from parameter axes K_{ch} and K_{pc}, with very small components from the other parameter axes. Axis 9 is oriented in a direction between the axes of K_{ch} and K_{pc}, but is nearly perpendicular to the axes of all other parameters. Similarly, the unit vector for axis 9, the second longest axis of the confidence region, also has the largest components from K_{ch} and K_{pc}, and almost no components from the other parameter axes. Axes 9 and 10 are perpendicular to each other, and are both in the plane of the K_{ch} and K_{pc} axes. The plane containing axes 9 and 10 contains values of the response surface very near the minimum.

The third longest axis, axis 8, has its largest components from parameter axes K_o and K_n. The four shortest axes of the confidence region, axes 1 through 4, contain mainly components from the head parameters. The confidence regions for the head parameters and the hydraulic conductivity parameters are nearly independent, because the axes which contribute to the confidence region for the head parameters are nearly perpendicular to the axes which contribute to the confidence region for the hydraulic conductivity parameters. However, the confidence region for the head parameters is not completely independent from the confidence region for the hydraulic conductivity parameters, since there are some small components of the longer six axes of the confidence region from the axes of the head parameters.

The table of relative contributions to the CV of the parameters (Table 7.7) shows that axes 9 and 10 contribute most of the uncertainty to three of the hydraulic conductivity parameters, K_{ch}, K_{pc},and K_k. Axis 8 contributes most of the uncertainty to the hydraulic conductivity parameters, K_o and K_n. The uncertainty in the head parameters comes from many different axes of the confidence region, including some of the largest axes of the confidence region. It was noted above that the head parameters have almost no projection in the direction of the six longest axes of the confidence region. However, they do have very small projections, and these very small projections multiplied by the length of the long axes yield some of the uncertainty in the head parameters.

Table 7.7 Relative contribution to the CV from each axis of the confidence ellipsoid based on the head data set

Parameters	U_1	U_2	U_3	U_4	U_5	U_6	U_7	U_8	U_9	U_{10}
K_{ch}	0.00	0.00	0.00	0.00	0.00	0.00	0.00	0.00	0.37	0.64
K_l	0.00	0.00	0.00	0.00	0.00	0.00	0.53	0.43	0.02	0.03
K_{pc}	0.00	0.00	0.00	0.00	0.00	0.00	0.00	0.00	0.06	0.94
K_k	0.00	0.00	0.00	0.00	0.00	0.00	0.00	0.00	0.06	0.94
K_o	0.00	0.00	0.00	0.00	0.00	0.00	0.00	0.90	0.03	0.07
K_n	0.00	0.00	0.00	0.00	0.00	0.00	0.00	0.89	0.03	0.07
H_1	0.00	0.00	0.03	0.27	0.03	0.00	0.04	0.08	0.48	0.08
H_2	0.01	0.04	0.22	0.50	0.13	0.01	0.00	0.01	0.09	0.00
H_3	0.38	0.03	0.17	0.05	0.00	0.25	0.00	0.04	0.04	0.03
H_4	0.03	0.61	0.08	0.01	0.00	0.27	0.00	0.00	0.00	0.00

The parameter space has yielded the following information. First, there is a large, multidimensional region in parameter space that has a value of the objective function near the minimum. The large parameter uncertainties come from more than one direction of parameter space. This situation is different from the multiparameter example in Chapter 5, where large uncertainties in the parameters were present, but these uncertainties came from only one axis of the confidence region. Second, three groups of parameters can be identified as having nearly independent confidence regions. The first group contains the parameters K_{ch}, K_{pc}, and K_k. The second group contains the parameters K_o and K_n. The third group contains the head parameters. Both the first and second group have large parameter uncertainties, but these uncertainties are due to different axes of the confidence region.

7.6.3 Parameter estimates based on ^{14}C data set

The model parameter space for the ^{14}C data can be compared to the model parameter space for the head data to determine the potential for ^{14}C data to stabilize the parameter estimates. The ^{14}C data set contains 18 data, 6 in the Nacimiento and 12 in the Ojo Alamo (Figure 7.6). The initial parameter estimates are chosen to be identical to the final parameter estimates using the head data. The final parameter estimates using only the ^{14}C data are listed in Table 7.8, along with the standard error and coefficient of variation. Figure 7.9 shows the steady state ^{14}C concentration distribution for the flow system using the final parameter estimates using only the ^{14}C data. This figure shows that the ^{14}C data exist only in the upper portion of the flow system, and samples from deeper formations would not result in any measurable concentrations of ^{14}C.

For the hydraulic conductivity parameters, the standard errors for K_{ch}, K_l, and K_{pc} are very large. No data are available in these units, and the ^{14}C data is virtually insensitive to these parameter values. The standard errors for K_o and K_n are about 0.2 orders of magnitude, while the standard error for K_k is about 4 orders of magnitude. For the head boundary parameters, node 1 has the largest standard error, because no ^{14}C data exists in the southern end of the model domain. The remaining head nodes have standard errors between 15 and 40 meters, similar to those using head data.

Table 7.8 Parameter estimates and uncertainties based on ^{14}C data set

Parameters	Initial Estimate	Final Estimate	Std. Error	CV
K_{ch}	1.1	1.100	787.2	19088.2
K_l	1.44e-04	0.208	292.9	396.7
K_{pc}	8.52e-01	0.715	3116.4	21386.4
K_k	6.11e-04	0.013	3.696	1.893
K_o	209.6	10.770	0.204	0.203
K_n	149.2	0.398	0.167	0.363
H_1	1805.0	1983.0	4153.1	2.218
H_2	1975.0	1991.0	33.2	0.017
H_3	1940.0	1997.0	15.0	0.008
H_4	1686.0	1714.0	39.8	0.023

Table 7.9 shows the fit of the simulated and the observed ^{14}C data. The actual differences between the simulated and observed data ^{14}C concentrations range from 0.05 to 11.1 pmc. The weighted differences ranged from 0.10 to 3.08. The residuals greater than zero outnumber residuals less than zero, and the average weighted residual is greater than zero. The value of the objective function at the minimum is 40.5. The goodness of fit is 5.0, larger than the goodness of fit for the head data. Again, the assigned standard errors are smaller than they should be, according to how well the data fit the model.

Table 7.9 Fit of observed and simulated ^{14}C data using parameter estimates based on ^{14}C data set

Data Identifier	Observed Data	Simulated Data	Difference	Weighted Difference
28n-c	51.20	52.59	-1.39	-0.15
39n-c	12.60	11.37	1.23	0.54
40n-c	19.90	17.63	2.27	0.91
48n-c	9.20	19.07	-9.87	-2.24
81n-c	1.40	0.03	1.37	2.74
82n-c	4.50	3.94	0.56	0.14
20o-c	37.90	32.97	4.93	0.63
22o-c	10.16	8.71	1.45	0.29
23o-c	50.50	54.40	-3.90	-0.52
32o-c	27.20	38.61	-11.41	-3.08
33o-c	40.30	29.78	10.52	2.63
34o-c	5.52	5.57	-0.05	-0.10
38o-c	8.33	11.25	-2.92	-1.27
52o-c	8.14	5.79	2.35	0.62
57o-c	2.79	0.48	2.31	0.62
58o-c	3.96	2.89	1.07	0.45
83o-c	8.85	4.28	4.57	2.54
84o-c	4.70	5.77	-1.07	-0.76
Average Weighted Residual				0.096
Number of Weighted Residuals greater than 0 : 11				
Number of Weighted Residuals less than 0.0 : 7				
Value at Objective Function Minimum = 40.49				
s^2 = 5.0				

7.6.4 Parameter space based on ^{14}C data set

Table 7.10 lists the axes of the confidence region for the final parameter estimates using the ^{14}C data set. The longest axis is axis 10; the second longest is axis 9. Both of these axes have significant components from the parameter axes K_{ch} and K_{pc}, a small component from K_l, and almost no components from the other parameters. Axis 8 is 18 units long, and is aligned closely with the parameter axis K_l. Axis 7 is 1.6 units long, and is aligned most closely with the axis of K_k. All other axes

Table 7.10 Axes of confidence region for parameter estimates based on ^{14}C data set

Axis Lengths	9.2e-04	8.0e-03	1.1e-02	5.2e-02	1.3e-01	2.9e-01	1.6e+00	1.8e+01	4.7e+02	2.9e+04
Parameters	U_1	U_2	U_3	U_4	U_5	U_6	U_7	U_8	U_9	U_{10}
K_{ch}	0.00	0.00	0.00	0.00	0.00	0.00	0.00	0.03	0.75	0.67
K_l	0.00	0.00	0.00	-0.04	0.04	0.00	0.05	-1.00	0.06	-0.01
K_{pc}	0.00	0.00	0.00	0.00	0.00	0.00	0.00	-0.05	-0.66	0.75
K_k	0.03	-0.01	0.01	-0.25	0.22	-0.17	-0.93	-0.03	0.00	0.00
K_o	-0.05	-0.02	0.01	0.65	0.69	0.31	-0.07	0.00	0.00	0.00
K_n	-0.03	0.04	-0.04	0.41	0.03	-0.91	0.07	-0.01	0.00	0.00
H_1	0.07	-0.03	0.02	-0.59	0.69	-0.22	0.35	0.06	0.00	0.00
H_2	0.45	-0.66	-0.60	0.04	-0.02	0.01	0.00	0.00	0.00	0.00
H_3	0.89	0.30	0.35	0.08	-0.01	0.00	0.00	0.00	0.00	0.00
H_4	0.05	0.69	-0.72	-0.03	0.04	0.05	-0.01	0.00	0.00	0.00

are less than one unit long. The table of relative contributions to the CV of the parameters (Table 7.11) shows that axis 10 contributes most of the uncertainty to three of the hydraulic conductivity parameters, K_{ch}, K_{pc},and K_l, and the parameter H_1.

Table 7.11 Relative contribution to the CV from each axis of the confidence region based on ^{14}C data set

Parameters	U_1	U_2	U_3	U_4	U_5	U_6	U_7	U_8	U_9	U_{10}
K_{ch}	0.00	0.00	0.00	0.00	0.00	0.00	0.00	0.00	0.00	1.00
K_l	0.00	0.00	0.00	0.00	0.00	0.00	0.00	0.00	0.01	0.99
K_{pc}	0.00	0.00	0.00	0.00	0.00	0.00	0.00	0.00	0.00	1.00
K_k	0.00	0.00	0.00	0.00	0.00	0.00	0.63	0.07	0.29	0.02
K_o	0.00	0.00	0.00	0.03	0.21	0.21	0.31	0.04	0.19	0.02
K_n	0.00	0.00	0.00	0.00	0.00	0.56	0.08	0.34	0.01	0.00
H_1	0.00	0.00	0.00	0.00	0.00	0.00	0.07	0.25	0.11	0.58
H_2	0.00	0.10	0.16	0.02	0.02	0.01	0.11	0.52	0.06	0.00
H_3	0.01	0.10	0.26	0.33	0.04	0.01	0.15	0.03	0.00	0.07
H_4	0.00	0.06	0.12	0.00	0.05	0.42	0.12	0.02	0.00	0.22

The confidence region using ^{14}C data can be compared to the confidence region using the head data by calculating angles of interaction. For the longest axes (axis 10 for ^{14}C data; axis 10 for head data), the angle of interaction is 8.9°, indicating that the orientations of the axes are not much different. For the second longest axes (axis 9 for both data sets), the angle of interaction is also 8.9°. Recall that the longest axes contain mainly uncertainties from the hydraulic conductivity parameters from the lower layers of the model. Because the axes are very long, even this small angle of

interaction reduces the uncertainty of the parameters using the joint data set. However, the uncertainty of the parameters is still be large, and the maximum uncertainty still occurs along this direction of parameter space. It is more difficult to predict the reduction in uncertainty for the other model parameters.

7.6.5 Joint parameter estimation

Joint parameter estimation using both hydraulic head and ^{14}C data is used to estimate the model parameters. For joint estimation, the weights for each data set are required. The weights can be chosen using any of the methods presented in Chapter 6. Table 7.12 contains the parameter estimates and uncertainties for all four weighting criteria. All four criteria weight the head data more heavily than the concentration data. The head weights all have $w_h = 1.0$, and the concentration weights range from $w_c = 0.1$ to $w_c = 0.52$.

Table 7.12 also contains some additional statistics about each set of parameter estimates, including the average CV, the CN, the volume of the confidence region, and the length of the longest axis of the confidence region. It also contains statistics about the fit of the observed and simulated data at each set of parameter estimates. S_h is the value of the head portion of the objective function evaluated at the set of parameter estimates, and S_c is the value of the concentration portion of the objective function evaluated at the same estimates. The s_h^2 statistic is S_h/n_h, and the s_c^2 statistic

Table 7.12 Parameter estimates and uncertainties for joint data set using four weighting criteria

	Head Data Only			Concentration Data Only			Joint Data Set; MINCN			Joint Data Set; RESID			Joint Data Set; MINLEN			Joint Data Set; MINVOL		
w_h	1.0			0.0			1.0			1.0			1.0			1.0		
w_c	0.0			1.0			0.10			0.19			0.24			0.54		
Parameters	Estimate	Std	Coeff. Var.	Estimate	Std	Coeff. Var.	Estimate	Std	Coeff. Var.	Estimate	Std	Coeff. Var.	Estimate	Std	Coeff. Var.	Estimate	Std	Coeff. Var
K_{ch}	1.10e+00	21.29	498.3	1.100	787.2	19088.2	1.10e+00	4.49	108.700	1.10e+00	4.50	108.950	1.10e+00	4.51	109.500	1.10e+00	4.29	104.200
K_l	1.44e-04	30.19	7.9	0.208	292.9	396.7	1.22e-03	4.37	1.500	1.39e-03	4.73	1.657	1.52e-03	4.67	1.655	2.41e-03	4.22	1.613
K_{pc}	8.52e-01	49.33	706.4	0.715	3116.4	21386.4	6.99e-01	5.80	37.240	7.00e-01	5.21	34.750	7.00e-01	4.74	30.570	7.00e-01	8.94	57.830
K_k	6.11e-04	44.46	13.8	0.013	3.696	1.893	1.64e-03	0.30	0.106	1.57e-03	0.26	0.093	1.55e-03	0.26	0.093	1.47e-03	0.35	0.123
K_s	2.10e+02	55.73	24.0	10.770	0.204	0.203	5.01e+00	0.22	0.308	5.67e+00	0.18	0.234	6.02e+00	0.15	0.198	7.32e+00	0.11	0.122
K_h	1.49e+02	52.05	23.9	0.398	0.167	0.363	1.64e-01	0.18	0.224	1.78e-01	0.14	0.188	1.88e-01	0.13	0.175	2.16e-01	0.10	0.151
H_1	1805.0	43.72	0.024	1983.0	4153.1	2.218	1803.0	28.42	0.016	1804.0	28.88	0.016	1804.0	29.74	0.016	1800.0	33.91	0.019
H_2	1975.0	23.20	0.012	1991.0	33.2	0.017	1971.0	16.14	0.008	1972.0	14.64	0.007	1973.0	13.81	0.007	1982.0	12.05	0.006
H_3	1940.0	13.33	0.007	1997.0	15.0	0.008	1952.0	8.27	0.004	1956.0	7.77	0.004	1959.0	7.45	0.004	1969.0	6.78	0.003
H_4	1686.0	13.25	0.008	1714.0	39.8	0.023	1679.0	10.69	0.006	1678.0	10.80	0.006	1677.0	11.10	0.007	1676.0	12.00	0.007
Average CV			127.44			4.1e+03			14.811			14.591			14.223			16.407
Condition Number			1.7e+05			2.8e+07			3.9e+04			4.3e+04			4.5e+04			5.1e+04
Volume of Region			4.73e-03			5.37e-05			1.25e-09			8.29e-10			4.86e-10			2.51e-10
Length of Max Axis			690			2.90e+04			131.2			121.3			111.9			117.8
S_h			58.7			0.0			62.7			63.8			66.0			70.7
S_c			0.0			40.5			100.7			97.5			85.2			72.1
s_h^2			1.06			0.00			1.14			1.16			1.20			1.28
s_c^2			0.00			2.22			5.59			5.41			4.73			4.00

is S_c/n_c, where n_h and n_c are the number of head and ^{14}C data respectively. The s^2 statistics give a measure of the fit between the observed and simulated data, and are used to compare fits among the different weighting methods. For the purpose of comparing fits, the number of parameters being estimated is not contained in the s^2 statistic.

It is important to note that the fit for each individual data set using the joint estimates is somewhat worse than the fit for each data set using the estimates from that data set. Each data set leads to a different set of parameter estimates, and the joint parameter estimates reflect the trade-off between the two data sets. For instance, using the parameter estimates based on the head data only, S_h is 58.7, while for the joint parameter estimates using the MINLEN criterion, S_h is 66.0. Similarly, using the parameter estimates based on the ^{14}C data only, S_c is 40.5, while for the joint parameter estimates using the MINLEN criterion, S_c is 85.2. The difference between S_h using the head data set and S_h using the joint data set is smaller than the difference between S_c using the ^{14}C data set and S_c using the joint data set, reflecting the fact that the head data is weighted more heavily than the ^{14}C data. Examining the s^2 statistics, the ^{14}C data always fits worse than the head data, for all sets of weights. However, as the relative ^{14}C weights increase, the fit of the ^{14}C data becomes better and the fit of the head data becomes worse.

The parameter estimates and uncertainties for all four weighting criteria are

similar, though definite patterns emerge. The standard errors and CV's for all parameters are somewhat reduced from those using only the head data. The parameters K_{ch}, K_l and K_{pc} all have standard errors near 5 orders of magnitude. Though these standard errors are reduced from those produced using head or ^{14}C data alone, they are still significant. The parameters K_k, K_o and K_n all have standard errors approximately between 0.1 and 0.3, much reduced from those using only head data. The uncertainty in K_k is significantly reduced from that using either data set alone, though the uncertainty in K_k increases as relative weighting of the ^{14}C data increases. For K_n and K_o, the uncertainties are nearly the same or somewhat larger than those using the ^{14}C data alone. Note that the uncertainties in K_n and K_o decrease as the relative weighting of the concentration data increases. The head parameters have standard errors between 7 and 33 meters, reduced by nearly a factor of two from those using either data set individually.

Comparing the different weighting criteria, the MINCN, RESID, and MINLEN criteria all have relatively small concentration weights. The parameter estimates are slightly different for each set of weights. The smallest average CV is produced by the MINLEN criterion, though the average CV's for the RESID criterion and MINCN criterion are not much larger. Both the MINLEN and the RESID criterion seem to strike a good balance between minimizing the condition number and minimizing the volume of the confidence region. It must be noted that the average CV's are dominated by the large CV's for parameters K_{ch} and K_{pc}.

Figure 7.10 shows the head distribution for the flow system using the joint parameter estimates using the MINLEN criterion. Comparing Figure 7.10 with Figure 7.8, the head distribution using only head data, the joint data set seems to produce parameter estimates which allow more flow through the lower layers of the system. The joint data set results in larger conductivities for the aquitards, which allows greater leakage into the lower model layers. Figure 7.11 shows the concentration distribution for the flow system using the same estimates.

The four weighting criteria all weight the head data more than the concentration data. For the parameters with the largest uncertainties, these weights reduce the parameter uncertainties as much as possible. However, for the parameters K_o and K_n, the ^{14}C data results in much better parameter estimates than the head data. Weighting the concentration data less than the head data does not result in the smallest possible uncertainties in these parameters. As the relative weight of the concentration data decreases, the fit of the ^{14}C data becomes worse. The estimates of those parameters which the ^{14}C data can estimate well (K_o and K_n in this case) becomes more uncertain.

7.6.6 Parameter space based on joint data set

Table 7.13 lists the axes of the confidence region for the final parameter estimates using the joint data set for the MINLEN criterion. The confidence region has many similarities to the confidence region for the head data set (Table 7.6). Axes 9

and 10 are the longest axes of the confidence region. Both have significant components from the parameter axes K_{ch} and K_{pc}, but small components from the other parameter axes. The third longest axis, axis 8, is nearly parallel to parameter axes K_l. The fourth and fifth longest axes, axes 7 and 6, have their largest components from parameter axes K_o and K_n.

Table 7.13 Axes of confidence region for parameter estimates based on joint data set at MINLEN weights

Axis Lengths	2.6e-03	4.3e-03	6.2e-03	1.2e-02	4.4e-02	1.6e-01	2.1e-01	2.9e-01	1.1e+02	1.3e+01
Parameters	U_1	U_2	U_3	U_4	U_5	U_6	U_7	U_8	U_9	U_{10}
K_{ch}	0.00	0.00	0.00	0.00	0.00	0.00	0.00	0.00	-0.97	0.25
K_l	0.00	-0.01	0.00	-0.04	0.14	-0.01	0.08	-0.99	0.01	0.06
K_{pc}	0.00	0.00	0.00	0.00	0.01	0.00	0.01	-0.06	-0.25	-0.97
K_k	-0.01	-0.10	0.01	-0.11	0.97	0.10	0.05	0.14	0.00	0.00
K_o	-0.01	0.00	0.00	0.00	-0.10	0.47	0.87	0.05	0.00	0.00
K_n	0.01	-0.01	-0.01	0.00	-0.05	0.88	-0.48	-0.05	0.00	0.00
H_1	0.01	0.02	-0.03	-0.99	-0.12	-0.01	-0.01	0.02	0.00	0.00
H_2	0.18	0.97	-0.13	0.01	0.10	0.01	0.01	0.00	0.00	0.00
H_3	0.95	-0.14	0.27	0.00	-0.01	-0.01	0.01	0.00	0.00	0.00
H_4	0.25	-0.18	-0.95	0.02	0.00	-0.01	0.01	0.00	0.00	0.00

The table of relative contributions to the CV of the parameters (Table 7.14) shows that axis 9 contributes most of the uncertainty to four of the hydraulic conductivity parameters, K_{ch}, K_l, K_{pc},and K_k. Axes 6 and 7 contribute most of the

uncertainty to the other two other hydraulic conductivity parameters, K_o and K_n. The uncertainty in the head parameters comes from many different axes of the confidence region.

Table 7.14 Relative contribution to the CV from each axis of the confidence ellipsoid based on the joint data set at MINLEN weights

Parameters	U_1	U_2	U_3	U_4	U_5	U_6	U_7	U_8	U_9	U_{10}
K_{ch}	0.00	0.00	0.00	0.00	0.00	0.00	0.00	0.00	1.00	0.00
K_l	0.00	0.00	0.00	0.00	0.00	0.00	0.00	0.03	0.79	0.19
K_{pc}	0.00	0.00	0.00	0.00	0.00	0.00	0.00	0.00	0.84	0.16
K_k	0.00	0.00	0.00	0.00	0.22	0.03	0.02	0.20	0.36	0.19
K_o	0.00	0.00	0.00	0.00	0.00	0.15	0.84	0.01	0.00	0.00
K_n	0.00	0.00	0.00	0.00	0.00	0.67	0.32	0.01	0.00	0.00
H_1	0.00	0.00	0.00	0.49	0.10	0.00	0.01	0.15	0.16	0.09
H_2	0.01	0.37	0.01	0.00	0.43	0.11	0.06	0.01	0.00	0.00
H_3	0.43	0.03	0.21	0.00	0.03	0.06	0.24	0.01	0.00	0.01
H_4	0.01	0.01	0.84	0.00	0.00	0.08	0.05	0.00	0.01	0.00

The error ratio matrix (Table 7.15) shows smallest error ratios result from prior information on K_{ch}, while the second smallest error ratios result from prior information on K_{pc}. Prior information on any of the parameters K_{ch}, K_{pc}, K_l, or K_k result in very small error ratios for the remaining parameters. Errors in any other parameters lead to very large error ratios for the parameters K_{ch}, K_{pc}, and K_l. Since these parameters have large uncertainties, the errors due to the error ratio may be within the parameter uncertainties. Regardless, prior information on the parameters K_{ch}, K_{pc}, and K_l are the

Table 7.15 Error ratio matrix for joint parameter estimates based on MINLEN criterion

	Parameters with prior information									
Estimated Parameters	K_{ch}	K_l	K_{pc}	K_k	K_o	K_n	H_1	H_2	H_3	H_4
K_{ch}	1.00	-58.60	3.28	-700.28	6.44	10.02	2626.75	-281.21	-683.16	1437.06
K_l	-0.01	1.00	-0.04	9.38	-0.04	0.00	-35.20	3.77	9.15	-19.26
K_{pc}	0.26	-14.97	1.00	-178.88	6.0	3.80	670.98	-71.83	-174.51	367.08
K_k	0.00	0.03	0.00	1.00	0.00	0.00	-1.33	0.14	0.35	-0.73
K_o	0.00	0.00	0.00	-0.01	1.00	0.00	0.03	0.00	-0.01	0.01
K_n	0.00	0.00	0.00	0.00	0.00	1.00	0.00	0.00	0.00	0.00
H_1	0.00	0.00	0.00	-0.04	0.00	0.00	1.00	-0.02	-0.04	0.09
H_2	0.00	0.00	0.00	0.00	0.00	0.00	0.00	1.00	0.00	0.00
H_3	0.00	0.00	0.00	0.00	0.00	0.00	0.00	0.00	1.00	0.00
H_4	0.00	0.00	0.00	0.00	0.00	0.00	0.01	0.00	0.00	1.00

most responsible since they lead to the smallest error ratios.

Based on examining the parameter space, three groups of parameters can be defined. The first group contains parameter K_{ch}, K_{pc}, K_l and K_k. For the joint data set, prior information on K_{ch} is the most efficient in reducing the overall parameter uncertainty, and leads to the smallest linearized error ratios. Prior information on any of the parameters in this group will reduce the uncertainty for all the parameters in the group. The second group contains the parameters K_o and K_n. Prior information on these parameters will not reduce the uncertainty of any of the parameters in the first group. Prior information on K_o or K_n will mainly reduce the uncertainty in these two parameters. The third group contains the head parameters. Prior information on the head parameters will not reduce the uncertainty in any of the hydraulic conductivity parameters significantly. The linearized error ratios show that the head parameters are the least responsible parameters for prior information.

7.6.7 Discussion of results for 10 parameter system

Estimating all 10 flow parameters in the model resulted in very large uncertainties for the hydraulic conductivities in the lower model layers. These large uncertainties dominated the model parameter space, and thus dominated the way the parameter space criteria selected the weights for joint parameter estimation. Prior information on these parameters with large uncertainties will efficiently stabilize the

parameter set. From the error ratio matrix, errors in the prior information for any of these parameters will not result in significant errors in the parameter estimates of the other model parameters.

Because the large uncertainties in the hydraulic conductivities of the lower model layers dominated model parameter space, the weighting criteria focused on reducing these large uncertainties. However, if the modeller were interested in estimating the hydraulic conductivity of the upper model layers as well as possible, the results would be disappointing, since the weighting criteria did not lead to the best estimates of these parameters. Since the uncertainties in the hydraulic conductivities of the upper model layers was small compared to the lower model layers, reducing the uncertainties in the upper model layers was not a priority for the weighting criteria. In fact, the weighting criteria that weighted the head data more than the ^{14}C data increased the uncertainties in the upper model layers.

For the second stage of parameter estimation, we wish to focus on estimating the hydraulic conductivities of the upper model layers as well as possible, given the data available. Based on the first stage, it is efficient and responsible to use prior information to define the parameter values for the lower four hydraulic conductivity parameters, K_{ch}, K_l, K_{pc} and K_k. These four parameters are specified at the parameter values from joint parameter estimation. Specifying the parameter values of the lower model layers will not significantly affect the parameter estimates for the upper model

layers.

7.7 Model calibration for 6 flow parameters

For the second stage of model calibration, only six model parameter are estimated. These parameters are the two hydraulic conductivity parameters, K_o and K_n, and the four head parameters. The same model and boundary conditions are used. The other four hydraulic conductivity parameters are specified at the values from the joint parameter estimates, which are very close to the prior parameter estimates. The model parameter space using hydraulic head and ^{14}C data is analyzed. The weighting criteria for the joint parameter estimates is the main focus. After estimation of the parameters using the joint data set is disussed, the effect of errors in the other model parameters is examined.

7.7.1 Parameter estimates and confidence region based on hydraulic head data set

The parameter estimates for this reduced parameter set using only hydraulic head data are nearly identical to the parameter estimates for the full parameter set using hydraulic head data. Table 7.16 contains the parameter estimates, standard errors, and CV's for the 6 parameters using only hydraulic head data. The standard errors and CV's are somewhat reduced from the full parameter set. With the full

parameter set, some of the longest axes of the parameter confidence region contained part of the uncertainty in these parameters. These long axes are now eliminated, and therefore the uncertainties in these parameters is somewhat reduced. However, the standard errors for the hydraulic conductivity parameters are still extremely large, suggesting these parameters are virtually non-identifiable using head data. The standard errors for the head parameters range from 9.8 to 25 meters.

Table 7.17 lists the axes of the confidence region for the 6 parameter set using the head data. Axes 5 and 6 are the longest axes, and have components only from the parameter axes K_o and K_n. Axes 1 through 4 contain components only from the head parameters. Again, the confidence regions for the hydraulic conductivity parameters and head parameters are nearly independent of each other. Note that axes 1 through 4 of the 6 parameter system are very similar to axes 1 through 4 of the 10 parameter system (Table 7.6). Also, axes 5 and 6 of the 6 parameter system are similar to axes 6 and 8 of the 10 parameter system. These similarities show that the confidence region for the parameters in the 6 parameter system is nearly the same as that for the 10 parameter system. The table of relative contributions to the CV of the parameters (Table 7.18) shows that axis 6 contributes most of the uncertainty to the two hydraulic conductivity parameters. The four smallest axes contribute most of the uncertainty to the head parameters.

Table 7.16 Parameter estimates and uncertainties for joint data set based on four weighting criteria; 6 parameter system

	Head Data Only			Concentration Data Only			Joint Data Set; MINCN			Joint Data Set; RESID			Joint Data Set; MINLEN			Joint Data Set; MINVOL		
w_h	1.0			0.0			1.0			1.0			0.60			0.19		
w_c	0.0			1.0			0.17			0.32			1.0			1.0		
Parameters	Estimate	Std	Coeff. Var.	Estimate	Std	Coeff. Var.	Estimate	Std	Coeff. Var.	Estimate	Std	Coeff. Var.	Estimate	Std	Coeff. Var.	Estimate	Std	Coeff. Var
K_o	209.6	33.79	14.560	10.750	0.137	0.135	5.368	0.148	0.202	5.361	0.102	0.140	7.668	0.073	0.082	9.336	0.063	0.065
K_h	149.2	33.77	15.530	0.397	0.130	0.276	0.216	0.119	0.178	0.234	0.089	0.141	0.258	0.066	0.112	0.348	0.062	0.135
H_1	1805.0	25.04	0.014	1836.0	352.08	0.192	1817.0	20.01	0.011	1812.0	21.28	0.012	1787.0	32.36	0.018	1766.0	48.37	0.027
H_2	1975.0	19.52	0.010	1991.0	16.95	0.009	1968.0	11.44	0.006	1975.0	9.44	0.005	1995.0	7.90	0.004	1994.0	6.50	0.003
H_3	1940.0	9.83	0.005	1997.0	9.48	0.005	1960.0	6.90	0.004	1969.0	5.96	0.003	1987.0	4.68	0.002	1988.0	4.18	0.002
H_4	1686.0	13.35	0.008	1714.0	33.18	0.019	1678.0	10.38	0.006	1677.0	11.09	0.007	1674.0	12.52	0.007	1699.0	13.51	0.008
Average CV			5.021			0.106			0.068			0.051			0.038			0.040
Condition Number			4716.0			321.0			89.5			92.9			98.6			135.9
Volume of Region			1.55e-07			1.01e-10			3.02e-11			1.10e-11			2.63e-12			1.96e-12
Length of Max Axis			19.1			0.251			0.219			0.169			0.126			0.143
S_h			58.7			0.0			64.4			73.5			89.2			101.8
S_c			0.0			40.5			94.1			73.2			62.5			56.7
s_h^2			1.06			0.00			1.17			1.33			1.62			1.85
s_c^2			0.00			2.22			5.22			4.07			3.47			3.15

Table 7.17 Axes of confidence region for parameter estimates based on head data; 6 parameter system

Axis Lengths	4.1e-03	6.1e-03	7.1e-03	1.4e-02	3.4e+00	1.9e+01
Parameters	U_1	U_2	U_3	U_4	U_5	U_6
K_o	0.00	0.00	0.00	0.00	-0.73	-0.68
K_n	0.00	0.00	0.00	0.00	0.68	-0.73
H_1	-0.06	-0.08	-0.49	-0.87	0.00	0.00
H_2	-0.23	-0.23	-0.81	0.49	0.00	0.00
H_3	-0.94	-0.19	0.27	-0.08	0.00	0.00
H_4	-0.25	0.95	-0.19	0.03	0.00	0.00

Table 7.18 Relative contribution to the CV from each axis of the confidence region based on head data; 6 parameter system

Parameters	U_1	U_2	U_3	U_4	U_5	U_6
K_o	0.00	0.00	0.00	0.00	0.03	0.97
K_n	0.00	0.00	0.00	0.00	0.03	0.97
H_1	0.00	0.00	0.07	0.88	0.00	0.04
H_2	0.01	0.03	0.40	0.55	0.00	0.01
H_3	0.68	0.06	0.17	0.05	0.04	0.00
H_4	0.02	0.65	0.03	0.00	0.28	0.02

7.7.2 Parameter estimates and confidence region based on ^{14}C data set

Table 7.16 also contains the parameter estimates and uncertainties for the ^{14}C data set when estimating only 6 parameters. The parameter estimates for this reduced

parameter set using only ^{14}C data are nearly identical to the parameter estimates for the full parameter set using the same data. The standard errors and CV's are again somewhat reduced from the full parameter set, for the same reasons explained above. The standard errors for the hydraulic conductivity parameters are near 0.13 orders of magnitude. The largest standard error is for parameter H_1, due to the scarcity of data in the southern end of the model.

Table 7.19 lists the axes of the confidence region for the 6 parameter set using the ^{14}C data. Axis 6 is the longest axis. Axes 4, 5 and 6 have the largest components from parameter axes K_o, K_n and H_1. Axes 1 through 4 have the largest components from H_1, H_2, and H_3. The six axes of the 6 parameter system follow the same pattern as axes 1 through 6 of the 10 parameter system (Table 7.10). The table of relative contributions to the CV of the parameters (Table 7.20) shows that axes 5 and 6 contributes most of the uncertainty to K_o, K_n, H_1, and H_4, while axes two and three contribute most of the uncertainty to H_2 and H_3.

The confidence region using ^{14}C data can be compared to the confidence region using the head data by calculating the angle of interaction. For the longest axes (axis 6 for ^{14}C data; axis 6 for head data), the angle of interaction is 37°. The axes have quite different orientations. However, using the head data, the longest axis is 19 units long, while for ^{14}C data, the longest axis is 0.25 units long. Though the axes have different orientations, the axis for ^{14}C data is much shorter than the axis for head

Table 7.19 Axes of confidence region based on ^{14}C data; 6 parameter system

Axis Lengths	8.1e-04	6.5e-03	9.0e-03	7.0e-02	1.3e-01	2.5e-01
Parameters	U_1	U_2	U_3	U_4	U_5	U_6
K_o	-0.01	0.03	-0.04	0.80	-0.54	-0.25
K_n	0.00	-0.02	0.04	0.44	0.25	0.86
H_1	0.02	0.01	0.01	-0.40	-0.80	0.44
H_2	0.43	0.78	0.46	0.01	0.01	-0.01
H_3	0.89	-0.29	-0.34	0.01	0.01	0.00
H_4	0.14	-0.55	0.82	0.02	-0.03	-0.05

Table 7.20 Relative contribution to the CV from each axis of the confidence ellipsoid based on the ^{14}C data; 6 parameter system

Parameters	U_1	U_2	U_3	U_4	U_5	U_6
K_o	0.00	0.00	0.00	0.26	0.41	0.33
K_n	0.00	0.00	0.00	0.02	0.02	0.96
H_1	0.00	0.00	0.00	0.03	0.44	0.53
H_2	0.00	0.50	0.34	0.02	0.05	0.09
H_3	0.03	0.22	0.63	0.04	0.07	0.01
H_4	0.00	0.05	0.21	0.01	0.08	0.65

data. The parameters are much better defined using the ^{14}C data; thus the joint data set may not improve the parameter estimates significantly over those using ^{14}C data alone. Remember that the longest axes contribute mainly to the uncertainty in the hydraulic conductivity parameters.

7.7.3 Joint parameter estimation for 6 parameter system

Joint parameter estimation using both hydraulic head and ^{14}C data is used to estimate the 6 model parameters. For joint estimation the weights for each data set can be chosen using any of the methods presented in Chapter 6. Before presenting the weights calculated using each method, the issue of weighting for this parameter set is discussed in a conceptual manner.

Table 7.16 contains the parameter estimates, uncertainties, and other statistics about the parameter estimates, including information about the fit for each data set. The head data produce better fits than the ^{14}C data at all sets of weights. However, even with the worse fit, the ^{14}C data estimate the two hydraulic conductivity parameters much better than the head data, and the ^{14}C data estimate the H_2 and H_3 about as well as the head data set. When the head data is weighted more heavily than the ^{14}C data, the fit of the calculated head data to the observed head data is better, since the parameter estimates are closer to those using only head data. At the same time, the fit for the ^{14}C data is worse, since the parameter estimates are farther from the estimates using only ^{14}C data. Since the calculated uncertainty depends on the fit of the data (see equations (4.2) and (4.3)), those parameters which the ^{14}C data estimate well (K_o and K_n in this case) is poorly served by weighting the head data more than the ^{14}C data. Conversely, if the ^{14}C data are weighted more heavily than the head data, the fit of the calculated ^{14}C data to the observed ^{14}C data is better,

since the parameter estimates are closer to those using only ^{14}C data. Those parameters which the ^{14}C data estimate well, K_o and K_n, benefit by weighting the ^{14}C data more than the head data. It makes sense to weight the ^{14}C data more heavily than the head data in this case, since the ^{14}C data produces better estimates of the hydraulic conductivity parameters than the head data.

Table 7.16 contains the parameter estimates and uncertainties for all four weighting criteria. The MINCN and RESID criteria weight the head data more heavily than the ^{14}C data. The RESID criterion produces weights which are somewhat different from the weights produced from the 10 parameter set. The RESID criterion weights the head data more heavily because s_h^2 is always smaller than s_c^2. The MINLEN and MINVOL criteria weight the ^{14}C data more heavily than the head data. As discussed above, this weighting makes sense conceptually, since the ^{14}C data produce better estimates than the head data for the most uncertain parameters.

The parameter estimates and parameter space change as the weights change. For K_n and K_o, the parameter estimates become larger as the ^{14}C weight increases. The uncertainties in these parameters also become decrease as the ^{14}C weight increases. For parameters H_1 and H_4, the parameter uncertainty increases as the ^{14}C weight increases. These parameters are more uncertain using ^{14}C data than head data, so this increase in parameter uncertainty is not surprising. For parameters H_2 and H_3, the parameter uncertainties decrease slightly as the ^{14}C weight increases.

Though individual parameter uncertainties move different directions as the ^{14}C weight increases, the overall parameter uncertainty generally decreases as the ^{14}C weight increases. The minimum overall parameter uncertainty, as measured by the average CV, is observed at the parameter estimates using the MINLEN weighting criterion. Weighting the head data more than the ^{14}C data, as required by the MINCV and RESID criteria, does not result in the lowest uncertainty joint parameter estimates.

7.7.4 Parameter space based on joint data set

If more reliable parameter estimates are required, the parameter space for the 6 parameter set can be examined to determine the most efficient and responsible parameters for prior information. Table 7.21 lists the axes of the confidence region for the final parameter estimates for the joint data set using the MINLEN parameter estimates. The longest axis, axis 6, has the largest component from parameter K_n, and the second largest component from axis K_o. Prior information on these two parameters would be the most efficient in reducing the overall parameter uncertainty.

Table 7.22 is the error ratio matrix for this parameter set. Prior information on K_n results in the smallest error ratios. Prior information on K_o also results in relatively small error ratios, as does prior information on H_1. Prior information on the other head parameters lead to larger error ratios for the hydraulic conductivity parameters. K_n is the most responsible parameter for prior information, while K_o and H_1 are also good

Table 7.21 Axes of confidence region based on joint data set at MINLEN weights; 6 parameter system

Axis Lengths	1.29e-03	3.64e-03	4.47e-03	1.76e-02	1.26e-01	5.50e-02
Parameters	U_1	U_2	U_3	U_4	U_5	U_6
K_o	-0.03	0.02	0.00	0.05	-0.53	-0.85
K_n	-0.01	0.02	0.05	0.05	0.85	-0.53
H_1	0.04	-0.03	-0.02	-1.00	0.02	-0.07
H_2	0.24	-0.95	0.22	0.04	-0.01	-0.03
H_3	0.96	0.20	-0.19	0.04	-0.01	-0.03
H_4	0.14	0.25	0.96	-0.02	-0.05	0.02

Table 7.22 Error ratio matrix based on joint data set at MINLEN weights; 6 parameter system

	Parameters with prior information					
Estimated Parameters	K_o	K_n	H_1	H_2	H_3	H_4
K_o	1.00	-0.58	-0.51	6.71	17.91	5.07
K_n	-1.08	1.00	0.81	-1.72	-4.29	9.24
H_1	-0.02	0.02	1.00	-0.46	-0.32	-0.26
H_2	0.01	-0.01	0.00	1.00	0.08	0.06
H_3	0.01	-0.01	-0.01	0.03	1.00	0.07
H_4	0.06	-0.05	-0.04	0.23	0.75	1.00

choices for prior information. Prior information on the other head parameters would not be as responsible if the modeller were interested in the estimates of K_o and K_n.

7.7.5 Effect of errors in other parameters

In calibrating the above model, several parameters were not estimated. These parameters are the effective porosity in each unit, the anisotropy for each unit, the initial concentration for ^{14}C at the boundary, and the longitudinal and transverse dispersivities. These parameters were assigned a specified value. It is important to determine whether errors in the specified values of these parameters influence the estimated parameters significantly. For this purpose, the linearized error ratio matrix can be computed for these transport parameters.

The resulting error ratio matrix is shown in Table 7.23. The parameters P_o and P_n are the effective porosity of the Ojo Alamo and Nacimiento respectively, and the parameters An_o and An_n are the anisotropy of the Ojo Alamo and Nacimiento.The parameters that have significant error ratios are the hydraulic conductivity parameters as a result of errors in c_{init}, α_L, and An_n. Errors in the boundary ^{14}C concentration may be magnified over three times when estimating the hydraulic conductivity parameters. Errors in α_L lead to largest error ratios for K_o and K_n, while errors in α_T lead to very small error ratios for K_n than K_o. The estimates of the hydraulic conductivity parameters are very sensitive to errors in the estimate of α_L. This sensitivity is problematic, since prior information on α_L is difficult to obtain. The parameter estimates are insensitive to errors in the anisotropy of K_o, but more sensitive to the anisotropy of K_n. These error ratios are consistent, since in the Ojo Alamo, the flow

Table 7.23 Error ratio matrix for transport parameters using parameter space based on joint data set at MINLEN weights; 6 parameter set

	Transport Parameters						
Estimated Parameters	P_o	P_n	c_{init}	α_L	α_T	An_o	An_n
K_o	0.55	0.52	-3.6	-9.0	-0.30	-0.01	0.61
K_n	-0.79	-0.71	3.3	11.5	0.86	0.01	-1.37
H_1	0.00	0.00	-0.01	0.02	0.00	0.00	0.00
H_2	0.00	0.00	0.01	-0.01	0.00	0.00	0.00
H_3	0.00	0.00	0.00	0.00	0.00	0.00	0.01
H_4	0.00	0.00	-0.02	0.00	0.01	0.00	0.01

direction is dominantly along the dip of the unit, and therefore not very sensitive to the anisotropy of K_o. In the Nacimiento, there is a small component of vertical flow, and the anisotropy of the unit does affect the flow field. Based on these linearized error ratios, estimating both c_{init} and α_L along with the flow parameters for this model would be more responsible than simply using prior information on these transport parameters. Using prior information for the other transport parameters is responsible, since the linearized error ratios are small.

Based on the above error ratio analysis, parameter estimation for the flow system is performed for 8 parameters: the six flow parameters and c_{init} and α_L. For c_{init}, the final parameter estimate is 79.5 pmc. For α_L, the final parameter estimates is 350 m. Both of these parameter estimates are close to their prior values, so the estimates for the flow parameters are similar to the parameter estimates using prior information

on c_{init} and α_L. The linearized error ratios show the potential for large errors when using prior information on c_{init} and α_L, but these prior estimates are close to the estimates using the calibration data, so no large errors occur.

7.8 Summary of model calibration for the San Juan Basin

A cross section model for the San Juan basin has been developed. Hydraulic head data, ^{14}C data, and independent information on parameter values have been used to calibrate this model in an efficient and responsible manner. The model has been calibrated in two stages.

In the first stage, 10 flow parameters were estimated, the hydraulic conductivity of the 6 model layers and the head boundary values at four nodal points. The joint estimates did reduce the uncertainty in the model parameters significantly over the head data set. However, estimating all 10 parameters resulted in large uncertainties for the hydraulic conductivities in the lower model layers in both single state and joint parameter estimates. These large uncertainties dominated the model parameter space, and thus dominated the way the parameter space criteria selected the weights for joint parameter estimation. The criteria weighted the head data more heavily than the concentration data. These weights reduced the uncertainty in the overall parameter estimates, but did not produce the best estimates for all model parameters. Prior information on the parameters in the lower model layers was found to be most

efficient in stabilizing the overall parameter set. Errors in the prior information for any of these parameters did not result in significant errors in the parameter estimates of the other model parameters.

In the second stage of model calibration, the focus was on obtaining the best possible estimates for the hydraulic conductivities in the upper model layers. Prior information was used to define the parameter values for the lower four hydraulic conductivity parameters, and only six model parameters were estimated: two hydraulic conductivity parameters and the four head parameters. The concentration data resulted in much better estimates of the hydraulic conductivity parameters than the head data set. For this parameter set, the MINLEN and MINVOL parameter space methods weighted the concentration data more heavily than the head data. These weights made sense conceptually, and resulted in the best estimates for the hydraulic conductivities in the upper model layers, and the minimum overall parameter uncertainties. The RESID and MINCN criteria weighted the head data more heavily than the ^{14}C data, a weighting scheme which did not result in the best parameter estimates. The error ratios for the parameters which were specified were generally small, with the exception of the initial concentration of ^{14}C and the longitudingal dispersivity.

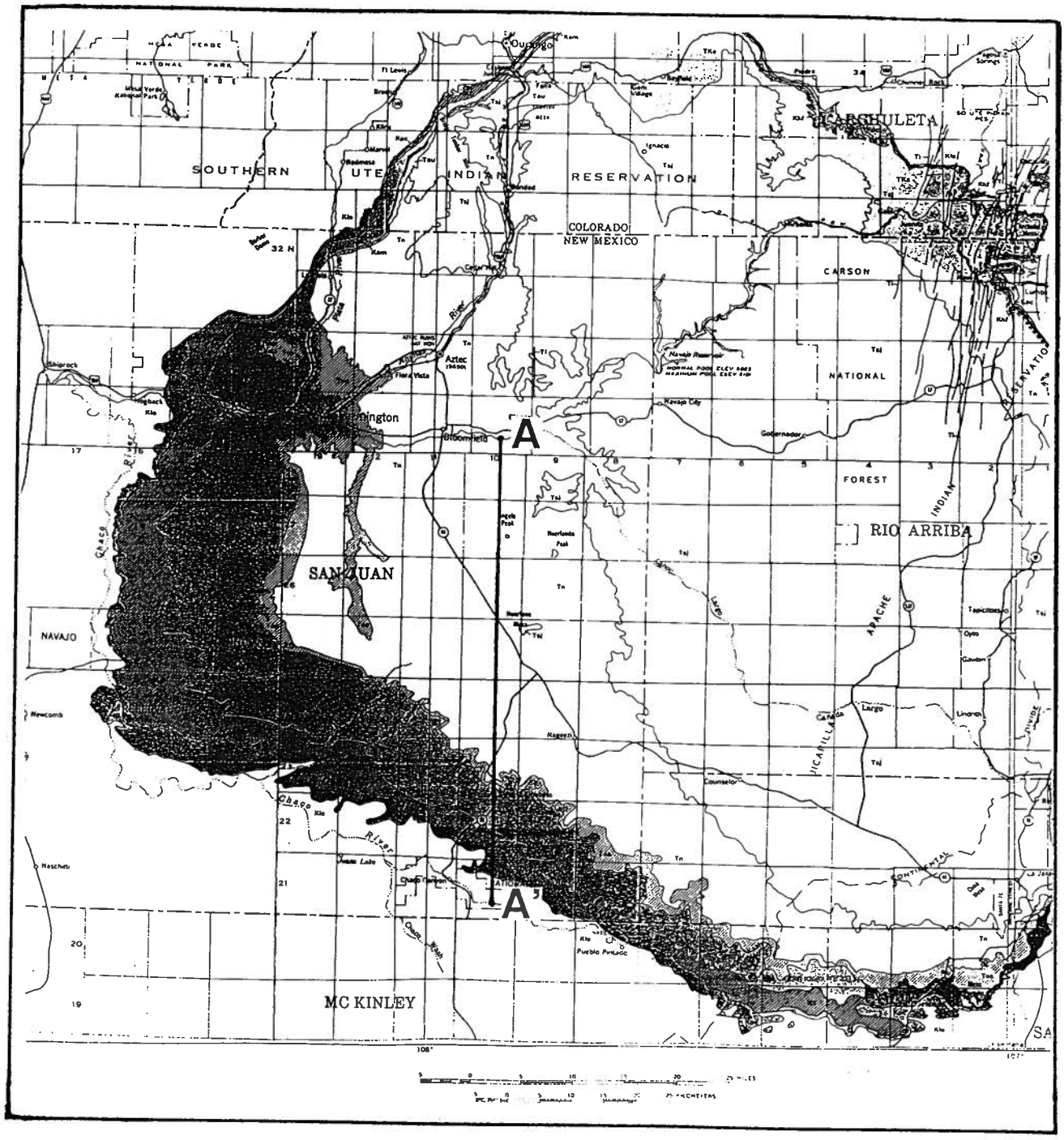

Figure 7.1 Plan view of the San Juan Basin showing outcrops of major units and the location of the modelled cross section. The white in the center of the basin represents the outcrop of the Nacimiento Formation. The shaded areas represent the outcrop area of the Ojo Alamo SS, Kirtland/Fruitland Shale, and Pictured Cliffs SS.

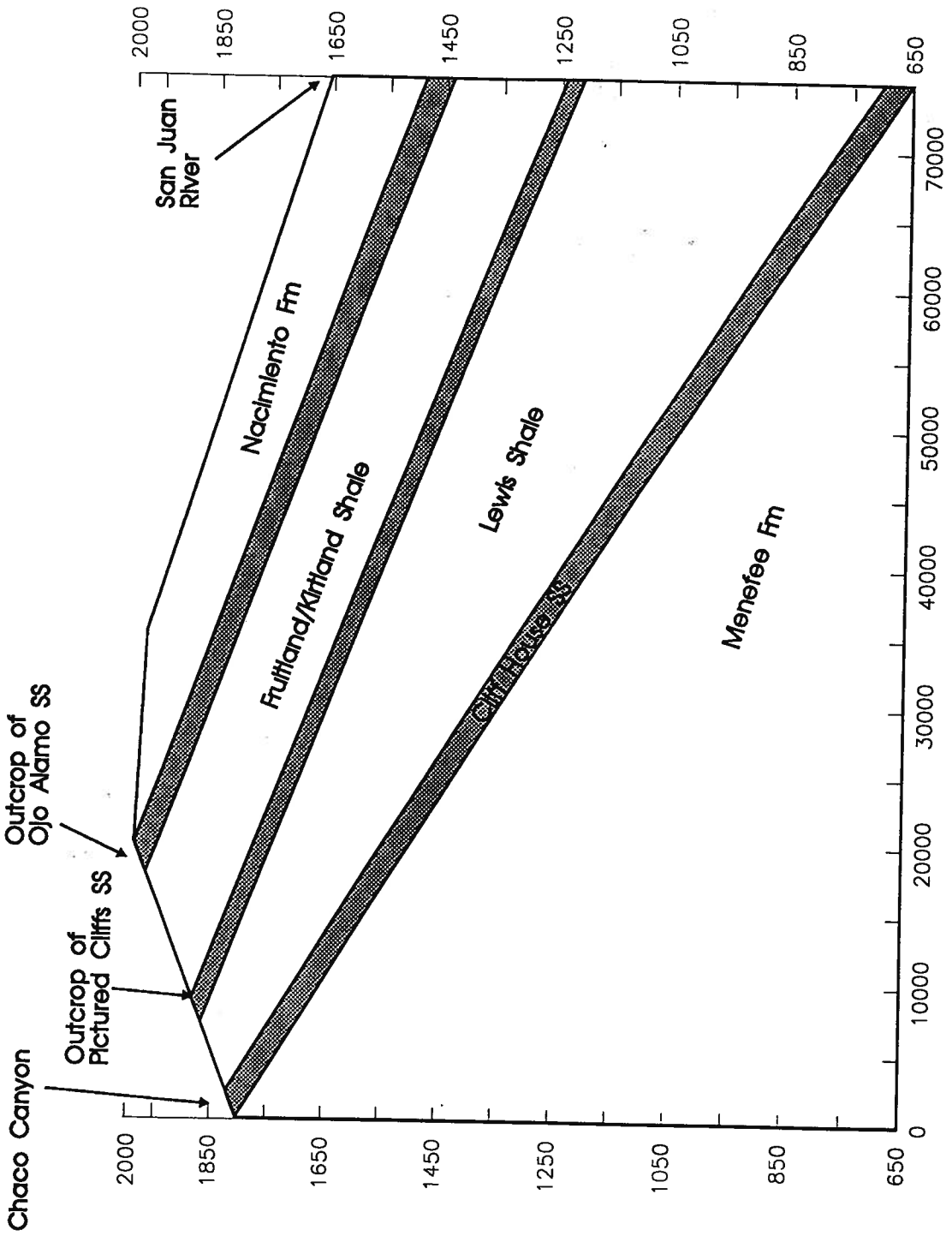

Figure 7.2 Generalized north-south cross section of the San Juan Basin along modelled cross section.

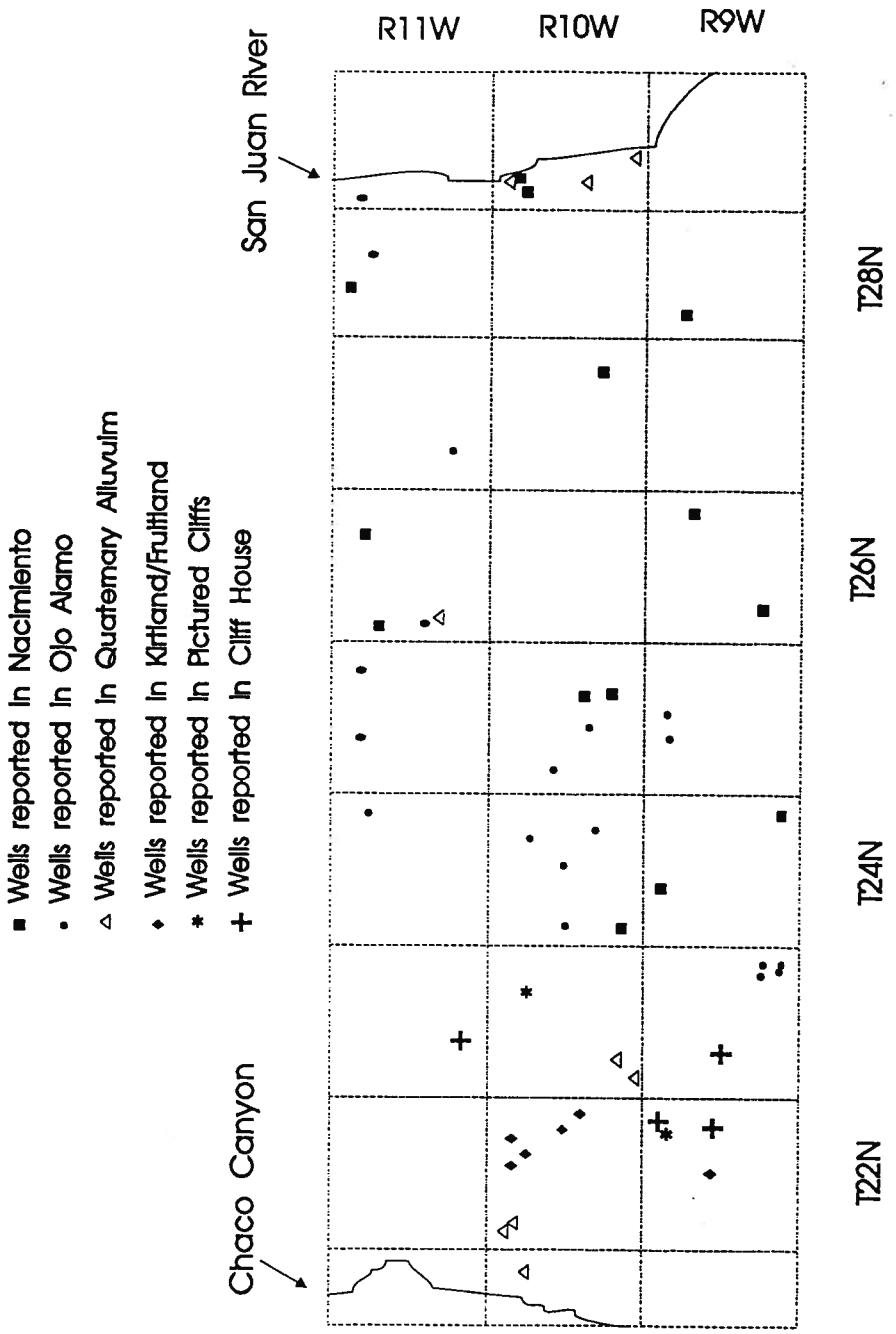

Figure 7.3 Location of wells with hydraulic head data in R9W, R10W and R11W from Chaco Canyon to the San Juan river.

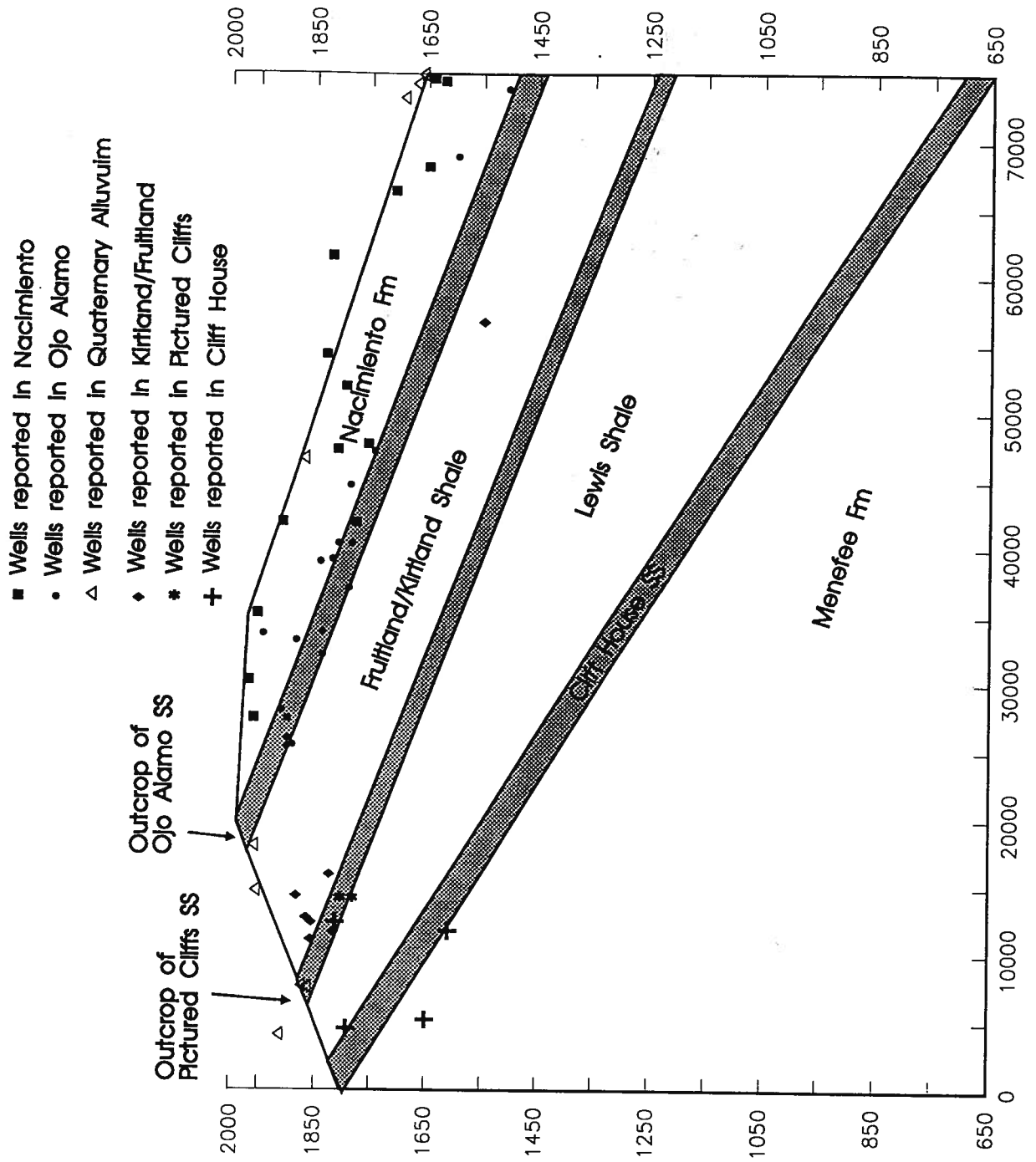

Figure 7.4 Location of midpoint of screened interval for wells in head data set along modelled cross section.

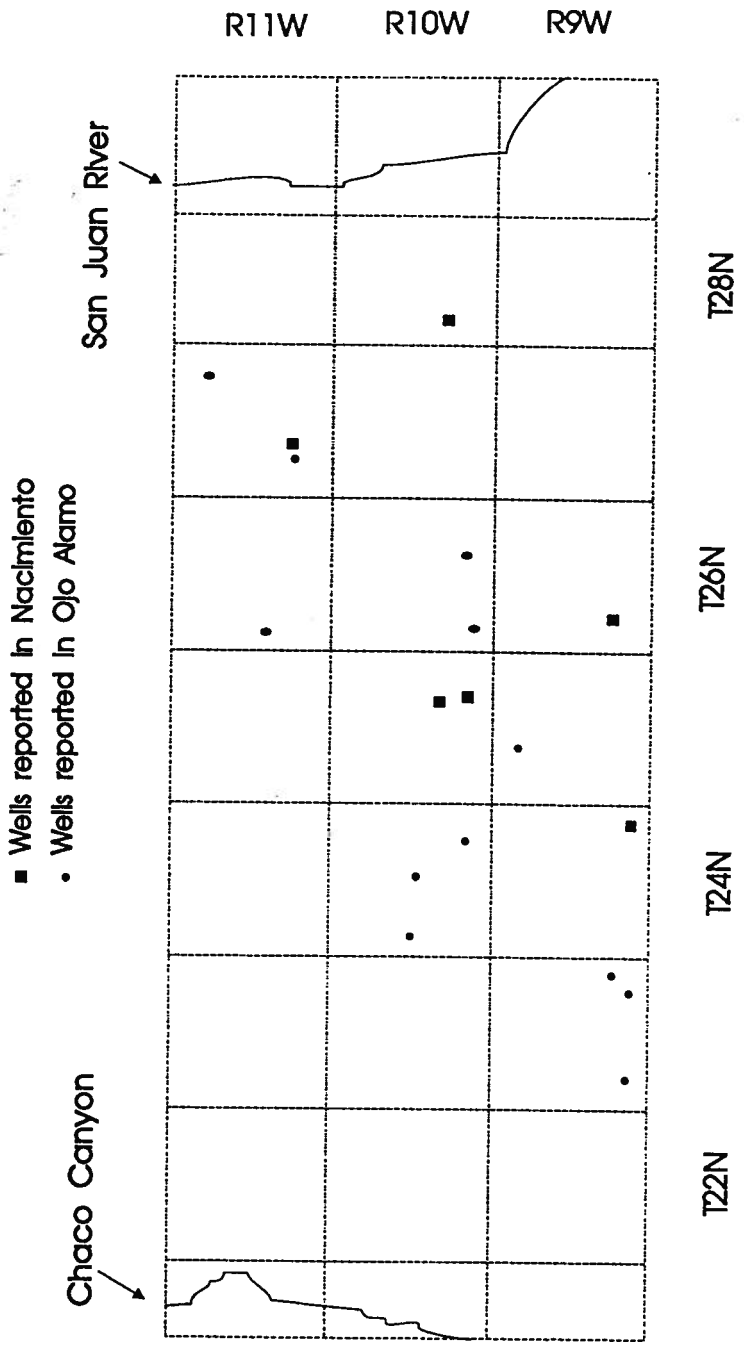

Figure 7.5 Location of wells with ^{14}C data in R9W, R10W and R11W from Chaco Canyon to the San Juan river.

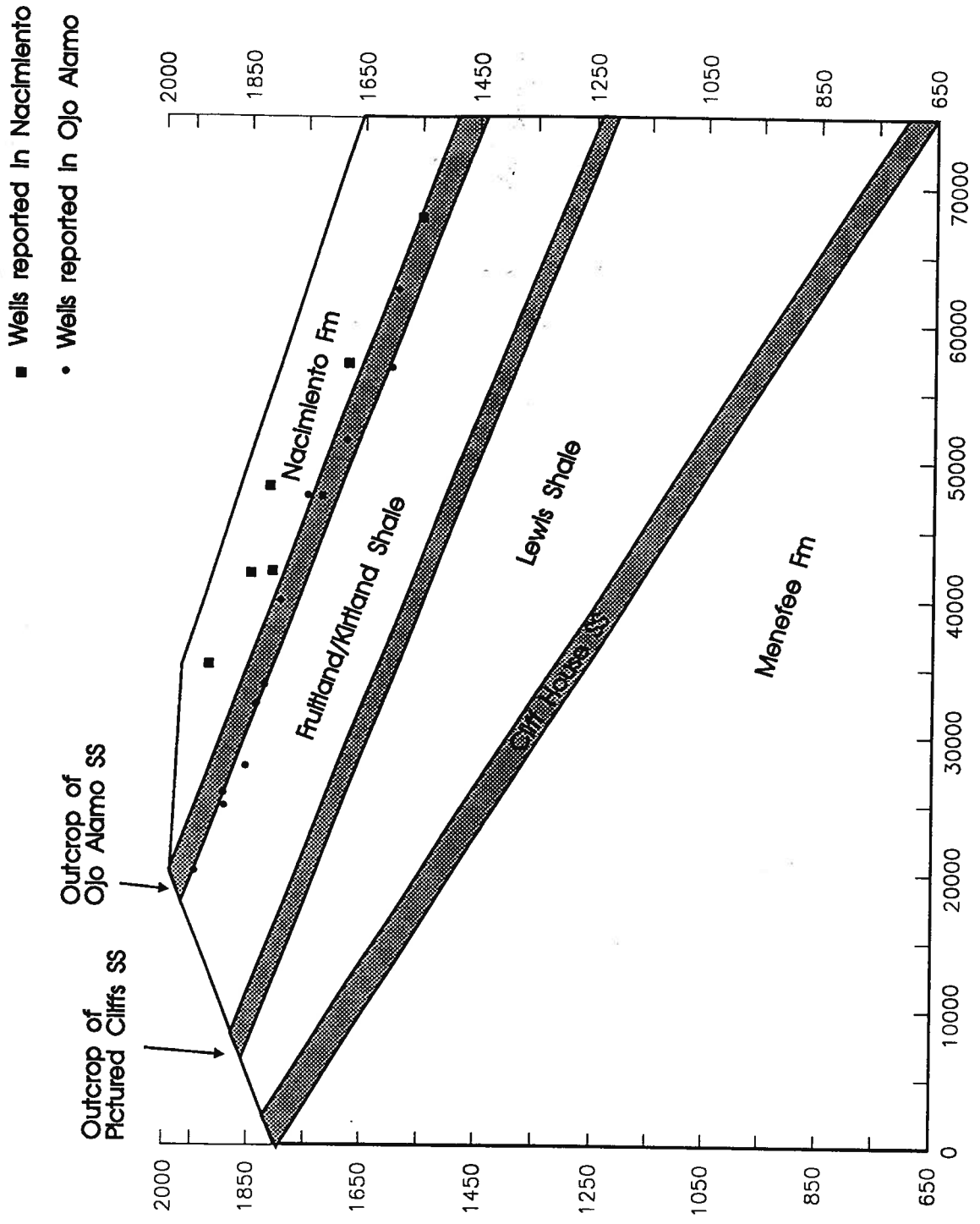

Figure 7.6 Location of midpoint of screened interval for wells with ^{14}C data along modelled cross section.

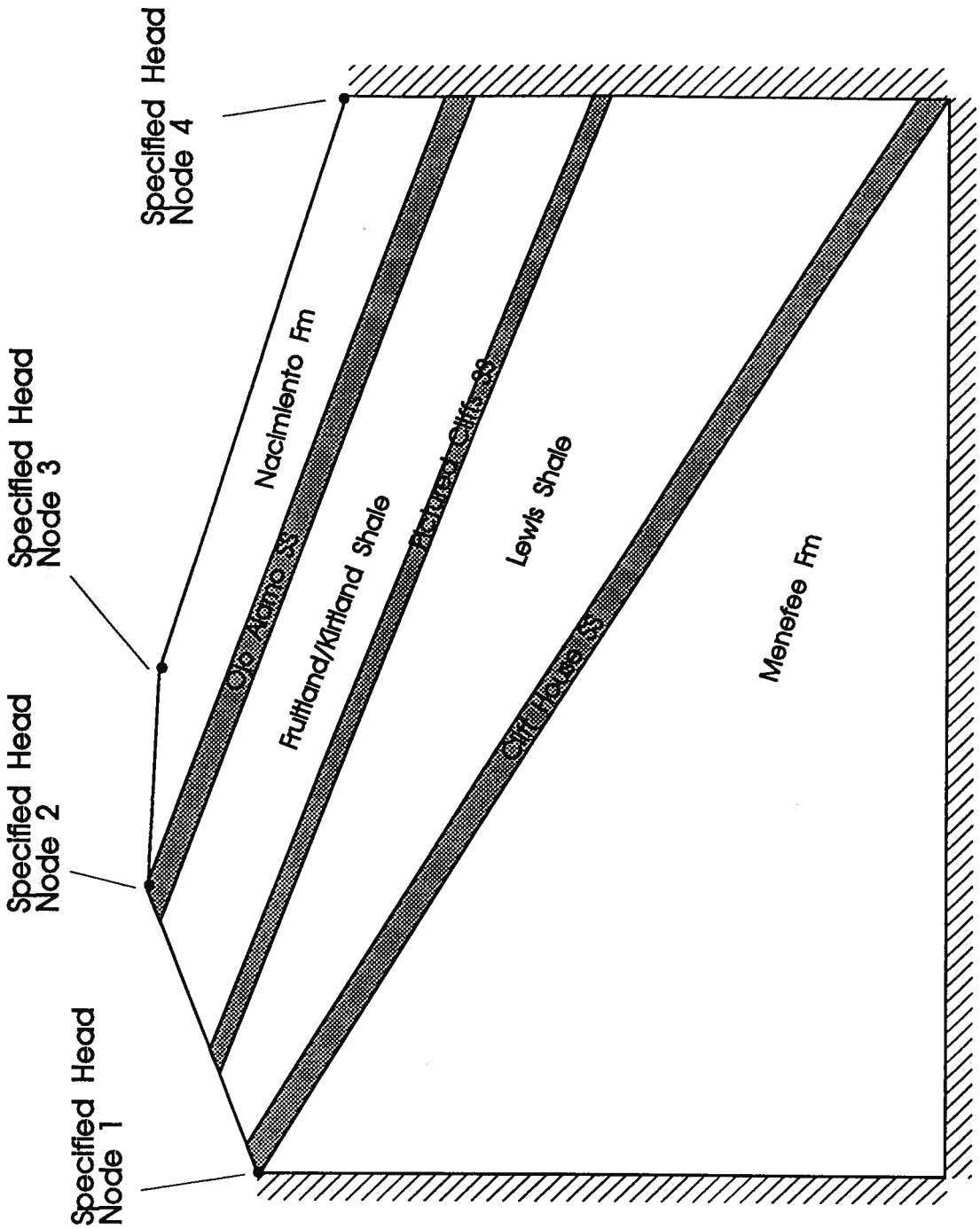

Figure 7.7 Conceptual cross section showing layering and model boundary conditions.

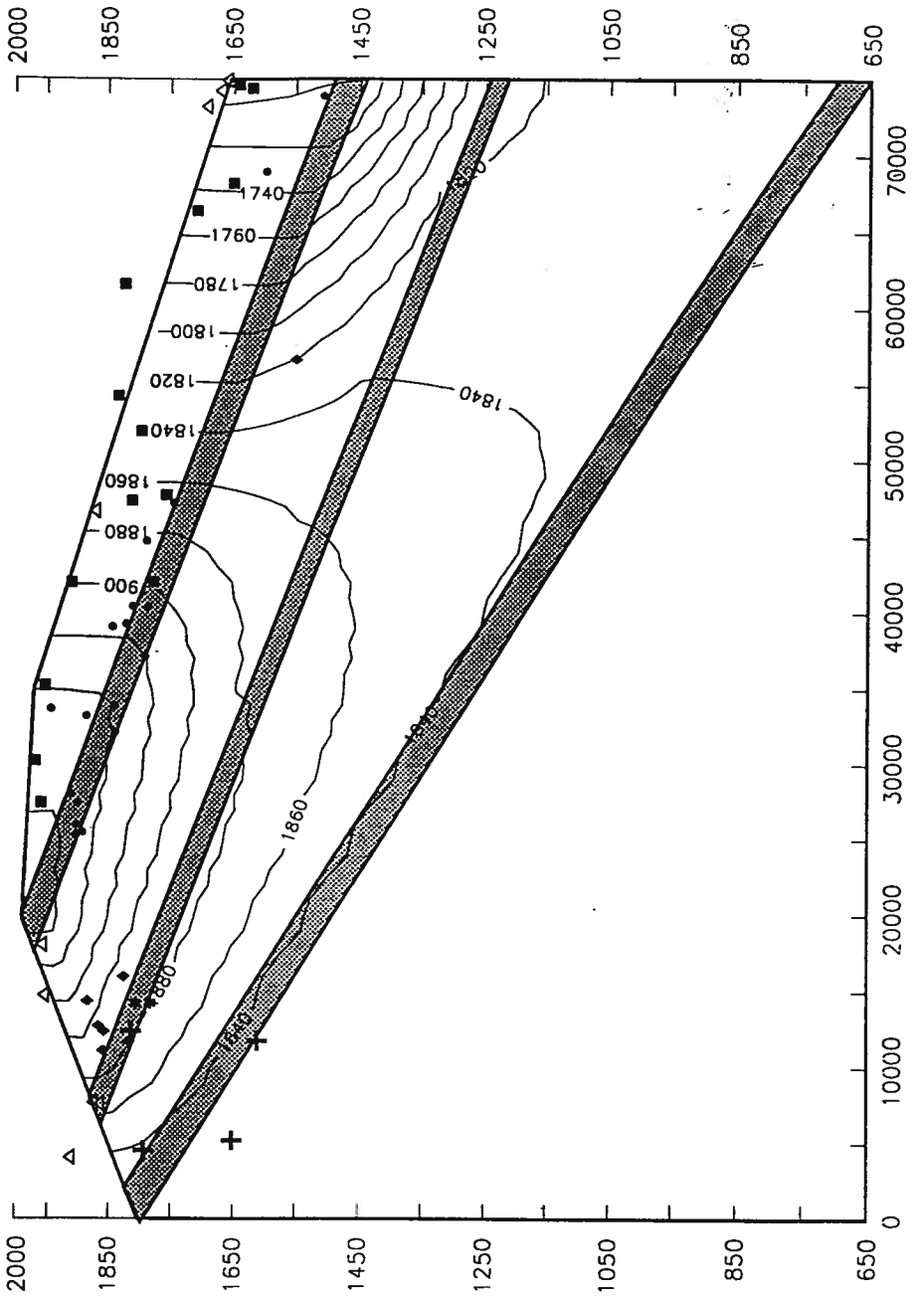

Figure 7.8 Head distribution based on final parameter estimates using the hydraulic head data data set.

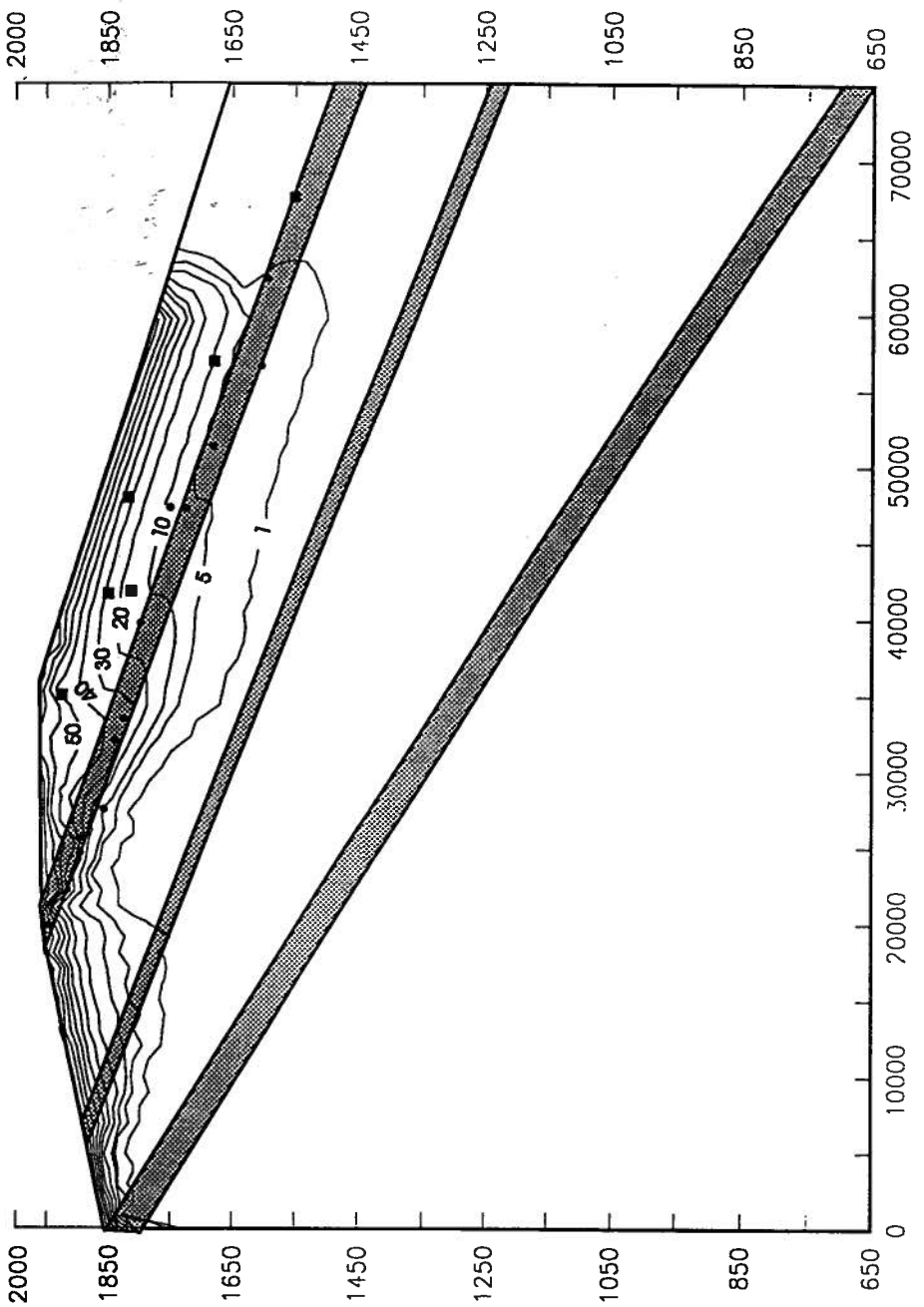

Figure 7.9 The ^{14}C distribution based on final parameter estimates from ^{14}C data set.

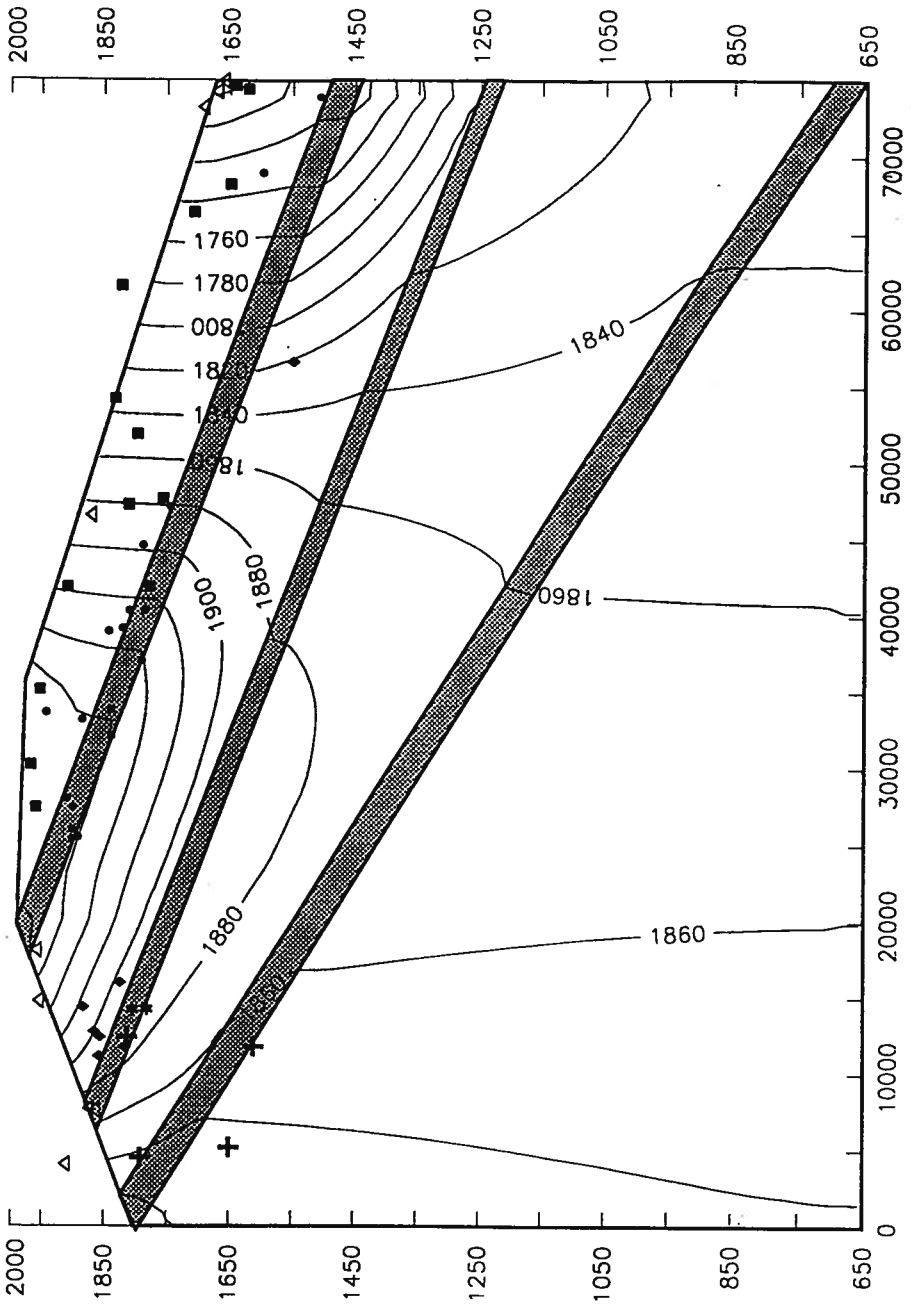

Figure 7.10 Head distribution based on final parameter estimates from joint data set.

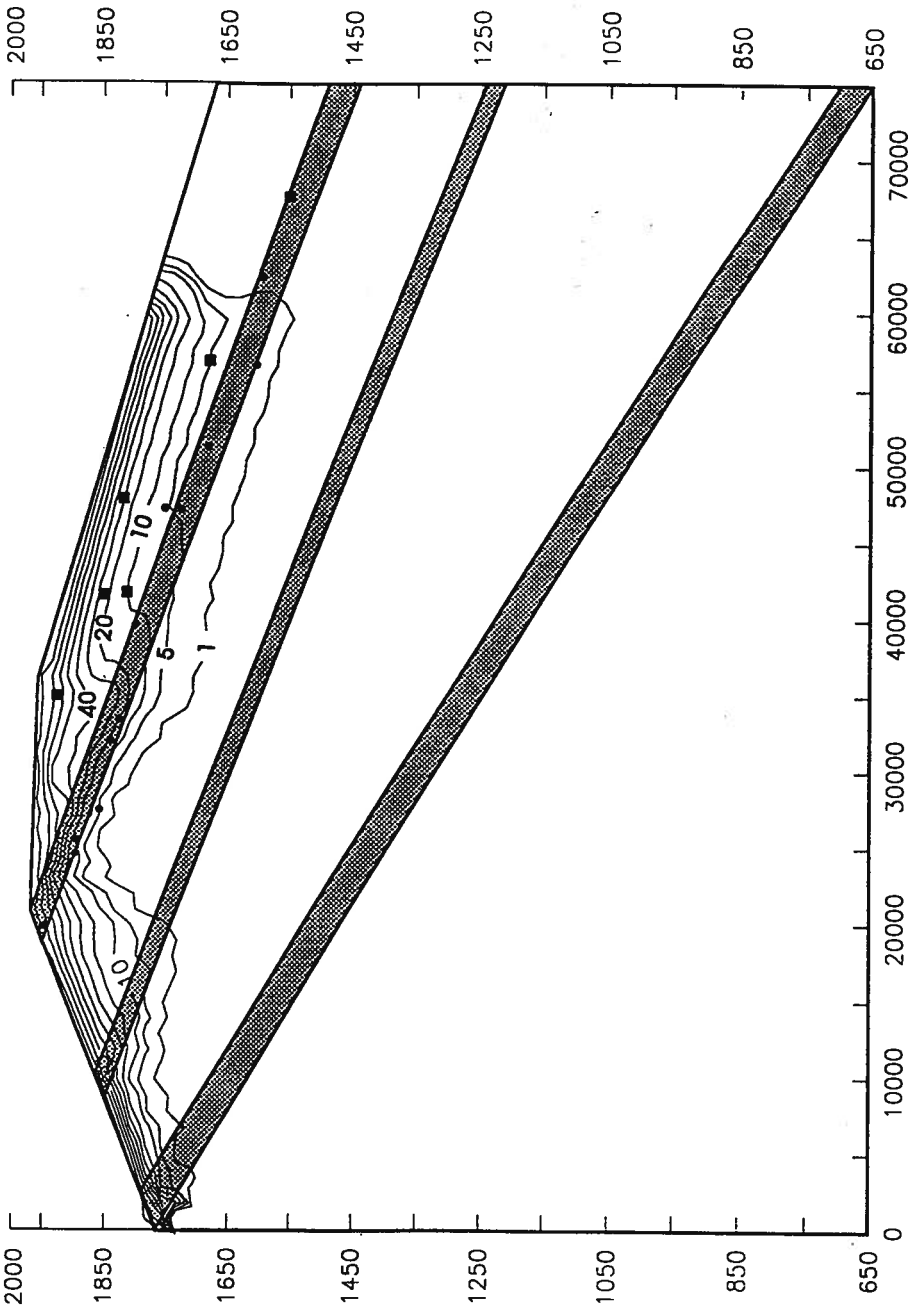

Figure 7.11 The ^{14}C distribution based on final parameter estimates from joint data set

CHAPTER 8. SUMMARY

The work in this thesis is devoted toward understanding parameter estimation for groundwater flow models. Parameter estimation using only hydraulic head data often results in ill-conditioned parameter estimates, leading to problems with non-unique and unstable parameter estimates with large uncertainties. Prior information on parameters or joint parameter estimation including tracer concentration data have been proposed to reduce the ill-conditioning of the parameter estimates. Prior information or joint estimation reduce the ill-conditioning of the parameter estimates in some situations, but in other situation they do not reduce the ill-conditioning of the parameter estimates significantly. The focus of the thesis has been to understand in what situations prior information or joint estimation will significantly improve the parameter estimates, and develop guidelines for using prior information and joint parameter estimation in an efficient and responsible manner.

The key contributions of this thesis are:

1. Parameter space analysis using response surfaces and linearized confidence regions is introduced. Response surfaces are used to understand conceptually how prior information and joint parameter estimation improve parameter estimates. Linearized confidence regions are used to extend the concepts to multiple parameter dimensions.
2. Guidelines are developed for the efficient and responsible use of prior

information in groundwater flow models. Efficient use of prior information involves identifying those parameters for which prior information will stabilize the parameter estimates the most. Responsible use of prior information involves those parameters for which errors in the prior information have the smallest influence on the parameter estimates.

3. Guidelines are developed to identify situations where joint parameter estimation will significantly improve parameter estimates over single state parameter estimation. Criteria are also developed and evaluated for weighting individual data sets in joint parameter estimation.

4. The above guidelines are used to develop and calibrate a groundwater flow model for the San Juan Basin, New Mexico. Hydraulic head data, ^{14}C data, and prior information on parameter values are used to calibrate the model. The most efficient and responsible use of prior information is identified. Weighting criteria are applied and evaluated to determine appropriate weights for the head and ^{14}C data.

REFERENCES

Baltz, E.H., Stratigraphy and regional tectonic implications of part of the Upper Cretaceous and Tertiary rocks, east-central San Juan Basin, New Mexico, U.S. Geol. Surv. Prof. Pap., 552, 1967

Baltz, E.H., S.R. Ash, and R.Y. Anderson, History of the nomenclature and stratigraphy of rocks adjacent to the Cretaceous-Tertiary boundary, western San Juan Basin, New Mexico, U.S. Geol. Surv. Prof. Pap., 524-D, 1966

Campana, M.F., and E.S. Simpson, Groundwater residence times and discharge rates using discrete-state compartment model and ^{14}C data, J. Hydrol., 72, 171-185, 1984

Carrera, J., State of the art of the inverse problem applied to the flow and solute transport equations, in Groundwater Flow and Quality Modelling, edited by E. Custodio et al., pp. 549-583, D. Reidel Publishing Co., 1988

Carrera, J., and S.P. Neuman, Estimation of aquifer parameters under transient and steady state conditions, 1. Maximum likelihood method incorporating prior information, Water Resour. Res., 22(2), 199-210, 1986a

Carrera, J., and S.P. Neuman, Estimation of aquifer parameters under transient and steady state conditions, 2. Uniqueness, stability, and solution algorithms, Water Resour. Res., 22(2), 211-227, 1986b

Carrera, J., and S.P. Neuman, Estimation of aquifer parameters under transient and steady state conditions, 3. Aplication to synthetic and field data, Water Resour. Res., 22(2), 228-242, 1986c

Chavent, G., About the stability of the optimal control solution of inverse problems, in Inverse and Improperly Posed Problems, edited by G. Anger, pp. 45-58, Akademie-Verlag, Berlin, 1979

Cooley, R.L., A method of estimating parameters and assessing reliability of models of steady state groundwater flow, 1. Theory and numerical properties, Water Resour. Res., 13(2), 318-324, 1977

Cooley, R.L., A method of estimating parameters and assessing reliability of models of steady state groundwater flow, 2. Application of statistical analysis, Water Resour. Res., 15(3), 603-617, 1979

Cooley, R.L., Incorporation of prior information on parameters into nonlinear regression groundwater flow models, 1. Theory, Water Resour. Res., 18(4), 965-976, 1982

Cooley, R.L., Exact Scheffe-type confidence intervals for output from groundwater models, 2. Combined use of hydrogeologic information and calibration data, Water Resour. Res., 29(1), 35-50, 1993

Cooley, R.L. and R.L. Naff, Regression modeling of groundwater flow, USGS Open File Report 85-180, 1985

Cooley, R.L., Konikow, L.F., and Naff, R.L., Nonlinear regression groundwater flow modeling of a deep regional aquifer system, Water Resour. Res., 22(13), 1759-1778, 1986

Copty, N., Y. Rubin, and G. Mavko, Geophysical-hydrological identification of field permeabilities through Bayesian updating, Water Resour. Res., 29(8), 2813-2825, 1993.

Dagan, G., Stochastic modeling of groundwater flow by unconditional and conditional probabilities: The inverse problem, Water Resour. Res., 21(1), 65-72, 1985.

Dagan, G., Time dependent macrodispersion for solute transport in anisotropic heterogeneous aquifers, Water Resour. Res., 24(9), 1491-1500, 1988

Dagan, G., and Y. Rubin, Stochastic identification of recharge, transmissivity and storativity in aquifer unsteady flow: A quasi-steady approach, Water Resour. Res., 24(10), 1698-1710, 1988.

Emsellen, Y., and G. de Marsily, An automatic solution for the inverse problem, Water Resour. Res., 7(5), 1264-1283, 1971

Fasset, J.E., and J.S. Hinds, Geology and fuel resources of the Fruitland Formation and Kirtland Shale of the San Juan Basin, New Mexico and Colorado, U.S. Geol. Surv. Prof. Pap., 676, 1971

Fontes, J. Ch., Environmental isotopes in groundwater hydrology, in Handbook of Environmental Isotope Geochemistry, edited by P.Fritz and J. Ch. Fontes, pp.75-134, Elsevier, New York, 1980

Fontes, J. Ch., and J.M. Garnier, Determination of the initial carbon-14 activity of the total dissolved carbon - A review of the existing models and a new approach, Water Resour. Res., 15, 399-413, 1979

Freeze, R.A., J. Massmann, L. Smith, T. Sperling, and B. James, Hydrogeological decision analysis, 1. A framework, Ground Water, 28(5) 738-766, 1990

Gailey, R.M., A.S. Crowe, and S.M. Gorelick, Coupled process parameter estimation and prediction uncertainty using hydraulic head and concentration data, Adv. Water Resour., 14(5), 301-314, 1991

Gavalas,G.R., P.C. Shah, and J.H. Seinfeld, Reservoir history matching by Bayesian estimation, Soc. Pet. Eng., J., 16(6), 337-350, 1976

Gelhar, L.W., and C.L. Axness, Three-dimensional stochastic analysis of macrodispersion in aquifers, Water Resour. Res., 19(1), 161-180, 1983

Graybill, F.A., Theory and Application of the Linear Model, Duxbury, North Scituate, Mass., 1976.

Gupta, S.K., D. Lal, and P. Sharma, An approach to determining pathways and residence time of groundwaters: Dual radiotracer dating, J. Geophys. Res., 86, 5292-5300, 1981

Hefez, E., V. Shamir, and J. Bear, Identifying the parameters of an aquifer cell model, Water Resour. Res., 11(6), 993-1004, 1975.

Hill, M.C., A computer program (MODFLOWP) for estimating parameters of a transient, three dimensional ground-water flow model using nonlinear regression, U.S. Geol. Sur. Open File Rep. 91-484, Denver, 1992

Hill, P.D., A review of experimental design procedures for regression and model discrimination, Technometrics, 20, 15-21,1978

Hoeksema, R.J., and P.K. Kitanidis, An application of the geostatistical approach to the inverse problem in two-dimensional groundwater modeling, Water Resour. Res., 20(7), 1003-1020, 1984

Jacquard, P., and C. Jain, Permeability distribution from field pressure data, Soc. Pet. Eng. J., 5(4), 281-294, 1965.

Kitanidis, P.K., and E.G. Vomvoris, A geostatistical approach to the inverse problem in groundwater modeling and one-dimensional simulations, Water Resour. Res., 19(3), 677-690, 1983.

Kleinecke, D., Use of linear programming for estimating geohydrologic parameters in groundwater basins, Water Resour. Res., 7(2), 367-375, 1971.

Krabbenhoft, D.P., M.P. Anderson, C.J. Bowser, and J.W. Valley, Estimating groundwater exchange with lakes, 1. The stable isotope mass balance method, Water Resour. Res. 26(10), 2445-2453, 1990a.

Krabbenhoft, D.P., M.P. Anderson, and C.J. Bowser, Estimating groundwater exchange with lakes, 2. Calibration of a three-dimensional, solute transport model to a stable isotope plume, Water Resour. Res. 26(10), 2455-2462, 1990b.

Kuczera, G. Improved parameter inference in catchment models, 1. Evaluating parameter uncertainty, Water Resour. Res., 19(5), 1151-1162, 1983a.

Kuczera, G. Improved parameter inference in catchment models, 2. Combining different types of hydrologic data and testing their compatability, Water Resour. Res., 19(5), 1163-1172, 1983b.

Marquardt, D.W., An algorithm for least-squares estimation of non-linear parameters, J. Soc. Ind. Appl. Math., 11(2), 431-441, 1963

Mendoza, C.A., R. Therrien, and E.A. Sudicky, ORTHOFEM users guide, University of Waterloo, Waterloo, Ontario, 14pp.,1992

Mishra, S., and S.C. Parker, Parameter estimation for coupled unsaturated flow and transport, Water Resour. Res., 25(3), 385-396, 1989.

Mook, W.G., Carbon-14 in hydrogeological studies, in Handbook of Environmental Isotope Geochemistry, edited by P.Fritz and J. Ch. Fontes, pp.49-74, Elsevier, New York, 1980

Neuman, S.P. and S. Yakowitz, A statistical approach to the inverse problem in aquifer hydrology, 1. Theory, Water Resour. Res., 15(4), 845-860, 1979.

Neuman, S.P., A statistical approach to the inverse problem of aquifer hydrology, 3. Improved solution method and added perspective, Water Resour. Res., 16(2), 331-346, 1980.

Nour-Omid, B., W.S. Dunbar, and A.D. Woodbury, Lanczos and Arnoldi methods for the solution of convection-diffusion equations, Comp. Meth. App. Mech. Eng., 88, 75-95, 1991

Pearson, F.J., Jr., and D.E. White, Carbon-14 ages and flow rates of water in the Carrizo Sand, Atascosa County, Texas, Water Resour. Res., 3, 251-261, 1967

Phillips, F.M., M.K. Tansey, L.A. Peeters, S. Cheng, and A. Long, An isotopic investigation of groundwater in the central San Juan basin, New Mexico: Carbon-14 dating as a basis for numerical flow modeling, Water Resour. Res. 25(10), 2259-2273, 1989

Phillips, F.M. and M.K. Tansey, An integrated isotopic/physical approach to a numerical model of groundwater flow in the San Juan Basin, Rep. 197, New Mexico Water Resour. Res. Inst., Las Cruces, 1984

Press, W.H., B.P.Flannery, S.A. Teukolsky, and W.T. Vettering, Numerical Recipes, Cambridge University Press, Cambridge, 1986

Ratowsky, D.A., Nonlinear Regression Modeling, Marcel Dekker, New York. 1984

Robertson, W.D. and J. Cherry, Tritium as an indicator of recharge and dispersion in a groundwater system in central Ontario, Water Resour. Res. 25(6), 1097-1109, 1989

Shah, P.C., G.R. Gavalas, and J.H. Seinfeld, Error analysis in history matching: The optimum level of parameterization, Soc. Pet. Eng. J., 18(3), 219-228, 1978

Sorooshian, S., and F. Arfi, Response surface sensitivity analysis methods for post calibration studies, Water Resour. Res., 18(5), 1531-1538, 1982.

Sorooshian, S., and V.K. Gupta, Automatic calibration of conceptual rainfall-runoff model parameters: The question of parameter observability and uniqueness, Water Resour. Res., 19(1), 260-268, 1983.

Sorooshian, S., and V.K. Gupta, The analysis of structural identifiability: Theory and application to conceptual rainfall-runoff models, Water Resour. Res., 21(4), 487-495, 1985.

Stallman, R.W. Numerical analysis of regional water levels to define aquifer hydrology, Trans. AGU, 37(4), 451-460, 1956

Stone, W.J., F.P. Lyford, P.F. Frenzel, N.H. Mizell, and E.T. Padgett, Hydrogeology and water resources of the San Juan Basin, New Mexico, Miner. Resour. Rep. N.M. Bur. Mines Miner. Resour.,6, 70pp,1983

Strecker, E.W., and W. Chu, Parameter identification of a groundwater contaminant transport model, Ground Water, 24, 56-62, 1986.

Sun, N., and W.W-G. Yeh, Identification of parameter structure in groundwater inverse problems, Water Resour. Res., 21(6), 869-883, 1985

Sun, N., and W.W-G. Yeh, Coupled inverse problems in groundwater modeling, 1. Sensitivity analysis and parameter identification, Water Resour. Res., 26(10), 2507-2525, 1990a

Sun, N., and W.W-G. Yeh, Coupled inverse problems in groundwater modeling, 2. Identifiability and experimental design, Water Resour. Res., 26(10), 2526-2551, 1990b

Tarantola, A. and B. Valette, Generalized nonlinear inverse problems using the least squares criterion, Rev. Geophys., 20(2), 219-232, 1982

Toorman, A.F., P.J. Wierenga, and R.G. Hills, Parameter estimation of hydraulic properties from one step outflow data, Water Resour. Res., 28(11), 3021-3028, 1992

Umari, A.R., R. Willis, and P.L.-F. Liu, Identification of aquifer dispersivities in two dimensional transient groundwater contaminant transport: An optimization approach, Water Resour. Res., 15(4), 815-831, 1979.

Vecchia, A.V., and R.L. Cooley, Simultaneous confidence and prediction intervals for nonlinear regression models with application to a groundwater flow model, Water Resour. Res., 23(7), 1237-1250, 1987.

Vogel, J.C., Investigation of groundwater flow with radiocarbon, in Isotopes in Hydrology, pp. 235-237, International Atomic Energy Agency, Vienna, 1967

Wagner, B.J. and S.M. Gorelick, A statistical methodology for estimating transport parameters: Theory and applications to one dimensional advective-dispersive systems, Water Resour. Res., 22(8), 1303-1315, 1986.

Wagner, B.J. and S.M. Gorelick, Optimal groundwater quality management under parameter uncertainty, Water Resour. Res., 23(7), 1162-1174, 1987.

Wang K., P.Y. Shen, and A.E. Beck, A solution to the inverse problem of coupled hydrological and thermal regimes, in Hydrological regimes and their subsurface thermal effects, edited by A.E. Beck, L. Stegena and G. Garven, AGU Monograph series, Washington, 1989

Weiss, R. and L. Smith, Parameter estimation using hydraulic head and environmental tracer data, in Proceedings, 1993 Ground Water Modeling Conference, Golden, Colorado, 60-70, 1993

Woodbury, A.D., and L. Smith, Simultaneous inversion of hydrogeologic and thermal data, 2. Incorporation of thermal data, Water Resour. Res., 24(3), 356-372, 1988

Woodbury, A.D., L. Smith, and W.S. Dunbar, Simultaneous inversion of hydrogeologic and thermal data, 1. Theory and application using hydraulic head data, Water Resour. Res., 23 (8), 1586-1606, 1987

Woodbury, A.D., W.S. Dunbar, B. Nour-Omid, Application of the Arnoldi algorithm to the solution of the advection-dispersion equation, Water Resour. Res., 26(10), 2579-2590, 1990

Xiang, Y., J.F. Sykes, and N.R. Thomson, A composite L1 parameter estimator for model fitting in groundwater flow and solute transport simulation, Water Resour. Res., 29(6), 1661-1673, 1993

Yakowitz, S. and L. Duckstein, Instability in aquifer identification: Theory and case studies, Water Resour. Res., 16(6), 1045-1064, 1980

Yeh, W. W-G., Optimal identification of parameters in an inhomogeneous medium with quadratic programming, Soc. Pet. Eng. J., 15(5), 371-375, 1975.

Yeh, W. W-G., and Y.S. Yoon, Parameter identification with optimum dimension in parameterization, Water Resour. Res., 17(3), 664-672, 1981

Yeh, W. W-G., Y.S. Yoon, and K.S. Lee, Aquifer parameter identification with kriging and optimum parameterization, Water Resour. Res., 19(1), 225-233, 1983.

Yeh, W. W-G., Review of parameter identification procedures in groundwater hydrology: The inverse problem, Water Resour. Res., 22 (2), 95-108, 1986